A SELECTED-ION FLOW TUBE STUDY OF SOME GAS-PHASE ION-MOLECULE REACTIONS OF POTENTIAL RELEVANCE TO THE CHEMISTRY OF DENSE INTERSTELLAR CLOUDS.

A thesis

presented for the Degree

of

Doctor of Philosophy in Chemistry

in the

University of Canterbury

by

Simon Antony Hudson Petrie

University of Canterbury

1991

To C., D., E., H., and S.

(They know who they are.)

ABSTRACT:

Results are reported for the studies of several systems of ion-molecule reactions of potential relevance to the chemistry of interstellar clouds. Measurements were obtained using a selected-ion flow tube operated at room temperature (300 ± 5 K) and using helium buffer gas at a pressure of 0.30 ± 0.01 Torr.

The proton affinities of C_4H_2 and C_2N_2 were determined by measurement of the rate coefficients for forward and reverse proton transfer reactions involving compounds of similar proton affinity. The results obtained were $PA(C_2N_2)$ = 674 ± 4 kJ mol^{-1} and $PA(C_4H_2)$ = 741 ± 4 kJ mol^{-1}: this latter quantity is significantly below the literature value, based on an earlier measurement obtained from ICR bracketing.

Isomerism of the ions C_2N^+, C_3N^+, CHN^+ and CH_2N^+ was investigated, using reactivity with various neutrals to distinguish between isomers. The ions CCN^+/CNC^+ and $CCCN^+/c\text{-}C_3N^+$ were distinguished on the basis of their reactivity with H_2: in both instances, the isomer featuring a terminal N atom reacted rapidly while the other isomer was unreactive. Identification of the isomers HCN^+/HNC^+ was complicated by the occurrence of tautomerisation of HCN^+ to the more stable isomer HNC^+ by the mechanism of 'forth and back' proton transfer which occurred with several neutral reagents: reaction with CF_4 was subsequently used to distinguish between these isomers, since HCN^+ reacted rapidly with CF_4 while HNC^+ was unreactive. The reactions of all of these isomeric systems were examined with several neutrals abundant in interstellar clouds. The ions $HCNH^+$ and CNH_2^+ could not be distinguished on the basis of reactivity with the neutrals surveyed: we cannot exclude the possibility that only one of these isomers, $HCNH^+$, was formed using the ion producing methods used.

The reactivity of several ions $C_3H_nN^+$ ($n = 1 \rightarrow 4$) and $C_3H_nO^+$ ($n = 0 \rightarrow 3$), with various neutrals, was investigated to ascertain the importance of these ions in the interstellar synthesis of acrylonitrile, tricarbon monoxide and propynal. Several ion-molecule reactions of CH_2CHCN were also studied to this end. The results indicate that $C_3H_nN^+$ ($n > 0$) and $C_3H_nO^+$ ($n > 0$) are unreactive with the

most prominent cloud constituents H_2 and CO; thus dissociative recombination of these ions should represent a significant source of the target molecules. Several ion-molecule reactions of the types $X^+ + CH_2CHCN$, and $C_3H_nN^+ + X$, produce ions which, on dissociative recombination, are expected to yield cyanopolyynes and cyclopropenylidene. Several reactions of the $C_3H_nO^+$ ions suggest pathways to higher-order polycarbon monoxides and dioxides.

The reactivity of the molecular ions of C_2N_2, C_4N_2 and C_3O_2 have also been studied, to gauge the likely consequences of reactions of such ions within interstellar clouds.

The thermochemistry of the reaction $HCN^+ + CF_4 \rightarrow CF_3^+ + HF + CN$ is explored with regard to the proposal that this reaction may be 'entropy-driven'.

The interstellar significance of a novel class of neutral-neutral reactions has been considered.

The reactivity of the ions $C_4H_n^+$ ($n = 0 \rightarrow 4$), $C_3H_nN^+$ ($n = 0 \rightarrow 4$), and $C_3H_nO^+$ ($n = 0 \rightarrow 3$) with the neutrals H_2, CO, C_2H_2 and HCN is discussed in greater detail. Previous studies have determined that ions featuring linear carbon-chain skeletons are more reactive with H_2 and with CO if they feature 'bare' (non-hydrogenated) terminal carbon atoms: the present study suggests that ions with bare terminal C atoms are also more reactive than ions where the terminal atom is N or O rather than C. This observation may be explained by the degree of carbene character evident in such ions. These results are also discussed with reference to the predominance of very highly unsaturated linear molecules within interstellar clouds.

TABLE OF CONTENTS:

ACKNOWLEDGEMENTS:

The following have, in various ways, assisted in the completion of this thesis:

My supervisor, Dr. Murray J. McEwan, and my assistant supervisor, Dr. Peter W. Harland.

My parents, Catherine and Derek Petrie, and my brother, Hamish, and sister, Elizabeth.

Staff members and fellow researchers, Dr. Colin G. Freeman, Paul F. Wilson, Dr. John S. Knight, Pravit Sudkeow, Dr. Sean C. Smith, Dr. Robert G.A.R. McLagan, Professor Leon F. Phillips, Ryan P.A. Bettens, Professor Eldon E. Ferguson, Dr. Michael Meot-Ner, Dr. Vincent G. Anicich, Kathryn M. McGrath, Barry A. Wells, Tania Chirnside, Brett R. Cameron, Roger F. Meads, Mark Morrison, David Marsden, and Katrina Mackle.

Chemistry Department technical staff in the Mechanical, Glassblowing and Electronics workshops, and the Secretarial offices.

The University of Canterbury, for the provision of a University of Canterbury scholarship, and the Chemistry Department, for the provision of a Teaching Assistantship.

The staff of the Physical Sciences and Engineering Libraries.

Friends, associates, and positive influences, Michael T., Tim, Annette & Fitz, Caligula the cat, Linda & Johnnie, Mary, Francisco, Jim, Lind & Andrew, Ian, Geoff & Liz, Brenda, Dave, Donna, Helen, Tony, Mark, Alex, Steve, Clarrie & Rosalie, Julian, Owen & Joy, Michael H., David, Jefferson Airplane, Libby & Richard, Gay, Rudi, Brian & Caitlin, Mark, John, Gabrielle, anyone else whose name I've omitted accidentally, and Nick, David, Grant, Andrew, and Phil.

Last but by no means least, Sandi McGowan.

LIST OF TABLES:

LIST OF FIGURES:

PUBLICATIONS:

The following publications are related to the research presented in this thesis:

Knight J.S., Petrie S.A.H., Freeman C.G., McEwan M.J, McLean A.D., DeFrees D.J.
J. Am. Chem. Soc. **110** (1988) 5286
Structural isomers of C_2N^+: a selected-ion flow tube study.

Petrie S.A.H., Freeman C.G., McEwan M.J., Meot-Ner (Mautner) M.
Int. J. Mass Spectrom. Ion Proc. **90** (1989) 241
The proton affinity of cyanogen and ion / molecule reactions of $C_2N_2^+$.

Petrie S., Freeman C.G., Meot-Ner M., McEwan M.J.,Ferguson E.E.
J. Am. Chem. Soc. **112** (1990) 7121
An experimental study of HCN^+ and HNC^+ ion chemistry.

Petrie S., Knight J.S., Freeman C.G., Maclagan R.G.A.R., McEwan M.J., Sudkeaw P.
Int. J. Mass Spectrom. Ion Proc. **105** (1991) 43
The proton affinity and selected ion-molecule reactions of diacetylene.

Petrie S., Freeman C.G., McEwan M.J., Ferguson E.E.
Mon. Not. Roy. Astron. Soc. **248** (1991) 272
The ion chemistry of HNC^+/HCN^+ isomers: astrochemical implications.

Petrie S.
Mon. Not. Roy. Astron. Soc. (1991) In press.
Interstellar reactions of kinetically excited radicals with molecular hydrogen.

Petrie S., Chirnside T.J., Freeman C.G., McEwan M.J.
Int. J. Mass Spectrom. Ion Proc. (1991) In press.
The ion-molecule chemistry of CH_2CHCN.

Petrie S., Freeman C.G., McEwan M.J.
Mon. Not. Roy. Astron. Soc. (1991) In preparation.
The ion-molecule chemistry of acrylonitrile: astrochemical implications.

Petrie S., Knight K.S., McGrath K.M., McEwan M.J., Freeman C.G.
J. Am. Chem. Soc. (1991) In preparation.
C_3N^+ isomerism: a selected-ion flow tube study.

Bettens R.P.A., Petrie S., McEwan M.J., Freeman C.G.
To be written.
A selected-ion flow tube study of the ion-molecule chemistry of $C_3H_nO^+$ (n = 0-3).

Petrie S., McEwan M.J., Freeman C.G., McGrath K.M.
To be written.
CH_2N^+ isomerism: a selected-ion flow tube study.

CHAPTER 1.

INTRODUCTION.

Section 1.1: The chemistry of the interstellar medium.

Dense interstellar clouds are among the least visually captivating objects in the night sky, since they appear usually as an absence or a paucity of stars in a particular line of sight. Yet these clouds are (in their own way) fascinating, since they constitute the largest storehouse of chemical substances within our Galaxy.

Conditions throughout most interstellar space (see **table 1.1**) are not at all conducive to the existence of molecules, even the simplest bimolecular structures: particle densities are phenomenally low, and so collisions are very infrequent, providing very little opportunity for chemistry to occur. In these conditions, ultraviolet and cosmic radiation provide efficient channels for the destruction of molecules: only the simplest species such as CH can be formed in competition with these destruction processes. Within this harsh environment, dense clouds exist as some sort of oasis for the chemist in a desert which is, in general, of interest only to the physicist and astrophysicist.

The density of a dense cloud is not great: a thousand particles per cubic centimetre is a typical cloud density - higher densities, up to 10^{10} particles per $cm^{3,}$ are found in particularly dense clumps of large clouds. Clouds can be

described as "dense" only in comparison to most reaches of interstellar space (where, in any given cubic centimetre, you are lucky to find any particles whatsoever). Because of the pressure gradient which decreases outwards from the cloud's centre, clouds (once formed) must be large enough to be gravitationally self-contained or else their lifespan will be short. Most clouds have diameters of a few parsecs and range in mass from several times the mass of the sun to several million solar masses. Most clouds are very cold (typically having a temperature of about 20K); they are also largely opaque to any electromagnetic radiation more energetic than microwave radiation, so ionizing and dissociating radiation cannot usually penetrate to the centre of a cloud (though cosmic rays can: under cloud conditions, cosmic rays act as much for the propagation of molecules as for their destruction). The cloud's opacity derives

---

Table 1.1: Physical conditions of gaseous bodies throughout the Universe. [1,2]

Object / system	T [a,b]	n [c]	P [d]	Composition [e]
Terrestrial atmosphere [f]	3×10^2	3×10^{19}	7.6×10^2	O_2, N_2, Ar
Solar core	1.5×10^7	$\sim 10^{26}$	$\sim 10^{14}$	H^+, He^{2+}, *e*
Solar photosphere	5.8×10^3	$\sim 10^{17}$	$10^1 \rightarrow 10^2$	H^+, He^+, *e*
Tenuous IS [g] space	$10^5 \rightarrow 10^6$	$\sim 10^{-2}$	$10^{-16} \rightarrow 10^{-15}$	H^+, H, He^{2+}, *e*
Diffuse IS cloud	$10^2 \rightarrow 10^4$	$10^{-2} \rightarrow 10^2$	$10^{-15} \rightarrow 10^{-13}$	H, He, CH
Dense IS cloud	$10^1 \rightarrow 10^2$	$10^3 \rightarrow 10^{10}$	$10^{-15} \rightarrow 10^{-8}$	H_2, He, CO
Intergalactic space	$> 10^4$?	$< 5 \times 10^{-9}$?	?	H^+, He^{2+}, *e* ?

Notes

a. All values are approximate and intended merely to give an indication of 'typical' conditions. There exists a continuum of physical conditions within, between and beyond the ranges tabulated here.
b. Temperature, in degrees Kelvin.
c. Particle density, in particles cm^{-3}.
d. Pressure, in torr.
e. Only the predominant chemical components are listed.
f. At sea level.
g. IS ≡ Interstellar.

in part from its large size and the large quantity of gas contained within, and also from the small grains of dust which are present and which serve to scatter or absorb any incident radiation.

Virtually all the information concerning cloud constituents has come from radio astronomy: radio-frequency spectra of molecular clouds feature lines which correspond to rotational excitation and de-excitation of particular molecules. The variety of chemicals identified within clouds is slight - to date, less than a hundred molecules, molecular ions and radicals have been observed as cloud components (see **table 1.2**) - but the existence of many exotic and unusual species within this list indicates that the chemistry occurring within these clouds differs substantially from that seen under normal terrestrial conditions. Common features of cloud constituents are single and triple C-C bonds, triple C-N bonds, a predominance of straight-chain organic species, an absence of branched-chain organics and a lack of inorganic, metal-containing, multifunctionalised and cyclic compounds. The detectability of a species within a cloud does not merely relate to its presence: to be observed, a species must not only be present in reasonable abundance but also (because most species are detected via rotational transitions) its rotational spectrum must be known and must contain lines of sufficient strength to be perceived in astronomical observations. Molecules which have a nonpolar or negligibly polar ground state will not, in general, be observed because their rotational spectra are weak or nonexistent. There are several observed but unidentified features in cloud spectra, and many molecules (e.g. CH_4, C_2H_2) which are very likely cloud components but are by their nature completely undetectable.

Several recent reviews treat the broad topic of interstellar chemistry [3,5,8-20] and related topics such as cloud physics,[21,22] observed cloud conditions,[23,24] interstellar dust,[25,26] interstellar modelling [27,28] and organic synthesis.[29,30]

Table 1.2: Molecules observed within interstellar clouds. [3-7] This table lists molecules detected in clouds but not those species which have only been identified in circumstellar shells, since ion-molecule chemistry is thought to be less important a process in the chemical evolution of the latter regions. There is also very strong evidence for the presence of polycyclic aromatic hydrocarbons (PAHs) in interstellar clouds, though no individual PAH has yet been identified as a cloud constituent.

CH·	CH^+	CN·	HCN
HNC	$HCNH^+$	CH_2NH	CH_3NH_2
CO	HCO·	HCO^+	HOC^+ (?)
H_2CO	CH_3OH	CS	HCS^+
H_2CS	CH_3SH	NH_2CN	OCN^- (?)
HNCO	$HCONH_2$	HNCS	$HOCO^+$
HCOOH	OCS	C_2	C_2H·
C_2H_2	CH_2CN·	CH_3CN	CH_3NC
H_2CCO	CH_3CHO	$HCOOCH_3$	CH_3OCH_3
CH_3CH_2OH	c-SiC_2	C_2S	C_3H·
c-C_3H_2	CH_3C_2H	C_2CN·	HC_2CN
CH_2CHCN	CH_3CH_2CN	C_2CO	HC_2CHO
CH_3COCH_3	C_2CS	C_2C_2H·	CH_3C_2CN
C_2C_2CH·	HC_2C_2CN	$CH_3C_2C_2H$	$C_2C_2C_2H$·
$CH_3C_2C_2CN$	$HC_2C_2C_2CN$	$HC_2C_2C_2C_2CN$	$HC_2C_2C_2C_2C_2CN$
H_2	H_3^+	NH_3	OH·
H_2O	H_3O^+	SiH_4 (?)	H_2S
HCl	N_2H^+	NO·	HNO
PN	NS·	NaOH (?)	SiO
SO	SiS		

Section 1.2: Ion-molecule reactions as a basis of interstellar chemistry.

Once astronomy and other broadly physical disciplines have determined the composition and the conditions which prevail within dense interstellar clouds, it becomes a problem in chemistry to explain the species which are present. The very low pressure within a cloud means that the only reactive processes which need be considered are unimolecular and bimolecular processes: three-body collisions (and, of course, those of higher order) are so exceedingly rare as to be totally unimportant. The low cloud temperatures additionally constrain viable reactions to be only those which are exoergic or thermoneutral and which lack activation energy barriers, since the reactive species to be considered in any collision will have negligible internal energy. The main experimental effort in modelling cloud chemistry has thus been in studying exothermic two-body reactions.

The processes which are held to be of some importance include radical-radical reactions, radiatively stabilised bimolecular association reactions,[31] some bimolecular reactions with activation barriers[32] (between neutral species of high abundance) and some processes occurring on interstellar dust grains;[33,34] but the predominant interstellar gas process is the reaction between a positive ion and a neutral, usually stable, molecule. **Positive ion-molecule reactions** are often very efficient under interstellar conditions, because they usually lack activation barriers (see **figure 1.1**) - thus when they are exoergic they occur at the collision rate. Support for the importance of ion-molecule reactions in interstellar chemistry comes from the generally good agreement between observed cloud

composition and expected composition (as inferred from model mechanisms comprising many hundreds of ion-molecule reactions) - though there are some aspects of the ion-molecule models which do not mirror well the cloud conditions. Notable shortcomings in the present models of ion-molecule reactions are:

Figure 1.1: Generalised reaction profiles for (a) exothermic and (b) endothermic positive ion-molecule reactions, and for (c) reaction between two neutral species. Ion-molecule reactions lack effective activation energy barriers, because of the long-range attractive electrostatic interaction between A^+ and B as they approach: the energy required for rearrangement into products is provided by this attraction, in most cases. The lack of an activation barrier is extremely important at 10K (a typical temperature in a cold interstellar cloud) where the mean internal energy of a thermalised ion or molecule is approximately 0.08 kJ mol^{-1}. The efficiency of ion-molecule reactions explains their predominance in the partially-ionised cloud environment.
[Figure adapted from reference 29].

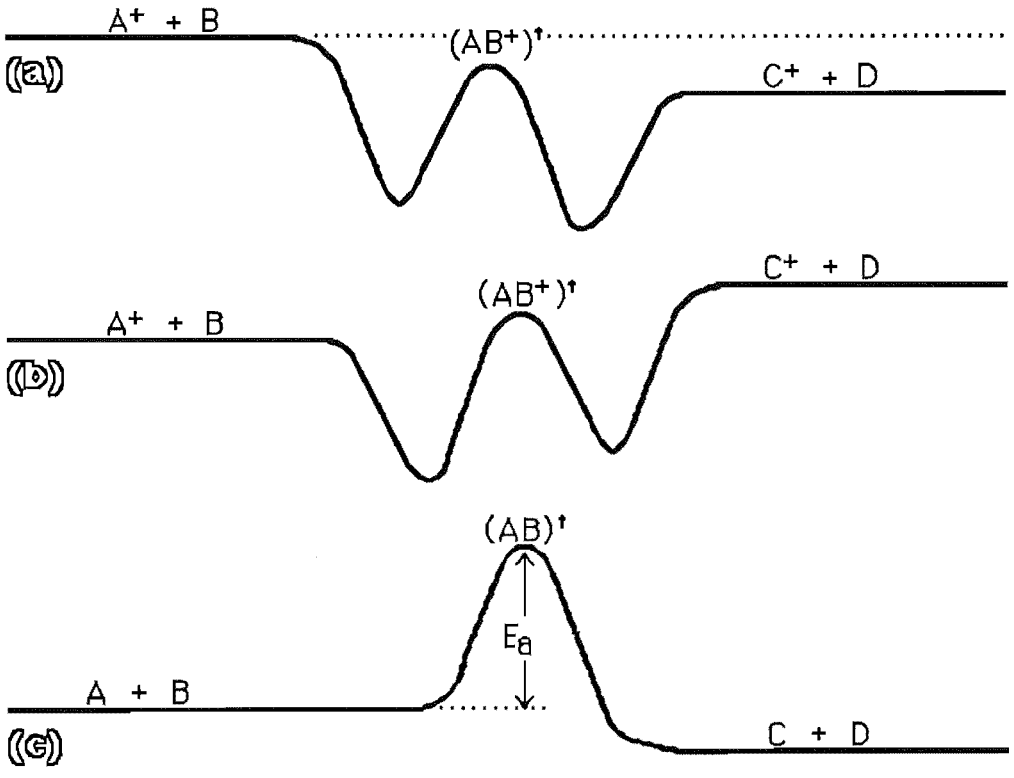

(i) The production of sulphur-bearing species.[35] According to models, production of H_2S and SO in the amounts observed requires some high-temperature processing, but these species are also seen in very cold clouds. It has also been suggested[34] that sulphur chemistry requires grain surface reactions.

(ii) Incorrect abundances obtained for nitrogen species in models suggest that the starting materials may be in a different form from that assumed. Models incorporating neutral-neutral processes are better able to account for the observed abundances of simple nitrogen-containing molecules.[36,37]

(iii) The formation of CH and CH^+ is held to require high temperatures and the presence of shock waves resulting from violent events - such as star formation - within the cloud.[38]

(iv) Predicted abundances of some polyatomic ions such as HC_3NH^+ and CH_3CNH^+ are at least an order of magnitude above the observational upper limits for these species.[39,40] Reactions between neutral species may account for this discrepancy.[41-43]

A notable success of ion-molecule chemistry has been in its modelling of the very large deviations, from terrestrial (and presumably interstellar) abundances, of the H/D ratios observed within interstellar molecules.[44-46] Very recently, models have been developed which account for the long-term, dynamical development of the cloud[36] or which include accretion processes onto dust grain surfaces:[47] these more sophisticated models claim better agreement with

observation than earlier, pseudo-time-independent ion-molecule models, although such agreement may merely reflect the greater degree to which more complex models can be 'fitted' to observed conditions in the absence of sufficient observational constraints on these conditions.

Ion production within cloud interiors is most typically by cosmic-ray bombardment of H_2 or He:[44,48]

$$\text{c.r.} + H_2 \rightarrow H_2^+ + e + \text{c.r.} \quad [.80] \quad (1.1a)$$

$$\text{c.r.} + H_2 \rightarrow H^+ + H + e + \text{c.r.} \quad [.04] \quad (1.1b)$$

$$\text{c.r.} + He \rightarrow He^+ + e + \text{c.r.} \quad [.16] \quad (1.1c).$$

A cosmic ray is most usually a proton, electron or α-particle having a kinetic energy of several MeV. The chief Galactic source of such cosmic rays is held to be Type I supernovæ. Calculations have shown that 2 MeV cosmic rays from such events have a range of several hundred parsecs within the diffuse interstellar medium;[49] each cosmic ray can initiate many ionisations, since only ~60 eV is lost per ionisation. Some of this energy is expended in translational excitation of the products, chiefly of the electron (typically $E_T \sim 30$ eV)[1] which thus may be able to induce further ionisation

$$H_2 + e \rightarrow H_2^+ + e + e' \quad (1.2).$$

An ionisation rate per hydrogen molecule $\zeta'_{H_2} \sim 1.1 \times 10^{-15}$ s^{-1} has been suggested as the mean Galactic value for cosmic-ray induced ionisation, but this rate will be lower within dense clouds because of the finite permeability of such a dense

region.[50] Models of dense cloud chemistry usually adopt an ionisation rate of 1×10^{-17} s^{-1}, reflecting the attenuation of cosmic rays by the gas and dust constituting the cloud.[13]

It is worth noting also that alternative methods of ionisation exist, even in the absence of irradiation. A process of chemi-ionisation has been suggested[48]

$$CH\cdot + O \rightarrow CHO^+ + e \qquad (1.3)$$

for which a rate coefficient $k_{1.3} = 7 \times 10^{-12}$ cm^3 $molec^{-1}$ s^{-1} has been estimated at 25K.[51] Such processes involving small, reactive neutrals may be important at relatively low pressures (i.e. on cloud fringes) and during the early stages of a cloud's development, when the abundance of these species is highest; however, cosmic-ray production of H_2^+ is considered the dominant primary process.

Subsequent reaction of H_2^+ with molecular hydrogen yields H_3^+, which is unreactive with H_2

$$H_2^+ + H_2 \rightarrow H_3^+ + H\cdot \qquad (1.4)$$

$$H_3^+ + H_2 \rightarrow \text{no reaction} \qquad (1.5)$$

$k_{1.4} = 2.0 \times 10^{-9}$ cm^3 $molec^{-1}$ s^{-1}

$k_{1.5} < 1 \times 10^{-14}$ cm^3 $molec^{-1}$ s^{-1}

and which thus persists to react with other chemicals present within the cloud - for example,

$$H_3^+ + CO \rightarrow CHO^+ + H_2 \qquad (1.6).$$

$$k_{1.6} = 1.7 \times 10^{-9}\ cm^3\ molec^{-1}\ s^{-1}$$

With such reactions, the synthetic chemistry of the cloud is under way. Subsequent reactions between progressively larger reactants (at, in general, progressively lower abundances) can succeed in producing quite large molecules such as the cyanopolyynes ($R(C_2)_nCN$, $n = 0 \rightarrow 5$ observed for R = H, $n = 0 \rightarrow 2$ observed for $R = CH_3$). Reaction classes of importance include charge-transfer, proton-transfer, atom abstraction, radiative association and dissociative recombination processes (see **figure 1.2**). Of these processes, the first three are studied with relative ease in the laboratory, and their implications for interstellar chemistry are well established.

Radiative association of ions with molecules, first suggested by Williams,[53] is held to be of importance in collisions involving polyatomic reactants.[31] Under cloud conditions, termolecular association reactions are precluded by the extremely low pressure (at $n=10^3$ particles cm^{-3} and T=10K, a molecule or ion is likely to undergo a *bimolecular* collision once every few weeks) and so reactions yielding products which require collisional stabilisation cannot occur. Association reactions *can* occur if the initially-formed collision complex can be stabilised by radiative de-excitation within the complex's lifetime. Typical frequencies for infra-red radiative stabilisation of collision complexes are in the range $k_r \sim 10^2 \rightarrow 10^3\ s^{-1}$,[54] which is many orders of magnitude below the normal range of vibrational frequencies (vibration being the mode through which fragmentation of the complex is liable to occur). For a long lifetime, the collision complex must possess several internal degrees of freedom wherein the

excess energy of the association may be partitioned (since the complex will easily dissociate otherwise) and thus, in general, this process is more feasible for more highly polyatomic products. The low cloud temperatures also favour long lifetimes: reactants possess essentially no internal energy and so, for dissociation to occur, essentially all of the internal energy of the collision complex must be localised in the bond between the initial fragments.

Figure 1.2: Important classes of interstellar ion-molecule reactions.

(a). Charge transfer $\mathbf{A^+ + X \rightarrow X^+ + A}$
Usually fast when exoergic; exoergic if IP(A) > IP(X)
e.g. $He^+ + CO \rightarrow (CO^+)^* + He$
$HC_3N^+ + NH_3 \rightarrow NH_3^+ + HC_3N$
but $He^+ + H_2 \not\rightarrow (H_2^+)^* + He$

(b). Proton transfer $\mathbf{AH^+ + X \rightarrow XH^+ + A}$
Fast when exoergic; exoergic if PA(X) > PA(A)
e.g. $H_3^+ + CO \rightarrow HCO^+ + H_2$
$HCO^+ + HCN \rightarrow HCNH^+ + CO$

(c). Atom abstraction $\mathbf{A^+ + XB \rightarrow AB^+ + X}$
Usually fast when exoergic and B = H
e.g. $CN^+ + H_2 \rightarrow HCN^+ + H.$
$\rightarrow HNC^+ + H.$
$HCN^+ + H_2 \rightarrow HCNH^+ + H.$

(d). Radiative association $\mathbf{A^+ + B \rightarrow AB^+ + h\nu}$
Always exoergic; efficient when collision complex $(AB^+)^*$ is long-lived.
e.g. $CH_3^+ + H_2 \rightarrow CH_5^+ + h\nu$
$CH_3^+ + HCN \rightarrow CH_3CNH^+ + h\nu$

(e). Dissociative recombination $\mathbf{AB^+ + e \rightarrow A + B}$
Always exoergic for some product channels; almost always exceedingly fast, except for monatomic ions.
e.g. $CH_5^+ + e \rightarrow CH_3\cdot + H_2$ [a]
$\rightarrow CH_2 + H_2 + H\cdot$ [a]
$\not\rightarrow CH_4 + H\cdot$ [b]
$H_3O^+ + e \rightarrow OH\cdot + H_2$
$\rightarrow H_2O + H\cdot$ [a]

Notes:
a. This product channel has not been identified.
b. This product channel is thought to be inactive.[52]

The observation of purely radiative association requires very low pressures to ensure that there is no collisional contribution to stabilisation, and so flow tube experiments have more often focussed on termolecular association.[55] Since radiative and termolecular association involve the same collision complex, it is frequently assumed that the strong inverse temperature dependences which are seen for termolecular association are indicative also of similarly strong dependences for radiative association. However, problems can arise with the extrapolation of theoretical studies in the absence of sufficient experimental results. Herbst et al,[55] inferring radiative association rate coefficients from observed termolecular association, describe a difference between theoretically calculated and experimentally derived radiative association rate coefficients of a factor of $10^{3.5}$ for the reaction

$$HCNH^+ + C_2H_2 \rightarrow [C_3H_4N]^+ \qquad (1.7).$$

$k_{1.7e} = 3.3 \times 10^{-16}$ cm^3 molec^{-1} s^{-1} (experimental)

$k_{1.7c} = 1.1 \times 10^{-12}$ cm^3 molec^{-1} s^{-1} (calculated)

The values quoted here are two-body rate coefficients giving the effective bimolecular rate for association, with the experimental results indicating that the collision complex is radiatively stabilised in fewer than one collision per 10^6, in contrast to the theoretical expectations. The discrepancy here is thought to arise from an incorrect structure assigned to the collision complex in the theoretical treatment. The very low rate coefficient in this instance is explained in terms of the predominant production of a cyclic metastable isomer rather than the lowest-energy structure (protonated C_2H_3CN). Such a metastable product would have a lower density of available vibrational and rotational states than the lowest-

energy species, and would thus have both a shorter lifetime as a collision complex and a lower probability of collisional stabilisation in laboratory studies.

Some direct experimental observations of radiative association have been made: the reaction

$$CH_3^+ + H_2 \rightarrow CH_5^+ + h\nu \qquad (1.8)$$

is important in the interstellar synthesis of methane, since

$$CH_3^+ + H_2 \rightarrow CH_4^+ + H\cdot \qquad (1.9)$$

is endoergic. Measurement of $k_{1.8} = 1 \times 10^{-13}$ cm^3 molec^{-1} s^{-1} at 13K using an ion trap technique[56] constitutes the first detection of radiative association at low temperatures and pressures.[57-59] Bimolecular association has also been observed in several association reactions involving nitriles at room temperature, which are found to be reasonably efficient at low pressures.[60-64] The only known mechanism for bimolecular association is that of radiative association. Ab initio calculations of the structures of the association complexes in these studies have enabled the association systems to be modelled. There is good agreement between measured and calculated lifetimes of the AB^+ complexes.[65,66]

Dissociative recombination of a positive ion with an electron

$$\mathbf{AB^+} + e \rightarrow \mathbf{A} + \mathbf{B} \qquad (1.10)$$

yields two neutral fragments and thus serves as the main terminating step in a chain of ion-molecule reactions initiated by cosmic-ray ionisation.[67-70] As such, it provides an upper limit to the degree of ionisation within a cloud (typically, about 10^{-8}). [71] Dissociative recombination reactions are *very* rapid - for triatomic or larger species, the recombination coefficients observed at room temperature are typically of the order of 10^{-6} cm^3 $molec^{-1}$ s^{-1}, [72] with $\alpha_{e(1.10)}$ tending to increase with the size of the molecular ion. The reactions also display a strong negative temperature dependence[73,74] and are thus even more rapid under interstellar conditions - though the variation with temperature diminishes as the size of the molecular ion increases. A notable exception to the general rapidity of these reactions is

$$H_3^+ + e \rightarrow H_2 + H\cdot \qquad (1.11a)$$

$$\rightarrow 3H\cdot \qquad (1.11b),$$

which, Smith and Adams claim on the basis of Flowing Afterglow - Langmuir Probe measurements, does not occur to any measurable extent: $\alpha_{e(1.11)} < 1.0 \times 10^{-11}$ cm^3 $molec^{-1}$ s^{-1}. [3,73] Interstellar H_3^+ is, as a consequence, given free rein in models to undergo further reactions with trace neutrals. This view has, however, been contested by Amano,[75] who finds a recombination coefficient $\alpha_{e(1.11)} = 1.8 \times 10^{-7}$ cm^3 $molec^{-1}$ s^{-1} in agreement with earlier, stationary-afterglow[76,77] and merged-beam measurements.[78,79] In any event, reaction of H_3^+ with CO to produce HCO^+ is likely to be a more rapid loss mechanism for H_3^+ than is dissociative recombination,[80,81] so the uncertainty regarding this process is not of critical concern in this field.

For triatomic and larger molecular ions, several products are usually possible from a dissociative recombination reaction - unless one bond is notably weaker than the others:

$$N_2H^+ + e \rightarrow N_2 + H\cdot \qquad [1.0] \qquad (1.12).$$

$$\alpha_{e(1.12)} = 1.7 \times 10^{-7}\ cm^3\ molec^{-1}\ s^{-1}\ (at\ 300K)^3$$

The product distributions of most dissociative recombinations are not well predicted by theory, since it is not intuitively obvious which of the collision complex's bonds will break most rapidly; several theories exist which treat the dissociation process in different ways, and which predict often very different results.[52,69,82,83] Until recently, experimental determination of product channels was not possible. An experiment applying spectroscopic techniques to a FALP apparatus[84] has identified one of the product channels for reaction of ground-state HCO_2^+ with an electron:

$$HCO_2^+ + e \rightarrow OH + CO \qquad [0.34] \qquad (1.13a)$$

$$\rightarrow H + CO_2 \qquad [?] \qquad (1.13b)$$

$$\rightarrow H + O + CO \qquad [?] \qquad (1.13c)$$

$$\alpha_{e(1.13)} = 3.4 \times 10^{-7}\ cm^3\ molec^{-1}\ s^{-1}\ (at\ 300K)$$

and similar studies have since been performed for H_3O^+ and N_2OH^+.[85]

A fundamental tenet of astrochemical modelling is that, in accordance with the prevailing temperature, reactants possess negligible internal or translational energy. This is necessarily true (to a very good approximation) for reactions not

involving molecular hydrogen, since preceding collisions with H_2 would have thermalised each reactant; but reactions of higher energy species with hydrogen can also be considered relevant.[86] If a reaction

$$\mathbf{AB^+ + CD \rightarrow AC^+ + BD} \qquad (1.14)$$

is exoergic, then the exoergicity of the reaction will be conferred as suprathermal energy of the products. Energy which is channeled into electronic or vibrational modes of a product is likely to be dissipated as electromagnetic radiation before this species can undergo collision with H_2, since the time between collisions greatly exceeds the lifetime of most feasible excited states; but translational energy cannot be quenched except by intermolecular collision, and in some cases this energy is sufficient to drive reactions. For example, in nitrogen chemistry, the reaction

$$N^+ + H_2 \rightarrow NH^+ + H\cdot \qquad (1.15)$$

is endoergic[87] for thermalised reactants ($\Delta H_{1.15} \sim +0.7$ kJmol^{-1}). The endoergicity of this reaction can be overcome for N^+ produced in some fashions - for example, by collision of He^+ (generated by cosmic-ray ionisation) with N_2 (which is not observed in interstellar clouds because of its nonpolar nature, but which is probably a species of comparable abundance to CO):

$$He^+ + N_2 \rightarrow (N_2^+)^{\#} + He \qquad (1.16a)$$

$$(N_2^+)^{\#} \rightarrow (N^+)^* + N\cdot \qquad (1.16b)$$

The N^+ thus produced has an excess translational energy of approximately 1.5 kJ mol^{-1}, which is sufficient to allow NH^+ formation on collision with H_2; nonreactive collisions still dominate, however, leading to thermalisation of the translationally excited N^+ in most cases.

$$(N^+)_{fast} + H_2 \rightarrow NH^+ + H\cdot \quad (1.17a)$$

$$\rightarrow N^+ + (H_2)_{fast} \quad (1.17b)$$

$k_{1.17a(0.038)} = 3.7 \times 10^{-10}$ cm^3 $molec^{-1}$ s^{-1} (@ KE_{cm} = 38 meV)

$k_{1.17a(0.26)} = 6.2 \times 10^{-10}$ cm^3 $molec^{-1}$ s^{-1} (@ KE_{cm} = 260 meV)

$k_c = 1.59 \times 10^{-9}$ cm^3 $molec^{-1}$ s^{-1}

(KE_{cm} is the centre-of-mass collision energy pertaining to the VT-SIFDT experimental results;[86] k_c is the collision rate coefficient according to Langevin theory). This notion of 'hot-ion' chemistry in cold clouds has also been treated recently by Brown et al.[41]

Negative ions may also play a rôle in cloud chemistry[88,89] - though such a rôle is almost certainly subservient to positive-ion chemistry, because of the necessarily lower total abundances of negative ions. Negative ions may be generated by attachment of low-energy electrons to molecules

$$\mathbf{AB} + e \rightarrow \mathbf{A^-} + \mathbf{B} \quad (1.18a)$$

$$\rightarrow \mathbf{AB^-} + h\nu \quad (1.18b)$$

or by UV-induced photoionisation of polar molecules

$$\mathbf{AB} + h\nu \rightarrow \mathbf{A^-} + \mathbf{B^+} \qquad (1.19).$$

Electron attachment competes with dissociative recombination as a loss mechanism for electrons - collision of an electron with a positive ion rather than a neutral molecule is favoured by the greater electrostatic attraction which is manifested between ions and electrons. Negative-ion production by electron attachment requires that the electrons be of low translational energy. Cosmic-ray ionisation produces high-energy electrons: some of this energy is rapidly expended in further ionisations (reaction 1.2), but a point is soon reached at which a medium-energy electron is incapable of further ionisation. Subsequently, the electron can only be quenched by collision with molecules:

$$e + H_2 \rightarrow e' + H_2 \qquad (1.20)$$

Such quenching processes are very inefficient: Cravath[90] has determined that, for quenching of a highly excited electron by elastic collisions in a neutral gas, only ~0.00026 of the electron's kinetic energy is lost per collision with H_2. Many thousands of collisions will be required to thermalise the electron, and within this time any interaction with a cation is likely to lead to neutralisation. Thus production of negative ions is only feasible if the degree of ionisation is sufficiently low.

Ultraviolet ionisation of molecules (reaction (1.19)), within the more sheltered reaches of a cloud, will occur principally as a byproduct of cosmic-ray ionisation, because of the opacity of clouds to external UV and the lack of other internal UV sources.[91]

Negative ions, if formed, are very efficiently destroyed by collision with positive ions:

$$AB^+ + CD^- \rightarrow AB + CD \quad (1.21a)$$

$$\rightarrow AC + BD \quad (1.21b).$$

The rate coefficients for these processes are faster even than for recombination of positive ions with electrons: values of $k_{1.21} \sim 10^{-3}$ cm^3 molec^{-1} s^{-1} have been estimated.[72]

Shocks are of importance in driving chemistry in some cloud regions: a shock wave may occur as the result of large-scale upheaval (such as nascent star formation) within a cloud, leading to an increase in local temperature and pressure. Temperatures of several thousand degrees may be attained, permitting a more varied chemistry including endothermic and barrier-inhibited reactions. Chemistry within shocked regions[36,92-98] has similarities with the chemistry of circumstellar envelopes,[43,99-101] and several molecules not seen in cold interstellar clouds have been seen in such envelopes.

Recent efforts in investigating interstellar chemistry have tended to concentrate on the above areas. In addition, as the interstellar chemistry of carbon, nitrogen and oxygen has become better-understood, much recent work has been done in studying the chemistry of the second-row elements, principally silicon,[102-110] phosphorus[111-113] and sulphur.[35,97,114-118] Evidence is accumulating also for the interstellar presence of polycyclic aromatic hydrocarbons (PAHs),[88,89,94,119-124]

which have been implicated as an intermediate stage between smaller molecules and dust grain formation.

Section 1.3: Laboratory study of ion-molecule reactions.

Several types of technique have been developed, mainly within the last twenty-five years, for the study of ion-molecule reactions.[125]

In ion cyclotron resonance spectroscopy (ICR),[126] ions are produced in a low-pressure chamber ($P <\sim 10^{-3}$ Torr), constrained by a magnetic field which induces cyclotron motion in the ions. Application of an electric field perpendicular to the magnetic field causes the ions to be propelled along the chamber. Reactions with neutrals can be studied, for example, by the change in ion signal as a function of the variation in pressure of a reactant neutral. The ICR technique, because of the wide pressure range attainable (four orders of magnitude: $\sim 10^{-7}$ - 10^{-3} Torr), is commonly used to study termolecular association processes.[60,62]

In the CRESU technique[127] [CRESU ≡ "Cinétique de Réactions en Ecoulement Supersonique Uniforme"], ion-molecule rate coefficients at very low temperatures are studied by supersonic expansion of a partially ionized gas stream through a Laval nozzle into a low-pressure chamber. The gas stream, which is thus internally cooled to very low effective temperatures, contains the ion source gas, the reactant gas and a buffer gas. Detection of the reactant and

product ions is effected by a mass-spectrometer. The CRESU technique is especially useful for studying ion-molecule reactions as a function of temperature, and at the temperatures relevant to dense interstellar cloud conditions. Reaction studies using CRESU have demonstrated[128] that the reaction

$$N^+ + H_2 \rightarrow NH^+ + H\cdot \qquad (1.15)$$

$k_{1.15} = 4.0 \times 10^{-11}$ cm^3 molec^{-1} s^{-1} [T = 20K]

$k_{1.15} = 2.2 \times 10^{-10}$ cm^3 molec^{-1} s^{-1} [T = 70K]

proceeds much more slowly at 20K than at 70K, due to an apparent slight endothermicity ($\Delta H_{1.15} \sim +0.7$ kJmol^{-1}), while the reaction

$$O_2^+ + CH_4 \rightarrow CH_3O_2^+ + H\cdot \qquad (1.22)$$

$k_{1.22} = 4.6 \times 10^{-10}$ cm^3 molec^{-1} s^{-1} [T = 20K]

$k_{1.22} = 5.8 \times 10^{-11}$ cm^3 molec^{-1} s^{-1} [T = 70K]

is considerably more rapid at the lower temperature, in accordance with a proposed mechanism involving rearrangement of a weakly-bound, short-lived complex.

A recent refinement of the CRESU technique features mass-selection of the reactant ions,[129] by a quadrupole mass spectrometer: this adaptation, CRESUS, has been used to measure the temperature dependence of the reaction

$$N_2^+ + H_2 \rightarrow N_2H^+ + H\cdot \qquad (1.23).$$

$k_{1.23} = 9.5 \times 10^{-10}$ cm^3 molec^{-1} s^{-1} [T = 20K][129]

$k_{1.23} = 2.1 \times 10^{-9}$ cm^3 molec^{-1} s^{-1} [T = 300K][130]

Because of the size of the reaction chambers employed, the CRESU techniques consume large flows of carrier gas. An alternative technique developed very recently by M.A. Smith and co-workers[131] uses similar production of a supersonic jet of internally cooled reactants, but produces a pulsed gas flow in a much smaller apparatus: its developers claim a reduction in buffer gas consumption of better than four orders of magnitude over the CRESU technique. Ion detection in this free jet flow reactor is by time-of-flight mass spectrometry, and temperatures as low as 0.5K have been attained for the study of the association process[132]

$$Ar^+ + Ar + Ar \rightarrow Ar_2^+ + Ar \qquad (1.24).$$

Effective temperatures attainable by this technique, for reactions involving molecular neutrals, are somewhat higher, since the reactant neutrals are at a higher rotational temperature (T_{rot} ~ 10 K; T_{rot} ~ 170 K for H_2).[131]

Some low-temperature data can also be obtained by ion trap methods using liquid-helium or liquid-nitrogen cooled instruments,[59,87,133] but the cooling method used in this instance reduces the chemical versatility of the technique[127] since fewer reagents are volatile at cryogenic temperatures.

Notwithstanding the widespread use of ICR and other techniques, most modelling of interstellar chemical processes has been performed using results produced from one of the many variants of the flow technique originally developed by Ferguson, Fehsenfeld and Schmeltekopf in 1963.[134,135] The **Flowing Afterglow** (FA) instrument was constructed after the isolation of a stationary afterglow in helium following electrical discharge ionisation[136] and found early applications in the measurement of reactions relevant to terrestrial upper-atmosphere chemistry.[134,137] The experimental development[138,139] and applications of the FA technique to ion-molecule chemistry[139,140] have been recently reviewed: the central features, and some indications of the versatility, of the technique are outlined below.

In the flowing afterglow apparatus (**see figure 1.3**), ions are generated within the reaction tube, typically by electron bombardment on the ion-producing gas. A

Figure 1.3: Schematic diagram of a typical flowing afterglow apparatus [Adapted from reference 141].

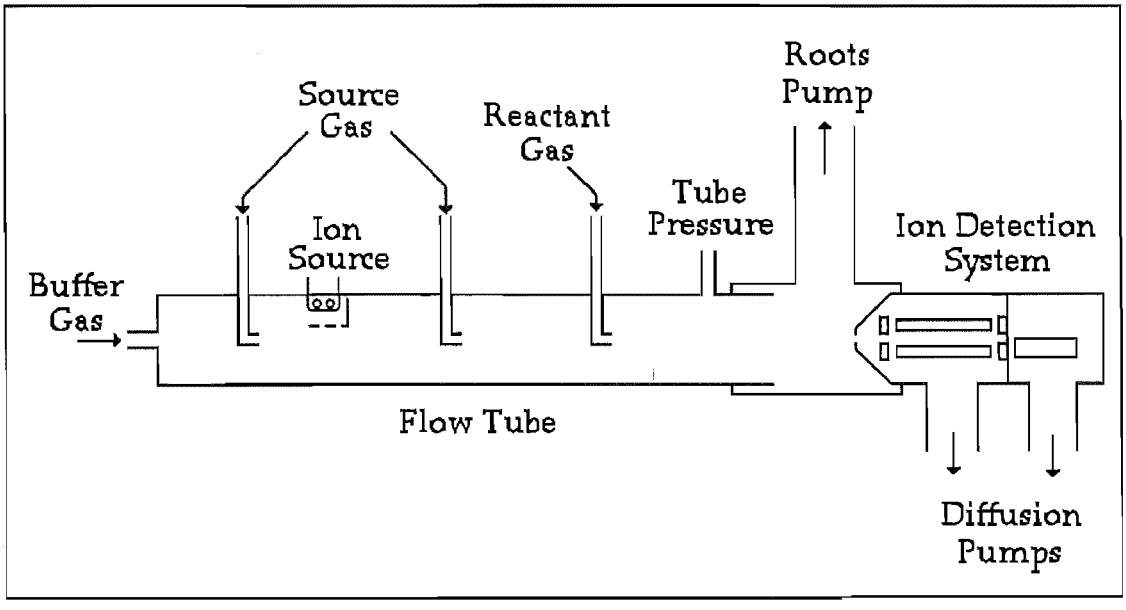

stream of unreactive buffer gas (with which the ion's source gas has been mixed) carries the resulting plasma along the tube towards the aperture at the end of the tube which leads into the mass spectrometer chamber wherein the ions are mass-selected and subsequently detected by a particle multiplier or equivalent device. As the plasma beam traverses the tube axis, it passes several gas inlet ports where a neutral reactant may be added. The reactivity of an ion is judged by the reduction in the initial reactant ion signal with added neutral, and product ions are detected mass-spectrometrically.

Most typically, the buffer gas is helium with a pressure in the range 0.1 to 1.0 Torr: to minimise the effects of radial diffusion (and hence maximise the signal intensity) the gas is rapidly pumped through the tube. The mass-spectrometer chamber, where a much lower pressure must be maintained, is pumped separately from the flow tube. Rate coefficients can be easily obtained from the FA: the comparatively high pressure of the reaction region represents a disadvantage in the modelling of astrochemical processes with respect to "low-pressure" techniques such as ICR (where the pressure is still several orders of magnitude above typical cloud pressures). A compensating advantage of FA is that excited states of the ions are usually rapidly quenched by collisions with the buffer gas.[142]

The basic refinement of the flowing-afterglow apparatus is the **Selected Ion Flow Tube** (SIFT), devised by Smith and Adams in the mid-70s.[143] The SIFT (see **figure 1.4**) differs from the FA in having a remote, differentially-pumped ion source chamber: ions are produced by electron impact in the ion source, the ion beam is focussed via a series of electrostatic lenses and is passed through a

quadrupole mass spectrometer so that the desired reactant ion is mass-selected. The ion beam, thus filtered, is then further focussed upon an aperture leading into the flow tube. This aperture is a specially-shaped Venturi inlet designed to minimise the effects of back-streaming of the buffer gas into the (very much lower pressure) ion source chamber.

The greater complexity of the SIFT over the FA technique means that the flight-path for the ion, from inception through possible reaction to eventual detection, is longer and more complex and thus signal losses (through diffusion and processing) are greater. In fact, diffusive loss for ions in a SIFT is substantially lower than the loss of ion signal through ambipolar diffusion in a FA plasma:[141] the major loss in ion signal occurs as a consequence of ion divergence after

---

Figure 1.4: Schematic diagram of a typical SIFT apparatus. The vertical lines before and after the quadrupole mass spectrometers (QMS) denote the position of electrostatic lenses, used for focussing [Adapted from reference 139].

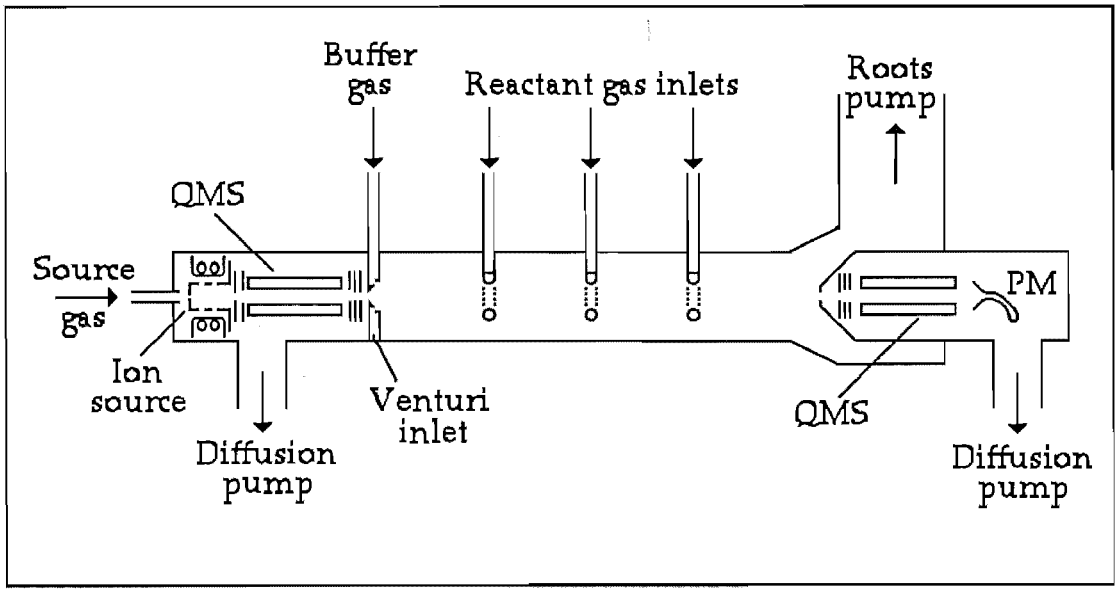

passage through the upstream quadrupole mass filter, before injection through the Venturi orifice. The disadvantage of lower signals is overridden by the increase in purity of the reactant ion beam, from which other ion masses, neutral contaminants, electrons and negative ions - all likely contaminants in the reaction tube of the FA - have been eliminated as far as possible. This means that product channels (especially) can be more confidently determined using the SIFT in preference to the FA.

Further adaptations of the SIFT technique expand the room-temperature, thermalised ion properties of the FA and the SIFT. These modifications (which had previously been applied to the FA device)[144,145] include the addition of a drift region[146] and of a variable-temperature incubating jacket[141,147] to the tube of the "standard" SIFT. A drift region is essentially an extension to the flow tube along which a voltage gradient can be applied, and is useful in artificially controlling the kinetic energy of the ion within this region: one possible application of such a technique is to determine the binding energy in a cluster ion or adduct - for example, in the study of the reaction

$$^{14}N_4^+ + {}^{15}N_2 \rightarrow {}^{14}N_2{}^{15}N_2^+ + {}^{14}N_2 \qquad (1.25),$$

the kinetics of ligand switching were investigated as a function of changing relative kinetic energy in a VT-SIFDT apparatus.[147]

Adding a variable-temperature jacket permits measurement of reaction rates over a wider range of temperatures (typically 80K to 500K), to study the variation in reaction rate with temperature. Fast ion-molecule reactions, and especially

interactions involving an ion and a polar neutral, are frequently seen to have a negative temperature dependence, since the efficiency of the ion's 'capture' by the neutral's dipole is enhanced at reduced relative velocities.[148,149] This means that at 10K, in an interstellar cloud, such processes can be very efficient indeed.[150]

Several other innovations to the FA technique have allowed access to information and to categories of reactions not amenable to study by the above "basic" versions of flow systems. These innovations include incorporation of Langmuir Probe, Laser-Induced Fluorescence, cold finger sampling techniques, and Gas Chromatography / Mass Spectrometry.

The Flowing Afterglow Langmuir Probe (FALP) was developed by Smith and coworkers,[151,152] and incorporates a probe[153] to investigate properties of the flow-tube plasma. The FALP has been used to study ion-electron dissociative recombination, electron attachment and positive ion-negative ion mutual neutralisation reactions, all of which are of some relevance to an understanding of the chemistry of interstellar clouds. Smith and Adams have developed a FALP instrument with a variable temperature incubating jacket (the VT-FALP)[154] which permits investigation of the temperature dependence of plasma processes.[73]

Analysis of the neutral products of ion-molecule reactions is also possible using special adaptations of the FA technique. Laser-induced fluorescence (LIF) was first coupled with a flowing-afterglow apparatus in 1982[155] to study the OH vibrational distribution of the reaction

$$O^- + HF \rightarrow OH + F^- \qquad (1.26).$$

More recently, the FALP technique has been combined with LIF by Adams, Herd and Smith[84] to permit accurate product determinations for astrophysically important dissociative recombination reactions. The investigation of the reaction

$$HCO_2^+ + e \rightarrow OH + CO \qquad [0.34] \qquad (1.13a)$$

by this modified FALP technique is worthy of note not only for the experimental innovation involved, and the chemical knowledge gained, but also for the rather lengthy chain of reactions performed in the reactor during the measurement:

$$He + e \rightarrow He^+ + 2e \qquad (1.27)$$

$$He^+ + 2He \rightarrow He_2^+ + He \qquad (1.28)$$

$$He_2^+ + Ar \rightarrow Ar^+ + He + He \qquad (1.29)$$

$$Ar^+ + H_2 \rightarrow ArH^+ + H_2 \qquad (1.30a)$$

$$\rightarrow H_2^+ + Ar \qquad (1.30b)$$

$$ArH^+ + H_2 \rightarrow H_3^+ + Ar \qquad (1.31)$$

$$H_3^+ + CO_2 \rightarrow HCO_2^+ + H_2 \qquad (1.32).$$

Addition of argon serves to remove metastable excited helium atoms (He*) from the downstream region of the tube, through the Penning ionisation process

$$He^* + Ar \rightarrow Ar^+ + He + e \qquad (1.33).$$

The He* species would otherwise continue to ionise reagent gases introduced downstream (thus obscuring the real rate of ion-electron recombination occurring). Addition of H_2 produces a plasma which does not recombine prematurely (as it were), since the reaction

$$H_3^+ + e \rightarrow H_2 + H\cdot \quad (1.11a)$$

$$\rightarrow 3H\cdot \quad (1.11b),$$

is immeasurably slow. Finally, addition of CO_2 produces the ion of interest, HCO_2^+, which can then recombine with the free electrons entrained in the buffer gas flow.

Physical isolation of products from reactions in a FA apparatus has proceeded by the trapping of neutral products on a liquid-nitrogen-cooled cold finger, followed by warming and analysis of the sample by GC/MS.[156-158]

It is significant that these innovations have involved FA systems at the expense of SIFT techniques: that this has been the case is understandable in view of the much larger ion signals (and, therefore, much more readily observable neutral products) obtained using the simpler flowing afterglow technique. Further developments may include SIFT analogues of some of the FA devices detailed above. A flow tube with selected-ion injection, variable temperature, drift region, Langmuir probe, and spectroscopic and physical product isolation capabilities would be a formidable instrument indeed ...

Section 1.4: Determination of reaction rates from flow data.

Whatever the nature of the flow technique employed, derivation of the rate coefficient for an observed reaction is essentially the same.

For a bimolecular reaction of the form

$$A^+ + B \rightarrow \text{products} \qquad (1.34),$$

the rate law is given as

$$\text{rate} = \frac{-d[A^+]}{dt} = k\,[A^+]_t\,[B]_t \qquad \{1.i\}$$

where k is the second-order rate coefficient and $[A^+]_t$ and $[B]_t$ are the concentrations of the reactants after a reaction interval of time **t**. In experiments using the SIFT (or other flow) technique, the ion signal $[A^+]$ is not monitored as a function of time but as a function of the neutral reactant concentration [B] and after a fixed reaction distance **z**. The rate law thus needs to be rewritten appropriately. The time elapsed is proportional to the distance travelled by the ion A^+, if its velocity v_{ion} is assumed to be independent of its axial and radial position within the tube:

$$\frac{dz}{dt} = v_{ion} \qquad \{1.ii\},$$

so rate $= \frac{-d[A^+]}{dz} = \frac{k}{v_{ion}} [A^+]_z [B]_z$ {1.iii}.

$[A^+]_z$ and $[B]_z$ are the distance-dependent reactant concentrations. In practice, the neutral reactant **B** is present in large excess and so reaction with the small concentration of the ion A^+ leaves it essentially undepleted - thus [B] can be treated as being independent of distance. As a consequence, the rate will exhibit pseudo-first-order behaviour as a function of distance:

$$\frac{-d[A^+]}{dz} = \frac{k}{v_{ion}} [A^+]_z [B] \qquad \{1.iv\}$$

$$\Rightarrow \quad \frac{-d[A^+]}{[A^+]_z} = \frac{k[B]}{v_{ion}} dz \qquad \{1.v\}$$

$$\Rightarrow \quad \int_0^z \frac{-1}{[A^+]} d[A^+] = \int_0^z \frac{k[B]}{v_{ion}} dz \qquad \{1.vi\}$$

$$\Rightarrow \quad \ln [A^+]_o - \ln [A^+]_z = \frac{k[B]z}{v_{ion}} \qquad \{1.vii\}$$

$$\Rightarrow \quad \ln\left(\frac{[A^+]_z}{[A^+]_o}\right) = \frac{-k[B]z}{v_{ion}} \qquad \{1.viii\}.$$

From this expression, it can be seen that if the ion velocity, the reaction distance and the ion signal $[A^+]_o$ at distance zero (that is, before any mixing of the reactants has occurred) are held constant while [B] is systematically varied, then a

plot of ln $[A^+]_z$ versus [B] will yield a line of slope -k z / v_{ion} and intercept ln $[A^+]_o$. In this manner, the rate coefficient can be determined

$$k = \ln\left(\frac{[A^+]_z}{[A^+]_o}\right) \frac{v_{ion}}{[B]\,z} \qquad \{1.ix\},$$

provided that all the quantities on the right-hand side of this expression {1.ix} are known.

$[A^+]_z$ is measured as the intensity of the signal due to the reactant ion's mass at the particle multiplier (the SIFT's detection device); $[A^+]_o$ cannot be conveniently measured, but it is treated as being equivalent to $[A^+]_{z,o}$ (that is, the ion signal due to A^+ after having passed through the reaction distance z while [B] = 0) - a correction factor is applied to compensate for effects of radial diffusive loss of the on-axis ion beam (since only those ions which are on-axis are able to be detected). Since the expression involves the ratio of the A^+ ion signals before and after reaction with B, the units of $[A^+]$ are unimportant.

The reaction distance z can be taken as the distance between the injection portal for the reactant neutral and the exit orifice of the SIFT tube - however, this supposes that mixing of the buffer gas and the reactant neutral is instantaneous. This is physically unreasonable, and in practice the reaction distance is 'end-corrected' to compensate for the axial and radial dependence of the reactant concentration [B]. This end correction is made on the basis of repeated measurements of a calibration reaction - for example,

$$C^+ + CH_4 \rightarrow \text{products} \qquad (1.35),$$

$$k_{1.35} = 1.4 \times 10^{-9}\ cm^3\ molec^{-1}\ s^{-1}$$

for which the value of the rate coefficient is well-established. The end correction can reasonably be assumed to be pressure-dependent, so calibration measurements are necessary at a representative range of pressures.[159]

The ion velocity $\mathbf{v}_{ion}$ can be measured by time-of-flight methods, but it is more customary to calculate it from experimental conditions as follows. Adams et al.[160] have demonstrated that the expression

$$\mathbf{v}_{ion} = 1.33\ \mathbf{v}_{buff} \qquad \{1.x\},$$

where $\mathbf{v}_{buff}$ is the calculated mean velocity of the buffer gas employed, usually gives good agreement with the measured $\mathbf{v}_{ion}$.[141] Thus all the quantities required to determine the rate coefficient for a reaction can be determined.

In practice, the analysis of results is a somewhat more complex matter since allowance should be made for radial and axial diffusion of the ions, and for the non-uniform velocity of the carrier gas as a function of position. Analysis of the relevant flow characteristics can provide correction factors for these effects, as has been explained elsewhere.[160,161] The correction factors applicable to the Canterbury SIFT are detailed in section 2.2.

Section 1.5: Study of isomeric systems by flow techniques.

It is apparent, from a description of the basic aspects of the flow-tube technique, that the SIFT does not directly offer any information on the structure of the reactants or of the product ions which are detected. In fact, the quadrupole mass spectrometers associated with flow-tube ion selection and detection are generally operated at resolutions much too low to discriminate between, for example, CO^+ and N_2^+. The use of the SIFT to determine the isomeric content of a reactant ion signal may therefore seem an odd and slightly quaint notion. The SIFT is not capable of delivering any structural information whatever: however, it can discriminate easily between two isomers of an ion if these isomers exhibit differing reactivity with some neutral species.

An ion signal **I** comprising only one species A^+ with negligible vibrational and electronic excitation will, as discussed in section (1.4), exhibit a linear decay of the logarithm of the ion signal when plotted against the concentration of the reactant neutral [B] (see **figure 1.5**). An ion signal comprising both A^+ and C^+ (where C^+ has the same mass-to-charge (m/z) ratio as A^+, but differs in its reactivity towards B) will not give a linear decay on such a ln(I)/[B] graph. The curved decay resulting (see **figure 1.6**) in such an instance is the sum of the two decays (each of which would describe a linear decay on a semilogarithmic graph) for A^+ and for C^+ reacting with B,

$$A^+ + B \rightarrow \text{products} \qquad (1.36)$$

$$C^+ + B \rightarrow \text{products} \qquad (1.37)$$

$$k_{1.36} \neq k_{1.37}$$

and if the ratio of A^+ to C^+ is known then $k_{1.36}$ and $k_{1.37}$ can be established. If the ratio of A^+ to C^+ in the initial ion signal is not known, then it becomes an exercise in curve-fitting to separate out the two linear components of the curve: this curve-fitting is usually achieved by applying an iterative computer program to the experimental data.[162]

A curved decay on a graph does not automatically indicate the existence of two isomers, however. Curved decays can result if the reaction being studied does not occur to completion but sets up an equilibrium in the reaction region; if the detection mass-spectrometer is unable to completely resolve between m/z (A^+) and contaminant ions having mass numbers one unit higher or lower; or if the reactant neutral B is added in sufficient concentration to significantly alter the

Figure 1.5: Semilogarithmic graph of ion signal decay versus reactant neutral partial pressure, in the case where the reactant ion signal contains only one ion form. The example shown is for the reaction of Ar^+ (m/z 40) with O_2, for which a rate coefficient $k = 4.92 \times 10^{-11}$ cm^3 $molec^{-1}$ s^{-1} was determined from the data depicted here. This is also the type of graph expected in the case where two forms of the reactant ion (two isomers or two forms with different internal energies) are present, but react at the same rate with the neutral - for example, both isomers may react at the collision rate.

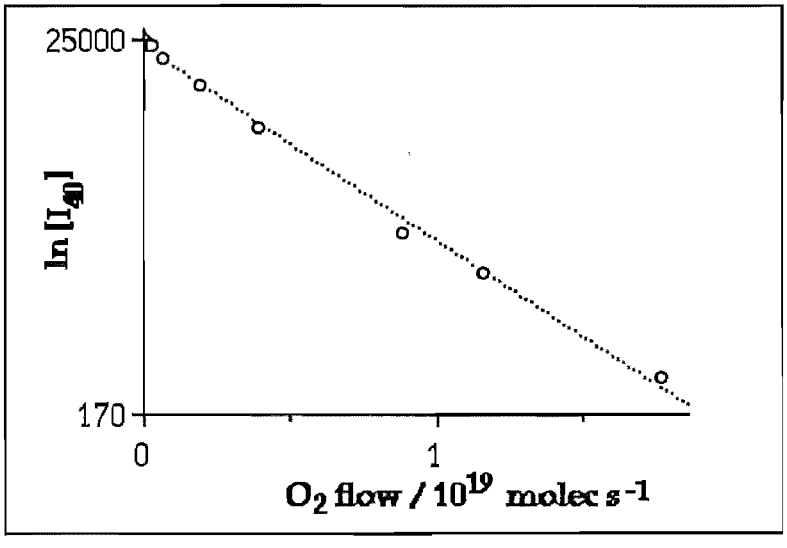

Figure 1.6: Semilogarithmic graph of ion signal decay versus reactant neutral partial pressure, in the case where the reactant ion signal comprises two forms of differing reactivity. The observed ion signal is the sum of two logarithmic decays and so does not display a linear relationship when graphed in this manner.

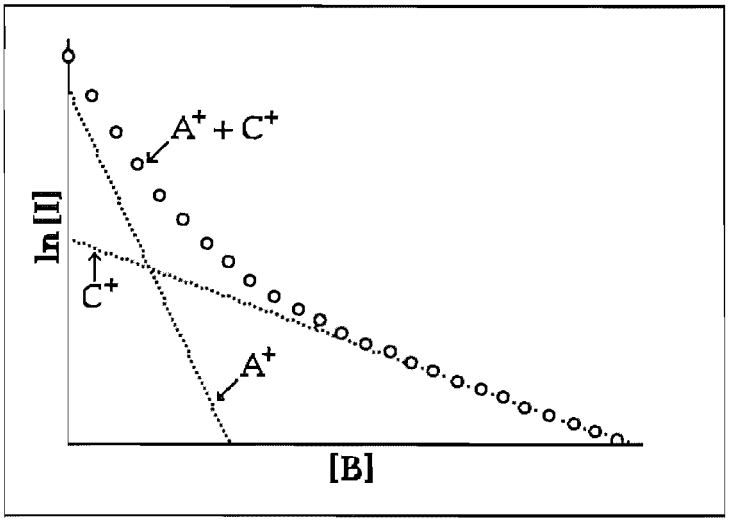

(a). The curved decay in this hypothetical example corresponds to reaction of two forms A^+ (which accounts for 76% of the total initial reactant ion signal) and C^+ (which accounts for the other 24%, and which reacts 6 times as slowly as A^+). The presence of such curvature may indicate isomerism, but can also arise when only one structure is present if a significant population of this form is vibrationally excited.

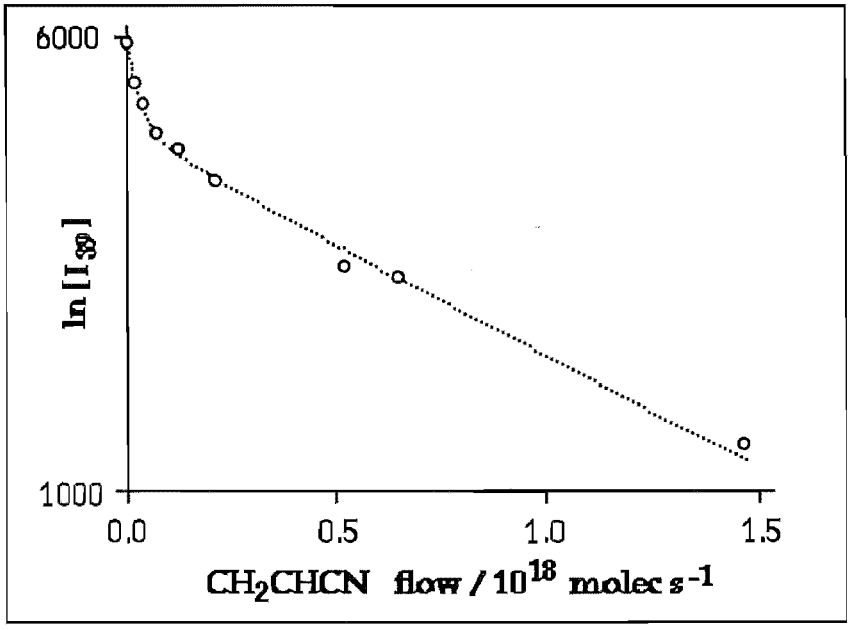

(b). Experimental decay curve observed for the reaction of $C_3H_3^+$ with CH_2CHCN. Two isomers of $C_3H_3^+$ react at distinctly different rates with CH_2CHCN: the curve fitted to the experimental data points describes the sum of two exponential terms, yielding $k = 3.97 \times 10^{-9}$ cm^3 $molec^{-1}$ s^{-1} for the more reactive $C_3H_3^+$ isomer (29% of the ion signal in this graph) and $k = 1.10 \times 10^{-10}$ cm^3 $molec^{-1}s^{-1}$ for the less reactive isomer.

mass flow of the buffer gas.[163] Each of these processes can give a curvature in results which appears suggestive of two ions of identical mass but differing reactivity. Curvature may also be exhibited if a secondary reaction or side reaction occuring in the tube generates a product ion of the same mass as the reactant ion A^+ being detected; or if the reaction under study has a termolecular mechanism (association reactions, for example:

$$A^+ + B + M \rightarrow AB^+ + M \qquad (1.38)),$$

and occurs more rapidly for **M** = **B** than for **M** = **X**, where **X** is the buffer gas being used. The nature of the curvature displayed by the last two processes is not so easily mistaken for differing reactivity of isomers.

Even in circumstances where the observed curvature is directly attributable to differing reactivity of two equal-mass ions A^+ and C^+, it does not follow that A^+ and C^+ are necessarily isomers. They may be ions of totally different general formula: for example, the m/z (29) signal produced from electron impact on 2-methyl propan-2-ol comprises $C_2H_5^+$ and CHO^+.[164] The ions A^+ and C^+ may differ only in their vibrational or electronic states: the ionisation process is sufficiently high-energy to permit the population of various excited states in many instances. Nevertheless, vibrational or electronic excitation of reactant ions is usually held to be unimportant for triatomic or larger species (which are, after all, the only species capable of exhibiting isomerism): triatomic species will generally have, at the energy of the excited vibrational state, a sufficiently high density of available vibrational / rotational states to make collisional relaxation by the buffer gas a facile process, and in a flow tube an ion will have several

thousand collisions with the buffer gas before entering the reaction region. Electronic excitation is more problematic, but the physical separation of the ion source from the flow tube means that, in a SIFT, sufficient time for electronic de-excitation has usually elapsed by the time the ion has reached the reaction region. Excitation should definitely be considered as a potential source of curvature in SIFT experiments, and every effort should be made to show whether any curvature exhibited is truly isomeric in origin and does not arise from some other process.

The low temperatures and pressures of interstellar clouds make them an ideal "breeding ground" for otherwise transient species: this is evident by the large number of radicals and molecular ions which have been detected in clouds (see table 1.2). It is logical, therefore, to expect that isomers which would (under terrestrial conditions) isomerise or tautomerise rapidly to more stable forms may exist as long-lived species within clouds. To date, the only vindication of this hypothesis is the widespread occurrence of both HCN and HNC in interstellar clouds. Other low-stability isomers such as H_2CC (vinylidene), HCOH (hydroxycarbene) and HCCNC (isocyanoacetylene) have been proposed as likely interstellar molecules[83,65] but have not yet been reported. A constant problem with the detection of such exotic compounds is the lack of laboratory measurements of their spectra: for this reason, the search for such isomers requires accurate spectra calculated by *ab initio* techniques.

Predictions concerning neutral isomers can be made upon the evidence of their ionic precursors, and thus there is some application of ion-molecule reaction measurements in this field. Differences in the reactivity of a pair of isomeric

ions can dictate the prospects for formation of related isomeric molecules. For example, if two ions XYZ^+ and XZY^+ are likely to be formed within interstellar clouds, and if XYZ^+ reacts with H_2 while XZY^+ is unreactive with H_2 and other common cloud constituents

$$XYZ^+ + H_2 \rightarrow XYZH^+ + H\cdot \qquad (1.39)$$

$$XZY^+ + H_2 \rightarrow \text{no reaction} \qquad (1.40)$$

then subsequent neutralization of $XYZH^+$ may yield the neutral XYZ while neutralization of XZY^+ (which, under cloud conditions, may be expected to occur predominantly by dissociative recombination) will most probably result in the breakage of an X–Z or Z–Y bond. Since with increasing molecular complexity the possibilities for the existence of two or more distinct isomers are enhanced, and since the reactive chemistry of any species is never entirely predictable (this thesis includes examples of unexpected consequences of isomerism for the ions CHN^+ and C_3N^+), experimental measurements are necessary to characterise the differences in reactivity of different isomers.

Section 1.6: Introduction to the present work.

The following nine chapters detail the results of experiments performed in the period from February 1987 to December 1990. I have endeavoured to stress the implications, of the present studies, for models of interstellar cloud chemistry.

Chapter Two offers a discussion of the experimental procedures used.

Chapter Three deals with the determination, by examination of proton-transfer kinetics, of the proton affinities (PAs) of C_2N_2 and C_4H_2. The study on C_4H_2 was originally carried out, to a large part, by John Knight[166] as a part of his Ph.D. research: I have thus dealt here only with measurements which were checked, or first performed, as a part of my own research. Some reactions of $C_2N_2^+$ with various neutrals are also reported in this chapter.

Chapter Four deals with investigations of isomerism in the ions C_2N^+ and C_3N^+. Most of the kinetic studies on C_2N^+ reactivity were performed by John Knight:[166] in consequence, I have concentrated here on the efforts which I made to interpret the observed isomeric ratios as a function of the techniques used to generate C_2N^+ in these experiments. John Knight also performed initial studies on C_3N^+ reactivity, which showed that two isomers of this ion exist under the conditions in the flow tube. In addition to a detailed examination of C_3N^+ isomerism, some reaction chemistry of the ion $C_4N_2^+$ is also reported.

Chapter Five deals with an investigation of isomerism in the ions CHN^+ and CH_2N^+. The existence of isomerism in these systems has been previously demonstrated by a variety of techniques, but the present work represents the first investigation into differences in isomer reactivity in these systems.

Chapter Six describes the reactivity of $C_3H_nN^+$ ions (n = 2 to 4), generated from acrylonitrile, with various neutrals. This work was undertaken to investigate

the chemistry of acrylonitrile within interstellar clouds. In addition, some reactions of ions with neutral CH_2CHCN were also performed.

Chapter Seven describes the reactivity of $H_nC_3O^+$ (n = 0 to 3) with various neutrals, and the implications of this reactivity for interstellar chemistry. In addition, the reactivity of $C_3O_2^+$ generated from carbon suboxide was also explored.

Chapter Eight explores the idea that kinetically-excited products of dissociative recombination reactions may be able to react with H_2 in cold interstellar clouds despite the fact that such reactions are inhibited by activation energy barriers.

Chapter Nine offers a comparison of the reactivities of the ion series $C_4H_n^+$, $C_3H_nN^+$ and $C_3H_nO^+$ with the neutrals H_2, CO, HCN and C_2H_2.

Finally, I discuss further work which could be undertaken to investigate some of the aspects left incompletely resolved by the present work.

CHAPTER 2.

EXPERIMENTAL.

Section 2.1: Equipment.

The measurements reported herein were obtained using a Selected-Ion Flow Tube originally constructed in this department during 1982 - 1985. Several modifications were made during the present work, in view of the projected conversion of the original SIFT into an instrument with variable-temperature and drift-region facilities. As a consequence, different versions of the instrument were used for different sets of experiments, as outlined below.

The measurements outlined in Chapters 3 and 4 were obtained principally upon the earliest working version of our SIFT. This instrument has been described previously by Knight[166] and by Knight et al[167] and will not be discussed extensively here. This version of the SIFT is illustrated in **figure 2.1**. A central feature of this version was the colinearity of the ion source chamber and the flow tube: in consequence, photons which were generated in the ionising process were able to traverse the entire axis of the ion source chamber and flow tube, and enter the detection chamber. The particle multiplier (PM), employed as the ion detection device, does not differentiate between ions and photons, and so was deployed in an off-axis configuration to minimise photon noise in the ion signal. Ions were deflected towards the PM by the application of a high positive voltage (+0.6kV) to the 'deflection electrode' situated approximately opposite the PM. A

consequence of this configuration was that the instrument was markedly mass-sensitive: ions having a higher mass were deflected less sharply (by the deflection electrode and by the high negative voltage (-2.6kV) applied to the PM) than were ions of comparatively low mass, and so heavier ions were detected less efficiently than ions having m/z <~ 50 amu.

The second working version of the SIFT, shown in **figure 2.2**, was used to obtain the measurements described in chapters 5, 6 and 7. Qualitative differences between versions are summarised in **table 2.1**.

Figure 2.1: Schematic diagram of Version 1 of the Canterbury SIFT (not to scale). The particle multiplier (PM) in this version of the SIFT was mounted off-axis to minimise photon noise from the ion source: ions were channeled to the PM by the application of a large positive voltage at the ion deflection electrode (IDE). The reactant gas inlets shown are of the 'finger' type: these were subsequently replaced by ring inlets.

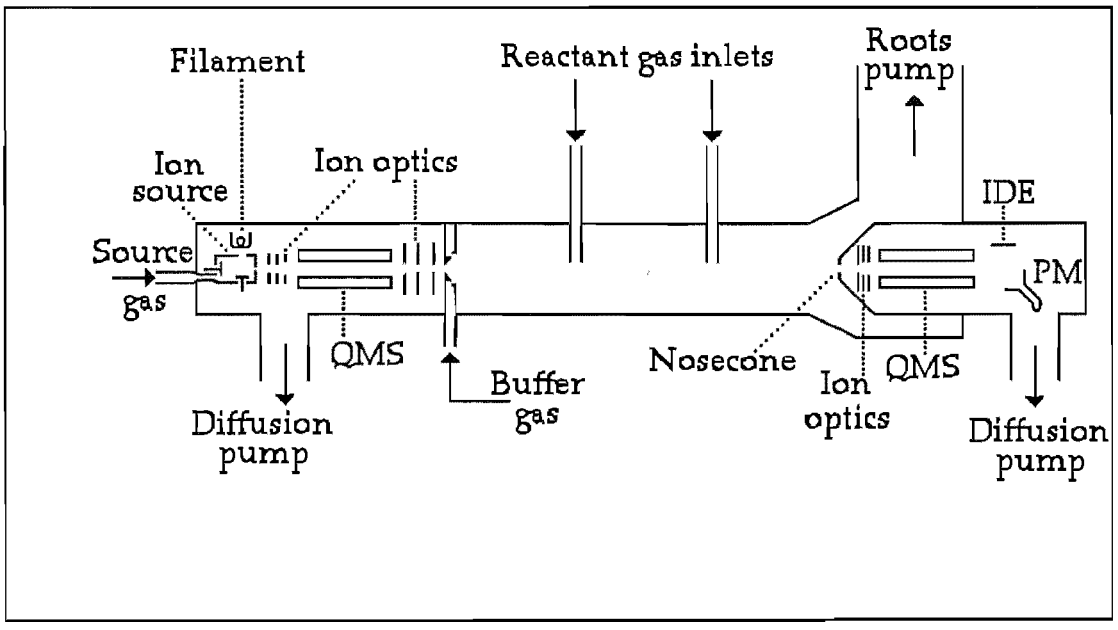

Figure 2.2: Schematic diagram of the Canterbury SIFT, Version 2 (not to scale). This version of the SIFT has an off-axis ion source chamber, and substantially modified upstream ion optics, ion source and Venturi orifice components. The position of the additional SIFT chamber, to be constructed, is shown: other projected modifications are the addition of a drift region and the incorporation of a variable-temperature facility.

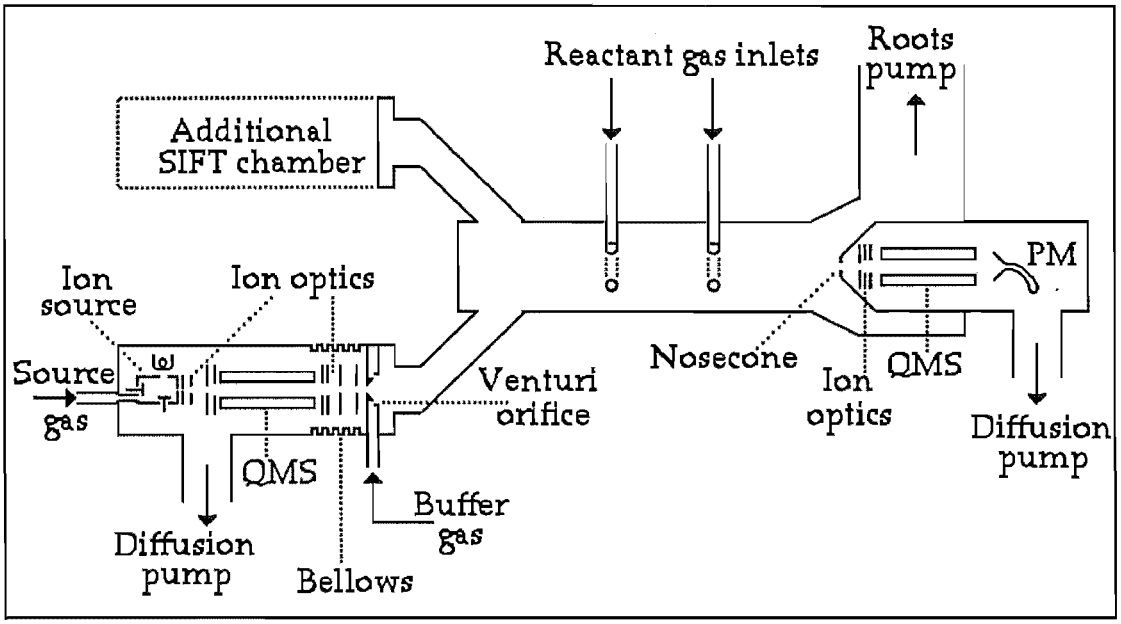

Table 2.1: A summary of differences between Version 1 and Version 2 of the Canterbury SIFT.

Version 1	Version 2
Low-pressure ion source, collinear with the flow tube axis.	High-pressure ion source, displaced off the flow tube axis.
Electrostatic lenses within ion source chamber configured as shown in reference 166.	Electrostatic lenses within ion source chamber designed using the SIMION program: configured as shown in figures 2.3, 2.4 and 2.6.
Finger-type reactant neutral inlets.	Ring-type reactant neutral inlets.
Particle multiplier (PM) displaced off flow tube axis; ion deflection electrode employed to divert ions towards PM.	PM collinear with flow tube axis; no deflection electrode necessary.

The SIMION electrostatic lens analysis program[168,169] was used to redesign the lens assemblies associated with the upstream quadrupole mass spectrometer. The lens assemblies SIFT1 and SIFT2, shown in **figures 2.3** and **2.4**, are the results of this analysis. SIFT1 is the design for the lens assembly to train the ions ejected from the ion source into the quadrupole field; SIFT2 focusses the ion beam emerging from the QMS into the Venturi inlet at the entrance of the flow tube. All lenses used in these designs are planar ring lenses, except for L6 for which a cylindrical lens appeared more effective. The lens assemblies actually constructed differed from the configurations shown, since mechanical limitations prevented the incorporation of lens L10 into the SIFT2 assembly. SIFT1 was not fabricated as a single assembly: instead, lenses L1 and L2 were attached to the ion source assembly, while the remaining lenses were mounted on the quadrupole filter anterior endplate. Because of the lack of physical connection between L2 and L3, the spacing between these lenses was variable - in practice, it was found that better ion signals were obtained when this spacing was reduced below the distance specified by SIMION. In addition, the lens L5 was eventually removed from the assembly with no visible impairment to the resulting ion signal.

The trajectory of an ion within the lens assembly is dependent upon the contours of the electric field within the assembly, the ion's initial energy, initial position and initial direction. Trajectory calculations were performed using SIMION, with a 'family' of ions used to approximate the range of trajectories likely to be focussed favourably by the lens configuration. **Figure 2.5** illustrates the passage of one such ion family through the lens assembly SIFT2. These calculations were used to determine approximately the optimum voltage settings for the

Figure 2.3: Redesigned ion optics, upstream of UQMS.

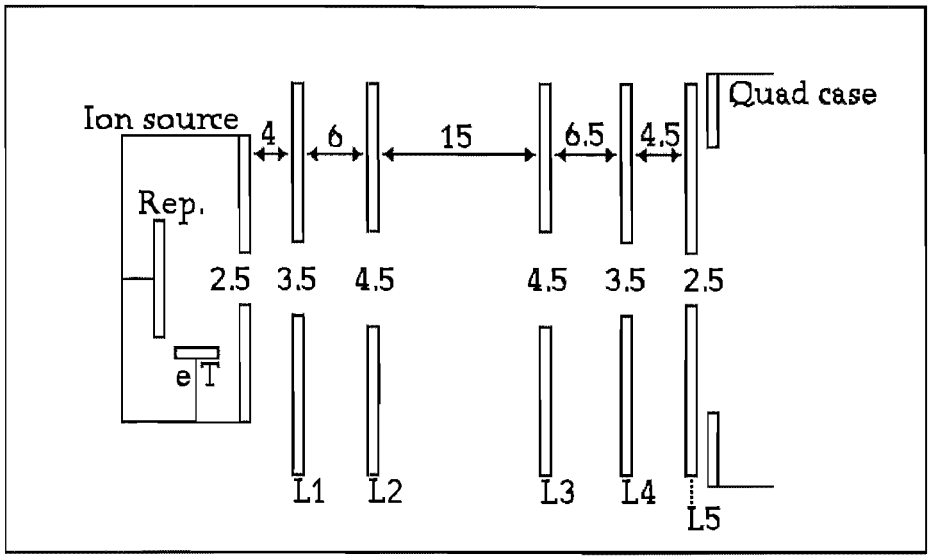

(a). Optics designed using SIMION program. The vertical scale of this diagram is twice the horizontal scale. Lens spacings are indicated by figures associated with arrows: lens apertures are indicated by isolated figures (All distances are in mm). (Rep. = repeller; eT = electron trap).

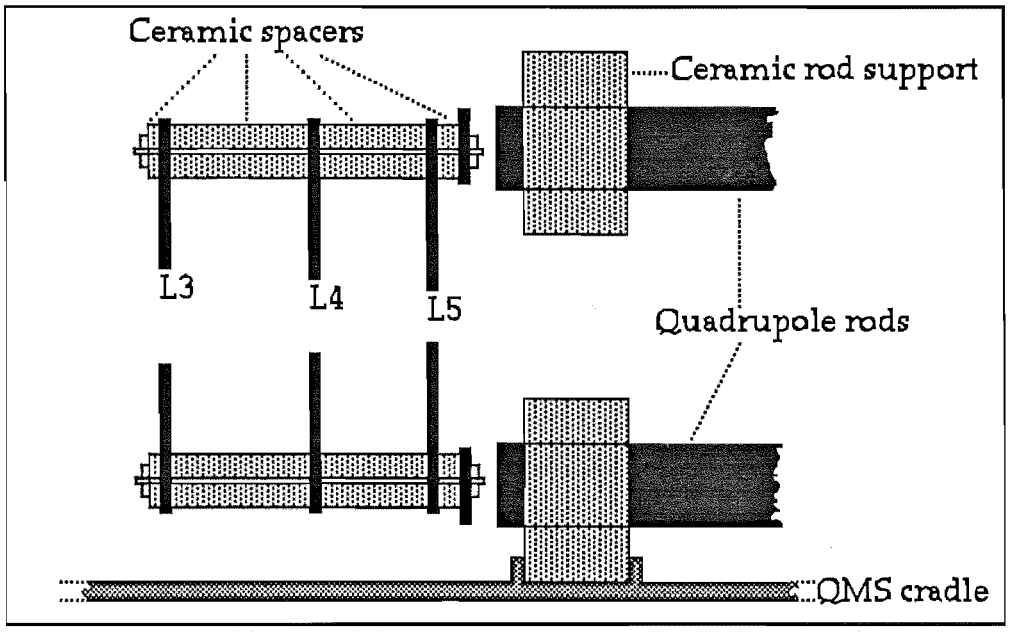

(b). The lens assembly comprising lenses 3,4 & 5, attached upstream of the ion source quadrupole. The assembly is fastened to the ceramic rod support by bolts (not shown) attached to the quadrupole endplate. Electrical connections to the quadrupole rods and to the lenses are not shown.

Figure 2.4: Redesigned ion optics, downstream of UQMS.

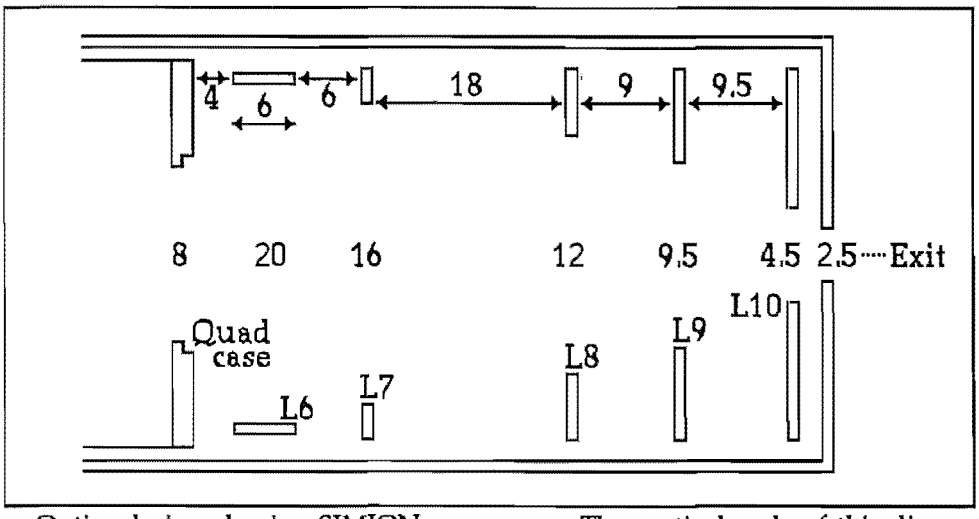

(a). Optics designed using SIMION program. The vertical scale of this diagram is twice the horizontal scale. Lens spacings are indicated by figures associated with arrows: lens apertures are indicated by isolated figures (All distances in mm).

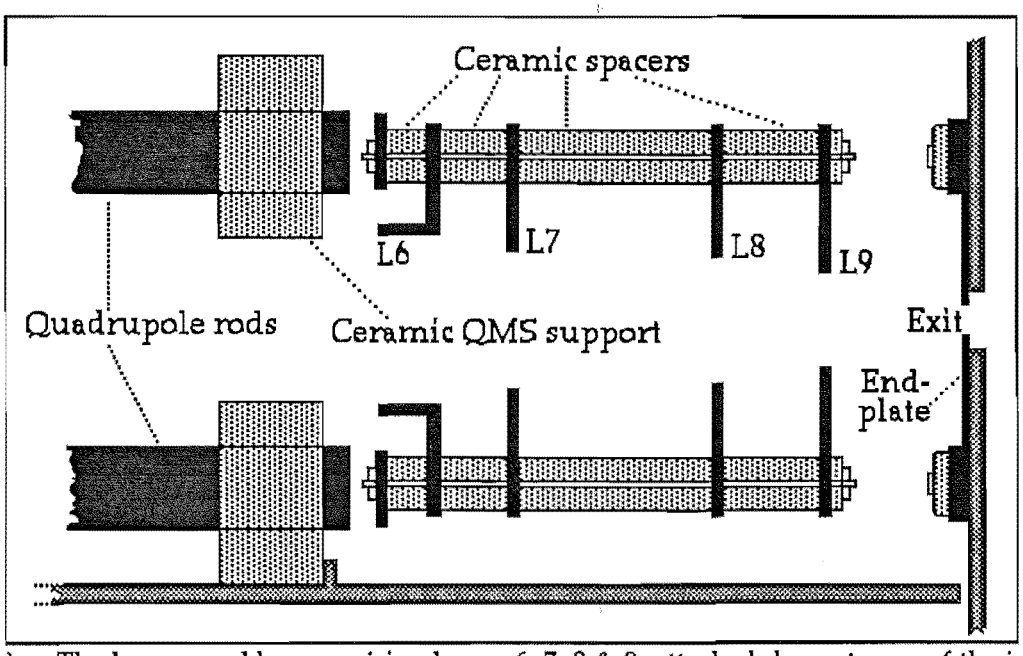

(b). The lens assembly comprising lenses 6, 7, 8 & 9, attached downstream of the ion source quadrupole. Lens 10 cound not be incorporated into the assembly due to mechanical limitations. Electrical connections to the quadrupole rods, the exit disc and the lenses are not shown.

Figure 2.5: Voltage contours and ion trajectories for the SIFT2 lens assembly, calculated using the SIMION program, for a repeller voltage of 50V. The red curves in the upper diagram show the voltage contours (10 V spacings), while the blue curves in the lower diagram illustrate the calculated efficiency of ion transmission at this voltage setting.

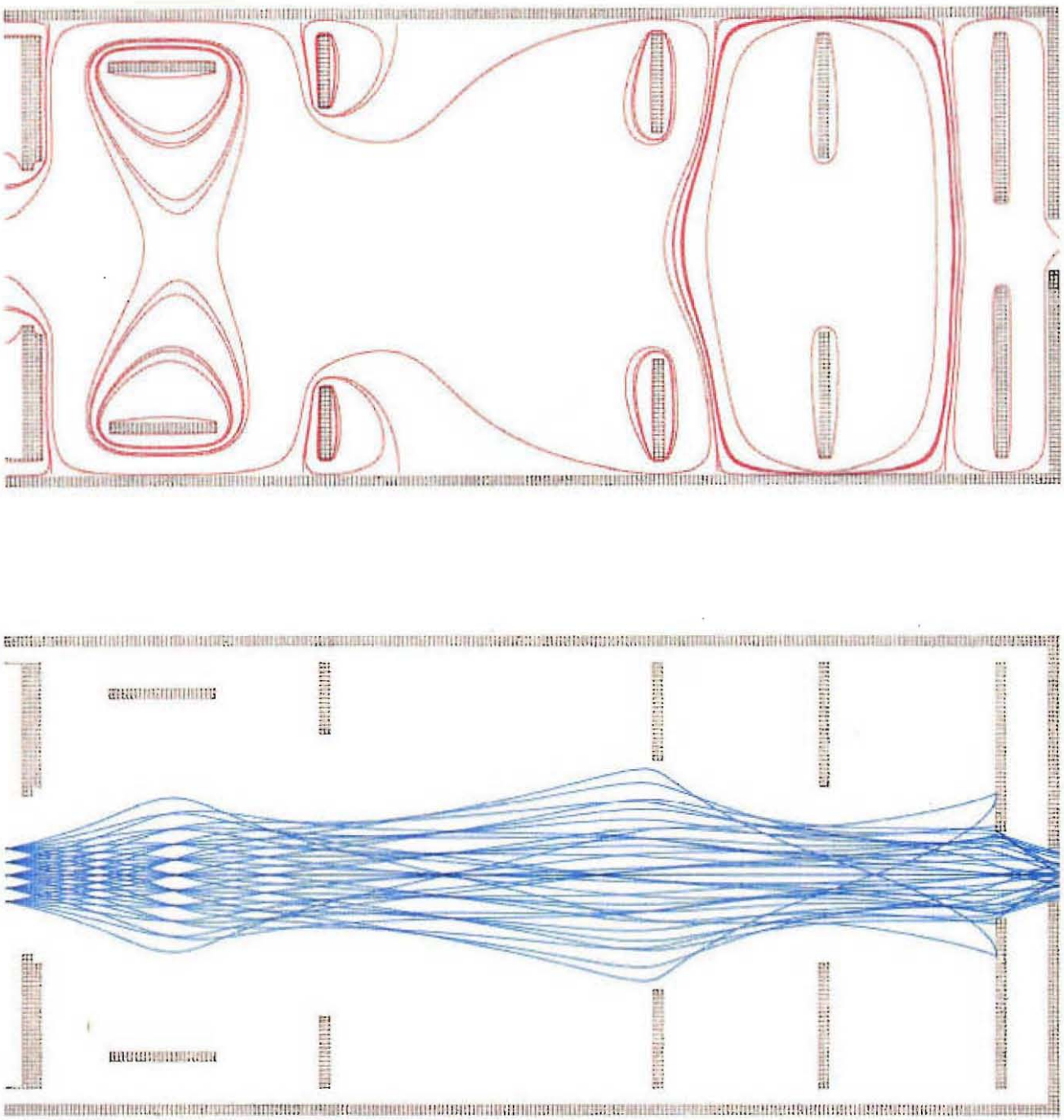

SIFT1 and SIFT2 assemblies. These calculated optimum settings are shown in **table 2.2**, in conjunction with the experimental optimum determined for a repeller setting of +10 V. It can be seen that the calculated and experimental optima do not agree closely, but this is not surprising given the differences between the designed assemblies and those constructed - principally, as mentioned previously, the exclusion of lens L10 in the experimental assembly. **Table 2.3** presents a more comprehensive display of optimum settings, for repeller voltages from +10 to +65 V, in the absence also of lens L5 (as mentioned above).

Table 2.2: Calculated optimum lens settings for repeller voltages of 10, 20 and 50 V. These settings were determined from trajectory calculations performed using the SIMION ion-optics design program. The experimental optimum found for a repeller setting of 10 V is shown also: differences between the calculated and observed optima may arise from differences in the constructed and designed ion optics assemblies.

Repeller voltage	10 V [a]	10 V [b]	20 V [a]	50 V [a]
Electron trap	5	7.5	10	20
L1	-50	-72.2	-100	-200
L2	3	3.0	12	23
L3	6	1.2	15	30
L4	-30	-66.7	-90	-50
L5	2	-13.5	5	5
Quad case	-5	0.0	-5	-5
L6	10	11.4	30	90
L7	-15	-85.9	-12	-6
L8	5	0.7	18.8	55
L9	-40	-171.4	-50	-60
L10	4	– [c]	15	42
Exit lens	0	1.4	0	0

Notes
a. Calculated lens voltage settings for this repeller voltage.
b. Observed optimum lens settings at 10 V repeller setting.
c. This lens was not constructed due to mechanical limitations.

In practice, optimum voltages applied to the lenses are larger in magnitude than those determined using SIMION. The observed ion signal is much more sensitive to the voltages on the repulsive lenses (to which positive voltages are applied) than to the settings on the attractive (negative) lenses. For example,

Table 2.3: Variation in optimum lens settings and observed ion currents with repeller voltage. All readings were made at an electron energy setting of 21.4 V, using argon as the ion source gas. The background pressure in the ion source chamber was 2.7×10^{-6} Torr (in absence of argon); when Ar was added, a pressure of 4.5×10^{-5} Torr was noted; the total pressure in the ion source chamber was 1.2×10^{-4} Torr - this includes an effect from the backstreaming of He buffer gas through the Venturi orifice. The ion signals recorded were due to Ar^+, selected at m/z 40.0 with the upstream QMS resolution set to 2.0 and the downstream QMS resolution at 8.0. In practice, the readings for the flow tube exit disc current and particle multiplier signal were obtained on a separate occasion, since the probe employed upstream resulted in a loss in ion transmission to these sites. The readings for the exit disc current and the PM signal have been adjusted to take into account minor differences in the ion source transmission characteristics on these two occasions: at a low repeller voltage especially, the focussing conditions can change due to oxidation of the lens surfaces.

Repeller voltage	10 V	20 V	35 V	50 V	65 V
Electron trap	5.2	10.2	15.0	30.0	45.0
L1	-80.0	-105.6	-100.6	-135.6	-180.7
L2	3.6	2.3	2.5	3.9	2.5
L3	1.1	1.0	1.0	1.2	1.2
L4	-129.6	-94.5	-139.3	-148.4	-204
L6	0.7	2.2	41.0	59.4	75.4
L7	-200	-198	-204	-199	-199
L8	0.4	1.6	11.7	14.9	21.3
L9	-116.7	-160.7	-132.3	-182.9	-200
Exit lens	0.4	0.7	0.6	7.9	11.6
Filament current	2.69 A	2.69 A	2.68 A	2.69 A	2.69 A
Emission current	237 nA	233 nA	237 nA	239 nA	238 nA
Exit lens current	2.1 nA	17.1 nA	52.8 nA	60.0 nA	56.0 nA
Probe current [a]	26 pA	192 pA	260 pA	320 pA	260 pA
Flow tube exit disc current	~ 0.1 pA	1.6 pA	2.3 pA	2.5 pA	2.3 pA
Particle multiplier signal	470 cps	2427 cps	3528 cps	3299 cps	3456 cps

Notes

a. Circular fine wire mesh probe, inserted 80.0 cm upstream of the flow-tube exit disc. A voltage bias of -2.74 V was applied to attract ions onto the probe. The same voltage was subsequently applied to the flow tube exit disc.

a small change (± 2 V) in the voltage on the attractive lens L8 may diminish the signal by a factor of 10, while a large change (± 50 V) on the repulsive lens L7 may have a negligible effect.

Trajectory calculations from SIMION show that the calculated optimum voltages do not result in substantial deceleration of the ions. The initial ion energy is largely determined by the voltage applied to the repeller. The large voltages commonly employed are likely to have an accelerating effect, so that the ions leaving the ion source chamber have high translational energy. Observations which verify this are the common occurrence of lower-mass ion signals due to breakup of the ion selected by the upstream QMS

$$C_2H_5^+ \rightarrow C_2H_3^+ + H_2 \qquad (2.1)$$

$$C_2H_5OH_2^+ \rightarrow H_3O^+ + C_2H_4 \qquad (2.2a)$$

$$\rightarrow C_2H_5^+ + H_2O \qquad (2.2b)$$

$\Delta H_{2.1} = +210$ kJ mol^{-1}

$\Delta H_{2.2a} = +136$ kJ mol^{-1}

$\Delta H_{2.2b} = +153$ kJ mol^{-1}

and the observation of proton transfer in the reaction

$$ArH^+ + He \rightarrow HeH^+ + Ar \qquad (2.3)$$

$\Delta H_{2.3} = +193$ kJ mol^{-1}.

These processes, which usually result in less than 10% depletion of the primary reactant ion signal, are all highly endothermic: they appear due to collision of

translationally (and internally) excited ions with the helium buffer gas, since they are impeded by a reduction in the magnitude of the voltages applied to the electrostatic lenses. Alternatively, the observed breakup could be occurring within the ion source chamber after passage through the QMS. In practice, this phenomenon is usually of minor concern since repeated collision with helium will thermalise all translationally hot ions before these ions can encounter neutral reactants: thus the translational excitation should not affect the observed chemistry beyond the possibility of misinterpreting products from breakup ions as minor products from the reaction of the ion of interest.

Figure 2.6: Schematic diagram of the ion source assembly (not to scale). This high-pressure ion source was used in the majority of reaction studies reported in this work, following replacement of the earlier ion source assembly. Pressures attained within the ion source during operation are thought to be of the order of 1 to 10 Torr; the chamber containing the ion source is maintained at approximately 10^{-4} Torr during normal operation. L1 and L2 are electrostatic lenses: electrical connections to these lenses are not shown.

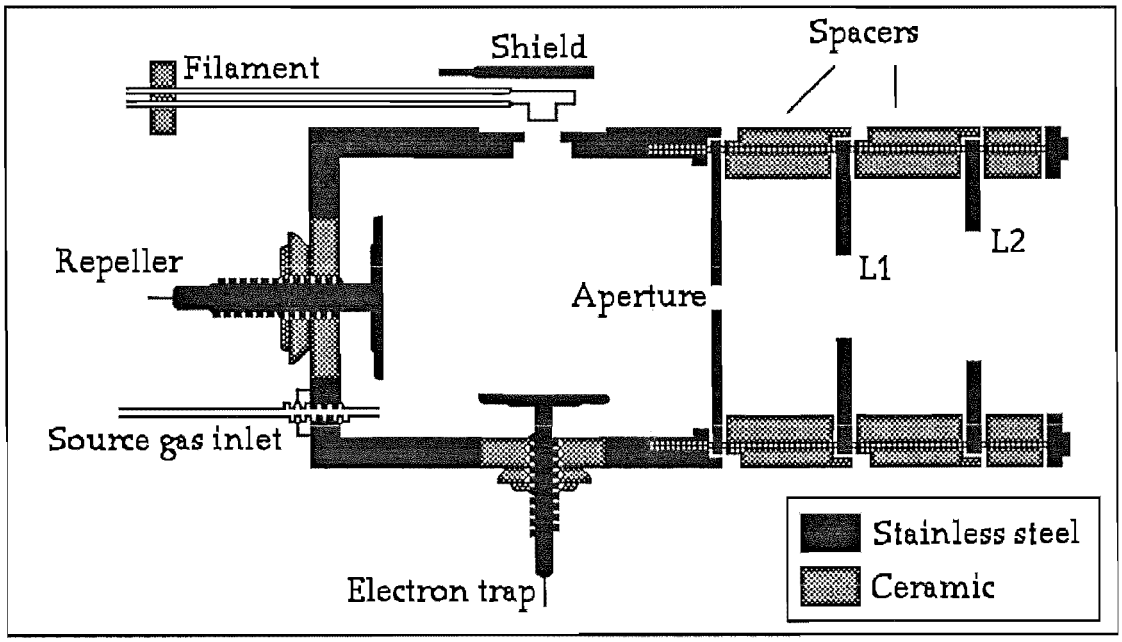

The variation in observed ion signal intensity with tube pressure is recorded in **table 2.4.** These results show that, for the probe situated 80 cm upstream from the flow tube exit disc, the maximum signal intensity is observed at a buffer gas pressure of ~0.35 Torr. This is contrary to expectation: ion loss through diffusion is less at higher tube pressure, so the observed ion signal should increase steadily with pressure. It is likely that, at high tube pressures, laminar flow of the buffer gas has not been reached at this distance: a greater degree of turbulence in the buffer gas from the Venturi nozzle injection would account for the diminished signal with increasing pressure. The suspicion of turbulence at this distance led to a relocation of the upstream reactant neutral inlet (portal 1): this inlet was repositioned at a distance of 66 cm upstream from the flow tube exit disc, to isolate it from the region of suspected turbulence. In practice, all the

Table 2.4: Variation in observed ion currents with tube pressure. All readings were made under the conditions detailed in table 2.3, using the lens settings for a repeller voltage of 20 V.

Pressure [a,b]	Q_{He} [a,c]	I_{ex} [a,d]	I_{probe} [a,e]	I_{disc} [a,f]	I_{pm} [a,g]
0.162 ± 0.002	45.6 ± 1%	12.2 ± 0.2	69 ± 2	<0.1 ± 0.2	5 ± √I
0.183	57.4	12.4	90	<0.1	36
0.225	80.0	11.2	118	0.2	254
0.265	99.6	11.0	132	0.6	737
0.305	122.2	10.1	130	1.0	1274
0.347	142.3	9.9	153	1.6	2026
0.389	164.9	8.9	138	2.2	2704
0.430	186.7	8.7	125	3.0	3239
0.448	195.4	9.0	114	2.7	3412

Notes

a. Uncertainties for each measurement appear at the top of each column.
b. Tube pressure, in Torr, of He buffer gas.
c. Helium flow in $cm^3\ s^{-1}$ at STP.
d. Observed ion current, in nA, on the ion source chamber exit lens.
e. Observed current, in pA, on ion probe inserted 80.0 cm upstream of flow tube exit orifice.
f. Observed current, in pA, on flow tube molybdenum exit disc.
g. Observed ion signal, in counts per second, from the particle multiplier.

rate measurements reported in this work were obtained at a tube pressure of 0.30 Torr, and usually involved addition of the reactant neutral at portal 2 (further removed than portal 1 from the region of suspected turbulence), so the effects of this turbulence are expected to be negligible. The low ion signal recorded at this probe at high tube pressure could also arise through a change in the optimum settings required in the ion source lens assemblies, due to more efficient braking of the ions by helium backstreaming into the ion source chamber from the Venturi orifice. This possibility was excluded since refocussing of the ion source lenses at a higher pressure could not improve the ion signal recorded on the probe. Thus, helium backstreaming has little effect on the ion transmission through the ion source chamber under these conditions. This is corroborated by the similarity seen in settings required for transmission of Ar^+ (m/z 40), N^+ (m/z 14) and He^+ (m/z 4): under low pressure conditions, these ions should all be focussed similarly by the same lens settings. In practice, different optimum settings were determined for these ions, but the differences were slight - all of these ions were focussed well by the optimum settings determined for He^+, and refocussing for N^+ and for Ar^+ resulted in only a small (< 20%) improvement in the ion signal observed for these ions. The signal observed at the flow tube exit disc, and at the particle multiplier, is seen to increase steadily with pressure, as expected: diffusive loss should decrease as the pressure increases.

Another modification to the original version of the SIFT was the replacement of the finger-type reactant neutral inlets with ring-type inlets, since such inlets were found by Upschulte et al.[159] to have a lower end correction than radial, spiral or finger inlets. The new inlets were constructed as shown in figure 3 in reference

159. The end corrections for these inlets were determined using the reaction of Ar^+ with O_2

$$Ar^+ + O_2 \rightarrow O_2^+ + Ar \qquad (2.4)$$

$$k_{2.4} = 4.5 \times 10^{-11} \text{ cm}^3 \text{ molec}^{-1} \text{ s}^{-1}$$

as a calibration reaction. Experiments were performed for a range of tube pressures from 0.22 to 0.38 Torr. Over this pressure range the rate coefficients $k_{2.4}$ determined for portal 2 (z_2 = 42.9 cm, where z is the actual distance from the neutral inlet to the SIFT exit disc) were independent of pressure and dictated an end correction of +1.8 cm, yielding an effective reaction distance z_2(eff) of 44.7 cm. The results for portal 1 were substantially more erratic: rates observed using the true distance z_1 = 70.9 cm were 20% too high, indicating a larger (and negative) end correction for this reaction distance. The observed behaviour for portal 1 most probably arises from turbulence in the region slightly upstream from this inlet: for this reason, portal 1 was not commonly used to determine rate coefficients, although it was routinely used to add various neutrals when it was desirable to effect an additional reaction in the tube prior to the reaction of interest.

No substantial changes were made to the neutral reactant glass handling line. The needle valve associated with portal 1 (in Version 1) was replaced, for greater flow sensitivity, by a variable leak valve of the same type as that used for portal 2. The variable leak valve associated with portal 2 was subsequently reconfigured in a manner illustrated in **figure 2.7**. This was done because of a phenomenon which was especially apparent when studying a fast reaction involving a 'sticky'

neutral reactant such as H_2O, NH_3 or HCN: for such reactions, a long time delay (often of up to two minutes) was apparent after reduction of the reactant neutral flow, before stabilisation of the reactant ion signal. This time delay could not be effectively reduced by changing the helium flush setting, and it was eventually decided that the delay arose because of the presence of a large 'dead volume' of gas which was not effectively swept out by the helium flush. Rearrangement of the tubing leading to and from the leak valve was performed as shown, and this rearrangement resulted in a reduction of the time delay to a much more acceptable interval of around five seconds.

Figure 2.7: The reconfiguration of the variable leak valve associated with portal 2. The diagram on the left illustrates the configuration used in Version 1 of the Canterbury SIFT: note that, following passage through the sapphire seat valve (in black), the reactant gas is admitted to a large dead volume before it encounters the helium flush. The arrangement shown on the right is that used in Version 2, so as to minimise the size of the dead volume after the sapphire seat valve.

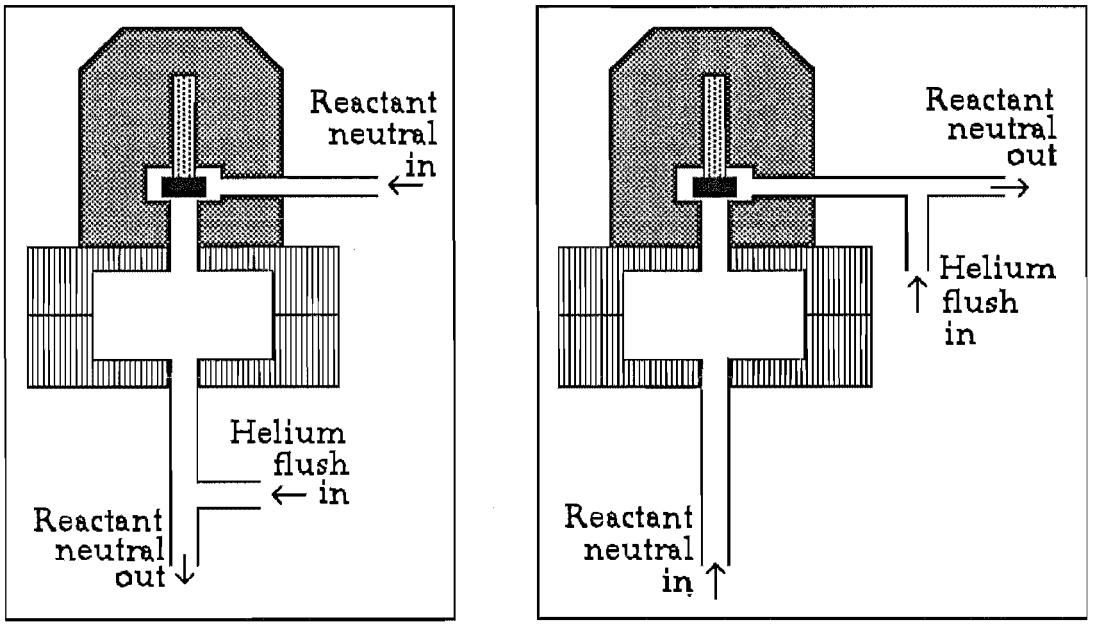

Other features of the instrumentation and equipment of the Canterbury SIFT are as detailed previously[166,167] and will not be described here.

Section 2.2: Data acquisition and analysis.

Data was gathered in a manner similar to that detailed by Knight[166]. The concentration of neutral reagent molecules within the tube was determined by using a pressure transducer to monitor the change in pressure, as a function of time, in the glass manifold (of known volume) of the gas inlet line. The changing pressure was recorded by an Apple IIe computer using an A/D converter. A program, 'Pressmonitor' (see **appendix 1**), was used to record the pressure. The reactant and product ion signals were recorded manually.

Following data collection, reaction rates were determined using a suite of programs connected by the menu program 'Options'. A program 'Meanflows' was used to convert the raw flow file from 'Pressmonitor' into a data file containing the averaged flow measurements in Torr s^{-1}, and the signals (in counts per second) recorded at each flow for each of the ions of interest. Analysis of the data file by the program 'Rascal' yielded a calculated reaction rate and a graph illustrating the fit of the calculated rate to the observed experimental data. The rate coefficient was corrected using the expression

$$k_{corr} = \frac{k}{C_2 (1 - \varepsilon)} \frac{\omega}{\gamma} \qquad \{2.i\},$$

in which C_2 is the radial diffusive correction, $(1 - \varepsilon)$ is the correction for axial diffusive loss and $\frac{\omega}{\gamma}$ is the correction for non-uniform velocity. These factors may be expressed:[159]

$$C_2 = 1 - \frac{2D^2 j_o^2}{r^2 v_{ion}^2} + \frac{6D^4 j_o^4}{r^4 v_{ion}^4} + \ldots \qquad \{2.ii\},$$

where r is the tube radius in cm, v_{ion} is the ion's velocity in cm s^{-1}, $j_o = 2.405$ [159] and D is the diffusion coefficient

$$D = 0.02354\, K_o \left(\frac{760}{P}\right) \left(\frac{T}{273.16}\right) \qquad \{2.iii\},$$

for pressure, P, in Torr and temperature, T, in degrees K; D is calculated using

$$K_o = 31.11 \sqrt{\mu} \qquad \{2.iv\}$$

(where μ is the reduced mass, in g mol^{-1}, of the ion in the relevant buffer gas) to determine the reduced mobility K_o.

$$\varepsilon = \left(\frac{\delta}{\omega r^2} + \frac{\gamma}{\omega} \frac{k[B]}{D}\right) \frac{D^2}{v_{gas}\, v_{ion}} \qquad \{2.v\},$$

for which k is the uncorrected rate coefficient for the reaction concerned in cm^3 $molec^{-1}$ s^{-1}, [B] is the neutral concentration in molec cm^{-3} and ω has the value

$$\omega = \frac{2}{1 + \frac{5.52\lambda}{Pr}} \qquad \{2.vi\},$$

where λ is the mean free path length (in cm) of the ion in the buffer gas at a background pressure of 1 Torr:

$$\lambda = 8.59\,\eta\sqrt{\frac{T}{m_{He}}} \qquad \{2.vii\}$$

for helium buffer gas, where η is the viscosity of the buffer gas. The eigenvalues γ and δ can be solved as detailed elsewhere; [171,172] using the expressions detailed above, for the reaction of $Ar^+ + O_2$, the correction factors have the values

$C_2 = 0.99038$

$(1 - \varepsilon) = 0.9940$

and $\frac{\omega}{\gamma} = 1.5469.$

A typical printout from the 'Rascal' program is given in **figure 2.8**. The 'Rascal' program additionally used, for each experimental run, a format file which listed the values of variables appropriate to the experiment: the date, reactant neutral inlet used, temperature, buffer gas pressure etc. This format file could be modified as required within the 'Rascal' program or created using a file editing program 'Studyfiles', which could also be used to edit the data files to be used by 'Rascal'. A further program, 'Prod rat', was used to produce a graph, from the data file, of the experimental product distribution. For reactions for which isomerism in the reactant ion signal was evident as discussed in section 1.5,

Figure 2.8: A sample printout from the "Rascal" computer program.

```
RATE COEFFICIENT:
---- -----------

C++02.13/6/89.R1                m/z = 12
Date: 13/6/89              Run #1          Data file C++02.13/6/89.R1
(CALIBRATION RXN)
T = 299.8 K                     P = .298 Torr of HE (Tylan flow = 256)
Portal 2                   Neutral vol = 143.6 cm^3
Corrected reaction distance = 42.9 cm

Neutral flow    ;   Ion signal
  (torr/s)      ;
----------------;----------------
   0            ;     2973
   .0653499999  ;     359
   .04471       ;     712
   .02899       ;     1132
   .01523       ;     1952
   5.696E-03    ;     2554
   0            ;     3499

k          = 6.43972645E-10
k (corr)   = (1.002 +/- .0296)E-9cm^3 molec^-1 s^-1

Intercept = 8.064 +/- .0323 ln. counts
          = 3178 +/- 101 ion counts
```

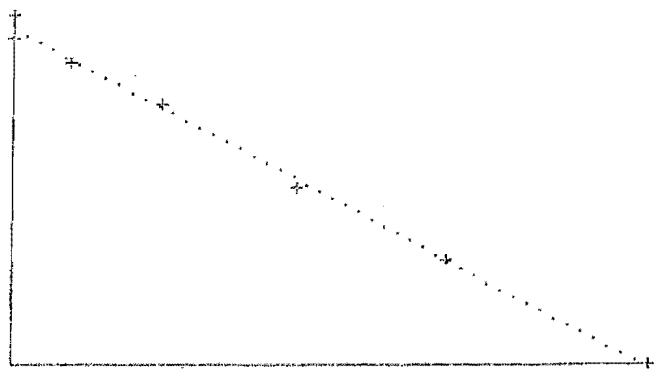

multiple exponential decays could be fitted to experimental data using the program 'Mule' which was adapted from the program 'Expon'[173] to also show a graph illustrating the fit of the calculated decays to the experimental results. Collision rate coefficients, which were calculated according to the ADO method of Su and Chesnavich,[174] were determined using the program 'Collirat'.

These programs are all listed in Appendix 1.

Section 2.3: Reagents and physical conditions.

Reagents used are as described previously,[166] with the following exceptions:

$C_4H_2O_2Cl_2$, fumaroyl dichloride (95%), was obtained from Aldrich.

$(CH_2CHCO)_2O$, acrylic anhydride (98% by ^1H nmr), was provided by Ryan Bettens at Monash University.

HCN, hydrocyanic acid, was produced in vacuo by the addition of KCN (Fluka, 98-99% cyanide) to 100% orthophosphoric acid.[175]

H_2S, hydrogen sulphide, was synthesised by the action of orthophosphoric acid upon sodium suphide ($Na_2S.xH_2O$, BDH, 30% Na_2S), according to the method of Melville and Gowenlock.[175]

C_3O_2, carbon suboxide, was produced by the action of phosporus pentoxide (Riedel - de Haën, 99+%) upon malonic acid (Riedel - de Haën, 99+%) upon heating, according to the methods of Miller & Fately[176] and Kim & Roebber.[177] Since C_3O_2 was used only as an ion source gas and not as a neutral reactant, it was not rigorously purified.

CH_3C_3N, methyl cyanoacetylene, was synthesised by the successive action of aqueous ammonia and phosphorus pentoxide upon methyl 2-butynoate ($CH_3C{\equiv}CCO_2CH_3$, Aldrich, 98%), according to the method of Durrant et al.[178]

C_4N_2, dicyanoacetylene, was synthesised by the action of ammonium hydroxide upon dimethyl acetylenedicarboxylate ($CH_3O_2CC{\equiv}CCO_2CH_3$, Aldrich, 99%), followed by heating in calcined sand, according to the method of Khanna et al.[179]

C_2H_2, acetylene, was obtained as instrument grade from NZIG and was further purified by vacuum distillation.

CO_2, carbon dioxide, was obtained from the sublimation of commercially-available dry ice and was further purified by vacuum distillation.

Kr, krypton (>99.9%) was obtained from Airco.

CH_3Cl, chloromethane (Industrial grade), was obtained from Virginia Chemicals.

CH_2CHCN, acrylonitrile (99+%), was obtained from Ajax Chemicals. To prevent poymerisation in the absence of air, a trace of the radical scavenger p-methoxy phenol was added.

CCl_4, carbon tetrachloride, was obtained from Riedel - de Haën (99+%) and from BDH (99.5%).

CF_4, carbon tetrafluoride, was obtained from Matheson Gas Products.

SF_6, sulphur hexafluoride (Instrument grade), was obtained from Air Products.

CF_3Br, bromotrifluoromethane, was obtained from Matheson Gas Products.

$CHCl_3$, chloroform, was obtained as solvent grade and was additionally purified by vacuum distillation.

$C_5H_5NO_2$, 1-amino-2-methoxy-cyclobutenedione, was prepared by the successive action of aqueous silver nitrate, methyl iodide and aqueous ammonia upon 3,4-dihydroxy-3-cyclobutene-1,2-dione (Aldrich, 98%), according to the method of Cohen and Cohen[180] and was purified by recrystallisation.

NH_2CN, cyanamide (99+%), was obtained from Aldrich.

C_2Cl_4, tetrachloroethylene (AR grade), was obtained from BDH.

C_6H_{10}, cyclohexene (99+%, stabilised with 0.05% hydroquinone), was obtained from Merck.

C_7H_8, toluene, was AR grade.

NO, nitric oxide (CP), was obtained from Matheson and was additionally purified by vacuum distillation.

$C_6H_5NH_2$, aniline (99%) was obtained from Aldrich.

CH_3CCH, propyne, was prepared according to the method of Brandsma.[181]

In all instances unless otherwise mentioned, measurements were made using helium (Technical or Instrument grade, stated purity 99.9%, obtained from NZIG) as the buffer gas at a pressure (within the flow tube) of 0.300 ± 0.005 Torr, at a room temperature of 300 ± 5 K. Neutral reactants were typically added at portal 2; ion source gases were added to the ion source at a pressure estimated to exceed 1 Torr in some circumstances. The pressures within the ion source chamber and the ion detection chamber (which were differentially pumped) were monitored by ion gauges and typically did not exceed 10^{-4} Torr and 10^{-5} Torr respectively. Exceptions to these conditions are identified within the text where appropriate. Other conditions are as described previously.[166] Except where otherwise stated, rate coefficients are quoted from the compilations of Anicich and Huntress[182] and Viggiano et al;[183] thermodynamic quantities (ΔH and ΔG, using the "ion convention"[184]) at 298K have been obtained from the compilations of Lias and co-workers.[184,185] Dipole moments have been obtained

from the C.R.C. Handbook of Chemistry and Physics;[186] polarisabilities have been obtained from Atkins[187] or Hirschfelder et al,[188] or calculated using the method given in the latter text.[188] Rate coefficients determined in this work are considered to have an uncertainty of ± 25%; product distributions are estimated to have an uncertainty of ± 15%.[166]

CHAPTER 3.

PROTON AFFINITY OF C_4H_2 AND C_2N_2.

Section 3.1: Determination of proton affinity by equilibrium measurements.

The proton affinity (PA) of a species **X** is a measure of the stability of the protonated species XH^+, and is defined as

$$PA\ (X) = \Delta H^\circ_f\ (X) + \Delta H^\circ_f\ (H^+) - \Delta H^\circ_f\ (XH^+) \qquad \{3.i\}.$$

It can be seen that PA(**X**) is the enthalpy change in the reaction

$$XH^+ \rightarrow X + H^+ \qquad (3.1).$$

Direct experimental study of such a reaction, or its reverse, is not usually feasible: thus for most species it is not possible to determine the absolute proton affinity. The technique normally adopted is to use some indirect method of study (involving comparison of **X** with a substance of well-characterised PA), yielding a proton affinity value for **X** relative to the PA of some standard substance. These indirect methods concern the proton-transfer equilibrium

$$XH^+ + B \rightleftharpoons BH^+ + X \qquad (3.2)$$

where $\Delta H^\circ = PA(X) - PA(B)$ {3.ii}.

If both the forward and reverse reactions involved can be separately studied, the enthalpy change can be determined from the equilibrium constant:

$$K = e^{-\Delta G^\circ / RT} \qquad \{3.iii\}$$

and $$K = k_f / k_b \qquad \{3.iv\}.$$

$$\therefore \quad \Delta G^\circ = -RT \ln (k_f / k_b) \qquad \{3.v\};$$

$$\Delta G^\circ = \Delta H^\circ - T\Delta S^\circ \qquad \{3.vi\}$$

$$\therefore \quad \Delta H^\circ = -RT \ln (k_f / k_b) + T\Delta S^\circ \qquad \{3.vii\}.$$

Some researchers contend that definition of the proton-transfer equilibrium coefficient as k_f / k_b does not give a reliable indication of the free-energy change from left to right. These workers[189,190] advocate applying a correction factor for equilibria in which the forward and reverse reactions have markedly different collision rates:

$$K = \frac{k_f / k_{(c)f}}{k_b / k_{(c)b}} \qquad \{3.viii\},$$

where $k_{(c)f}$ and $k_{(c)b}$ are the calculated collision rate coefficients. The equilibrium constant is, in this model, defined as the ratio of the efficiencies of the forward and reverse reactions; this ratio will often be markedly different from k_f / k_b, if **X** is substantially more or less polar or polarisable than **B**.

This modification to K yields

$$\Delta H^\circ = -RT \ln \left[\frac{k_f / k_{(c)f}}{k_b / k_{(c)b}}\right] + T\Delta S^\circ \qquad \{3.ix\}$$

where ΔH° = PA(**X**) - PA(**B**). In this chapter, this model incorporating allowances for variations in collision rate will not be used.

To determine ΔH°, and hence the change in proton affinity, the change in entropy must be known. The usual method employed, in the absence of measurements at different temperatures, is to estimate ΔS° on the basis of changing rotational symmetry[185] from left to right of the equilibrium:

$$\Delta S^\circ = R \ln \left[\frac{\sigma_B \, \sigma_{XH^+}}{\sigma_X \, \sigma_{BH^+}}\right] \qquad \{3.x\}$$

where σ_x is the rotational symmetry number of **X**. A problem inherent in this calculation is that it assumes a knowledge of the configuration of the protonated species XH^+ and BH^+: if the shapes of these ions are not known, but estimated, uncertainty is introduced into this expression for ΔS°. There are other potential sources of inaccuracy in this method of calculation: however, it is a simple

means of estimating the entropy change and so is commonly used in deriving PA values.

In some circumstances, it is not possible to examine equilibrium (3.2) sufficiently closely to obtain an equilibrium constant: if this is the case, then the experimental technique of 'bracketing' may be employed instead. Bracketing involves studying the reaction of a protonated species XH^+ with a series of bases $B_{1\rightarrow n}$ which have well-established PA values. The extent

$$XH^+ + B_i \rightarrow B_iH^+ + X \qquad (3.3)$$

of reaction (3.3) for differing B_i allows interpolation of PA(X) at some position within the sequence of $PA(B_{1\rightarrow n})$ values. The disadvantage of the bracketing technique is that it is intrinsically more uncertain than determination of proton affinities from the proton-transfer equilibrium constant: an exothermic proton-transfer reaction may not be observable if other reaction channels are more energetically favourable, and an endothermic proton-transfer process may still occur as a slow reaction. PA values found by bracketing are especially uncertain for compounds which have uncommonly high or uncommonly low PA, since there are relatively few compounds in such ranges to which cross-reference can be made. In this chapter, equilibrium measurements are described which allow the determination of $PA(C_2N_2)$ and $PA(C_4H_2)$, these compounds having PA values towards the lower end of the scale.

Section 3.2: The proton affinity of C_2N_2.

Dicyanogen, N≡C–C≡N, is a likely constituent of interstellar clouds, since molecules containing CN functional groups comprise a large minority of the interstellar molecules detected to date. However, NCCN itself will not be easily detectable since it lacks a permanent dipole moment and will not, thus, be visible in the radio window. A less stable isomer, CNCN (isocyanogen) has better prospects for detection since its microwave spectrum has recently been calculated[191] and since it also possesses a substantial dipole moment (μ = -0.705 debye).[191,192] Identification of this isomer within clouds would be a very good indication of the probable presence of the more stable NCCN isomer also.

While C_2N_2 has not been detected in the interstellar environment, it has been considered as a precursor to the CN· radical within cometary comae:[193] it has also been identified within the stratosphere of Titan[194] at a level of 0.01 → 0.1 ppm. In Titan's atmosphere, C_2N_2 is thought to arise via the reaction

$$CN\cdot + HCN \rightarrow C_2N_2 + H\cdot \qquad (3.4)$$

$\Delta H_{3.4} = -45$ kJ mol^{-1}

$k_{3.4} = 1.8 \times 10^{-14}$ cm^3 molec^{-1} s^{-1} @ 300 K.[195]

This reaction has a calculated activation barrier[196] of $E_a \sim 17$ kJ mol^{-1} and so will be prohibitively slow in cold interstellar clouds: for this reason, any C_2N_2 formed in the interstellar environment would most probably occur through shock processes or via (as yet unidentified) ion-molecule reactions. The most logical precursor to C_2N_2 in an ion-molecule mechanism is its protonated form,

$NCCNH^+$: this ion has much better prospects for interstellar detection since it possesses a very large dipole moment, $\mu = -6.448 \pm 0.003$ debye.[191] To accurately assess ion-molecule mechanisms for C_2N_2 formation within clouds, a knowledge of the relevant thermochemical factors is necessary. One of these factors is the proton affinity, $PA(C_2N_2)$.

The proton affinity of C_2N_2 was determined by studying the proton-transfer equilibria involving C_2N_2, CH_3Cl, and C_2H_4:

$$C_2N_2H^+ + C_2H_4 \rightleftharpoons C_2H_5^+ + C_2N_2 \quad (3.5)$$

$$C_2N_2H^+ + CH_3Cl \rightleftharpoons CH_3ClH^+ + C_2N_2 \quad (3.6)$$

$$C_2H_5^+ + CH_3Cl \rightleftharpoons CH_3ClH^+ + C_2H_4 \quad (3.7)$$

A compilation of thermochemical values relevant to these proton-transfer equilibria, including results from the present work, is shown in **table 3.1.**

Table 3.1: Thermochemical values pertinent to determination of $PA(C_2N_2)$.

Parameter	Value [a]	Method of determination	Reference
$\Delta H°_f(C_2H_4)$	52.2 ± 1 kJ mol^{-1}	-	184
$\Delta H°_f(C_2H_5^+)$	902 ± 1 kJ mol^{-1}	Appearance potential	197,198
$PA(C_2H_4)$	680 ± 2 kJ mol^{-1}	PA standard value	185
	682 ± 7 kJ mol^{-1}	SIFT bracketing	199
	680 ± 2 kJ mol^{-1}	ICR bracketing	200
$PA(CH_3Cl)$	~ 682 kJ mol^{-1}	ICR bracketing	184,201,202
	673 ± 4 kJ mol^{-1}	SIFT studies	203[b]
$PA(C_2N_2)$	674 ± 8 kJ mol^{-1}	ICR bracketing	204
	681 kJ mol^{-1}	MP3//6-31+G** calculation	204
	678 ± 8 kJ mol^{-1}	SIFT bracketing	205
	657 kJ mol^{-1}	CEPA-1/SCF calculation	191
	674 ± 4 kJ mol^{-1}	SIFT studies	203[b]

Notes
a. in kJ mol^{-1}.
b. This work.

Reactant ions were generated by the following techniques:

$C_2N_2H^+$ was produced in the ion source (P ~ 8×10^{-5} Torr) from a 1:40 mixture of C_2N_2 in H_2:

$$H_2^+ + C_2N_2 \rightarrow C_2N_2H^+ + H\cdot \quad (3.8)$$

$$H_3^+ + C_2N_2 \rightarrow C_2N_2H^+ + H_2 \quad (3.9)$$

and

$$C_2N_2^+ + H_2 \rightarrow C_2N_2H+ + H\cdot \quad (3.10)$$

$\Delta H_{3.8} = -412$ kJ mol^{-1}

$k_{3.9} = 2.2 \times 10^{-9}$ cm^3 molec^{-1} s^{-1}

$k_{3.10} = 9.6 \times 10^{-10}$ cm^3 molec^{-1} s^{-1} [203]

Attempts were made to produce **$C_2H_5^+$** in the ion source, using

$$H_3^+ + C_2H_4 \rightarrow C_2H_3^+ + H_2 + H_2 \quad [0.7] \quad (3.11a)$$

$$\rightarrow C_2H_5^+ + H_2 \quad [0.3] \quad (3.11b)$$

$$CH_3^+ + CH_4 \rightarrow C_2H_5^+ + H_2 \quad (3.12)$$

$k_{3.11} = 2.3 \times 10^{-9}$ cm^3 molec^{-1} s^{-1}

$k_{3.12} = 1.2 \times 10^{-9}$ cm^3 molec^{-1} s^{-1}.

These techniques were unsatisfactory: upon injection of the m/z 29 ion signal into the flow tube, breakup of the primary ions occurred giving

$$(C_2H_5^+)^* \rightarrow C_2H_3^+ + H_2 \quad (3.13)$$

$\Delta H_{3.13} = +210$ kJ mol^{-1}.

The endothermicity of this reaction indicates that under the injection conditions (i.e. the voltage settings on the ion source components and the electrostatic lenses), a significant proportion of the ions being injected have an excitation energy of this magnitude. This excitation is most probably in the form of translational energy as discussed in chapter 2. It was not possible to reduce the injection energy sufficiently to avoid breakup of the primary ions while maintaining an acceptable signal intensity.

To circumvent this problem, chemical ionisation was used to form $C_2H_5^+$ within the flow tube, via reaction (3.12): CH_3^+ (from methane) was injected from the ion source, and CH_4 was added at the tube's first inlet port. The $C_2H_5^+$ signal produced, using gentler conditions and at higher pressure than in the ion source, did not display any tendency to undergo breakup.

CH_3ClH^+ was also generated within the flow tube, since efforts to produce it in the ion source (using a 1:20 mixture of CH_3Cl in H_2) led to breakup analogous to that observed for $C_2H_5^+$:

$$(CH_3ClH^+)^* \rightarrow CH_2Cl^+ + H_2 \qquad (3.14)$$

$$\Delta H_{3.14} = +192 \text{ kJmol}^{-1}.$$

A 1:10 mixture of CO:H_2 was used to produce a mixture of the ions HCO^+/COH^+ in the ion source: injection of this isomeric mixture into the flow tube gave CH_3ClH^+ by proton transfer to CH_3Cl (which was added at the tube's first inlet port):

$$HCO^+ + CH_3Cl \rightarrow CH_3ClH^+ + CO \quad (3.15)$$

$$COH^+ + CH_3Cl \rightarrow CH_3ClH^+ + CO \quad (3.16)$$

$\Delta H_{3.15} = -87$ kJ mol^{-1}

$\Delta H_{3.16} = -225$ kJ mol^{-1} .[164,206]

The results obtained for the proton-transfer equilibria are shown in **table 3.2**; the PA values calculated from these measurements are given in **table 3.3**. The measurements, and the determination of the PA values from the measurements, are discussed below.

Table 3.2: Proton transfer reactions studied to determine PA(C_2N_2).

Reactants	Products [a]		k_{obs} [b]	k_c [c]
$C_2N_2H^+ + C_2H_4$	$C_2H_5^+ + C_2N_2$ $C_2H_5^+.C_2N_2$	[0.92] [0.08]	0.90	1.11
$C_2H_5^+ + C_2N_2$	$C_2N_2H^+ + C_2H_4$ $C_2H_5^+.C_2N_2$	[0.40] [0.60]	0.21	1.12
$C_2N_2H^+ + CH_3Cl$	$CH_3ClH^+ + C_2N_2$	[1.0]	0.16	2.23
$^{37}CH_3ClH^+ + C_2N_2$	$C_2N_2H^+ + CH_3Cl$	[1.0]	≥0.20 0.25 [d]	0.96
$C_2H_5^+ + CH_3Cl$	$CH_3ClH^+ + C_2H_4$ $C_2H_5^+.CH_3Cl$	[0.80] [0.20]	0.079	2.05
$^{37}CH_3ClH^+ + C_2H_4$	$C_2H_5^+ + CH_3Cl$	[1.0]	0.83	1.12

Notes

a. Product channels reported in brackets, where more than one product was detected.
b. Observed rate coefficient, in units of 10^{-9} cm^3 molec^{-1} s^{-1}.
c. Calculated ADO collision rate coefficient, using the theory of Su and Chesnavich.[172]
d. Determined by ICR measurement.[207]

3.2.1. $C_2N_2H^+ + C_2H_4 \rightleftharpoons C_2H_5^+ + C_2N_2$

$C_2N_2H^+ + C_2H_4$: Injection of $C_2N_2H^+$ into the flow tube at high injection energy gave signals at m/z 27 and m/z 53. The signal at m/z 27, which had an intensity of 30% of that of the parent ion (m/z 53) was ascribed to breakup:

$$(C_2N_2H^+)^* \rightarrow HCN^+ + CN\cdot \qquad (3.17a)$$

$$\rightarrow CNH^+ + CN\cdot \qquad (3.17b)$$

$\Delta H_{3.17a} = +717$ kJ mol^{-1}

$\Delta H_{3.17b} = +643$ kJ mol^{-1}.

Table 3.3: $\Delta G°$, $\Delta H°$, and PA values calculated from the proton transfer equilibria studied to determine PA(C_2N_2).

Equilibrium	k_f [a]	k_r [a]	$\Delta G°$ [b]	$T\Delta S°$ [b,c]	$\Delta H°$ [b]	PA[d]
$C_2N_2H^+ + C_2H_4 \leftrightarrow C_2H_5^+ + C_2N_2$	0.83	0.084	-5.7	0	-5.7	674.3 ± 2 [e]
$C_2N_2H^+ + CH_3Cl \leftrightarrow CH_3ClH^+ + C_2N_2$	0.16	0.25	1.1	1.0	2.1	674.6 ± 4 [e] 672.2 ± 4 [f]
$C_2H_5^+ + CH_3Cl \leftrightarrow CH_3ClH^+ + C_2H_4$	0.063	0.83	6.5	1.0	7.5	672.5 ± 2 [f]

Notes

a. k_f is the observed rate coefficient for proton transfer in the forward direction, k_r is the proton transfer rate coefficient in the reverse direction.

b. In units of kJ mol^{-1}.

c. The entropy corrections are calculated on the basis of the rotational symmetry numbers detailed in table 3.4.

d. Proton affinity of neutral indicated, in kJ mol^{-1}, referenced to PA (C_2H_4) = 680 kJ mol^{-1}. An additional uncertainty in PA (C_2H_4), of ± 2 kJ mol^{-1}, is not included in the figures above. PAs quoted for the second equilibrium above are calculated with reference to the appropriate PAs derived from the first and third equilibria measurements: this illustrates the internal consistency of the results.

e. PA(C_2N_2).

f. PA(CH_3Cl).

Addition of C_2H_4 indicated the following as product ions:

m/z 28, 29, 41, 54, 56, 57, 69, 81.

Reduction of the injection energy allowed the breakup ion, m/z 27, to be eliminated: products observed in this instance, due solely to reactions of $C_2N_2H^+$ and associated secondary reactions, were m/z 29, 57, 69, 81. It was possible to assign the signals at m/z 57 and 69 as products of secondary reactions, since the ratio of these ion signals to the total product ion signals converged towards zero at low C_2H_4 flows. Thus the reaction of $C_2N_2H^+$ with C_2H_4 involves proton transfer and adduct formation:

$$C_2N_2H^+ + C_2H_4 \rightarrow C_2H_5^+ + C_2N_2 \quad [0.92] \quad (3.18a)$$

$$\rightarrow C_2N_2.H^+.C_2H_4 \quad [0.08] \quad (3.18b)$$

$k_{3.18} = 9.0 \times 10^{-10}$ cm^3 molec^{-1} s^{-1}.

Further reactions, of $C_2H_5^+$ with C_2H_4, account for the products at m/z 57 and 69:

$$C_2H_5^+ + C_2H_4 + He \rightarrow C_4H_9^+ + He \quad (3.19)$$

$$C_4H_9^+ + C_2H_4 \rightarrow C_5H_9^+ + CH_4 \quad (3.20)$$

$\Delta H_{3.19} = -188$ kJ mol^{-1}

$\Delta H_{3.20} = -96$ kJ mol^{-1}.

The enthalpies quoted above apply for formation and reaction of sec-$C_4H_9^+$, the most probable ion structure for association of $C_2H_5^+$ with C_2H_4 in the absence of

rearrangement. Formation of t-$C_4H_9^+$ is more exothermic (for reaction (3.19)) and gives $\Delta H_{3.20}$ = -24 kJ mol^{-1}.

Reactions occurring from the breakup ion HCN^+/HNC^+ with C_2H_4 were responsible for product ions at m/z 28, 41, 54 and 56. The structure of the ion m/z 28 is uncertain:

$$HCN^+ + C_2H_4 \rightarrow HCNH^+ + C_2H_3\cdot \quad (3.21a)$$

$$\rightarrow C_2H_4^+ + HCN \quad (3.21b)$$

$\Delta H_{3.21a}$ = - 287 kJ mol^{-1}

$\Delta H_{3.21b}$ = - 298 kJ mol^{-1}

$$HNC^+ + C_2H_4 \rightarrow HCNH^+ + C_2H_3\cdot \quad (3.22a)$$

$$\rightarrow C_2H_4^+ + HCN \quad (3.22b)$$

$$\rightarrow C_2H_4^+ + HNC \quad (3.22c)$$

$\Delta H_{3.22a}$ = - 213 kJ mol^{-1}

$\Delta H_{3.22b}$ = - 224 kJ mol^{-1}

$\Delta H_{3.22c}$ = - 159 kJ mol^{-1}.

All of these possible processes, involving H-atom transfer and charge transfer, are exothermic. $C_2H_4^+$ can account for the signal at m/z 41:

$$C_2H_4^+ + C_2H_4 \rightarrow C_3H_5^+ + CH_3. \quad [0.9] \quad (3.23a)$$

$$\rightarrow C_4H_7^+ + H. \quad [0.1] \quad (3.23b)$$

$k_{3.23}$ = 1.0 x 10^{-9} cm^3 $molec^{-1}$ s^{-1} [208,209]

however, a small signal at m/z 55 is also expected for this reaction, which was not detected. The origins of the ions at m/z 54 and m/z 56 are uncertain.

The rate coefficient which we observed for the reaction of $C_2N_2H^+ + C_2H_4$ compares well with the result of Deakyne et al,[204] and in reasonable agreement with the result of Raksit and Bohme,[205] when allowance is made for the differences in experimental technique. Raksit and Bohme, using 0.20 Torr of H_2 as a buffer gas, reported a substantially larger product channel for adduct formation (30%) than we detected with He as a buffer at a pressure of 0.30 Torr. This difference can be accounted for by the greater efficiency of H_2 (in comparison to He) in collisional stabilisation of the collision complex to permit adduct formation.

$C_2H_5^+ + C_2N_2$: To study the reaction of $C_2H_5^+$ with C_2N_2, $C_2H_5^+$ was produced as indicated above by chemical ionisation involving addition of CH_4 to the flow tube. Sufficient CH_4 was added to completely quench the injected m/z 15 signal (CH_3^+). The reactant ion profile, in addition to the ion of interest (m/z 29, $C_2H_5^+$), also contained impurity signals at m/z 41 ($C_3H_5^+$) and m/z 19 (H_3O^+, water contaminant):

$$C_2H_5^+ + H_2O \rightarrow H_3O^+ + C_2H_4 \qquad (3.24)$$

$$k_{3.24} = 3.5 \times 10^{-9}\ cm^3\ molec^{-1}\ s^{-1}$$

The signal at m/z 41 is a mystery: $C_2H_5^+ + CH_4$ does not produce $C_3H_5^+$.[182,210] Possibly $C_3H_5^+$ arises from a C_2H_4 impurity in the methane

$$CH_3^+ + C_2H_4 \rightarrow C_3H_5^+ + H_2 \qquad [0.5] \qquad (3.25a)$$

$$k_{3.25} = 1.0 \times 10^{-9} \text{ cm}^3 \text{ molec}^{-1} \text{ s}^{-1},$$

but this reaction should produce a comparable signal at m/z 27 ($C_2H_3^+$) which was not evident.[210,211] In any event, as with H_3O^+, this contaminant ion signal was less than 5% of the intensity of the major ion $C_2H_5^+$.

Upon addition of C_2N_2, product signals were detected at m/z 53, 62, 67 and 81. m/z 62 was attributed to an unidentified secondary reaction, because of its rapid disappearance at low C_2N_2 flows; m/z 67 was found to result from a side reaction involving CH_3^+ (arising from incomplete conversion from CH_3^+ to $C_2H_5^+$ in the reaction distance between port 1, the CH_4 inlet and port 2, the C_2N_2 inlet):

$$CH_3^+ + C_2N_2 + He \rightarrow CH_3.C_2N_2^+ + He \qquad (3.26).$$

Having interpreted these additional products, the reaction between $C_2H_5^+$ and C_2N_2 is found to consist of proton transfer and adduct formation channels:

$$C_2H_5^+ + C_2N_2 \rightarrow C_2N_2H^+ + C_2H_4 \qquad [0.4] \qquad (3.27a)$$

$$\rightarrow C_2H_4.H^+.C_2N_2 \qquad [0.6] \qquad (3.27b)$$

$$k_{3.27} = 2.1 \times 10^{-10} \text{ cm}^3 \text{ molec}^{-1} \text{ s}^{-1}.$$

The product ratio given here is that observed in the limiting case of low C_2N_2 flows. This ratio was not constant over the range of C_2N_2 partial pressures employed in the experiment: the ratio $I_{53} : I_{81}$ decreased from 0.67 at low flows to

~ 0.1 at the highest flows used. This suggests that $C_2N_2H^+$ participates in further unidentified reactions with C_2N_2 or CH_4.

3.2.2. $C_2N_2H^+ + CH_3Cl \rightleftharpoons CH_3ClH^+ + C_2N_2$

A problem associated with the study of this equilibrium is that the ions $C_2N_2H^+$ and $CH_3{}^{37}ClH^+$ both give a signal at m/z 53. Therefore, the ion signal at m/z 51 (corresponding to $CH_3{}^{35}ClH^+$) was monitored in all experiments pertaining to this equilibrium, and the $CH_3{}^{37}ClH^+$ content of the m/z 53 signal was calculated on the basis of the natural isotope ratio for ^{35}Cl:^{37}Cl (75.77 : 24.23).

$C_2N_2H^+ + CH_3Cl$: For the reaction of $C_2N_2H^+$ with CH_3Cl, the only product channel observed was proton transfer as shown in table 3.2.

$CH_3ClH^+ + C_2N_2$: Reaction of CH_3ClH^+ with C_2N_2 presented some difficulties. Proton transfer was again the only channel apparent, but an accurate determination of the reaction rate was not obtainable. Since CH_3ClH^+ was generated by chemical ionisation within the flow tube, the tube contained appreciable partial pressures of both the neutrals C_2N_2 and CH_3Cl. Thus the reverse reaction was also able to occur, reducing the apparent rate of the forward reaction. Extrapolation of the slope of ln(CH_3ClH^+ ion signal) versus C_2N_2 partial pressure at low C_2N_2 partial pressures yielded the rate coefficient reported here, which is best regarded as a lower limit. This rate is, however, well supported by an ICR measurement[207] giving a rate for the proton transfer process

of 2.5 x 10^{-10} cm^3 $molec^{-1}$ s^{-1}: thus the lower limit found by SIFT measurement appears to have reasonable accuracy.

3.2.3. $C_2H_5^+ + CH_3Cl \rightleftharpoons CH_3ClH^+ + C_2H_4$

$C_2H_5^+ + CH_3Cl$: Product analysis for this reaction was uncomplicated, with proton transfer and adduct formation channels seen:

$$C_2H_5^+ + CH_3Cl \rightarrow CH_3ClH^+ + C_2H_4 \quad [0.80] \quad (3.28a)$$

$$\rightarrow CH_3Cl.H^+.C_2H_4 \quad [0.20] \quad (3.28b)$$

$k_{3.28} = 7.9 \times 10^{-11}$ cm^3 $molec^{-1}$ s^{-1}

$CH_3ClH^+ + C_2H_4$: Proton transfer was the only channel observed here, with the rate for proton transfer found as listed in table 3.2. In this instance, although both C_2H_4 and CH_3Cl were present in the tube, equilibration within the flow tube was not considered a significant problem (as it had been in the study of the proton transfer reactions involved in equilibrium (3.5)) since reaction of CH_3ClH^+ with C_2H_4 is much faster than the reaction of $C_2H_5^+$ with CH_3Cl.

Determination of symmetry factors for calculation of $PA(C_2N_2)$ and $PA(CH_3Cl)$:

Ion structures assumed, in the determination of entropy changes during proton transfer, are as shown in **table 3.4.**

A bond-protonated form is assumed in determination of σ for $C_2H_5^+$. If this ion has, instead, the structure $CH_3–CH_2^+$, σ = 1 and the PA values determined from reactions involving C_2H_4 will be in error by 1.7 kJ mol^{-1} owing to the change in entropy during the reaction. The bond-protonated form is, however, the most stable form of $C_2H_5^+$ according to ab initio calculations.[212] An additional point to note from table 3.4 is that, although there are three perpendicular twofold rotational axes of symmetry for C_2H_4, σ = 4 (rather than 8) for this species since only four different and indistinguishable orientations exist for this molecule.[187]

For protonated CH_3Cl, the Cl–H bond is assumed not to be colinear with the C–Cl bond: if these bonds are colinear, then σ = 3 for this species. However, this change in symmetry number would not alter the derived value of $PA(C_2N_2)$, since this quantity is not directly determined from $PA(CH_3Cl)$.

Table 3.4: Rotational symmetry numbers for X and XH^+, used in determining $PA(C_2N_2)$.

X	σ_X	XH^+	σ_{XH^+}
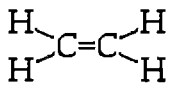	4	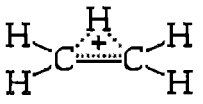	2
N≡C–C≡N	2	N≡C–C≡$\overset{+}{N}$–H	1
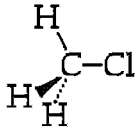	3	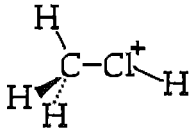	1

Protonated C_2N_2 is assumed to be nonlinear: a recent ab initio calculation[191] indicates that $NCCNH^+$ may well be a linear ion, but $\sigma = 1$ whether this ion is linear or not. Thus our derived value of $PA(C_2N_2)$ should not be in error even if this assumed structure is not correct.

Using these structures and the rate coefficients for proton transfer shown in table 3.3,

$PA(C_2N_2) = 674.3 \pm 4$ kJ mol^{-1} from $K_{3.5}$,

and $PA(CH_3Cl) = 672.5 \pm 4$ kJ mol^{-1} from $K_{3.7}$.

Using $K_{3.6}$ and the $PA(CH_3Cl)$ value determined above, $PA(C_2N_2) = 674.6 \pm 6$ kJ mol^{-1}: thus the thermochemical values determined from equilibria (3.5), (3.6) and (3.7) are consistent and in mutual agreement. These values are in agreement with the values determined earlier[185] but the uncertainties for $PA(C_2N_2)$ and $PA(CH_3Cl)$ are substantially less than for earlier determinations of these quantities.

Section 3.3: Some reactions of $C_2N_2^+$.

The $C_2N_2^+$ ion was easily generated by electron bombardment of C_2N_2 within the ion source. Some reactions of this ion with various neutrals are presented in table 3.5.

As can be seen from the efficiency of the reaction with hydrogen, $C_2N_2^+$ will be depleted rapidly within interstellar clouds and thus its reactions with other neutral species will not be of significance to models of interstellar chemistry. Channels evident in the other reactions of $C_2N_2^+$ are principally charge transfer, association, and atom transfer processes. Charge transfer was seen in all the reactions where IP(C_2N_2) > IP(X), similar to earlier findings for the reactions of $C_2N_2^+$ with C_4H_2,[213] HC_3N,[214] acetone and biacetyl.[215,216] A more interesting finding, relating to the reaction of $C_2N_2^+$ with HCN, is discussed in chapter 5.

Table 3.5: Reactions of $C_2N_2^+$ + X.

X	Products [a]		k_{obs} [b]	k_c [c]	-ΔH [d]
H_2	$C_2N_2H^+ + H\cdot$		0.96	1.51	235
CO	$C_2N_2.CO^+$		0.11	0.79	–
CO_2	$C_2N_2O^+ + CO$	[0.58]	0.0041	0.77	–
	$C_2N_2.CO_2^+$	[0.42]			–
H_2O	$H_2O^+ + C_2N_2$	[0.09]	2.6	2.4	97
	$C_2N_2H^+ + OH\cdot$	[0.91]			129
C_2H_2	$C_2H_2^+ + C_2N_2$	[≥0.95]	0.58	1.03	212
	$C_2N_2.C_2H_2^+$	[≤0.05]			–
C_2H_4	$C_2H_4^+ + C_2N_2$	[≥0.95]	1.3	1.1	299
	$C_4H_3N_2^+ + H\cdot$	[≤0.05]			–

Notes

a. Product channels reported in brackets, where more than one product was detected.
b. Observed rate coefficient, in units of 10^{-9} cm^3 $molec^{-1}$ s^{-1}.
c. Calculated ADO collision rate coefficient, using the theory of Su and Chesnavich.[172]
d. Reaction exothermicity in units of kJ mol^{-1}. Taken from the tabulation of Lias et al,[184] unless otherwise stated.

Section 3.4: The proton affinity of C_4H_2.

H–C≡C–C≡C–H, diacetylene, is formed as a combustion intermediate in flames;[217] ions derived from C_4H_2 have also been identified within flames, in connection with soot formation.[218] Extraterrestrial occurrences of C_4H_2 include Titan's atmosphere.[194,219,220] It is also considered partly responsible for stratospheric haze in the atmospheres of Uranus[221] and Neptune.[222] The molecule's lack of a permanent dipole moment renders it invisible to radio astronomers, but it is a very likely component of dark clouds: the detection of methyldiacetylene, CH_3C_4H, is very suggestive of the presence of diacetylene within interstellar clouds.[223] Herbst has argued[224] that the formation of diacetylene and more complex hydrocarbons in interstellar clouds requires a high abundance of neutral atomic carbon in the cloud's formative years, to permit reaction pathways such as

$$C_3H_4^+ + C \rightarrow C_4H_3^+ + H\cdot \qquad (3.29)$$

$$C_4H_3^+ + e \rightarrow C_4H_2 + H\cdot \qquad (3.30)$$

$\Delta H_{3.29}$ = -399 kJ mol^{-1}

$\Delta H_{3.30}$ = -568 kJ mol^{-1}.

Reactions of protonated diacetylene, $C_4H_3^+$, with H_2, CO and hydrocarbons have been investigated,[225-227] but there has been little study of the reactions of ions with C_4H_2.[204,228] The work detailed in this section was undertaken as a result of the report by Deakyne et al[204] of a value PA(C_4H_2) = 180 ± 1 kCal mol^{-1} (≡ 753 ± 4 kJ mol^{-1}), obtained by ICR bracketing measurements, that was considerably higher than the value obtained by Knight et al,[166] of PA(C_4H_2) = 738 ± 4 kJ mol^{-1}. This

latter value was obtained (on the University of Canterbury SIFT) by proton transfer equilibrium measurements involving BrCN and C_4H_2, and C_2H_5I and C_4H_2. A summary of the literature values of $PA(C_4H_2)$ and related quantities is given in **table 3.6**.

In the present work,[233] an attempt was made to determine $PA(C_4H_2)$ by studying the three proton-transfer equilibria involving C_4H_2, BrCN and CH_3NO_2:

$$C_4H_3^+ + CH_3NO_2 \rightleftharpoons CH_3NO_2H^+ + C_4H_2 \quad (3.31)$$

$$BrCNH^+ + CH_3NO_2 \rightleftharpoons CH_3NO_2H^+ + BrCN \quad (3.32)$$

$$C_4H_3^+ + BrCN \rightleftharpoons BrCNH^+ + C_4H_2 \quad (3.33)$$

Table 3.6: Thermochemical values pertinent to determination of $PA(C_4H_2)$.

Parameter	Value [a]	Method of determination	Reference
$PA(CH_3NO_2)$	750	PA standard value	185
	751.5 ± 12	FA bracketing	229
	756.1	ICR studies	230
	748.5	ICR bracketing	231
PA(BrCN)	748 ± 2	SIFT studies	167
	746 ± 2	ICR bracketing	232
	747 ± 2	SIFT studies	233[b]
$PA(C_4H_2)$	753 ± 4	ICR bracketing	204
	777.4	MP3//6-31G** calculation	204
	734	MP4SDQ/6-311G** calculation	233
	741	CEPA-1/SCF calculation	234
	741 ± 4	SIFT studies	233[b]

Notes
a. in kJ mol^{-1}.
b. This work.

The reactant ions were all injected into the flow tube from the ion source, thus avoiding any problems with competing reverse reactions occurring in the tube (c.f. the reaction of CH_3ClH^+ with C_2N_2, in section 3.2.2).

$C_4H_3^+$ was produced from acetylene

$$C_2H_2^+ + C_2H_2 \rightarrow C_4H_2^+ + H_2 \quad [0.35] \quad (3.34a)$$

$$\rightarrow C_4H_3^+ + H\cdot \quad [0.65] \quad (3.34b)$$

$k_{3.34} = 1.3 \times 10^{-9}$ cm^3 molec^{-1} s^{-1} [208,210]

from vinyl acetylene, CH_2=CH–C≡CH; and from a 1:10 mixture of diacetylene in hydrogen

$$H_2^+ + C_4H_2 \rightarrow C_4H_3^+ + H\cdot \quad (3.35)$$

$$H_3^+ + C_4H_2 \rightarrow C_4H_3^+ + H_2 \quad (3.36)$$

$\Delta H_{3.35} = -484$ kJ mol^{-1}

$\Delta H_{3.36} = -321$ kJ mol^{-1};

$$C_4H_2^+ + H_2 \not\rightarrow C_4H_3^+ + H\cdot \quad (3.37),$$

$k_{3.37} < 5 \times 10^{-13}$ cm^3 molec^{-1} s^{-1} [226]

Knight et al[166] found that these various methods of $C_4H_3^+$ generation gave no evidence for the formation of different $C_4H_3^+$ isomers. Giles et al[226] also observed results consistent with the existence of only one stable $C_4H_3^+$ isomer. In the present work, we found the rate coefficients and product distributions for the reactions of $C_4H_3^+$ with BrCN and with CH_3NO_2 to be independent of the

method of ion generation, and thus we conclude that all of these techniques yield only protonated diacetylene as $C_4H_3^+$.

$BrCNH^+$ was produced from a 1:10 mixture of BrCN in H_2:

$$H_2^+ + BrCN \rightarrow BrCNH^+ + H\cdot \quad (3.38)$$

$$H_3^+ + BrCN \rightarrow BrCNH^+ + H_2 \quad (3.39)$$

$$BrCN^+ + H_2 \rightarrow BrCNH^+ + H\cdot \quad (3.40)$$

$\Delta H_{3.38} = -486$ kJ mol^{-1}

$\Delta H_{3.39} = -323$ kJ mol^{-1}

$\Delta H_{3.40} = -140$ kJ mol^{-1}.

Injection of m/z 106 ($^{79}BrCNH^+$) from the ion source could not be accomplished without substantial contamination from neighbouring masses ($^{79,81}BrCN^+$). Instead, the mass spectrometer was set at m/z 112 and the resolution adjusted until a small signal at m/z 108 ($^{81}BrCNH^+$) was obtained without contamination.

$CH_3NO_2H^+$ was produced from a 1:10 mixture of CH_3NO_2 in H_2:

$$H_2^+ + CH_3NO_2 \rightarrow CH_3NO_2H^+ + H\cdot \quad (3.41)$$

$$H_3^+ + CH_3NO_2 \rightarrow CH_3NO_2H^+ + H_2 \quad (3.42)$$

$$CH_3NO_2^+ + H_2 \rightarrow CH_3NO_2H^+ + H\cdot \quad (3.43)$$

$\Delta H_{3.41} = -490$ kJ mol^{-1}

$\Delta H_{3.42} = -327$ kJ mol^{-1}

$\Delta H_{3.43} = -64$ kJ mol^{-1}.

Injection of $CH_3NO_2H^+$ at m/z 62 was accompanied by contaminating signals due to $CH_3NO_2^+$, NO_2^+ and NO^+, the latter two species arising from breakup subsequent to injection:

$$CH_3NO_2H^+ \rightarrow NO_2^+ + CH_4 \quad (3.44a)$$

$$\rightarrow NO^+ + CH_3OH \quad (3.44b)$$

$\Delta H_{3.44a} = +194.5$ kJ mol^{-1}

$\Delta H_{3.44b} = +78$ kJ mol^{-1}.

Adjustment of the mass spectrometer resolution permitted elimination of the m/z 61 ($CH_3NO_2^+$) signal, and operation at low repeller voltages allowed injection without detectable breakup to form NO_2^+, but formation of NO^+ by breakup was unavoidable. The NO^+ ion is generally unreactive, and there was no indication of any reaction of NO^+ with the neutrals used.

The results, for reaction of the ions $CH_3NO_2H^+$, $BrCNH^+$ and $C_4H_3^+$ with the appropriate neutrals, are given in **table 3.7**; the proton affinity values are calculated from these results in **table 3.8**, using the structures detailed in **table 3.9** to determine the entropy changes as with the determination of $PA(C_2N_2)$ in section 3.2. These results are interpreted below.

3.4.1 $C_4H_3^+ + CH_3NO_2 \rightleftharpoons CH_3NO_2H^+ + C_4H_2$

$CH_3NO_2H^+ + C_4H_2$: The reaction between $CH_3NO_2H^+$ and C_4H_2 is fast, but does not exhibit proton transfer. Rather, the only product seen is at m/z 42,

corresponding to $C_2H_4N^+$, $C_2H_2O^+$, or CNO^+. Of these possibilities, all of which require complicated rearrangement of the reactants, the most exothermic channel corresponds to

$$CH_3NO_2H^+ + C_4H_2 \rightarrow CH_3CNH^+ + C_2H_2 + CO_2 \qquad (3.45)$$

$$\Delta H_{3.45} = -494 \text{ kJ mol}^{-1},$$

Table 3.7: Proton transfer reactions studied to determine PA(C_4H_2).

Reactants	Products [a]		k_{obs} [a]	k_c [a,b]	k_{lit} [a,c]
$CH_3NO_2H^+ + C_4H_2$	$C_2H_4N^+ + C_2H_2 + CO_2$ [d]	[1.0]	1.1	1.20	1.1[e]
$C_4H_3^+ + CH_3NO_2$	$CH_3NO_2H^+ + C_4H_2$	[0.45]	3.1	2.90	2.45 [e]
	$C_2H_4N^+ + C_2H_2 + CO_2$ [d]	[0.30]			
	m/z 68 [f]	[0.25]			
$CH_3NO_2H^+ + BrCN$	$BrCNH^+ + CH_3NO_2$	[0.66]	0.80	2.34	0.81[g]
	$CH_3NO_2H^+.BrCN$	[0.34]			
$^{81}BrCNH^+ + CH_3NO_2$	$CH_3NO_2H^+ + BrCN$	[0.90]	1.5	2.87	1.7 [g]
	m/z 121[f]	[0.09]			
	$CH_3NO_2H^+.BrCN$	[0.01]			
$^{81}BrCNH^+ + C_4H_2$	$C_4H_3^+ + BrCN$	[0.20]	0.69	1.08	0.53 [e]
	$C_4H_3^+.BrCN$	[0.80]			
$C_4H_3^+ + BrCN$	$BrCNH^+ + C_4H_2$	[0.75]	2.4	2.1	1.3 [e]
	$C_4H_3^+.BrCN$	[0.25]			

Notes

a. See footnotes (a) - (c) for table 3.5.
b. Calculated using $\alpha(C_4H_2) = 7.33 \times 10^{-24}$ cm^3, as determined theoretically by Fowler and Diercksen.[235]
c. k_{lit} is the literature value for the reaction rate, from the reference quoted.
d. The product ion at m/z 42 is identified as CH_3CNH^+ on the basis of this being the most exothermic channel. The neutral products were not established.
e. Taken from reference 166.
f. This product was not identified.
g. Taken from reference 167.

though CH_3NCH^+ is another highly exothermic option (ΔH = -451 kJ mol^{-1}). Other possibilities are less likely on the basis of being less exothermic: formation of any product at m/z 42 requires extensive rearrangement, necessitating a long-lived collision complex, and for long complex lifetimes rearrangement is likely to yield the product having the lowest possible energy. Also, there exists a greater likelihood of activation energy barriers for such rearrangement if the eventual free energy gain is less. The absence of proton transfer in this reaction is not, in itself, at all conclusive: the reverse direction must be examined also.

Table 3.8: $\Delta G°$, $\Delta H°$, and PA values calculated from the proton transfer equilibria studied to determine $PA(C_4H_2)$.

Equilibrium	k_f [a]	k_r [a]	$\Delta G°$ [a]	$T\Delta S°$ [a,b]	$\Delta H°$ [a]	PA [c]
$CH_3NO_2H^+ + C_4H_2$ $\leftrightarrow C_4H_3^+ + CH_3NO_2$	0	1.4	+ [d]	0	+	< 750 [e]
$CH_3NO_2H^+ + BrCN$ $\leftrightarrow BrCNH^+ + CH_3NO_2$	0.53	1.35	2.3	0	2.3	748±2 [f]
$BrCNH^+ + C_4H_2$ $\leftrightarrow C_4H_3^+ + BrCN$	0.14	1.8	6.4	0	6.4	741±4 [e]

Notes

a. See footnotes (a) - (b) for table 3.3.
b. The entropy corrections are calculated on the basis of the rotational symmetry numbers detailed in table 3.9.
c. Proton affinity of neutral indicated, in kJ mol^{-1}, referenced to PA (CH_3NO_2) = 750 kJ mol^{-1}.
d. Inferred $\Delta G > 0$ from $k_f < k_r$ (that is, $K < 1$).
e. $PA(C_4H_2)$.
f. PA(BrCN).

$C_4H_3^+$ + CH_3NO_2: The observation of proton transfer as the major channel (45%) for the fast reaction between $C_4H_3^+$ and CH_3NO_2 is immediately in conflict with the finding, by Deakyne et al,[204] that $PA(C_4H_2) > PA(CH_3NO_2)$. The existence, in addition to proton transfer, of competing exothermic channels

$$C_4H_3^+ + CH_3NO_2 \rightarrow C_2H_4N^+ + C_2H_2 + CO_2 \quad [0.30] \quad (3.46a)$$

$$\rightarrow \text{m/z 68} \quad [0.25] \quad (3.46b)$$

$\Delta H_{3.46a}$ = -500 kJ mol^{-1} for m/z 42 = CH_3CNH^+

$\Delta H_{3.46b}$ = -457 kJ mol^{-1} for m/z 42 = CH_3NCH^+

(with the product at m/z 68 being unidentified) ensures that proton transfer cannot occur on every collision, but the observation of proton transfer in this direction and the absence of any proton transfer channel for the reaction of $CH_3NO_2H^+$ with C_4H_2 indicates that proton transfer is exothermic from $C_4H_3^+$ to CH_3NO_2. That is, $PA(CH_3NO_2) > PA(C_4H_2)$.

Table 3.9: Rotational symmetry numbers for X and XH^+, used in determining PA (C_4H_2).

X	σ_X	XH^+	σ_{XH^+}
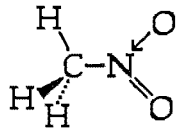	1	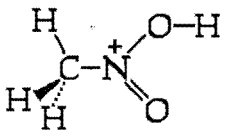	1
H–C≡C–C≡C–H	2	H–C≡C–C=C$^+$(H)H	2
Br–C≡N	1	Br–C≡N$^+$–H	1

It is not possible, from the results for this equilibrium system, to calculate the difference in PAs from the equilibrium constant $K_{3,31}$ (because of the competing product channels observed for reaction in both directions). The absence of these channels from the earlier ICR measurements[204] can be explained in terms of the extensive rearrangement required for these channels, necessitating a long-lived (collisionally stabilised) collision complex. At ICR pressures, such collisional stabilisation is improbable and so proton transfer is the only channel detected. This explanation does not, however, resolve the conflict between the two sets of data: the ICR results indicate $PA(C_4H_2) > PA(CH_3NO_2)$, while our results indicate the reverse.

3.4.2 $CH_3NO_2H^+ + BrCN \rightleftharpoons BrCNH^+ + CH_3NO_2$

$CH_3NO_2H^+ + BrCN$: Proton transfer is the main product channel for this reaction (66%). The overall reaction rate coefficient (8.0×10^{-10} cm^3 molec^{-1} s^{-1}) is below the calculated collision rate coefficient ($k_c = 2.34 \times 10^{-9}$ cm^3 molec^{-1} s^{-1}), which suggests thermoneutral or endothermic proton transfer. The efficiency, $k_f / k_{(c)f}$, of the proton transfer channel is 0.25: that is, 25% of collisions result in proton transfer.

$^{81}BrCNH^+ + CH_3NO_2$: Proton transfer is again the main product channel, with an efficiency of 0.47. The sum of these efficiencies is substantially below the value of unity expected. This deficiency is not adequately explained by the presence of a minor product channel at m/z 121 (the nature of this product being

unidentified), since neither the forward nor the reverse reaction occurs at the collision rate - thus reaction is not saturated in either direction, and so proton transfer is not hindered by competition with the other channels evident. The low value of $r_f + r_r = 0.72$ indicates that the reaction is close to thermoneutral.[236] The absence of hindrances to the proton transfer channels permits calculation of the free energy difference:

$$K_{3.32} = k_f / k_r = 0.39$$

$$\Delta G°_{3.32} = -RT \ln (K_{3.32})$$

$$\therefore \quad \Delta G°_{3.32} = 2.3 \text{ kJ mol}^{-1} \text{ at } 300K.$$

An uncertainty of ± 20% is ascribed to each rate coefficient, and ± 10% to the determination of each product ratio, corresponding to an overall uncertainty of ± 1.2 kJ mol^{-1} in the free energy calculation. From $\Delta G°_{3.32}$, and from $T\Delta S°$ as listed in table 3.9, it can be determined that

$$PA(CH_3NO_2) - PA(BrCN) = 2.3 \pm 2 \text{ kJ mol}^{-1}.$$

This value is in good agreement, within the uncertainties of the respective techniques, with the difference in PAs for the two compounds as determined by bracketing[185] and by an earlier SIFT measurement of this proton transfer equilibrium.[167] The earlier SIFT study did not report the unidentified product at m/z 121 for the reaction of $^{81}BrCNH^+$ with CH_3NO_2.

3.4.3 $BrCNH^+ + C_4H_2 \rightleftharpoons C_4H_3^+ + BrCN$

$^{81}BrCNH^+ + C_4H_2$: Adduct formation (80%) was the major product channel in evidence for this reaction, with (20%) proton transfer observed also. Competition between these channels is possible and is of concern in cases where adduct formation is the dominant channel, since the extent of proton transfer may be reduced by competition. However, the reaction is observed to be reproducibly slower than the calculated collision rate, suggesting that proton transfer is not hindered by competing association for this reaction.

$C_4H_3^+ + BrCN$: Proton transfer accounts for 75% of the collisions for this fast reaction, with adduct formation as the alternative product channel. The overall reaction is seen to occur at the collision rate. The sum of the proton transfer efficiencies is seen to be close to unity ($r_f + r_r = 0.91$), indicating that proton transfer is not substantially influenced by competing processes in either direction. The energetics of proton transfer can be calculated:

$$K_{3.33} = k_f / k_r = 0.077$$

$$\therefore \quad \Delta G°_{3.33} = 6.4 \pm 1.2 \text{ kJ mol}^{-1}.$$

$$\therefore \quad PA(BrCN) - PA(C_4H_2) = 6.4 \pm 2 \text{ kJ mol}^{-1}$$

(where the additional uncertainty is the $\pm$ 1 kJ mol^{-1} uncertainty in $T\Delta S°$). From the latter two equilibria, the difference in proton affinity between CH_3NO_2 and C_4H_2 can be determined:

$$PA(C_4H_2) = PA(CH_3NO_2) - 8.7 \pm 4 \text{ kJ mol}^{-1}.$$

This evaluation of $PA(C_4H_2) = 741 \pm 4$ kJ mol^{-1} is qualitatively supported by the conclusion, from the results obtained for equilibrium (3.31), that the proton affinity of C_4H_2 is below that of CH_3NO_2. Thus, while arithmetic triangulation of the results to achieve a self-consistent result is not possible because of the existence of competition for some of the proton transfer reactions, the results are seen to be in mutual agreement. The proton affinity determined for C_4H_2 is in good agreement with most of the values shown in table 3.6: the disagreement with the experimental value of Deakyne et al,[204] and hence with the literature value,[184] suggests that this literature value needs to be revised.

CHAPTER 4.

ISOMERISM OF C_2N^+ AND C_3N^+.

Section 4.1: C_2N^+.

In 1981, Haese and Woods[237] proposed that the reactions

$$C^+ + HCN \rightarrow C_2N^+ + H\cdot \quad (4.1)$$

$$C^+ + HNC \rightarrow C_2N^+ + H\cdot \quad (4.2)$$

$k_{4.1} = 3.5 \times 10^{-9}$ cm^3 molec^{-1} s^{-1} [238]

would selectively produce the CNC^+ and CCN^+ isomers respectively, since these are the products expected on consideration of the ion-dipole interaction and since the products would have insufficient energy to overcome the isomerisation barrier. On the basis of these considerations, they suggested that these two C_2N^+ isomers would display differences in their reactivity which could be significant in the modelling of interstellar cloud chemistry.

Theoretical calculations[237,239-241] and experimental studies[237,241-245] have verified that there are two distinct isomers of the C_2N^+ ion. Calculations at varying levels of theory indicate that ground-state CCN^+ is substantially higher in energy than ground-state CNC^+, and that there exists a sizeable barrier to isomerisation. Thus, the two species CCN^+ and CNC^+ are expected to display differences in reactivity. A summary of experimental and theoretical results (including a set

of calculations performed by DeFrees and McLean[241] as part of our study of the reactivity of the isomeric C_2N^+ system) is found in **table 4.1.**

The present study,[241] which was undertaken to demonstrate the differing reactivity of the CCN^+/CNC^+ ions in a flow tube, represents a continuation of work originally conducted earlier in this laboratory.[166] Other studies of C_2N^+ reactivity have been performed,[245-247] including an independent study of C_2N^+ isomerism by Bohme and co-workers,[245] but no earlier experimental investigations had dealt with the difference in reactivity of the two species.

Table 4.1: Experimental and theoretical heats of formation[a] of C_2N^+ species.

Ref.	ΔH_{CCN^+}	ΔH_{CNC^+}	$\Delta H_{(CCN^+ - CNC^+)}$	$\Delta H_{((TS) - CNC^+)}$
b	1761± 50, 1720 ± 17	1523 ± 50	197 ± 67	–
c	–	–	–	469
d	1761 ± 105	1556 ± 84	204 ± 20	–
e	1715 ± 29	–	–	–
f	–	–	118	–
g	1726 ± 12	1620 ± 11	106 ± 23	–
h	–	–	88 ± 25	195 ± 25
i	1715	1620	95	–

Notes

a. in kJ mol^{-1}.
b. Electron impact upon HC_3N and C_2N_2, Dibeler et al;[242] as interpreted by Haese and Woods.[237]
b. 4-31G-SCF calculations, Hopkinson.[239]
c. DZ+P-SCF and CI-SCF calculations, Haese and Woods.[237]
d. Electron impact on C_2N_2, Smith.[243]
e. CI(SDQ) calculations, Yoshimine and Kraemer.[240]
f. 'Monochromatic' electron impact on CH_3CN, CH_3NC and C_2N_2, Harland and McIntosh.[244]
g. MP4/6-311++G(df,pd) calculations, DeFrees and McLean.[241]
h. Tabulated literature values, Lias et al.[184]

A variety of methods was employed to produce C_2N^+. Chemical ionisation techniques permitted the production of C_2N^+ in the flow tube by reaction of C^+ (injected from the ion source) with HCN and with C_2N_2:

$$C^+ + HCN \rightarrow CCN^+ + H\cdot \quad (4.1a)$$

$$\rightarrow CNC^+ + H\cdot \quad (4.1b)$$

$\Delta H_{4.1a} = -5$ kJ mol^{-1}

$\Delta H_{4.1b} = -100$ kJ mol^{-1}

$$C^+ + C_2N_2 \rightarrow CCN^+ + CN\cdot \quad (4.3a)$$

$$\rightarrow CNC^+ + CN\cdot \quad (4.3b)$$

$\Delta H_{4.3a} = +40$ kJ mol^{-1}

$\Delta H_{4.3b} = -55$ kJ mol^{-1}.

Alternatively, C_2N^+ was injected from the ion source where it was formed by electron bombardment upon the source gas C_2N_2, HC_3N or CH_3CN.

The reactions of CCN^+ and CNC^+ with several neutral reagent gases are detailed in **tables 4.2** and **4.3**. In view of the practical difficulties of obtaining pure CCN^+ or pure CNC^+, no attempts were made to characterise differences in the product distributions due to CCN^+/CNC^+, except where only one isomer was reactive (in which instance the products observed are clearly due solely to this isomer).
The reaction with CH_4 was used to distinguish between CCN^+ and CNC^+:

$$CCN^+ + CH_4 \rightarrow \text{products} \quad (4.4)$$

$$CNC^+ + CH_4 \rightarrow \text{products} \quad (4.5)$$

$k_{4.4} = 7.0 \times 10^{-10}$ cm^3 molec^{-1} s^{-1}

$k_{4.5} = 4.0 \times 10^{-12}$ cm^{3}molec^{-1} s^{-1}.

A semilogarithmic graph of the ion signal at m/z 38 versus CH_4 concentration clearly showed a curved decay corresponding to the differing reactivity of two components of the m/z 38 ion signal (**see figure 4.1**). These components were identified as isomers since the addition of a substantial flow of N_2 from the first

Table 4.2: Reactions of $CCN^+ + X$.

X	Products [a]		k_{obs} [b]	k_c [c]	$-\Delta H$ [d,e]
H_2	$CH_2N^+ + C$	[0.90]	0.90	1.53	62
	$C_2H_2N^+$	[0.10]			–
CH_4	$C_2H_3^+ + HCN$	[0.60]	0.70	1.12	399
	$CH_2N^+ + C_2H_2$	[0.10]			477
	$C_3H_2N^+ + H_2$	[0.30]			512
NH_3	$CH_2N^+ + HCN$		1.9	2.29	598
H_2O	$HCO^+ + HCN$	[0.92]	1.63	2.55	525
	$CH_2N^+ + CO$	[0.08]			648
C_2H_2	$C_3H^+ + HCN$	[0.92]	1.6	1.10	225
	$CH_2N^+ + C_3$	[0.08]			186
HCN	$C_3HN_2^+$		0.42	3.48	–
N_2	no reaction		<0.0001	0.77	–
O_2	$C_2NO^+ + O$	[>0.97]	0.4	0.70	–
	$O_2^+ + C_2N\cdot$	[<0.03]			–
N_2O	$C_2NO^+ + N_2$	[0.73]	1.0	0.93	–
	(or $CN_3^+ + CO$)				–
	$NO^+ + C_2N_2$	[0.22]			518
	$N_2O^+ + C_2N\cdot$	[0.05]			–
CO_2	$C_2NO^+ + CO$		1.1	0.83	–

Notes

a. Product channels reported in brackets, where more than one product was detected.
b. Observed rate coefficient, in units of 10^{-9} cm^3 $molec^{-1}$ s^{-1}.
c. Calculated ADO collision rate coefficient, using the theory of Su and Chesnavich.[172]
d. Reaction exothermicity in units of kJ mol^{-1}. Taken from the tabulation of Lias et al,[184] unless otherwise stated.
e. Calculated using $\Delta H_f(CCN^+) = 1726$ kJ mol^{-1}.

inlet port did not alter the curved decay evident upon the subsequent addition of CH_4 from the second inlet port. In the case of curvature arising from a substantial extent of vibrational excitation of the ion at m/z 38, addition of N_2 should efficiently quench the vibrationally excited component. The fraction of the more reactive component at m/z 38 was not affected by the addition of N_2: thus vibrational excitation could be excluded as the cause of the observed reactivity.

Table 4.3: Reactions of $CNC^+ + X$.

X	Products [a]		k_{obs} [a]	k_c [a]	$-\Delta H$ [a,b]
H_2	no reaction		<0.0001	1.53	–
CH_4	$C_2H_3^+ + HCN$	[0.60]	0.004	1.12	293
	$CH_2N^+ + C_2H_2$	[0.10]			371
	$C_3H_2N^+ + H_2$	[0.30]			406
NH_3	$CH_2N^+ + HCN$		1.9	2.29	492
H_2O	$HCO^+ + HCN$	[0.92]	0.07	2.55	419
	$CH_2N^+ + CO$	[0.08]			542
C_2H_2	$C_3H^+ + HCN$	[0.92]	0.7	1.10	119
	$CH_2N^+ + C_3$	[0.08]			80
HCN	$C_3HN_2^+$		0.42	3.48	–
N_2	no reaction		<0.0001	0.77	–
O_2	no reaction		<0.0001	0.70	–
N_2O	$C_2NO^+ + N_2$	[0.73]	0.40	0.93	–
	(or $CN_3^+ + CO$)				–
	$NO^+ + C_2N_2$	[0.22]			412
	$N_2O^+ + C_2N\cdot$	[0.05]			–
CO_2	no reaction		<0.0001	0.83	–

Notes

a. See footnotes (a) - (d) for table (4.2).

b. Calculated using $\Delta H_f(CNC^+) = 1620$ kJ mol^{-1}.

The isomeric composition of the C_2N^+ ion signal, produced by a variety of techniques, was determined using the reactivity of m/z 38 with CH_4. These results are tabulated in **table 4.4.** It should be noted that all of the chemical ionisation methods, employing reaction (4.3), produce approximately 10% CCN^+ whereas this reaction should produce CNC^+ only. Similarly, all the electron-impact techniques produce approximately 20% CCN^+. The occurrence of substantial CCN^+ arising from electron impact is to be expected given the structure of the source gases used and the highly energetic nature of the ionisation process, but the apparent formation of CCN^+ from reaction (4.3) is not thermodynamically feasible for ground-state reactants. It is therefore presumed

---

Figure 4.1: Experimentally observed decay curve for reaction of C_2N^+ (generated from electron impact upon C_2N_2) with CH_4. This graph of ln(reactant ion signal) versus reactant neutral flow is not well fitted by a single exponential decay, indicating that two C_2N^+ isomers are reacting at different rates with CH_4. These results show that the more reactive isomer, CCN^+ (which accounts for ~ 20% of the m/z 38 ion signal) reacts with CH_4 with a rate coefficient $k = 7.8 \times 10^{-10}$ cm^3 $molec^{-1}$ s^{-1}; the rate observed for reaction of the less reactive isomer, CNC^+, is $k = 2.4 \times 10^{-12}$ cm^3 $molec^{-1}$ s^{-1}.

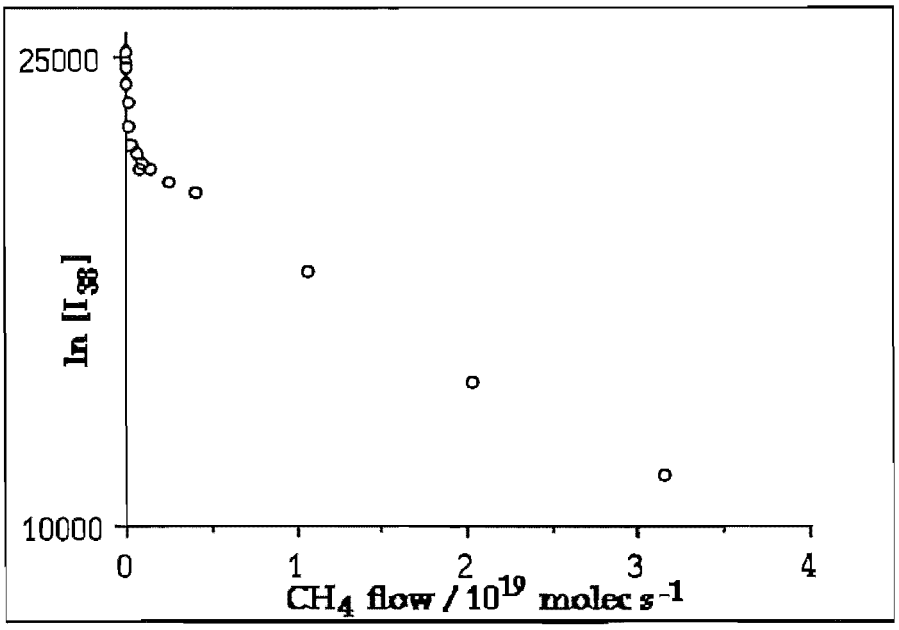

that the CCN^+ arises from an excited fraction of the C^+ ion signal, rather than from ground state (^2P) C^+: the most likely metastable excited state of C^+ is (^4P).

$$C^+(^4P) + C_2N_2 \rightarrow (CNC^+)^* + CN\cdot \qquad (4.6)$$

$$\Delta H_{4.6} = -565 \text{ kJ mol}^{-1}$$

$$(CNC^+)^* \rightarrow (CCN^+)^* \qquad (4.7a)$$

$$(CCN^+)^* \rightarrow (CNC^+)^* \qquad (4.7b).$$

The excited-state C^+ produces internally excited C_2N^+, which has sufficient internal energy to overcome the barrier to isomerisation: thus the immediate product ion resulting is able to oscillate between the CCN^+ and CNC^+ structures. The resulting distribution of CCN^+:CNC^+ might be expected to be governed by the thermal equilibrium constant for $CCN^+ \leftrightarrow CNC^+$:

Table 4.4: Isomeric composition of C_2N^+ produced from various sources.

Method [a]	Site [b]	%CCN^+ [c]
$e + HC_3N$	IS	18
$e + CH_3CN$	IS	22
$e + C_2N_2$	IS	20
$C^+(CH_4)$ [d] $+ C_2N_2$	FT	11
$C^+(CO)$ [d] $+ C_2N_2$	FT	11
$C^+(CO/He)$ [d,e] $+ C_2N_2$	FT	8
$C^+(CO_2)$ [d] $+ C_2N_2$	FT	11
$C^+(CCl_4)$ [d] $+ C_2N_2$	FT	12

Notes

a. Method of C_2N^+ generation employed.
b. Site of m/z 38 production. IS = ion source; FT = flow tube.
c. Determined by reaction with CH_4.
d. Gas from which C^+ was produced by electron impact.
e. Using a 1:30 mixture of CO in He.

$$CNC^+ + 195\ kJ\ mol^{-1} \leftrightarrow (TS)^* \leftrightarrow CCN^+ + 89\ kJ\ mol^{-1} \qquad (4.8),$$

where (TS)* denotes the transition state for isomerisation. The enthalpy values used here, and subsequently, are those tabulated by Lias et al,[184] with the exception of $\Delta H_f(CNC^+)$ and $\Delta H_f(TS)^*$, for which the values calculated by DeFrees and McLean[241] are used in the calculations presented below. The equilibrium constant calculated here assumes that the transition state is the only barrier to isomerisation, and that the isomeric distribution can be explained in terms of an Arrhenius-type rate constant for crossing of this barrier in both directions (that is, for $CCN^+ \rightarrow CNC^+$ and for $CNC^+ \rightarrow CCN^+$):

$$K_{4.7} = k_f / k_b$$

$$k_f = e^{-E_{a,f}/RT}$$

$$k_b = e^{-E_{a,r}/RT}$$

$$E_{a,f} = 195\ kJ\ mol^{-1}$$

$$E_{a,r} = 89\ kJ\ mol^{-1}$$

$$\therefore \quad K_{4.7} = e^{(E_{a,r}-E_{a,f})/RT}$$

$$\therefore \quad K_{4.7} = 2.9 \times 10^{-17} \text{ @ } 300\ K.$$

It is clear, however, that this value drastically underestimates the observed CCN^+ fraction, and this can be rationalised since the product ions at m/z 38 have far too short a residence time in the flow tube (t ~ 20 ms) to achieve a thermal distribution in the face of such a large isomerisation barrier. Rather, the factor governing the CCN^+ / CNC^+ distribution is the CCN^+ / CNC^+ density-of-states ratio at the transition state energy: C_2N^+ from reaction (4.6) is initially produced

with ample energy to overcome the barrier, but loses this energy after repeated collisions with the He buffer gas in the flow tube.

Troe[248] has determined the vibrational harmonic density of states to be

$$\rho_{vib,h}(E) = \frac{(E + a(E)E_z)^{s-1}}{(s-1)! \prod_{i=1}^{s} (h\nu_i)} \qquad \{4.i\}$$

where E is the energy of the species above the zero-point energy E_z, a(E) is a correction factor, S is the number of modes (including degenerate modes) of vibration, and ν_i is the fundamental frequency of the ith vibrational mode. a(E) can be calculated according to the expression

$$a(E) = 1 - B\omega \qquad \{4.ii\},$$

where

$$B = (S - 1)\frac{(S + (r + d)/2)}{S}\frac{\sum_{i=1}^{S} \nu_i^2}{(\sum_{i=1}^{S} \nu_i)^2} \qquad \{4.iii\}$$

for which $r = n_1 + 2n_2$, where n_i is the number of i-dimensional rotors, and d = 2 for linear molecules, d = 3 for nonlinear molecules;

and

$$\log_{10} \omega = -1.0506(E/E_z)^{0.25} \text{ for } E \geq E_z \qquad \{4.iv\},$$

and

$$\omega^{-1} = 5(E/E_z) + 2.73\sqrt{E/E_z} + 3.51 \text{ for } 0.1 \leq E/E_z \leq 1 \qquad \{4.v\}.$$

This treatment neglects the contribution of rotational energy level spacings to the density of states. There is a general formula[249] for the density of states

$$\underset{k=0}{N}_{v\,r}(E) = \frac{Q_r'\,(E + a_k\,Ez)^{v\,-1+\frac{r}{2}}}{\Gamma(v+\frac{r}{2})\prod_{i=1}^{v} h\nu_i} \qquad \{4.vi\}$$

which includes vibrational and rotational contributions, but solution of this expression (in which Q_r' is the rotational partition function, E is the energy above the zero-point energy E_z of the v oscillators, and a_k is equivalent to the factor a(E) in equation {4.i}) is not required since rotation will only affect the density of vibrational states if the molecule possesses rotational modes which contribute to its internal energy. In the case of a linear species such as CCN^+ or CNC^+, all the rotational energy is external and thus remains uncoupled from vibrational energy. This simplifies the density of states ratio Ψ

$$\Psi\,(E,R) = \frac{\rho^1_{vib,h}\,(E)\;(1/\sigma_1 B_1)}{\rho^2_{vib,h}\,(E)\;(1/\sigma_2 B_2)} \qquad \{4.vii\},$$

where E signifies internal, and R, external, energy, and σ is the rotational symmetry number of the species in question, and for which

$$B_i = \frac{h}{8\,\pi^2\,c\,I_i} \qquad \{4.viii\},$$

(where I is the moment of inertia) since for a harmonic-oscillator rigid-rotor, the density of rotational states is proportional to $1/\sigma B$.

Thus $$\Psi\ (E,R) = \frac{\rho^1_{vib,h}\ (E)}{\rho^2_{vib,h}\ (E)} \frac{(\sigma_2\ h\ /\ 8\ \pi^2\ c\ I_2)}{(\sigma_1\ h\ /\ 8\ \pi^2\ c\ I_1)} \qquad \{4.ix\},$$

$\therefore$ $$\Psi\ (E,R) = \frac{\rho^1_{vib,h}\ (E)}{\rho^2_{vib,h}\ (E)} \frac{\sigma_2\ I_1}{\sigma_1\ I_2} \qquad \{4.x\}.$$

This density-of-states ratio can now be calculated. Using the geometries calculated for CCN^+ and for CNC^+ by deFrees and McLean[241] (see **table 4.5**), the required moments of inertia and the rotational symmetry numbers can be determined. From these values and from the calculated vibrational frequencies,[241] Ψ can be determined as a function of C_2N^+ energy:

Table 4.5: Calculated geometries of CCN^+ and CNC^+.

Parameter [a]	CCN^+	CNC^+
ν_1 [b]	2257	1294
ν_2	1077	1963
ν_3 [c]	207	183
r(C–N) [d]	1.149	1.227
r(C–C)	1.383	–
I [e]	6.879×10^{-46}	6.000×10^{-46}
σ [f]	1	2

Notes
a. Calculated by DeFrees and McLean.[241]
b. Vibrational frequencies, cm^{-1}.
c. Doubly degenerate frequency.
d. Bond length, Angstroms.
e. Moment of inertia, kg m^2.
f. Rotational symmetry number.

$$\Psi\ (E,R) = 2.293\ \frac{\rho_{CCN^+}}{\rho_{CNC^+}} \qquad \{4.xi\}.$$

The variation of Ψ with energy is illustrated in **table 4.6.** The resulting graph (see **figure 4.2**) shows that, at the calculated transition state energy, 1/4 of the C_2N^+ ions will be in the form CCN^+. This is very close to the isomeric ratio observed for the electron impact techniques in which C_2N^+ is injected from the ion source: at low pressures (P ~ 10^{-4} Torr) such as those in the ion source region, the time between collisions is long in comparison to the likely timescale for interconversion across the isomerisation barrier. In consequence, collisional deexcitation of the ions is inefficient and the isomer ratio produced is similar to the ratio at the transition state energy. In the case of C_2N^+ ions produced within the flow tube by the chemical reaction (4.6), the pressure is several orders of magnitude higher (P ~ 0.3 Torr) and so collision is much more frequent.

Table 4.6: CCN^+/CNC^+ density of states ratio, Ψ, as a function of energy.

Energy [a]	ρ_{CCN^+} [b]	ρ_{CNC^+} [b]	Ψ (E,R) [c]
-20	0.9645	8.6284	0.2563
-10	1.2846	10.0217	0.2939
0	1.6678	11.5570	0.3309
10	2.1197	13.2412	0.3671
20	2.6460	15.0810	0.4023
30	3.2521	17.0835	0.4365
40	3.9438	19.2554	0.4696
50	4.7266	21.6036	0.5017
60	5.6062	24.1349	0.5326
70	6.5882	26.8563	0.5625
80	7.6781	29.7746	0.5913
90	8.8816	32.8967	0.6191
100	10.2413	36.2294	0.6458

Notes

a. Energy, in kJ mol^{-1}, relative to calculated transition state energy.

b. Density of states, in $(cm^{-1})^{-1}$, for CCN^+ and for CNC^+.

c. Calculated density of states ratio $\rho_{CCN^+}:\rho_{CNC^+}$.

Collisional deexcitation now competes much more efficiently with isomerisation, so the isomer ratio from reaction of $C^+(^4P)$ reflects the density of states ratio at an energy significantly above the transition state energy, where Ψ > 0.33. The observed CCN^+/CNC^+ ratio from the reaction of C^+ with C_2N_2 is thus consistent with less than 40% $C^+(^4P)$ in the m/z 12 signal: determination of the exact fraction of metastable C^+ required to account for the observed ratio is not possible given the uncertainty in the relative energy values and in the relative rates of isomerisation and collisional deexcitation.

The results of rate measurements and product analyses for CCN^+/CNC^+ reactions can be compared with those obtained in an independent study of C_2N^+ chemistry by Bohme et al.[245] The two studies are, in general, in good agreement, with few major differences. Bohme et al used the technique of electron impact upon

Figure 4.2: Calculated CCN^+ / CNC^+ density of states ratio.

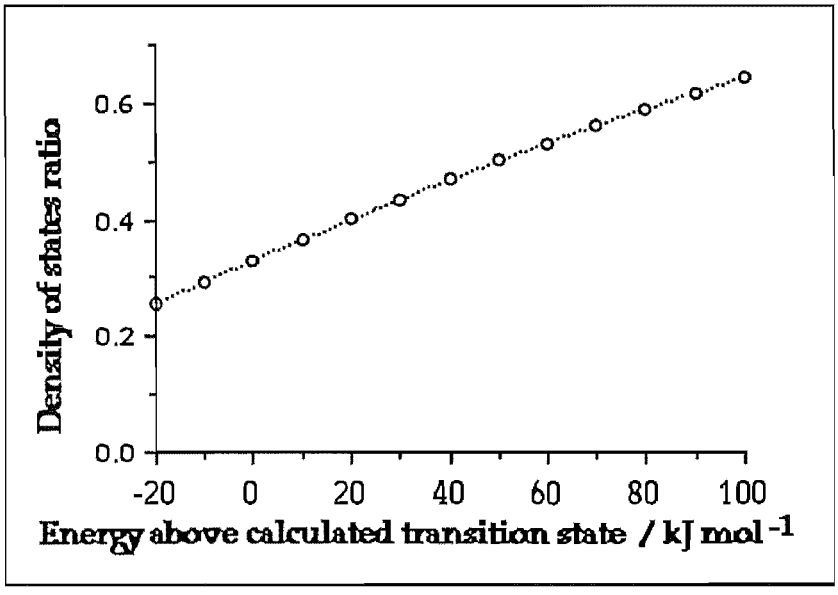

C_2N_2 to produce C_2N^+: their observed isomeric ratio of 0.25:0.75 for CCN^+:CNC^+ is in good agreement with our findings for this method (see table 4.4), and with the ratio expected from the density-of-states ratio at the transition state energy. They used the reaction of C_2N^+ with O_2

$$CCN^+ + O_2 \rightarrow C_2NO^+ + O \qquad (4.9)$$

$$CNC^+ + O_2 \rightarrow \text{no reaction} \qquad (4.10)$$

$$k_{4.9} = 3.0 \times 10^{-10}\ cm^3\ molec^{-1}\ s^{-1}$$

$$k_{4.10} < 1.0 \times 10^{-13}\ cm^3\ molec^{-1}\ s^{-1}$$ [245]

to distinguish the ions. Product analyses for CNC^+ were conducted by addition of sufficient O_2 to remove all CCN^+: thus, in their study, differences in the product distributions for CCN^+ and CNC^+ are reported for the reactions with H_2O, OCS and CS_2. In our study, separate product analyses in this manner were not attempted due to the difficulties in allowing for the possible reactivity of the primary products with the O_2 (or other titrant) added to remove CCN^+.

Significant differences in the rate coefficients and product distributions obtained by the two studies are:

(i). For the reaction of CCN^+ with H_2, the rate coefficient which we obtained was $9.0 \times 10^{-10}\ cm^3\ molec^{-1}\ s^{-1}$, significantly larger than the value $k_{obs} = 3.0 \times 10^{-10}\ cm^3\ molec^{-1}\ s^{-1}$ reported by Bohme et al. The disagreement between these results is not covered by the estimated uncertainty of the rate coefficient determinations (±40% in the study of Knight et al,[241] ±50% by Bohme et al[245]).

(ii). For the reactions of C_2N^+ with N_2O and C_2H_2, we observed slight but reproducible curvature evident in the experimental graphs for decay of the m/z 38 ion signal with added reactant, and on this basis determined $k_{CCN^+} > k_{CNC^+}$ for these reactions. Bohme et al reported $k_{CCN^+} = k_{CNC^+}$ for reaction with each of these reactants.

(iii). Bohme et al reported a 30% product channel for production of $C_2NO^+ + H_2$ from the reaction of CCN^+ with H_2O, which we did not observe.

(iv). Bohme et al reported a 20% product channel ($C_3O^+ + NO\cdot$) for the reaction $CCN^+ + CO_2$, which we did not observe.

Bohme et al also determined that the reaction of C^+ with HCN

$$C^+ + HCN \rightarrow CCN^+ + H\cdot \qquad (4.1a)$$

$$\rightarrow CNC^+ + H\cdot \qquad (4.1b)$$

$\Delta H_{4.1a} = -5$ kJ mol^{-1}

$\Delta H_{4.1b} = -100$ kJ mol^{-1}

produces CCN^+ and CNC^+ in a ratio ~ 1:3, in contrast to the expectations of Haese and Woods[237] that this reaction could only produce CNC^+. This result is in conflict also with the finding of Daniel et al,[250] in a crossed ion beam - molecular beam study, that CNC^+ is the sole product of the above reaction. The production of CCN^+ requires that reaction (4.1a) is exothermic, which is in doubt given the uncertainty in the tabulated heats of formation; it should also be noted that the

CCN^+ fraction observed here may arise solely from, or be enhanced due to, reaction of the metastable C^+ (^4P) with HCN.

The rapid reactivity which we observed for the reaction of CCN^+ with H_2 shows that this is the only reaction of CCN^+ liable to be of importance in interstellar cloud chemistry, since this reaction will ensure that the ion is depleted before it can undergo reactions with any other cloud components. The lack of reactivity for CNC^+ with H_2 indicates that reactions of CNC^+ with 'trace' cloud components (notably the rapid rates observed for its reactions with HCN, NH_3 and C_2H_2) will be relevant to cloud chemistry. Reactions of CNC^+ with CH_4, C_2H_2 and HCN are observed to result in lengthening of the carbon skeleton in the product ions: in this manner CNC^+ is expected to contribute to the production of more complex molecules in interstellar clouds.

The interstellar chemistry of CCN^+ is closely linked with that of HCN/HNC: reaction of C^+ with CHN is likely to be the major source of interstellar CCN^+

$C^+ + HCN$	$\rightarrow$	$CCN^+ + H\cdot$	[0.25?][245]	(4.1a)
$C^+ + HNC$	$\rightarrow$	$CCN^+ + H\cdot$	[1.0?][237]	(4.2a)

and the reaction of CCN^+ with H_2

$CCN^+ + H_2$	$\rightarrow$	$HCNH^+ + C$	[0.90]	(4.10a)
	$\rightarrow$	$C_2H_2N^+$	[0.10]	(4.10b)

indicates that most CCN^+ is rapidly converted to protonated HCN/HNC. $HCNH^+$ is unreactive with H_2 and CO, and dissociative recombination of this ion is expected to yield both HCN and HNC:

$$HCNH^+ + e \rightarrow HCN + H\cdot \quad (4.11a)$$

$$\rightarrow HNC + H\cdot \quad (4.11b)$$

$$\rightarrow CN\cdot + H_2 \quad (4.11c).$$

In this context, the chemistry of CCN^+ serves mainly to 'cycle' CHN between the molecular and protonated forms and hence is of no apparent synthetic significance to cloud chemistry, except for the small channel in reaction (4.10) leading to the adduct ion $C_2H_2N^+$. The reactivity of this $C_2H_2N^+$ ion has not yet been explored, but its apparent lack of reaction with H_2 suggests that (assuming that channel (4.10b) occurs under interstellar, as well as laboratory, conditions) its reactivity with other interstellar molecules will be relevant to models of cloud chemistry.

Section 4.2: C_3N^+.

The cyanoethynyl radical CCCN· was first reported, upon the basis of its calculated rotational spectrum,[251] as a constituent of the circumstellar envelope IRC+10216.[252] A subsequent detection of CCCN· within the cold cloud TMC-1 was reported by Friberg et al;[253] the isocyanoethynyl radical CCNC· has also been proposed as an interstellar species,[254] but has not yet been detected.

$C_3N\cdot$ is likely to be formed in the interstellar environment by dissociative recombination of ionized or protonated cyanoacetylene

$$HC_3N^+ + e \rightarrow C_3N\cdot + H\cdot \quad (4.12)$$

$$HC_3NH^+ + e \rightarrow HCCCN + H\cdot \quad (4.13a)$$

$$\rightarrow C_3N\cdot + H_2 \quad (4.13b)$$

or by cosmic-ray-induced UV photodissociation of HC_3N (that is, resulting from UV radiation produced by the interaction of cosmic rays with other interstellar molecules). In this context, the UV photolysis of HC_3N has been explored by Halpern et al.[255] The molecular ion C_3N^+ can also be formed by high-energy phenomena involving HC_3N: for example, in the cosmic-ray ionisation of HC_3N within interstellar clouds.

In 1986 Knight[166] reported the preliminary results of measurements performed on the Canterbury SIFT demonstrating differing reactivity for two isomers of the formula C_3N^+. These ions, produced by electron impact upon HC_3N in the ion source, displayed differences in their reactivity with H_2 (**see figure 4.3**) and with CH_4. For reaction of the more reactive isomer (~90% of the m/z 50 ion signal) with H_2, $k_{obs} = 9.1 \times 10^{-10}$ cm^3 $molec^{-1}$ s^{-1} was reported: the remaining isomer at m/z 50 appeared unreactive.

My initial studies of C_3N^+ reactivity, performed using HC_3N as the source gas, confirmed this pattern of reactivity: curvature characteristic of two isomeric forms at m/z 50 was seen in the reactions of C_3N^+ with CO_2, HCN and O_2 as well as with H_2 and CH_4. However, the product distributions of these reactions were

not easily characterized since injection of m/z 50 could not be accomplished without the accompanying injection of a signal at m/z 51, as large as (or larger than) the C_3N^+ signal. In most instances the reactivity of this HC_3N^+

Figure 4.3: Experimentally observed decay curve for reaction of C_3N^+ (generated from electron impact upon HC_3N) with H_2. (a). Graph covering the entire range of H_2 flows. (b). Graph highlighting the initial rapid decay. The absence of linearity in this decay curve very clearly demonstrates the existence of two forms of C_3N^+, with k = 1.0×10^{-9} cm^3 $molec^{-1}$ s^{-1} for the reactive form (accounting for 90% of the m/z 50 ion signal in this instance).

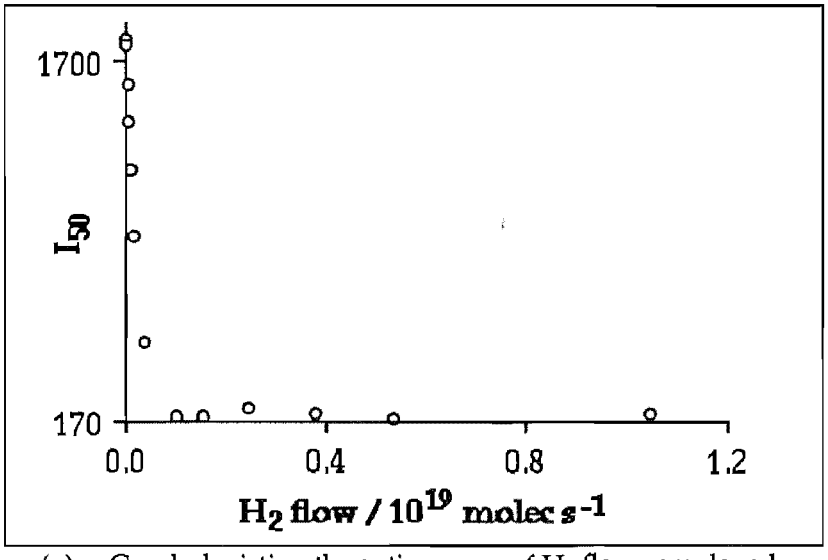

(a). Graph depicting the entire range of H_2 flows employed.

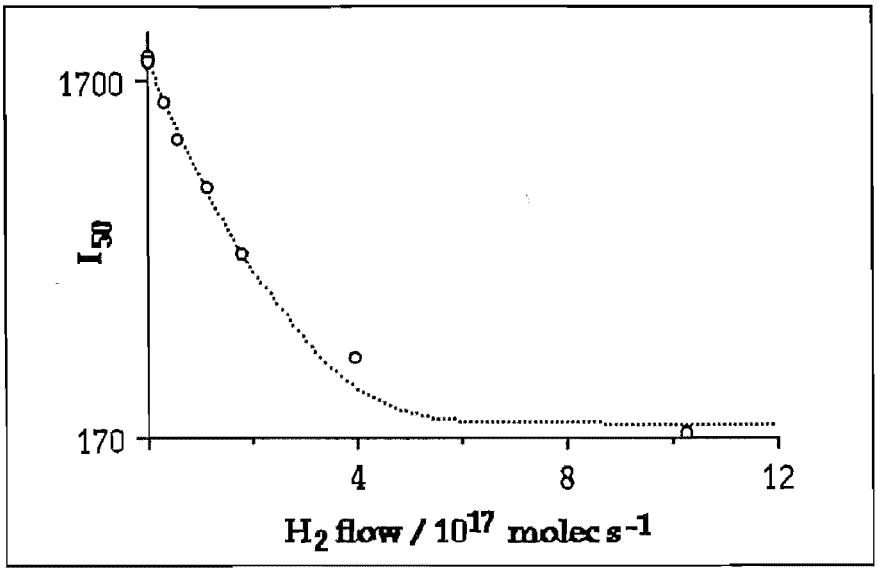

(b). Graph showing the initial decay due to the more reactive isomer

contaminant was almost as rapid as that of the more reactive C_3N^+ form, complicating product analysis. For this reason, and due to difficulties[256,257] in reproducing an earlier successful[258] synthesis of cyanoacetylene, alternative sources of the C_3N^+ ion were sought.

Methyl cyanoacetylene, $CH_3–C{\equiv}C–C{\equiv}N$, was initially chosen: it was felt that cleavage of the methyl group during ionisation would be likely to give rise to a "purer" C_3N^+ signal - that is, one less contaminated by a signal at m/z 51. However, when methylcyanoacetylene was employed as a source gas the signal at m/z 50 was accompanied by contaminating signals at m/z 51 (50% as large as at m/z 50) and at m/z 49 (20%). The signal at m/z 49 is a problem - improving the resolution of the upstream quadrupole mass spectrometer would allow injection of m/z 50 essentially uncontaminated by neighbouring masses, but m/z 49 can only be C_4H^+:

$$CH_3–C{\equiv}C–C{\equiv}N + e \rightarrow C_4H^+ + H_2 + N\cdot + 2e \qquad (4.14)$$

If a sizeable signal at m/z 49 is produced, then production of $C_4H_2^+$ and $C_4H_3^+$ is also very likely - and $C_4H_2^+$ cannot be distinguished from C_3N^+ on the basis of mass. For this reason, therefore, CH_3C_3N was not employed further as a source of C_3N^+.

Dicyanoacetylene, $N{\equiv}C–C{\equiv}C–C{\equiv}N$, was selected next: cleavage of either CN group during ionisation will produce C_3N^+, and since the source gas contains only C and N atoms, contamination at neighbouring masses should not be a significant problem.

Table 4.7: Reactions of C_3N^+ + X.

X	Products [a,b]		k_1 [a,c]	k_2 [d]	k_c [a]	$-\Delta H$ [a,e]
H_2	$HC_3N^+ + H\cdot$	[0.90]	0.81	<0.0005	1.50	158
	HC_3NH^+	[0.10]				721
CH_4	$C_2H_2N^+ + C_2H_2$	[0.18]	0.97	<0.001	1.08	334
	(or $C_3H_4^+ + CN\cdot$)					214 [f]
	$HC_3N^+ + CH_3\cdot$	[0.50]				156
	$HC_3NH^+ + CH_2$	[0.18]				256
	$C_3N.CH_3^+ + H\cdot$	[0.14]				180 [g]
NH_3	$NH_3^+ + C_3N\cdot$	[0.80]	2.0	2.0	2.22	241
	$CH_2N^+ + C_2HN$	[0.20]				–
H_2O	$CH_2N^+ + C_2O$	[0.03]	0.90	0.05	2.46	- [h]
	$HC_3N^+ + OH\cdot$	[0.67]				95
	$HC_3NO^+ + H\cdot$	[0.30]				>317
N_2	$C_3N_3^+$		0.02	<0.0005	0.73	–
O_2	$C_3NO^+ + O$	[0.58]	0.50	0.01	0.67	>34 [i]
	$C_2N^+ + CO_2$	[0.42]				529 [j]
CO	$C_3N.CO^+$		0.54	<0.001	0.80	–
C_2H_2	$HC_5N^+ + H\cdot$	[0.95]	1.02	>0.06 [k]	1.03	–
	$H_2C_5N^+$	[0.05]				–
HCN	$HC_3N^+ + CN\cdot$	[0.98]	2.2	0.23	3.33	76
	$C_3N.HCN^+$	[0.02]				–
CO_2	$C_3NO^+ + CO$		0.35	<0.001	0.79	– [l]
C_2N_2	$C_4N_2^+ + CN\cdot$	[0.21]	1.3	0.07	1.04	49
	$C_3N.C_2N_2^+$	[0.79]				–

Notes

a. See footnotes (a) - (d) for table (4.2).

b. Products and product ratios listed are for the reactions of the $CCCN^+$ isomer, generated by electron bombardment on a 1:20 mixture of C_4N_2 in He.

c. Rate coefficient observed for reaction of the more reactive C_3N^+ isomer, determined in this study as $CCCN^+$.

d. Rate coefficient observed for reaction of the less reactive C_3N^+ isomer, determined in this study as c-C_3N^+.

e. ΔH for the reaction $CCCN^+$ + X, calculated on the basis of $\Delta H_f(CCCN^+)$ = 1850 kJ mol^{-1} according to Harland and Maclagan.[259]

f. Assuming a $CH_2{=}C{=}CH_2^+$ structure for the $C_3H_4^+$ ion.

g. Calculated using $\Delta H_f(CH_3C{\equiv}C{-}C{\equiv}N^+)$ = 1378 kJ mol^{-1}; a more likely product structure is $C{\equiv}C{-}C{\equiv}NCH_3^+$, which might be expected to have a lower heat of formation.

h. The occurrence of this channel requires $\Delta H_f(C_2O) < 661$ kJ mol^{-1}.

(table 4.7 cont'd)

i. Calculated using $\Delta H_f(C_3NO^+) < 1567$ kJ mol^{-1} (see footnote (l)).
j. Calculated assuming a CCN^+ structure for C_2N^+.
k. See text for discussion.
l. The occurrence of this channel requires $\Delta H_f(C_3NO^+) < 1567$ kJ mol^{-1}.

Ionisation of C_4N_2 in the ion source produced a large signal at m/z 76 ($C_4N_2^+$, typically 2000 counts per second (cps)), with smaller sizeable signals at m/z 50 (C_3N^+, ~ 250 cps), m/z 48 (C_4^+, ~ 200 cps) and m/z 26 (CN^+, ~ 200 cps). Injection of m/z 50 could be accomplished satisfactorily with negligible contamination by m/z 48. Most often, dicyanoacetylene was used as a source gas in the form of a 1:20 solution in helium, since neat C_4N_2 displayed a propensity to attack the ion-source filament to an excessive degree.

Rate coefficients and product distributions could be determined for $C_3N^+ + \mathbf{X}$ for a wide variety of neutral reagents, as summarised in **table 4.7**. One surprising observation, apparent from the reaction of $C_3N^+ + H_2$ (see **figure 4.4**), was that C_3N^+ generated from C_4N_2 is essentially all (≥ 95%) in the more reactive form, and thus this method of generation cannot be used to determine the reactivity of the less reactive form with reagents **X**. For this reason it was felt necessary to synthesise further HC_3N, and this was done using the method of Moreu and Bongrand.[260,261]

Subsequently, problems were encountered in attempting to satisfactorily resolve between the signal at m/z 50 (C_3N^+) and the substantially larger signal at m/z 51 (HC_3N^+): the two adjacent signals could not be resolved except by operating the downstream quadrupole mass filter at an unacceptably high resolution (r = 8.9), at which setting the signal at m/z 50 was, at a few counts per second, too small to

permit accurate rate measurements or determination of the isomer ratio. The flow tube was then dismantled and cleaned: upon reassembly, the performance of the downstream mass spectrometer was substantially enhanced. The resolution at the appropriate mass range was investigated by injection (at m/z 52) of $C_2N_2^+$, generated by electron bombardment of C_2N_2 in the ion source. At a resolution setting of r=8.2 on the downstream mass spectrometer, the ion signal due to $C_2N_2^+$ was maximised at m/z 52.0 (I ~ 2000 cps) and decreased rapidly with decreasing m/z: at m/z 51.3 and below, I < 1 cps (see **figure 4.5**). This indicates that at this resolution setting, a reactant ion signal comprising both C_3N^+ and HC_3N^+ can be satisfactorily resolved: at a setting on the downstream mass spectrometer of m/z 50.0, no HC_3N^+ will be transmitted by the quadrupole. Subsequent injection of a 1:6 mixture of C_3N^+ and HC_3N^+ showed (see **figure 4.6**) that, although at m/z settings between 50.0 and 51.0 the ion signal did not

Figure 4.4: Experimental decay curve for reaction of C_3N^+ (generated from electron impact upon C_4N_2) with H_2. For C_3N^+ produced by this method, less than 5% is unreactive towards H_2, as shown by the arrow which denotes the best-fit intercept for this isomer. Ionisation of C_4N_2 produces less c-C_3N^+ than does ionisation of HC_3N.

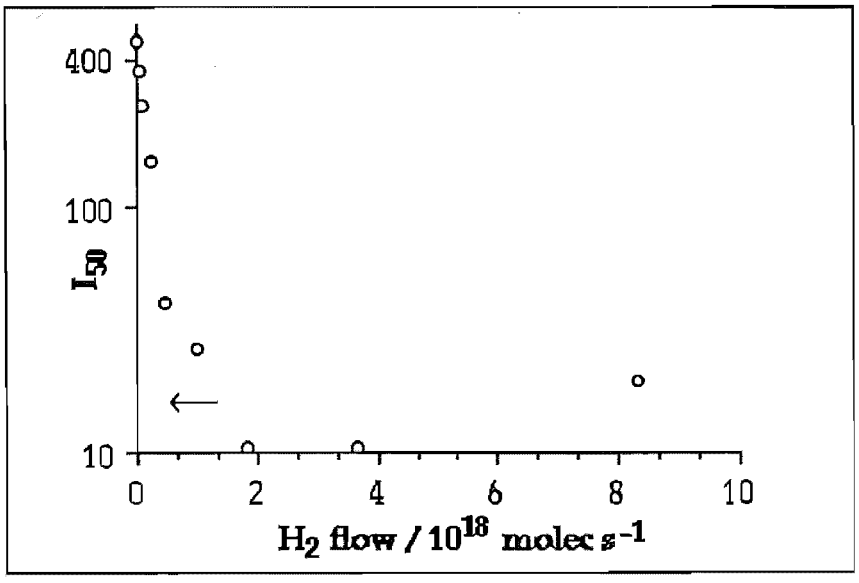

decrease to zero, it did decrease to a low value consistent with two well-resolved adjacent-mass signals. This permitted us to determine the isomeric ratio for C_3N^+, confident that the signal at m/z 50 contained no contamination from m/z 51. The reactivity of the C_3N^+ ion signal thus obtained was consistent with that observed previously: 90% of the C_3N^+ reacted at virtually the collision rate, whereas the remaining 10% was unreactive. The reactivity of this minority C_3N^+ isomer with various neutrals **X** is also listed in table 4.7.

The observation that the largest proportion of the m/z 50 ion signal was the most reactive component suggested very strongly that this reactive component was $CCCN^+$ and that this isomer is higher in energy than the less reactive component, for which $CCNC^+$ and a cyclic C_3N^+ ion are possible structures.

Figure 4.5: Mass spectrum obtained from $C_2N_2^+$ in the region of m/z 52, using a resolution setting of 8.2 upon the downstream Q.M.S. The signal at m/z 53 is most probably due to $C_2N_2H^+$ from reaction of $C_2N_2^+$ with H_2O within the flow tube: alternatively, some contribution to this m/z 53 signal may arise from injection of $^{12}C^{13}CN_2^+$ from the ion source.

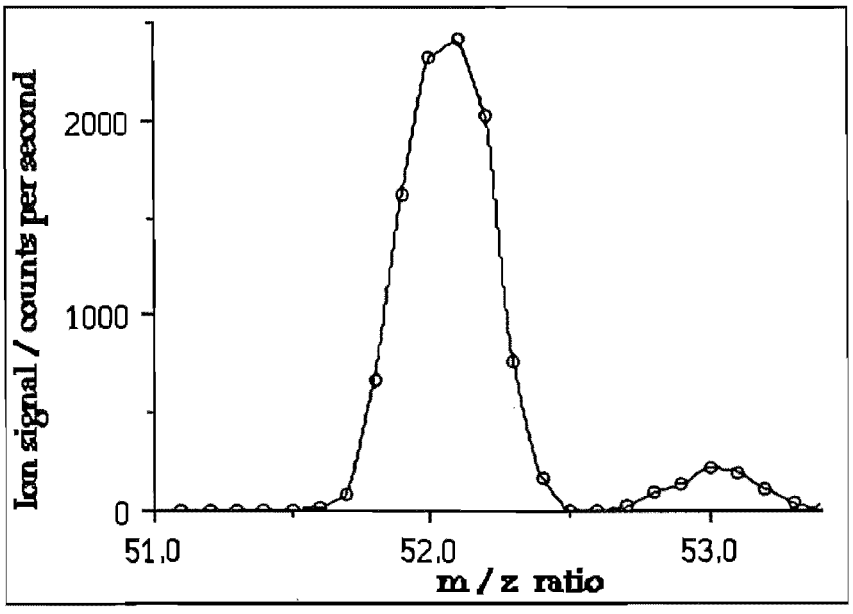

Harland and Maclagan[259] have studied the C_3N^+ system both experimentally and theoretically. In their study, the appearance energy of the $CCCN^+$ isomer was established by near-monochromatic electron impact ionisation of HC_3N: $AP(CCCN^+) = 17.78 \pm 0.08$ eV, corresponding to $\Delta H_f(CCCN^+) = 1850$ kJ mol-1. A sharp break in the ionisation efficiency curve was observed at around 18.7 eV, which they interpreted as indicating the formation of a higher-energy isomer identified as $c\text{-}C_3N^+$ on the basis of this isomer's calculated heat of formation. Harland and Maclagan's identification of $CCCN^+$ as the lowest-energy C_3N^+ isomer appears in serious disagreement with our observation that the more abundant isomer of C_3N^+ produced from HC_3N is very substantially more reactive with a wide variety of neutral reagents than is the less abundant C_3N^+

Figure 4.6: Mass spectrum obtained from C_3N^+ and HC_3N^+ in the region of m/z 50, using a resolution setting of 8.2 upon the downstream Q.M.S. The shoulders of the m/z 50 and m/z 51 peaks are not completely resolved at m/z 50.5, but the spectrum seen for injection of $C_2N_2^+$ (see figure 4.5) indicates that this resolution setting is suitable for complete separation of adjacent-mass ions in this mass range: that is, no HC_3N^+ ions will contribute to the signal at m/z 50. The signal at m/z 52 is probably a mixture of HC_3NH^+ and $H^{12}C_2{}^{13}CN^+$ ions.

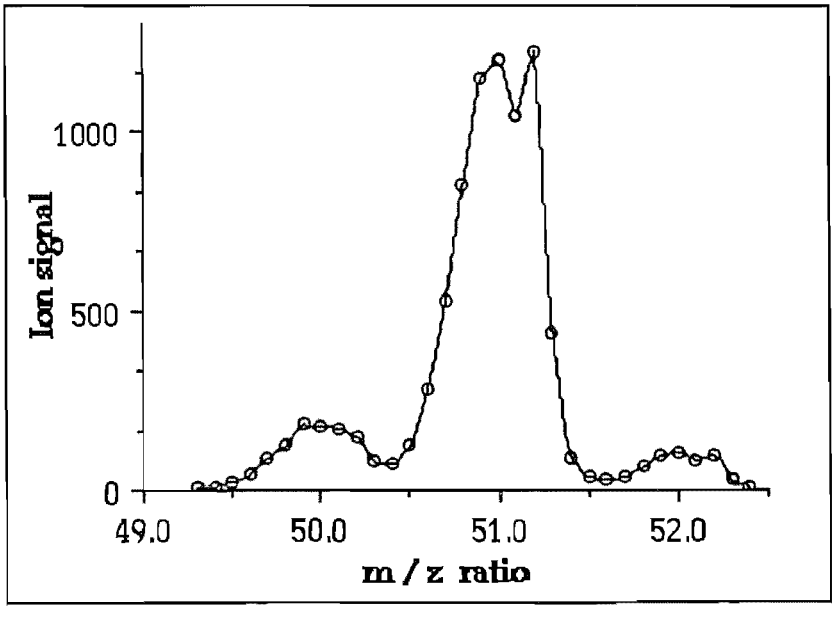

isomer. The general characteristic that ion-molecule reactions usually lack activation energy barriers suggests very strongly that the more reactive an isomer, the higher its heat of formation. Indeed, the only previously reported ion-molecule reaction in which a higher-energy isomer is the less reactive form is in the reaction of N_2OH^+ isomers with NO,[262,263] where the collision complex from the higher-energy ion $HNNO^+$ must undergo substantially greater rearrangement than that of $NNOH^+$ to have access to the only available exothermic product channel.

The difference in heats of formation of the two N_2OH^+ isomers is much smaller than the difference in the heats of formation of the C_3N^+ isomers as determined from appearance potentials. For this reason, it is tempting to deduce that the appearance potential at 18.7 eV is indicative of the barrier height to isomerisation to the less reactive form of C_3N^+. This explanation reconciles the experimental results but leaves unresolved the discrepancy between theory and experiment: a higher-energy isomer should not be universally less reactive than the lowest-energy form. A test for this hypothesis (that the appearance potential for the less abundant isomer may represent the isomerisation barrier, rather than the heat of formation of this isomer) is to investigate the proportion of the C_3N^+ isomers produced in situations in which the structure of the reactants does not appear to favour formation of the $CCCN^+$ isomer.

Reactions which have been reported[167,214,238,247,264,265] to produce C_3N^+ are

$$He^+ + HC_3N \rightarrow C_3N^+ + H\cdot + He \qquad [0.31] \qquad (4.15)$$

$$\Delta H_{4.15} = -655 \text{ kJ mol}^{-1}$$

$$k_{4.15} = 7.9 \times 10^{-9} \text{ cm}^3 \text{ molec}^{-1} \text{ s}^{-1}$$

$$CN^+ + C_2N_2 \rightarrow C_3N^+ + N_2 \qquad [0.10] \qquad (4.16)$$

$\Delta H_{4.16} = -251$ kJ mol^{-1}

$k_{4.16} = 1.4 \times 10^{-9}$ cm^3 molec^{-1} s^{-1}

$$C_2^+ + C_2N_2 \rightarrow C_3N^+ + CN\cdot \qquad [0.30] \qquad (4.17)$$

$\Delta H_{4.17} = -20$ kJ mol^{-1}

$k_{4.17} = 1.5 \times 10^{-9}$ cm^3 molec^{-1} s^{-1}

$$C_2^+ + HCN \rightarrow C_3N^+ + H\cdot \qquad [1.0] \qquad (4.18)$$

$\Delta H_{4.18} = -65$ kJ mol^{-1}

$k_{4.18} = 2.65 \times 10^{-9}$ cm^3 molec^{-1} s^{-1}

and

$$C_2^+ + HC_3N \rightarrow C_3N^+ + C_2H\cdot \qquad [0.50] \qquad (4.19)$$

$\Delta H_{4.19} = +66$ kJ mol^{-1}

$k_{4.19} = 4.8 \times 10^{-9}$ cm^3 molec^{-1} s^{-1},

where the ΔH values are calculated using $\Delta H_f(CCCN^+) = 1850$ kJ mol^{-1}, as determined by Harland.[266] Reaction (4.19) has been studied both by Raksit and Bohme[214,247] and by Knight et al:[167,267] the former determined C_3N^+ to be the major product, whereas Knight et al detected products at m/z 48 (C_4^+), m/z 49 (C_4H^+) and m/z 51 (HC_3N^+) but did not find any C_3N^+ to be produced by this reaction. Note that production of C_3N^+ is quite sizeably endothermic, according to Harland's value for $\Delta H_f(CCCN^+)$.

We determined the isomeric distribution of C_3N^+ produced by reactions (4.16), (4.17) and (4.18). This was done by injection of the reactant ions (C_2^+ from electron impact upon C_4N_2, CN^+ from electron impact upon C_2N_2) from the ion source into the flow tube, addition of the reactant neutrals (HC_3N or C_2N_2) at portal 1, and addition of N_2 at portal 2. Since the C_3N^+ ions are produced by reactions which occur throughout the tube's length, the rate of C_3N^+ removal by addition of N_2 will not allow easy determination of the rate of reaction of the C_3N^+ with N_2: however, since N_2 is unreactive with any of the other species in the flow tube, suppression of the m/z 50 ion signal by added N_2 indicates that $CCCN^+$ formed by the reaction under consideration has reacted with nitrogen. This method thus ascribes a lower limit to the fraction of $CCCN^+$ isomers within the C_3N^+ ion signal. The results are summarised in **table 4.8.** These results clearly indicate that $CCCN^+$ is the major or only form of C_3N^+ to be produced by all of these reactions. Thus (contrary to our earlier suspicions) $CCCN^+$ is indeed the lowest-energy isomer, supporting the relative C_3N^+ energies calculated by Maclagan.[259]

Table 4.8: Isomeric composition of C_3N^+ produced from various sources.

Method [a]	Site [b]	%$CCCN^+$
e + HC_3N	IS	90 ± 2 [c]
e + HC_3N/He [d]	IS	90 ± 2 [c]
e + C_4N_2	IS	≥ 95 [c]
C_2^+ + C_2N_2	FT	≥ 98 [e]
CN^+ + C_2N_2	FT	≥ 95 [e]
C_2^+ + HC_3N	FT	≥ 90 [e]

Notes

a. Method of C_3N^+ generation employed.
b. Site of m/z 50 production. IS = ion source; FT = flow tube.
c. Determined by reaction with H_2.
d. Using a 1:20 mixture of HC_3N in He.
e. Determined by reaction with N_2.

Having demonstrated that $CCCN^+$ is indeed the lowest-energy isomer, it then becomes necessary to explain how this ion can be more reactive than the higher-energy form, to which we ascribe, in accordance with the findings of Harland and Maclagan,[259] the structure c-C_3N^+. A species with higher ΔH_f will be less reactive than a lower energy species if there are significantly higher barriers to the reaction of this high-energy species. Similar arguments have been presented for the lability and stability of transition metal complexes. There are, however, no apparent precedents in ion-molecule chemistry to explain why the barriers for reaction of c-C_3N^+ with the majority of reagents used here should be so much larger than those for $CCCN^+$. An alternative explanation is that the isomer with higher ΔH_f will be less reactive if its product channels are endothermic while the lower-energy isomer has exothermic channels possible. Such a scenario requires that the reaction products from the higher-energy isomer have unusually high heats of formation. Why should this be so?

One possible rationale is found in the structure of the c-C_3N^+ ion as determined by Harland and Maclagan.[259] The bond lengths of the C_3N^+ ring (see **figure 4.7**) are very similar to those expected for an aromatic heterocycle, and very different from the expected values for a singly- or doubly-bonded system. If the c-C_3N^+ ion were aromatic - that is, if it possessed 6 π electrons delocalised around the 4-membered ring - then it might well have a lower heat of formation than that expected upon the basis of ring strain (which must be considerable, since the ion seems to have a bicyclo structure: compare the length of bond c with that expected for a C–C single bond). Formation of products, or of a stable collision complex, might involve the loss of this aromatic character, and thus necessitate an endothermic reaction to give products. Theoretical calculations exploring

the structures, and heats of formation, of possible products such as c-C_3NH^+ and c-$C_3NH_2^+$, would be very useful in testing this hypothesis. A problem with this hypothesis is that the existence of a 6 π electron cloud in a four-centre molecular orbital seems implausible, and is not reflected by the calculated electronic configuration.[259] An alternative explanation, involving two 2 π systems associated with the two rings present, is also unsatisfactory since the 'central' C–C bond would be a part of both π systems, which would suggest a shorter C–C bond length than has been calculated in this instance. It seems more probable, though less helpful in explaining the observed unreactivity of the cyclic species, that c-C_3N^+ is not aromatic but possesses equivalent bond order (1.5) to aromatic species.

Figure 4.7: c-C_3N^+ structure. Comparison of calculated bond lengths with literature values for various bond types.

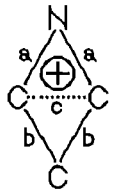

Bond	Length (Angstroms)	Reference
a	1.350	259
b	1.386	259
c	1.542	259
C–N single bond	1.472 - 1.479	186
C=N double bond	1.30	260
C–N bond (aromatic heterocycle)	1.352 ± 0.005	186
C–C single bond	1.541 ± 0.003	186
C=C double bond	1.337 ± 0.006	186
C–C bond (aromatic compound)	1.395 ± 0.003	186

Our studies of C_3N^+ reactivity indicate that $CCCN^+$ is exceptionally reactive - it reacted with near-unit efficiency with virtually all of the reagents tested (see table 4.7). The rapid reaction with hydrogen shows that $CCCN^+$ will be rapidly depleted within interstellar clouds; the products of this reaction

$$CCCN^+ + H_2 \rightarrow HC_3N^+ + H\cdot \quad [0.90] \quad (4.20a)$$

$$\rightarrow HC_3NH^+ \quad [0.10] \quad (4.20b)$$

$$k_{4.20} = 8.1 \times 10^{-10}\ cm^3\ molec^{-1}\ s^{-1}$$

are both of importance in the interstellar synthesis of cyanoacetylene.[167,267] The reaction of $CCCN^+$ with CO may also be of some interstellar significance: this reaction

$$CCCN^+ + CO \rightarrow C_3N.CO^+ \quad (4.21)$$

$$k_{4.21} = 5.4 \times 10^{-10}\ cm^3\ molec^{-1}\ s^{-1}$$

$$k_{4.21} > 5.1 \times 10^{-26}\ cm^6\ molec^{-2}\ s^{-1}$$

is observed to occur at an appreciable fraction of the apparent bimolecular collision rate at 0.3 Torr, so the analogous radiative association process may also occur rapidly under interstellar conditions.

Other $CCCN^+$ reactions are unlikely to play a significant rôle in interstellar cloud chemistry, although they may be important in the chemistry of hydrogen-free planetary atmospheres such as that of Titan. The reaction with C_2H_2, for example, is of relevance to the synthesis of cyanodiacetylene, HC_5N, in such an

environment: Kunde et al[194] have reported the detection of several polyynes, including HC_3N, in the Titanian atmosphere.

Although apparently too slow to be of any relevance to the chemistry of extraterrestrial environments, the reaction with N_2 is notable: to our knowledge, this reaction is the only such association reaction yet reported. The structure of the $C_3N_3^+$ ion formed, which must represent an adduct ion collisionally stabilised with reasonable efficiency ($k_{obs} \sim 0.03\ k_c$), is a matter for conjecture (and worth theoretical investigation). The only reaction for which a $C_3N_3^+$ product has been reported previously is

$$C_4N_4^+ + C_2N_2 \rightarrow C_3N_3^+ + C_3N_3\cdot \qquad (4.22a)$$

$$\rightarrow C_5N_5^+ + CN\cdot \qquad (4.22b)$$

described by Raksit and Bohme[247] as part of a SIFT study of C_2N_2 ion-molecule chemistry: no product ratio or rate coefficient is reported for this reaction, but it appears from the data given[247] to be slow, $k_{4.22} < 0.1\ k_c$. The same study of C_2N_2 chemistry reported also the reaction of the $CCCN^+$ ion with C_2N_2, giving $C_5N_3^+$ as the major product with some production of $C_4N_2^+$ also. Raksit and Bohme's product analysis for this reaction is in excellent agreement with the products determined in our own experiments: however, our rate coefficient is larger than their value of $\sim 4.5 \times 10^{-10}$ cm^3 molec^{-1} s^{-1}.

The reaction with CH_4 may be compared with the reactions of C_5N^+ and C_7N^+ with methane, which have been studied using Fourier transform mass spectrometry.[269,270] C_5N^+ and C_7N^+ have structures very similar to that of

$CCCN^+$ (differing merely by the number of C≡C– linkages present), and so a similar reactivity is expected. In fact, few similarities in reactivity are observed, although the major channel for reaction of all three ions is H–atom abstraction. The product ion at m/z 40 may be accompanied by C_2H_2 formation, showing a parallel to a minor channel seen for C_5N^+ and C_7N^+. Prominent channels for the reaction of C_5N^+ and C_7N^+ which were not observed in the present study are hydride transfer (23% of products for each of C_5N^+ and C_7N^+) and formation of $C_3H_3^+$ accompanied by neutral cyano(poly)yne formation (5% and 10% for C_5N^+ and C_7N^+, respectively). These reaction channels are substantially exothermic for C_3N^+ also, so their absence in this instance suggests differences in the mechanism of reactivity of C_3N^+ when compared with these larger C_5N^+ ions. These differences may in fact arise because of the differences in experimental technique: the studies involving C_5N^+ and C_7N^+ ions use an ICR-based technique, in which reactant ions are not thermalised because of the low pressures. This is illustrated by the occurrence of hydride transfer in the reactions of C_4N^+ and C_6N^+,[270] even though such a product channel is highly endothermic for ground-state reactants. Thus the differences in product channels may merely reflect the more quiescent conditions and longer collision complex lifetimes pertinent to SIFT studies.

In the present study, determination of the products due to the less reactive isomer, c-C_3N^+, was not attempted due to the difficulties associated with obtaining a pure signal of this isomer. No source of C_3N^+ gave better than 10% of c-C_3N^+ at m/z 50, and the only convenient technique (electron impact upon cyanoacetylene) also gave very large signals at m/z 51. It was not, therefore, thought to be feasible to attempt to determine which of the observed products

were due to c-C_3N^+ rather than to $CCCN^+$ or $HCCCN^+$ or various secondary reactions. A far better technique in this respect would be one involving electron impact upon some cyclic C_3N-containing species such as azetidine

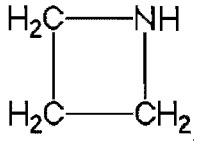

or some less saturated analogue. Alternatively, if injection of m/z 50 from HC_3N could be accomplished cleanly (without contamination at m/z 51), addition of sufficient N_2 upstream would remove all the $CCCN^+$ allowing an unfettered glimpse of the c-C_3N^+ reactivity.

Figure 4.8: Experimentally observed decay curve for reaction of C_3N^+ (generated from electron impact upon HC_3N) with NH_3. The interpolated line describes the decay curve expected for $k = 2.0 \times 10^{-9}$ cm^3 $molec^{-1}$ s^{-1}. No difference in reactivity between the two isomers is apparent.

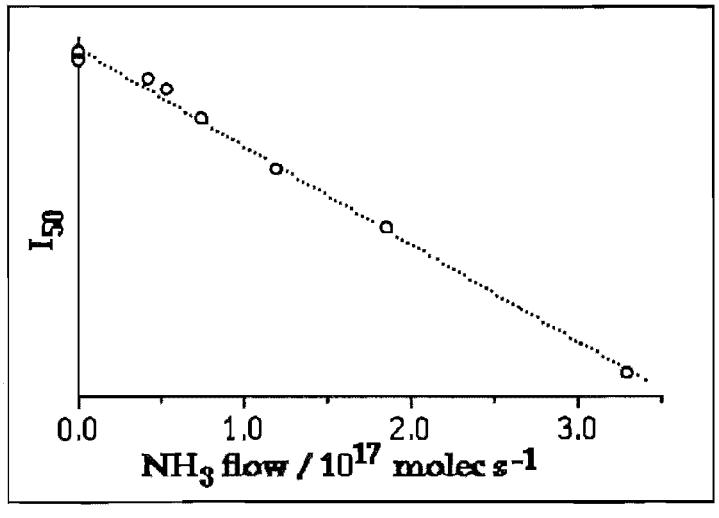

Figure 4.9: Experimentally observed decay curves for reaction of C_3N^+ (generated from electron impact upon HC_3N) with C_2H_2. Analysis is complicated by the production of $C_4H_2^+$ (also at m/z 50) from the reaction of HC_3N^+ with C_2H_2. The line plotted in graph (b) is for c-C_3N^+ (10% of the initial m/z 50 ion signal) reacting with C_2H_2 at a rate k = 6.1 x 10^{-10} cm^3 $molec^{-1}$ s^{-1}, which represents a lower limit for this reaction rate.

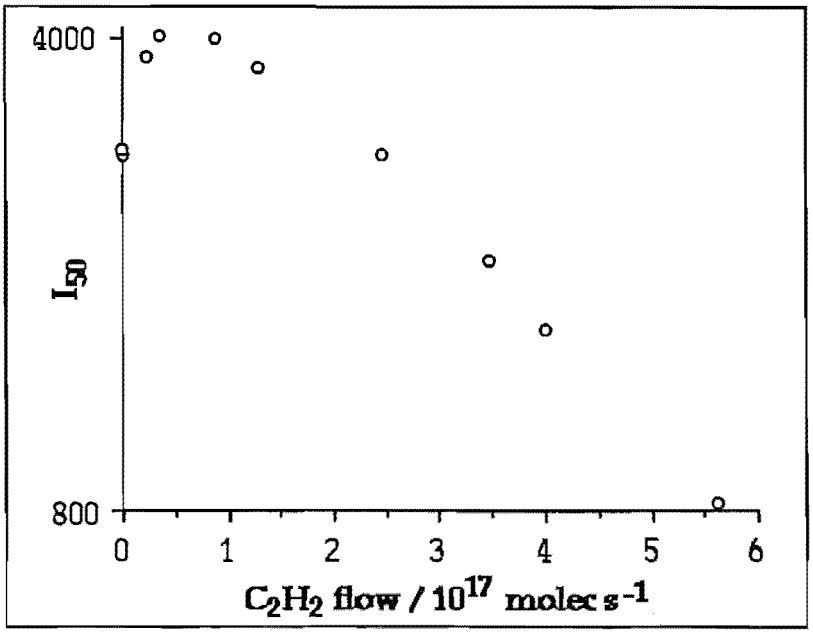

(a). Typical experimental data set.

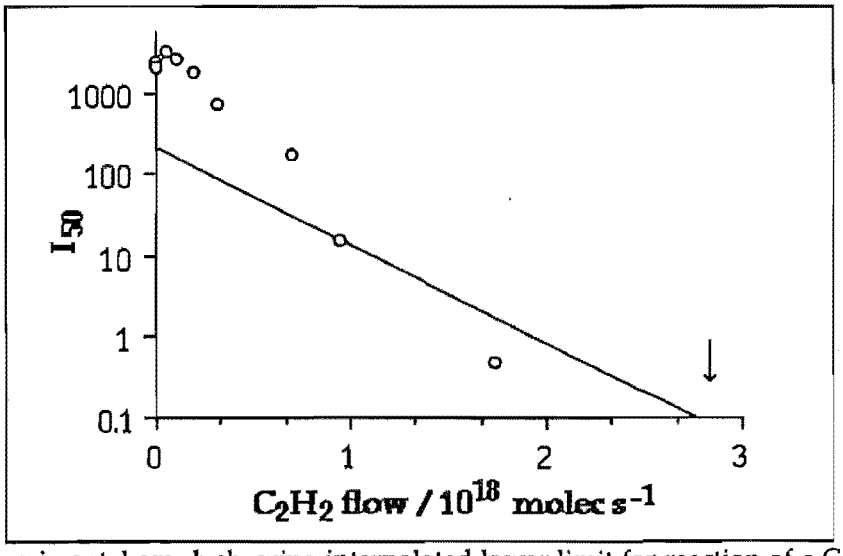

(b). Experimental graph showing interpolated lower limit for reaction of c-C_3N^+ with C_2H_2. (The arrow denotes further experimental points, out of graph range, below the interpolated line).

Although a satisfactory product analysis was too difficult in the circumstances prevailing, c-C_3N^+ is plainly much less reactive than $CCCN^+$: its complete unreactivity with H_2 and CO indicates that, once produced in the interstellar medium - for example, by cosmic-ray ionisation of HC_3N - it should persist for a substantial length of time, aiding detection. The most important interstellar reactions involving c-C_3N^+ are likely to be those with NH_3 (see **figure 4.8**), HCN and C_2H_2 as well as dissociative recombination with an electron. The rate of reaction of c-C_3N^+ with C_2H_2 could not be accurately determined in our study: a major product of the reaction of $HC_3N^+ + C_2H_2$ is $C_4H_2^+$ (+ HCN) at m/z 50, and the contribution from this product during the course of the reaction precluded a rate determination. However, a lower limit of $k \geq 6.0 \times 10^{-10}$ cm^3 $molec^{-1}$ s^{-1} can be ascribed on the basis of the amount of C_2H_2 required for complete removal of all forms of m/z 50 (see **figure 4.9**): thus the reaction of c-C_3N^+ with C_2H_2 is presumed to occur rapidly.

Section 4.3: $C_4N_2^+$.

Having synthesised dicyanoacetylene to investigate the chemistry of C_3N^+, we performed a brief study of the reactivity of the ion $C_4N_2^+$ with various neutrals (see **table 4.9**). Neither C_4N_2 nor its molecular ion have been detected in the interstellar environment, but this is not surprising in view of the symmetry of these species which would render them invisible at radio wavelengths. Yung[272] has proposed that the reaction of CN· with HC_3N should lead to the production of C_4N_2 in the atmosphere of Titan. This reaction has since been studied by Halpern et al:[196]

$$CN\cdot + HC_3N \rightarrow C_4N_2 + H\cdot \quad (4.23a)$$

$$\rightarrow HCN + C_3N\cdot \quad (4.23b)$$

$\Delta H_{4.23a} = -33$ kJ mol^{-1}

$\Delta H_{4.23b} = -21$ kJ mol^{-1}

$k_{4.23} = (1.70 \pm 0.08) \times 10^{-11}$ cm^3 molec^{-1} s^{-1}.

Table 4.9: Reactions of $C_4N_2^+ + X$.

X	Products [a]		k_{obs} [a]	k_c [a]	$-\Delta H$ [a]
H_2	no reaction		<0.001	1.49	–
CH_4	$C_4N_2H^+ + CH_3\cdot$		0.46	1.04	> 205 [b]
NH_3	$NH_3^+ + C_4N_2$		1.8	2.12	159
H_2O	$C_4N_2H^+ + OH\cdot$		0.56	2.35	> 144 [b]
N_2	no reaction		<0.001	0.69	–
O_2	$C_4N_2O^+ + O$ $C_4N_2O_2^+$	[0.70] [0.30]	0.004	0.62	169 [c] –
CO	$C_4N_2.CO^+$		0.075	0.74	–
C_2H_2	$C_2H_2^+ + C_4N_2$ $C_4N_2.C_2H_2^+$	[0.20] [0.80]	1.2	0.97	39 –
HCN	$C_4N_2.HCN^+$		1.2	3.12	–
CO_2	no reaction		<0.001	0.72	–
C_2N_2	$C_4N_2.C_2N_2^+$		0.40	0.94	–

Notes

a. See footnotes (a) - (d) for table (4.2).

b. Based on an upper limit $\Delta H_f(C_4N_2H^+) > 1248$ kJ mol^{-1}. [271]

c. Calculated assuming a $(N{\equiv}C)_2C{=}C{=}O^+$ structure for $C_4N_2O^+$.

The products of reaction (4.23) were not determined in the study by Halpern et al, but C_4N_2 is assumed to be the major product. The apparent existence of a small activation energy barrier (E_a ~ 6 kJ mol^{-1}) implies that this reaction will not be a significant source of interstellar C_4N_2, but it is able to account for C_4N_2 production in the warmer (T ~ 150K) atmosphere of Titan.

Very few ion-molecule studies involving C_4N_2 or $C_4N_2^+$ have been reported. Raksit and Bohme[247] determined that $C_4N_2^+$, presumably having the structure $C_2^+ \cdot C_2N_2$, is a minor product of the reaction of C_3N^+ with C_2N_2 (see also table 4.7). Bohme et al[271] also studied the reaction

$$C_4N^+ + CH_3CN \rightarrow C_2H_3^+ + C_4N_2 \quad [0.60] \quad (4.24a)$$

$$\rightarrow C_4N_2H^+ + C_2H_2 \quad [0.40] \quad (4.24b)$$

$k_{4.24} = 3.1 \times 10^{-9}$ cm^3 molec^{-1} s^{-1}

in which the products appear to include neutral and protonated dicyanoacetylene. The $C_4N_2H^+$ produced in this reaction was observed to proton-transfer rapidly to CH_3CN, suggesting PA(C_4N_2) < PA(CH_3CN) (788.0 kJ mol^{-1}).[185] This reaction suggests that C_4N_2 is indeed a likely constituent of interstellar clouds, since CH_3CN has been identified within dark clouds and since C_4N^+ is formed rapidly by the reaction of C^+ with HC_3N and is likely to be unreactive with H_2 at cloud temperature:

$$C^+ + HC_3N \rightarrow C_4N^+ + H\cdot \quad (4.25)$$

$$C_4N^+ + H_2 \rightarrow C_3H^+ + CHN \quad (4.26)$$

$k_{4.25} = 6.1 \times 10^{-9}$ cm^3 molec^{-1} s^{-1} [167,267]

$k_{4.26} = 2.2 \times 10^{-11}$ cm^3 molec^{-1} s^{-1} at 296K.[271]

The low rate constant observed for reaction (4.26) suggests that a barrier exists to inhibit this reaction. C_4N^+ should thus persist to allow reaction (4.24) to occur to some extent. For this reason, the reactions of C_4N_2 with various ions, and $C_4N_2H^+$ with various neutrals, are relevant to interstellar chemistry. The reactivity of $C_4N_2^+$, as described here, is also of potential interstellar relevance.

In the present study, $C_4N_2^+$ was generated in the ion source by electron impact on a 1:20 mixture of dicyanoacetylene in helium.

As demonstrated in table 4.9, the product channels evident in the reactions of $C_4N_2^+$ with the neutrals surveyed are adduct formation, atom abstraction and charge transfer. In this respect, the reactivity of $C_4N_2^+$ is similar to that of $C_2N_2^+$ generated from dicyanogen (as was seen in section 3.3). One unexpected observation is that $C_4N_2^+$ is unreactive with H_2, even though H-atom abstraction is highly exothermic:

$$C_4N_2^+ + H_2 \rightarrow C_4N_2H^+ + H\cdot \qquad (4.27)$$

$$\Delta H_{4.27} < -207 \text{ kJ mol}^{-1}.$$

The exothermicity of this reaction is calculated using Bohme's[271] experimental upper limit to $\Delta H_f(C_4N_2H^+)$. The failure of this reaction suggests that it is inhibited by a substantial activation barrier: if this is so, then $C_4N_2^+$ should be unreactive with interstellar hydrogen also. H-atom abstraction does occur in the reactions with CH_4 and H_2O, which are exothermic to a similar degree - there does not appear to be any barrier in these instances, though the reactions proceed with less than unit efficiency. Prodnuk et al[273] have commented that H-atom

abstraction reactions are commonly barrier-inhibited when the neutral reactant is H_2, but not otherwise: this is in accord with the results reported here.

Adduct formation is the most common channel, evident in the reactions with O_2, CO, HCN, C_2H_2 and C_2N_2. The rapidity of the termolecular association channels with CO, C_2H_2 and HCN indicate that radiative association may be an important reactive process of $C_4N_2^+$ within interstellar clouds. Cyclization of such adducts might well lead to aromatic ions which could be involved in gas-phase production of polycyclic aromatic hydrocarbons (PAHs) - though this is highly conjectural, especially since the structure of these adduct ions is not known from these SIFT studies. A major channel in the reaction with O_2 is O-atom abstraction: note that O-atom abstraction from CO_2 does not occur, perhaps indicating that this is an endothermic channel (there is no guarantee that the structure ascribed to $C_4N_2O^+$, based on the only structure explored in the compilation of ion thermochemistry[184] is correct in this instance: a more likely form is $ONCCCCN^+$, for which no thermochemical information is available) but more likely showing that the reaction with CO_2 is inhibited by a more substantial activation barrier than is the reaction with O_2.

Charge-transfer occurs in the reactions with C_2H_2 and NH_3: these represent pathways for neutralization of $C_4N_2^+$ in dense clouds. Since $C_4N_2^+$ does not react with H_2 and may not react rapidly with CO under interstellar conditions, dissociative recombination is an important reaction for removal of the ion: the most likely product channel is obviously

$$C_4N_2^+ + e \rightarrow C_3N\cdot + CN\cdot \qquad (4.28)$$

$$\Delta H_{4.28} = -609 \text{ kJ mol}^{-1},$$

since this is the most exothermic channel not involving rearrangement.

CHAPTER 5.

ISOMERISM OF CHN^+ AND CH_2N^+.

Section 5.1: CHN^+.

During the course of our brief study of $C_2N_2^+$ chemistry,[203] we investigated the reaction of $C_2N_2^+$ with HCN:

$$C_2N_2^+ + HCN \rightarrow CHN^+ + C_2N_2 \quad [0.20] \quad (5.1a)$$

$$\rightarrow C_2N_2H^+ + CN\cdot \quad [0.75] \quad (5.1b)$$

$$\rightarrow [C_2N_2.H.CN]^+ \quad [0.05] \quad (5.1c)$$

$k_{5.1} = 2.7 \times 10^{-9}$ cm^3 molec^{-1} s^{-1}.

The reaction rate and product distribution observed are both in serious disagreement with the findings of Inoue and Cottin,[274] who reported

$$C_2N_2^+ + HCN \rightarrow C_3N_3^+ + H\cdot \quad [1.0] \quad (5.1d)$$

$k_{5.1} = 1.5 \times 10^{-11}$ cm^3 molec^{-1} s^{-1}.

The discrepancies between these results arise from the differences in the experimental techniques used. Inoue and Cottin's experiments were performed in a mass spectrometer chamber containing C_2N_2 and HCN. Reactions were assigned upon the basis of the signals observed for various ions as a function of pressure: clearly, since the reaction chamber contained a multiplicity of possible

reactant ions at all pressures, the possibility for misinterpretation of the reaction chemistry involved was fairly high. In the SIFT, in contrast, a $C_2N_2^+$ ion signal can be injected free of contamination by any other ions and thus the product distribution obtained is much more reliable.

The product channels observed by us for reaction (5.1) appear, initially, to all be very straightforward processes. The major channel is hydrogen atom abstraction to form protonated dicyanogen (5.1b), and charge-transfer (5.1a) and adduction (5.1c) processes account for minor products. However, the apparent charge-transfer channel presents a problem. The ionisation potential of HCN is higher than that of C_2N_2 (IP(HCN) = 1312 ± 1 kJ mol^{-1}, while IP(C_2N_2)= 1290 ± 1 kJ mol^{-1}) and, therefore, charge-transfer in this manner is endothermic. An endothermic channel could not be expected to account for such a large fraction (20%) of the products of a collision-rate reaction, especially when the major product is strongly exothermic as is the case here ($\Delta H_{5.1b}$ = -140 kJ mol^{-1}). The existence of sufficient metastable excited $C_2N_2^+$ to account for the apparent charge-transfer channel is unlikely: therefore the product signal at (m/z = 27) is interpreted not as HCN^+ but as HNC^+. Formation of HNC^+ is energetically favourable (see **table 5.1**) but requires a substantially more complicated mechanism than merely the transfer of an electron. HNC^+ could be accounted for by the initial formation of a collision complex

$$C_2N_2^+ + HCN \rightarrow [C_2N_2^+.HCN] \qquad (5.2)$$

with substantial internal rearrangement of the complex preceding its dissociation into the observed products $C_2N_2H^+$ (+ CN·) and HNC^+ (+ C_2N_2). This type of

mechanism is supported by the detection of a primary product at m/z = 79, corresponding to the collisionally stabilised addition product $HC_3N_3^+$.

Having proposed that HNC^+ and not HCN^+ is being produced in this reaction, it becomes necessary to demonstrate this, and to this end we require a method of distinguishing HCN^+ from HNC^+. The different energies of HNC^+ and HCN^+ suggest that HCN^+ will display a higher gas-phase acidity than will HNC^+ - thus, HCN^+ should undergo proton transfer reactions more readily than HNC^+:

$$HCN^+ + X \rightarrow XH^+ + CN\cdot \qquad (5.3)$$

$$HNC^+ + X \rightarrow \text{no reaction} \qquad (5.4)$$

provided PA (CN· at C) < PA (X) < PA (CN· at N).

Table 5.1: Experimental and theoretical thermochemistry of CHN^+.

$\Delta H_f(HCN^+)$ [a]	$\Delta H_f(HNC^+)$ [a]	$\Delta H_f(TS)$ [a,b]	Method	Reference
1447	–	–	from IP(HCN)	184
–	1407	–	experimental bracketing	275
1437	1350	–	theoretical calculation [c]	276
–	1360	–	theoretical calculation [d]	277
–	1370	1572	theoretical calculation [e]	278
–	≤ 1373	–	experimental value [f]	279,280

Notes

a. Heats of formation are expressed in kJ mol^{-1}.
b. TS = transition state for isomerisation of CHN^+.
c. Green's function calculation of ionization potentials, using literature values[184] for $\Delta H_f(HCN)$ and $\Delta H_f(HNC)$
d. SCF calculation, adjusted to experimental $\Delta H_f(HCN^+)$.[184]
e. MP2/6-31G**/6-31G+ZPE calculations, adjusted to experimental $\Delta H_f(HCN^+)$.[184]
f. This work (see text for discussion).

The proton affinities of CN· have not been measured directly, but can be calculated from known heats of formation:

$$H^+ + CN\cdot \rightarrow HCN^+ \quad (5.5a)$$

$$\rightarrow HNC^+ \quad (5.5b).$$

$PA(\underline{C}N\cdot) = -\Delta H_{5.5a}$ and $PA(C\underline{N}\cdot) = -\Delta H_{5.5b}$ [where the underlined character indicates the site of protonation]. Using the appropriate ΔH_f values,[184] $PA(\underline{C}N\cdot) = 518 \pm 10$ kJ mol^{-1} and $PA(C\underline{N}\cdot) = 592 \pm 10$ kJ mol^{-1}. On the basis of these values, reaction with a species **X** for which PA(**X**) is between 518 and 592 kJ mol^{-1} should serve to distinguish HCN^+ from HNC^+, and may additionally allow refinement of $\Delta H_f(HCN^+)$ and $\Delta H_f(HNC^+)$.

The expectation that proton transfer would allow discrimination between HCN^+ and HNC^+ was not initially borne out by the experiments which were attempted (see **table 5.2**). Various neutrals with proton affinities within the appropriate range were tested for reaction with CHN^+, and none showed any proton-transfer reaction channels, or any reproducible curvature in the graph of ln (ion signal) versus reactant neutral pressure. The CHN^+ signal was obtained by various techniques (chiefly chemical ionisation and electron bombardment methods - see **table 5.3**) in an effort to find a technique which produced observable fractions of each isomer. The main method of CHN^+ production used was electron impact on HCN: this method was chosen partly for its simplicity and partly because it was felt that the ionisation process would produce initially HCN^+, with subsequent isomerisation to the more stable HNC^+ (provided that the initially formed HCN^+ possessed sufficient energy to overcome the barrier to

interconversion). The expectation was, therefore, that the m/z = 27 signal from this method should contain appreciable fractions of each isomer, simplifying the task of detecting curvature in the experimental graphs for reaction of CHN^+ with the neutral, **X**.

That this was not observed to be the case was most perplexing: reactions of CHN^+ with CO, CO_2, O_2, N_2O and C_2N_2 were studied in an effort to differentiate HCN^+ and HNC^+. Curvature was not seen in the semilogarithmic plots of ion signal against reactant neutral flows in any of these reaction studies, indicating either that only one isomer was present or that there was no observable difference in the reactivity of the two isomers. Of the reactants listed in table 5.2, CO, CO_2 and

Table 5.2: Reactions of CHN^+ + X, which failed to distinguish between HCN^+ and HNC^+.

X	Products [a]		k_{obs} [b]	k_c [c]	PA(X) [d]	IP(X) [e]
CO	$HCO^+ + CN\cdot$		0.0029	0.91	594	14.0139
O_2	$O_2^+ + HCN$	[.70]	0.50	0.77	422	12.071±.001
	$HCNO^+ + O$	[.20]				
	$NO+ + HCO\cdot$	[.10]				
C_2N_2	$C_2N_2H^+ + CN\cdot$		1.7	1.24	674 [f]	13.37 ± .01
N_2O	$N_2O^+ + HCN$	[.54]	1.2	1.04	581	12.886
	$HCNO^+ + N_2$	[.44]				
	$NO^+ + CHN_2$	[.02]				
CO_2	$CO_2^+ + HCN$	[.60]	0.0015	0.98	548	13.773±.002
	$CHN.CO_2^+$	[.40]				

Notes

a. Product channels reported in brackets, where more than one product was detected.
b. Observed rate coefficient, in units of 10^{-9} cm^3 $molec^{-1}$ s^{-1}.
c. Calculated ADO collision rate coefficient, using the theory of Su and Chesnavich.[172]
d. Proton affinity in units of kJ mol^{-1}. Taken from the tabulation of Lias et al,[185] unless otherwise stated.
e. Ionisation potential in units of kJ mol^{-1}. Taken from the tabulation of Lias et al,[184] unless otherwise stated.
f. Taken from reference 203.

N_2O were chosen on the basis of PA; O_2 and C_2N_2 were selected on the basis of IP, so that different rates were expected for proton transfer and/or for charge transfer with these reactants. The failure to see the desired channels for N_2O, O_2 and C_2N_2 was readily explained by the presence of other exothermic product channels for these reactants, but the very slow reaction rates seen for reaction of CHN^+ with CO and CO_2 were much more mysterious. Proton transfer from HCN^+ to CO or to CO_2 should occur rapidly, especially in the absence of competing product channels.

The dilemma posed by this apparent unreactivity of CHN^+ with CO and CO_2 was eventually resolved by recognising the following reaction mechanism occurred.

Table 5.3: Methods used for generating CHN^+ for reaction studies.

Code	Method	Site [a]	Comments
i	$Ar^+ + HCN \rightarrow CHN^+$	FT	CN^+ a minor product channel; CH_2N^+ formed from subsquent rapid reaction with HCN. Not a 'clean' source.
ii	$Ar^+ + HCN \rightarrow CHN^+$	IS	from a 10:1 mixture of Ar and HCN. Satisfactory in terms of size of CHN^+ ion signal: little contamination from adjacent masses.
iii	$CN^+ + H_2 \rightarrow CHN^+$	FT	CN^+ from $e + C_2N_2$ in ion source. Problems with CH_2N^+ contamination, small CHN^+ signal. Should give mostly HNC^+.
iv	$CN^+ + H_2 \rightarrow CHN^+$	IS	from a 20:1 mixture of H_2 and C_2N_2. Satisfactory.
v	$e + C_6H_5NH_2 \rightarrow CHN^+$	IS	Aniline used in an effort to generate HNC^+ free from HCN^+. Contamination at m/z = 27 by $C_2H_3^+$. Small signal obtained. Unsatisfactory.
vi	$e + HCN \rightarrow CHN^+$	IS	Satisfactory. Large signal at m/z = 27,little contamination from neighbouring masses.

Notes

a. Site of CHN^+ production. (FT = within the flow tube; IS = within the ion source)

A reactant **X** capable of accepting a proton from HCN^+ but not from HNC^+ may, upon collision with HCN^+, produce HNC^+ rather than XH^+. Such a process can take place because the collision complex has a sufficiently long lifetime for a second proton transfer to occur after proton transfer from HCN^+ to **X** - that is, proton transfer from XH^+ to NC:

$$HCN^+ + X \rightarrow (XH^+.CN)^* \quad (5.6a)$$

$$(XH^+.CN)^* \rightarrow (XH^+.NC)^* \quad (5.6b)$$

$$(XH^+.NC)^* \rightarrow X + HNC^+ \quad (5.6c).$$

Thus when no product channels apart from proton transfer are available for a reaction of HCN^+ with **X** (as is essentially the case for CO and CO_2), the major product channel will be isomerisation from HCN^+ to HNC^+. This change in the composition of the m/z= 27 ion signal is not detectable by the mass spectrometer and thus this isomerisation is not directly observable in the SIFT.

To demonstrate this isomerisation process, a reaction is required which distinguishes between HCN^+ and HNC^+ in some observable manner. The reactions of CHN^+ with CF_4 and with SF_6 were finally found to distinguish satisfactorily between HCN^+ and HNC^+:

$$HCN^+ + CF_4 \rightarrow CF_3^+ + HF + CN\cdot \quad (5.7)$$

$$HNC^+ + CF_4 \rightarrow \text{no reaction} \quad (5.8)$$

$k_{5.7} = 1.2 \times 10^{-9}$ cm^3 molec^{-1} s^{-1}

$k_{5.8} < 1.0 \times 10^{-11}$ cm^3 molec^{-1} s^{-1}

$$HCN^+ + SF_6 \rightarrow SF_5^+ + HF + CN\cdot \qquad (5.9)$$

$$HNC^+ + SF_6 \rightarrow HNCF^+ + SF_5\cdot \qquad (5.10)$$

$k_{5.9} = 1.3 \times 10^{-9}$ cm^3 molec^{-1} s^{-1}

$k_{5.10} = 1.2 \times 10^{-9}$ cm^3 molec^{-1} s^{-1}.

The reaction with CF_4 (5.7 & 5.8) was especially useful because it allowed direct determination of the HCN^+ / HNC^+ ratio in the m/z = 27 ion signal: the HCN^+ was that fraction of the m/z = 27 signal which disappeared upon addition of (sufficient) CF_4. **Figure 5.1** demonstrates the degree of curvature evident in the semilogaithmic graphs.

Figure 5.1: Experimental graph showing the reaction of CHN^+ with CF_4. HCN^+ reacts at the collision rate, while HNC^+ is unreactive: thus the isomeric ratio can be very easily determined. In this experiment, HCN^+ constituted 64% of the m/z 27 ion signal.

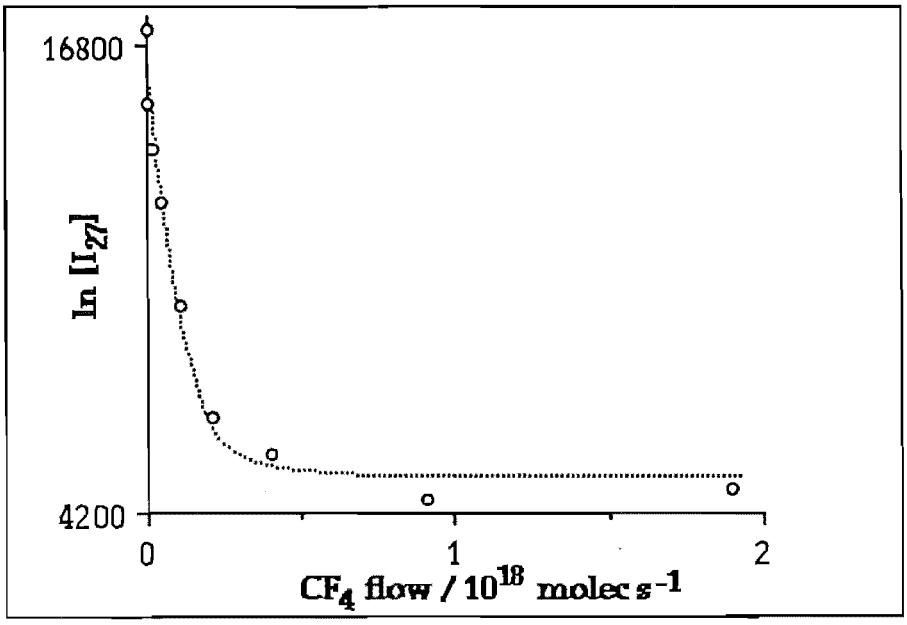

Reaction (5.7) may occur via proton-transfer ($PA(CF_4) \sim 527$ kJ mol^{-1}):[185]

$$HCN^+ + CF_4 \rightarrow (CF_4H^+.CN)^* \quad (5.7a)$$

$$(CF_4H^+.CN)^* \rightarrow (CF_4H^+)^* + CN\cdot \quad (5.7b)$$

$$(CF_4H^+)^* \rightarrow CF_3^+ + HF \quad (5.7c)$$

involving a mechanism in which isomerisation of HCN^+ to HNC^+ does not occur because the collision complex is weakly bound and so has too short a lifetime to permit the intramolecular rearrangement required for HNC^+ formation. Note that the mechanism above is one of several possible: others include fluoride ion transfer from CF_4 to HCN^+ (producing HCNF, which subsequently rearranges and dissociates as HF + CN·) and loss of HF rather than CN· in step (5.7b) above (followed by dissociation of CF_3CN^+ to give CF_3^+ + CN·). The mechanism for reaction of HCN^+ with SF_6 is similarly uncertain ($PA(SF_6)$ has not been determined) but most likely is analogous to that for reaction (5.7).

Reactions (5.7) to (5.10) permitted determination of the rate of isomerisation of HCN^+ by CO or by CO_2, by a method analogous to that detailed by Freeman et al.[206] For an experiment in which CHN^+ is injected into the flow tube, the isomerising gas CO_x (x = 1 or 2) is introduced at portal 1 with ensuing reaction

$$HCN^+ + CO_x \rightarrow HNC^+ + CO_x \quad (5.11),$$

and the titrating gas CF_4 is added at portal 2, the relevant equations for the changing concentrations of the ionic species involved are

$$[HCN^+]_{z_2} = [HCN^+]_0 \, (e^{-j_{5.11}z_1}) \, (e^{-j_{5.7}\, z_2}) \qquad \{5.i\}$$

$$[HNC^+]_{z_2} = [HNC^+]_0 + \left([HCN^+]_0(1-e^{-j_{5.11}(z_1-z_2)})\right) + \left([HCN^+]_0 \, (e^{-j_{5.11}(z_1-z_2)})(1-e^{-j_{5.11}z_2/(j_{5.7}+j_{5.11})})\right) \qquad \{5.ii\}$$

$$[CF^+]_{z_2} = [HCN^+]_0 \, e^{-j_{5.11}(z_1-z_2)} \, (1 - e^{-j_{5.7}z_2/(j_{5.7}+j_{5.11})}) \qquad \{5.iii\}$$

(where z_i is the reaction length for portal i, and

$$j_i = C \, k_i \, f_B \qquad \{5.iv\}$$

where f_B is the flux, in molec s^{-1}, of the reactant neutral B added to the tube and C has the form

$$C = \frac{\gamma}{\omega} \frac{(1-\varepsilon)}{\pi \, r^2 \, v_{buff}^2} \qquad \{5.v\}$$

(for which $\frac{\gamma}{\omega}$ and ε are flow coefficients as defined in section 2.2, r is the flow tube radius, and v_{buff} is the buffer gas velocity within the flow tube)). Solution of equations {5.i}-{5.iii}[281] yields the expression

$$C \, k_{5.11} \, f_{CO_x} \, z_1 = \ln(X^0_{HCN^+}) - \ln(X_{HCN^+} \, (1 - \beta)) \qquad \{5.vi\}$$

$$\therefore \qquad k_{5.11} = \frac{[\ln(X^0_{HCN^+}) - \ln(X_{HCN^+} \, (1-\beta))]}{C \, f_{CO_x} \, z_1} \qquad \{5.vii\},$$

$$X_{HCN^+} = \frac{[HCN^+]}{[HCN^+] + [HNC^+]}, \quad X = X^\circ \text{ at } f_{CO_x} = 0 \qquad \{5.viii\},$$

$$\beta = X^0_{HCN^+} (K'_{CO_x} - K_{CO_x}) \qquad \{5.ix\}$$

with $$K_{CO_x} = e^{j5.11z_1} \qquad \{5.x\}$$

and $$K'_{CO_x} = e^{j5.11(z_1 - z_2)} \qquad \{5.xi\}.$$

From equations {5.v}, {5.vii}, {5.ix} and {5.x} above, it can be seen that solution of $k_{5.11}$ requires prior solution of β, and solution of β requires prior solution of $k_{5.11}$. Thus solution of $k_{5.11}$ must be an iterative process, with some approximate value of $k_{5.11}$ initially being chosen to define approximately the parameter β. Since isomerisation was seen to be rapid, with relatively small flows of CO_x being required to effect noticeable changes in the HCN^+ / HNC^+ isomer ratio, the ADO rate coefficients[172] for collision of $CHN^+ + CO_x$ were selected as the initial approximation to $k_{5.11}$:

$$k_{c,5.11} = 9.19 \times 10^{-10} \text{ cm}^3 \text{ molec}^{-1} \text{ s}^{-1} \text{ for } CO_x = CO$$

$$k_{c,5.11} = 9.28 \times 10^{-10} \text{ cm}^3 \text{ molec}^{-1} \text{ s}^{-1} \text{ for } CO_x = CO_2.$$

Under the operating conditions employed in the Canterbury SIFT (T = 300K, P = 0.300 Torr of He), values of the other parameters required were

$$r = 3.66 \text{ cm}$$

$$v_{buff} = 8133 \text{ cm s}^{-1}$$

$$z_1 = 82.7 \text{ cm}$$

$$z_2 = 42.7 \text{ cm}$$

$$\frac{\gamma}{\omega} = 0.6465$$

$$\varepsilon = 5.385 \times 10^{-3}$$

$\therefore$ $$C = 2.310 \times 10^{-10} \text{ s cm}^{-3}.$$

The isomerisation experiments were performed by establishing a CHN^+ signal by injection of m/z 27 from HCN in the ion source and varying the flow of CF_4 in order to determine X_{HCN^+} for the flow of CO_x being applied. A range of CO flows, from $f_{CO} = 0$ to 2.7×10^{17} molec s^{-1}, was employed; CO_2 flows used ranged from $f_{CO_2} = 0$ to 1.6×10^{17} molec s-1 (see **tables 5.4 & 5.5**). $k_{5.11}$ was determined as the slope of the resulting graph (see **figures 5.2 & 5.3**) of $[\ln(X^0_{HCN^+}) - \ln(X_{HCN^+}(1 - \beta))]$ versus $Cf_{CO_x}z_1$.

The values found after three iterations (convergence was obtained rapidly) were

$$k_{5.11} = (4.63 \pm 0.4) \times 10^{-10} \text{ cm}^3 \text{ molec}^{-1} \text{ s}^{-1} \text{ for } CO_x = CO,$$

and $$k_{5.11} = (5.01 \pm 0.7) \times 10^{-10} \text{ cm}^3 \text{ molec}^{-1} \text{ s}^{-1} \text{ for } CO_x = CO_2.$$

Once the rate of isomerisation by CO_x was established, the reactions of HNC^+ with various neutrals (see **table 5.6**) were studied by addition at portal 1 of sufficient CO_x to convert >99 % of HCN^+ to HNC^+. Product channels then identified for the reaction of the ion signal at m/z = 27 with the relevant neutrals were inferred to be entirely due to HNC^+ (though care was taken to verify that none of the products observed arose from reaction of some primary product with the isomerising gas CO_x).

Having assigned the products due to HNC^+, products due to HCN^+ were inferred (see **table 5.7**) by studying the product ratios for reaction of the m/z = 27 ion signal (in the absence of the isomerising gas) with various neutrals: the proportion of HNC^+ to HCN^+ in the reactant ion signal was determined by titration with CF_4 or SF_6 and the proportions of each product channel due to HNC^+ were subtracted

from the observed total for each product channel. In some cases (because of cumulative uncertainties), product ions could not be ruled out as minor product channels for the reaction of HCN^+ with the neutral in question - for example,

$$HCN^+ + N_2O \rightarrow N_2O^+ + HCN \quad [>0.90] \quad (5.12a)$$

$$\rightarrow HCNO^+ + N_2 \quad [<0.10] \quad (5.12b)$$

Table 5.4: Calculation of the rate of HCN^+ isomerisation by CO.

First iteration: using $k_{isom} = 9.19 \times 10^{-10}$ cm^3 molec^{-1} s^{-1} (calculated collision rate)

$C f_{CO} z_1$ [a]	j_{isom} [a]	X_{HCN^+} [a]	β [a]	$\ln(X°_{HCN^+})-\ln(X_{HCN^+}(1-\beta))$ [a]
0	0	0.7325	0	0
4.11×10^8	4.564×10^{-3}	0.631	0.1080	0.263
7.53×10^8	8.364×10^{-3}	0.547	0.1575	0.463
1.316×10^9	1.463×10^{-2}	0.434	0.1896	0.734
2.961×10^9	3.290×10^{-2}	0.232	0.1482	1.310
5.215×10^9	5.795×10^{-2}	0.0851	0.0066	2.160

Second iteration: using $k_{isom} = 4.38 \times 10^{-10}$ cm^3 molec^{-1} s^{-1} (from first iteration)

$C f_{CO} z_1$	j_{isom}	X_{HCN^+}	β	$\ln(X°_{HCN^+})-\ln(X_{HCN^+}(1-\beta))$
0	0	0.7325	0	0
4.11×10^8	2.175×10^{-3}	0.631	0.0596	0.211
7.53×10^8	3.986×10^{-3}	0.547	0.0977	0.395
1.316×10^9	6.971×10^{-3}	0.434	0.1427	0.677
2.961×10^9	1.568×10^{-2}	0.232	0.1920	1.363
5.215×10^9	2.762×10^{-2}	0.0851	0.1680	2.337

Third iteration: using $k_{isom} = 4.68 \times 10^{-10}$ cm^3 molec^{-1} s^{-1} (from second iteration)

$C f_{CO} z_1$	j_{isom}	X_{HCN^+}	β	$\ln(X°_{HCN^+})-\ln(X_{HCN^+}(1-\beta))$
0	0	0.7325	0	0
4.11×10^8	2.32×10^{-3}	0.631	0.063	0.214
7.53×10^8	4.26×10^{-3}	0.547	0.103	0.401
1.316×10^9	7.45×10^{-3}	0.434	0.148	0.684
2.961×10^9	1.68×10^{-2}	0.232	0.192	1.363
5.215×10^9	2.95×10^{-2}	0.0851	0.161	2.328

Notes

a. See text for definition of parameters.

$$HNC^+ + N_2O \rightarrow HNCO^+ + N_2 \quad [0.55] \quad (5.13a)$$

$$\rightarrow NO^+ + HNCN \quad [0.45] \quad (5.13b).$$

In these experiments, CHN^+ was produced by electron impact upon HCN and the resultant m/z = 27 ion signal was found to contain 70% HCN^+, by titration with CF_4. The product signal at m/z = 43, corresponding to $HCNO^+$ / $HNCO^+$, was probably due to reaction of HNC^+ only, but a small product channel at this mass due to HCN^+ could not be ruled out given the uncertainty in the product ratio determination and in the HCN^+ / HNC^+ ratio, or on the basis of available energy ($\Delta H_{5.12b}$ = -266 kJ mol^{-1}). The structures of the ions at m/z = 43 are those conjectured to be most likely on the grounds of minimal rearrangement to products.

Figure 5.2: Graph showing calculated rate of isomerisation of HCN^+ by CO. The parameters calculated are from table 5.4, and yield a slope of $(4.63 \pm 0.4) \times 10^{-10}$ cm^3 $molec^{-1}$ s^{-1}; this slope is equal to the rate coefficient for isomerisation to HNC^+, and is about half the calculated collision rate. The results shown are from the third iteration, and reflect a change of 1.1% from the rate determined from the second iteration: since the convergence at this stage appeared sufficiently rapid, no further iterations were performed.

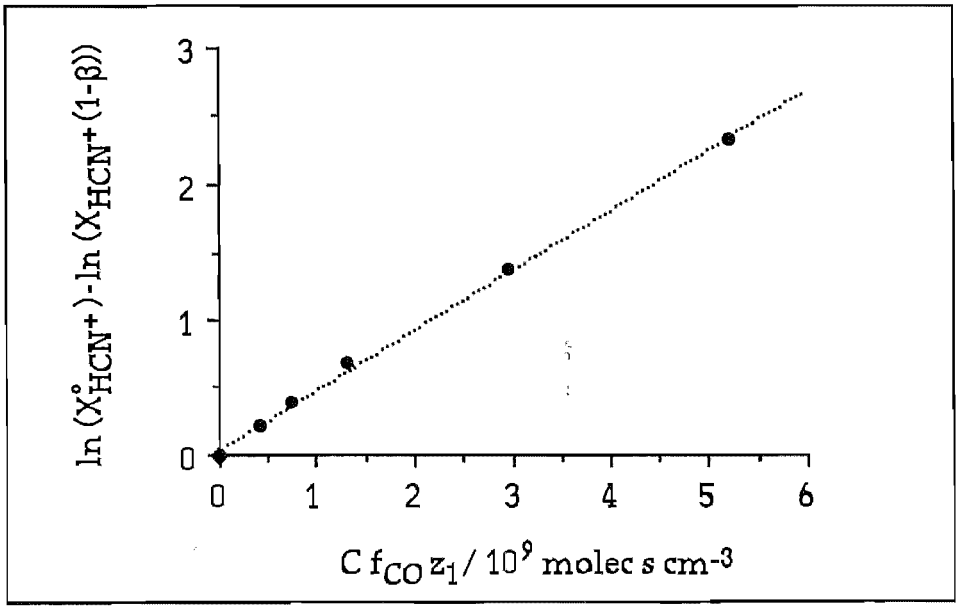

For the reactions with C_2H_2, both isomers were observed to react at the collision rate:

$$HCN^+ + C_2H_2 \rightarrow C_2H_2^+ + HCN \quad [>0.85] \quad (5.14a)$$

$$\rightarrow C_2H_3^+ + CN\cdot \quad [<0.15] \quad (5.14b)$$

$$HNC^+ + C_2H_2 \rightarrow C_2H_2^+ + HCN \quad [>0.50] \quad (5.15a)$$

$$\rightarrow C_2H_3^+ + CN\cdot \quad [<0.15] \quad (5.15b)$$

$$\rightarrow C_3H_2N^+ + H\cdot \quad [>0.35] \quad (5.15c).$$

Table 5.5: Calculation of the rate of HCN^+ isomerisation by CO_2.

First iteration: using $k_{isom} = 9.28 \times 10^{-10}$ cm^3 molec^{-1} s^{-1} (calculated collision rate)

C f_{CO_2} z_1 [a]	j_{isom} [a]	X_{HCN^+} [a]	β [a]	$\ln(X°_{HCN^+})-\ln(X_{HCN^+}(1-\beta))$ [a]
0	0	0.7325	0	0
4.55×10^8	5.102×10^{-3}	0.591	0.1420	0.339
8.58×10^8	9.625×10^{-3}	0.519	0.1905	0.669
1.685×10^9	1.891×10^{-2}	0.381	0.1680	0.865
3.076×10^9	3.451×10^{-2}	0.209	0.1169	1.408

Second iteration: using $k_{isom} = 5.42 \times 10^{-10}$ cm^3 molec^{-1} s^{-1} (from first iteration)

C f_{CO_2} z_1	j_{isom}	X_{HCN^+}	β	$\ln(X°_{HCN^+})-\ln(X_{HCN^+}(1-\beta))$
0	0	0.7325	0	0
4.55×10^8	2.980×10^{-3}	0.591	0.0777	0.295
8.58×10^8	5.621×10^{-3}	0.519	0.1248	0.478
1.685×10^9	1.104×10^{-2}	0.381	0.1770	0.848
3.076×10^9	2.016×10^{-2}	0.209	0.1888	1.463

Third iteration: using $k_{isom} = 5.01 \times 10^{-10}$ cm^3 molec^{-1} s^{-1} (from second iteration)

C f_{CO_2} z_1	j_{isom}	X_{HCN^+}	β	$\ln(X°_{HCN^+})-\ln(X_{HCN^+}(1-\beta))$
0	0	0.7325	0	0
4.55×10^8	2.75×10^{-3}	0.591	0.0725	0.290
8.58×10^8	5.20×10^{-3}	0.519	0.119	0.471
1.685×10^9	1.02×10^{-2}	0.381	0.172	0.842
3.076×10^9	1.86×10^{-2}	0.209	0.191	1.466

Notes

a. See text for definition of parameters.

Product channels (5.14b) and (5.15b) were not observable, since the product ions have m/z = 27 and are thus indistinguishable from CHN^+. These product channels could not be excluded, given the uncertainty in the rate coefficient determination and upon the basis of exothermicity ($\Delta H_{5.14b}$ = -128 kJ mol^{-1}; $\Delta H_{5.15b} \geq$ -54 kJ mol^{-1}). The channels positively identified for reactions (5.14) and (5.15) are more exothermic than these possible proton-transfer channels, but proton transfer is often able to compete efficiently with more exothermic processes: for example, in the reaction of $C_4H_3^+$ with CH_3NO_2 as described in section 3.4, a barely exothermic proton transfer channel was seen to accompany production of CH_3CNH^+ with an exothermicity of several hundred kJ mol^{-1}.[282]

Figure 5.3: Graph showing calculated rate of isomerisation of HCN^+ by CO_2, using parameters from table 5.5. The rate coefficient for isomerisation to HNC^+ is (5.01 ± 0.7) x 10^{-10} cm^3 $molec^{-1}$ s^{-1}. As with figure 5.2, the graph shows the results of the third and final iteration.

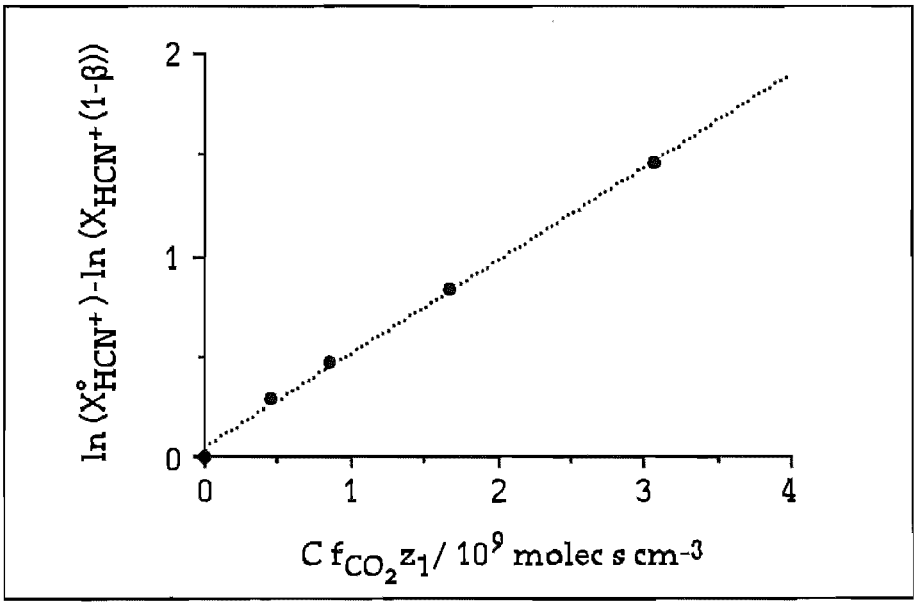

Similarly, $C_2H_3^+$ could not be excluded as a product of the reactions with CH_4:

$$HCN^+ + CH_4 \rightarrow HCNH^+ + CH_3\cdot \quad [>0.85] \quad (5.16a)$$

$$\rightarrow C_2H_3^+ + NH_2\cdot \quad [<0.15] \quad (5.16b)$$

$$HNC^+ + CH_4 \rightarrow HCNH^+ + CH_3\cdot \quad [>0.85] \quad (5.17a)$$

$$\rightarrow C_2H_3^+ + NH_2\cdot \quad [<0.15] \quad (5.17b).$$

Table 5.6: Reactions of $HNC^+ + X$.

X	Products [a]		k_{obs} [a]	k_c [a]	$-\Delta H$ [b]
SF_6	$HNCF^+ + SF_5\cdot$		1.2	1.2	~ 132
CF_4	no reaction		<0.005	1.0	–
CO	no reaction		<0.002	0.91	–
CO_2	products [c]		0.0012	0.98	–
N_2O	$HNCO^+ + N_2$	[.55]	1.1	1.04	440
	$NO^+ + HNCN$	[.45]			> 0
O_2	$HNCO^+ + O$	[.75]	0.36	0.77	109
	$NO^+ + HCO\cdot$	[.25]			344
CH_4	$HCNH+ + CH_3\cdot$	[≥ 85%] [d]	1.1	1.2	134
C_2H_2	$C_2H_2^+ + HCN$	[≥ 50%] [d]	1.5	1.2	138
	$C_3H_2N^+ + H\cdot$	[≥ 35%] [d]			255
N_2	no reaction		< 0.001	0.84	–
H_2	$CH_2N+ + H\cdot$		0.70	1.54	208

Notes

a. See footnotes (a) - (c) for table (5.2).
b. Reaction exothermicity in units of k] mol^{-1}. Taken from the tabulation of Lias et al,[184] unless otherwise stated.
c. See text for discussion.
d. A minor channel (≤ 15%) is also possible for $C_2H_3^+$ formation. See text.

These reactions (excluding the "invisible" channels (5.16b) and (5.17b)) were observed to occur upon virtually every collision, which means that channels leading to $C_2H_3^+$ could not exceed 15% of the product distribution given the uncertainty in the rate coefficient determination. Production of $C_2H_3^+$ is exothermic for HCN^+ ($\Delta H_{5.16b}$ = -72 kJ mol^{-1}) and possibly exothermic for HNC^+, within experimental uncertainty ($\Delta H_{5.17b} \geq +2 \pm 12$ kJ mol^{-1}), but is unlikely in view of the high exothermicity of the competing H-atom transfer (5.16a, 5.17a) and the improbability of breakage of the C-N bond during reaction.

Table 5.7: Reactions of HCN^+ + X.

X	Products [a]		k_{obs} [a]	k_c [a]	- ΔH [a]
SF_6	SF_5^+ + HF + CN·		1.3	1.2	49
CF_4	CF_3^+ + HF + CN·		1.2	1.0	? [b]
CO	HNC^+ + CO	[.99]	0.46	0.91	~ 74
	HCO^+ + CN·	[.01]			73
CO_2	HNC^+ + CO_2	[>.99]	0.50	0.98	~ 74
	CO_2^+ + HCN	[.003]			-16
N_2O	N_2O^+ + HCN	[>.90]	1.2	1.04	69
	$HCNO^+$ + N_2	[<.10]			266
O_2	O_2^+ + HCN		0.50	0.77	147
CH_4	$HCNH^+$ + CH_3·	[>0.85] [c]	1.1	1.2	208
C_2H_2	$C_2H_2^+$ + HCN	[>0.85] [c]	1.5	1.2	212
N_2	no reaction		< 0.001	0.84	–
H_2	CH_2N^+ + H·	[>.90]	0.86	1.54	282
	HNC^+ + H_2	[<.10]			74

Notes
a. See footnotes (a) - (c) for table (5.2), (b) for table (5.6).
b. See text for discussion.
c. A minor channel (≤ 15%) is also possible for $C_2H_3^+$ formation: see text.

For the reactions with O_2, both isomers were observed to react with similar efficiencies: only HCN^+ displayed charge transfer, suggesting IP(HNC) < IP(O_2) since the rate coefficient observed for $HNC^+ + O_2$ was only half the calculated rate coefficient.

$HNC^+ + O_2$	$\rightarrow$	$HNCO^+ + O$	[0.75]	(5.18a)
	$\rightarrow$	$NO^+ + HCO\cdot$	[0.25]	(5.18b)
	$\not\rightarrow$	$O_2^+ + HNC$		(5.18c)

The absence of channel (5.18c) thus implies IP(HNC) < 12.071 eV, which is lower than a value of 12.5 ± 0.2 eV obtained by charge exchange bracketing from HNC^+ generated from CH_3NC,[275] but which is in agreement with our determination of $\Delta H_f(HNC^+) \leq 1373$ kJ mol^{-1} from the proton-transfer isomerisation of HCN^+ by CO.

The similarity of the rate coefficients for reaction of HCN^+ and HNC^+ with O_2 ($k_{HCN^+} = 1.4\ k_{HNC^+}$) ensured that there was insufficient curvature evident [in the experimentally obtained graph of ln(ion signal at m/z 27) versus O_2 concentration] to identify two reactive components. For this reason O_2 could not be used as a means of distiguishing HCN^+ from HNC^+, hence its position in table 5.2 among the other reagents that did not, by themselves, permit discrimination of HCN^+/HNC^+.

The reactions with CO_2 deserve further mention. In the absence of CO (added, to effect isomerisation, from the first inlet port), a very slow decay in the m/z 27 ion signal was evident, with a product signal at m/z 44 indicating the presence of

charge transfer to CO_2. This is, of course, in competition with a fairly rapid isomerisation:

$$HCN^+ + CO_2 \rightarrow HNC^+ + CO_2 \quad [0.997] \quad (5.19a)$$

$$\rightarrow CO_2^+ + HCN \quad [0.003] \quad (5.19b).$$

The very slow charge-transfer process represented by channel (5.19b) is entirely consistent with known thermochemical values. IP(CO2) - IP(HCN) = 17 ± 1 kJ mol^{-1}, and on the basis of the Arrhenius expression for the upper limit to the rate of an endothermic process,

$$k_{5.19b} \leq k_c\, e^{-\Delta H_{5.19b}/RT}$$

$$\therefore \quad k_{5.19b} \leq 2.0 \times 10^{-3}\, k_c \quad @\,300K$$

$$\therefore \quad k_{5.19b} \leq 2.0 \times 10^{-12}\ cm^3\ molec^{-1}\ s^{-1},$$

which is in accord with the observed effective rate coefficient $k_{5.19b} = 1.5 \times 10^{-12}$ $cm^3\ molec^{-1}\ s^{-1}$. Upon the addition of CO, essentially complete conversion of HCN^+ to HNC^+ could be effected: reaction of the m/z 27 ion signal with CO_2 then exhibited an adduct signal only ($HNC.CO_2^+$, m/z = 71). This product signal was not evident in the absence of CO, which suggests that it may have arisen by a ligand-switching mechanism

$$HNC^+ + CO + He \rightarrow HNC.CO^+ + He \quad (5.20)$$

$$HNC.CO^+ + CO_2 \rightarrow HNC.CO_2^+ + CO \quad (5.21)$$

rather than by simple termolecular association of HNC^+ with CO_2. The adduct produced by the proposed reaction (5.20), $HNC.CO^+$ (m/z = 55), was not detected, but a weakly-bound adduct might not survive the ion sampling system downstream from the flow tube.

The absence of proton transfer from HNC^+ to CO indicates that this process is endothermic (as indeed is required by the forth-and-back proton transfer mechanism invoked for isomerisation of HCN^+ by CO). A mildly endothermic proton-transfer process might still be observable, in the absence of competing product channels, so the absence of such a proton-transfer channel in the case of HNC^+ with CO suggests that this process is considerably endothermic ($\Delta H \geq +10$ kJ mol^{-1}). However, the absence of an expected product channel is not an adequate basis for establishing thermochemistry and so the threshold for $\Delta H_f(HNC^+)$ is best expressed as ≤ 1373 kJ mol^{-1}.

Other systems in which ion-molecule reactions are involved in isomerisation are HCO^+/HOC^+ and $HNNO^+/NNOH^+$. HOC^+, which has been studied by Freeman et al,[166,206] is seen to undergo conversion to the lower-energy isomer HCO^+ by reaction with CO and with H_2:

$$HOC^+ + CO \rightarrow HCO^+ + CO \qquad (5.22)$$

$$k_{5.22} = 6.0 \times 10^{-10} \text{ cm}^3 \text{ molec}^{-1} \text{ s}^{-1}$$

$$HOC^+ + H_2 \rightarrow H_3^+ + CO \qquad [0.57] \qquad (5.23a)$$

$$\rightarrow HCO^+ + H_2 \qquad [0.43] \qquad (5.23b)$$

$$k_{5.23} = 4.7 \times 10^{-10} \text{ cm}^3 \text{ molec}^{-1} \text{ s}^{-1}.$$

The reaction with H_2 is interpreted as involving initial proton transfer (which is endothermic by ~ 3 kJ mol^{-1})[263] to H_2, followed by rotation of CO within the collision complex and subsequent proton transfer back to CO, yielding HCO^+. The low efficiency of this isomerisation process reflects the endothermicity of the initial proton transfer to H_2 and the relatively low probability of CO rotation within the complex before fragmentation: CO has a very small dipole moment (μ = 0.112 debye), so the forces inducing rotation will be weak compared with those for HCN^+ isomerisation by **X**: rotation of the $(NC\cdots H\mathbf{X}^+)$ complex is favoured by the large dipole moment (μ = 1.45 debye) of CN.

Conversion of $HNNO^+$ to the more stable isomer $NNOH^+$ has not been directly observed,[262] but this isomerisation has been implicated in the reaction with NO which has been analysed by Ferguson:[263]

$$HNNO^+ + NO \rightarrow NO^+ + N_2 + OH\cdot \qquad (5.24)$$

$k_{5.24} = 1.4 \times 10^{-11}$ cm^3 $molec^{-1}$ s^{-1}.

This reaction, which is observed to proceed more slowly than the corresponding reaction of the lower-energy isomer $NNOH^+$,[262] is interpreted in terms of a mechanism involving exothermic proton transfer to NO, rotation of NNO within the collision complex, exothermic proton transfer to NNO, and subsequent dissociative charge transfer:

$$ONNH^+ + NO \rightarrow (ONN\cdots HNO)^+ \qquad (5.24a)$$

$$(ONN\cdots HNO)^+ \rightarrow (NNO\cdots HNO)^+ \qquad (5.24b)$$

$$(NNO\cdots HNO)^+ \rightarrow (NNOH\cdots NO)^+ \qquad (5.24c)$$

$$(NNOH\cdots NO)^+ \rightarrow NO^+ + N_2 + OH\cdot \qquad (5.24d).$$

The necessity for such a complicated mechanism is that thermochemistry constrains the neutral products to be N_2 and OH·, the formation of which requires substantial rearrangement of the collision complex. It is quite conceivable that this reaction also results in the direct conversion of a fraction of the $HNNO^+$ to $NNOH^+$ via dissociation of the complex following step (5.24c), but this has not been experimentally verified.

In the present work, further experiments were performed to investigate the ratio of HCN^+/HNC^+ isomers produced in various reactions. The results of these experiments are summarised in **table 5.8**. It might intuitively be expected that any reaction of the form

$$\mathbf{X}^+ + HCN \rightarrow HCN^+ + \mathbf{X} \qquad (5.25a)$$

$$\rightarrow HNC^+ + \mathbf{X} \qquad (5.25b)$$

would tend to form predominantly HCN^+, since this higher-energy ion can be produced by a simple charge exchange while HNC^+ can only be produced by rearrangement of an excited HCN^+ product (or within an $\mathbf{X}\cdots HCN^+$ collision complex). If the barrier to isomerisation is high, as Koch et al[278] have calculated, then isomerisation can occur only within the collision complex unless reaction (5.25a) is sufficiently exothermic to allow the unimolecular reaction

$$(HCN^+)^* \rightarrow (HNC^+)^* \qquad (5.26)$$

$$E_a \sim 120 \text{ kJ mol}^{-1}$$

to occur also. For a simple charge transfer reaction, collision complexes should be comparatively short-lived, and much of the excess energy released by charge

Table 5.8: Miscellaneous other reactions.

Reaction	Products [a]		k_{obs} [a]	k_c [a]	$-\Delta H$ [a]
$Ar^+ + SF_6$	$SF_5^+ + Ar + F\cdot$	[>.99] [b]	1.54	1.0	209
$CN^+ + H_2$	$HCN^+ + H\cdot$	[0.57] [c]	1.79	1.5	130
	$HNC^+ + H\cdot$	[0.43] [c]			204
$C_2N_2^+ + HCN$	$HNC^+ + C_2N_2$	[0.20]	2.7	3.3	52
	$C_2N_2H^+ + CN\cdot$	[0.75]			133
	$C_3N_3H^+$	[0.05]			–
$O^+ + HCN$	$NO^+ + CH\cdot$	[0.55]	3.9	4.4	118
	$HCN^+ + O$	[0.15] [c]			2
	$HNC^+ + O$	[0.06] [c]			76
	$CHO^+ + N\cdot$	[0.19]			400 [d]
	$CO^+ + NH$	[0.05]			80
$Ar^+ + HCN$	$HCN^+ + Ar$	[0.74] [c]	0.38	3.5	209
	$HNC^+ + Ar$	[0.26] [c]			283
$N^+ + HCN$	$HCN^+ + N$	[0.91] [c]	– [e]	4.6	91
	$HNC^+ + N$	[0.09] [c]			165
$N_2^+ + HCN$	$HCN^+ + N_2$	[0.78] [c]	0.39 [f]	3.8	191
	$HNC^+ + N_2$	[0.22] [c]			265
$Kr^+ + HCN$	$HCN^+ + Kr$	[0.78] [c]	– [e]	3.1	39
	$HNC^+ + Kr$	[0.22] [c]			113
$CO_2^+ + HCN$	$HCN^+ + CO_2$	[0.59] [c]	3.4	3.4	17
	$HNC^+ + CO_2$	[0.41] [c]			91
$CN^+ + HCN$	$HCN^+ + CN\cdot$	[0.45] [c]	2.7 [f]	3.8	48
	$HNC^+ + CN\cdot$	[0.55] [c]			122
$CN^+ + CO$	$CO^+ + CN\cdot$		0.39	0.92	7

Notes

a. See footnotes (a) - (c) for table (5.2), (b) for table (5.6).
b. Minor product seen [~.001] at m/z = 89, corresponding to SF_3^+.
c. Product ratio determined by reaction of CHN^+ with CF_4.
d. Calculated exothermicity for formation of HCO^+. $-\Delta H$ = 262 kJ mol^{-1} for production of COH^+.
e. Rate coefficient not determined.
f. Rate coefficient not determined in this work. Literature value quoted from the compilation of Anicich & Huntress.[182]

transfer should be localised within the ionic product: thus, isomerisation should occur reasonably efficiently for those charge-transfer reactions which have an exothermicity greater than E_a. The efficiency of HNC^+ production by this method will depend upon the competition between the unimolecular isomerisation (5.26) and the collisional quenching of internally excited CHN^+ by He. Charge-transfer reactions less exothermic than E_a should not result in noticeable isomerisation of HCN^+.

Of the reactions $\mathbf{X}^+ + HCN$ in table 5.8, those with $\mathbf{X} = N_2$ and Ar have sufficiently exothermic charge-transfer channels to allow subsequent isomerisation; for $\mathbf{X} =$ $N\cdot$, O, Kr, CO_2 and $CN\cdot$, no HNC^+ should be produced if the reaction initially occurs as the transfer of an electron from HCN to $\mathbf{X}^+$. This expectation is not well met by the data observed.

The observation of ~20-25% HNC^+ formation in the reactions of Ar^+ and N_2^+ is quite consistent with the expectation that some HNC^+ should be produced by charge-transfer in these instances, but several of the other reactions also produce comparable yields of HNC^+. How ?

One possibility is that the reactant ions may possess vibrational or rotational excitation. In all cases, ions were produced in the ion source by electron bombardment: the high energies of the electrons emitted from the filament easily permit production of excited ions, which might not be adequately quenched by repeated collisions with the He buffer gas. Metastable electronic excitation, for example, might account for the production of some HNC^+ in the reactions with N^+ and Kr^+. The lowest metastable electronic state of N^+ is the

$^1D_2$ state, which lies 183 kJ mol^{-1} above the ground state ($^3P_0$). The lowest such states for Kr^+ are the $^2P_{0\frac{1}{2}}$ and $^4P_{2\frac{1}{2}}$ states, which are 64.3 kJ mol^{-1} and 1350 kJ mol^{-1}, respectively, above the ground state ($^2P_{1\frac{1}{2}}$).[283]

Other factors are likely to apply in the reactions of O^+, CN^+ and CO_2^+. With O^+, several product channels are evident, and some of the products (NH, HCO^+) require rearrangement. If such rearrangement can occur for these products, it is reasonable to expect that it can occur also to produce HNC^+.

The reaction of CN^+ may involve charge-transfer or H-atom abstraction: the latter process will tend to favour HNC^+ production, so the HNC^+ formed in this reaction can be taken as a lower limit of the extent of H-atom transfer in this reaction. Similarly, the reaction of CN^+ with H_2 (which we have studied also) appears to produce a ~1:1 mixture of the two isomers.

Charge-transfer from CO_2 is only slightly exothermic, and for this reason (and since a $CO_2.HCN^+$ complex features many vibrational and rotational modes among which internal energy may be partitioned) the collision complex may be relatively long-lived. HNC^+ can be produced by forth-and-back proton transfer within such a complex:

$$CO_2^+ + HCN \rightarrow (OCO\cdots HCN)^+ \quad (5.27a)$$

$$(OCO\cdots HCN)^+ \rightarrow (OCOH\cdots CN)^+ \quad (5.27b)$$

$$(OCOH\cdots CN)^+ \rightarrow (OCOH\cdots NC)^+ \quad (5.27c)$$

$$(OCOH\cdots NC)^+ \rightarrow (OCO\cdots HNC)^+ \quad (5.27d)$$

$$(OCO\cdots HNC)^+ \rightarrow HNC^+ + CO_2 \quad (5.27e).$$

This mechanism seems satisfactory to account for the especially high efficiency of HNC^+ production in this charge-transfer process.

Another factor which must be addressed is that the HCN^+/HNC^+ ratio might be dependent upon the quantity of HCN added in the above experiments. Specifically, is HCN^+ converted to HNC^+ in reactions with neutrals such as HCN? A mechanism of forth-and-back proton transfer suggests that HCN should be efficient in isomerising HCN^+

$$HCN + HCN^+ \rightarrow (HCNH\cdots CN)^+ \qquad (5.28a)$$

$$(HCNH\cdots CN)^+ \rightarrow (HCNH\cdots NC)^+ \qquad (5.28b)$$

$$(HCNH\cdots NC)^+ \rightarrow HCN + HNC^+ \qquad (5.28c)$$

$$\Delta H_{5.28a\text{-}c} = 74 \text{ kJ mol}^{-1},$$

since PA(HCN) > PA(CN), but in practice the formation of $HCNH^+ + CN\cdot$ is substantially more exothermic than formation of HNC^+ and so $HCNH^+$ is seen to be the major product:

$$HCN^+ + HCN \rightarrow HCNH^+ + CN\cdot \qquad (5.28d)$$

$$\Delta H_{5.28d} = 413 \text{ kJ mol}^{-1}$$

$$k_{5.28d} = 2.50 \times 10^{-9} \text{ cm}^3 \text{ molec}^{-1} \text{ s}^{-1}.$$

A small difference between the rate of reaction (5.28d) and the corresponding reaction rate for HNC^+

$$HNC^+ + HCN \rightarrow HCNH^+ + CN\cdot \qquad (5.29)$$

$$\Delta H_{5.29} = 339 \text{ kJ mol}^{-1}$$

$$k_{5.29} = 3.22 \times 10^{-9} \text{ cm}^3 \text{ molec}^{-1} \text{ s}^{-1}$$

suggests that the two ions may react differently. Furthermore, since the higher energy isomer is observed to react at a slightly slower rate than the lower-energy isomer (although the difference in rates is within the ascribed uncertainty of the measurements) and significantly below the calculated ADO collision rate (k_c = 3.8 x 10^{-9} cm^3 $molec^{-1}$ s^{-1}), there exists the possibility that some apparently unreactive HCN^+ + HCN collisions do result instead in forth-and-back isomerisation to HNC^+. Experiments which were performed by us attempted to examine this possibility, using CF_4 to investigate the HCN^+/HNC^+ ratio as a function of HCN flow, but the results are not conclusive. A rate coefficient of $k_{5.28a\text{-}c}$ = (2.75 ± 3) x 10^{-10} cm^3 $molec^{-1}$ s^{-1} was obtained: clearly, the uncertainty of this value (derived principally from the large uncertainties in $k_{5.28d}$ and $k_{5.29}$) is too great to exclude the possibility that channel (5.28d) is the only channel accessible in reaction of HCN^+ with HCN.

Further experiments with isotopically substituted reactants attempted to resolve this issue. The reaction

$$DCN^+ + HCN \rightarrow HNC^+ + DCN \qquad (5.30a)$$

is exothermic by a similar degree to the isomerisation of HCN^+ by HCN, although differences in the zero-point energies of the respective reactants and products will have a small thermochemical effect. Channel (5.30a) is, of course, in competition with the more exothermic process

$$DCN^+ + HCN \rightarrow DCNH^+ + CN\cdot \qquad (5.30b)$$

as well as the channels

$$\rightarrow \quad DNC^+ + HCN \qquad (5.30c)$$

$$\rightarrow \quad HCN^+ + DCN \qquad (5.30d),$$

although in view of the near-thermoneutral nature of reaction (5.30d), this channel is likely to be of very low efficiency. An estimate of $\Delta H_{5.30d} \sim 6$ kJ mol^{-1} can be obtained from the literature values of ZPE(HCN)[284] and ZPE(HCN$^+$)[285] and the estimated values for the deuterated isotopomers of these species:[286] the endothermicity of this reaction, with so many exothermic channels available, ensures that channel (5.30d) will be of very little importance. Any observed products at m/z 27 are thus likely to originate from channel (5.30a), while products at m/z 29 arise from channel (5.30b). A small channel corresponding to reaction (5.30c) is likely to be unobservable because of the rapid subsequent reaction of this isomer with HCN. In our experiments, channel (5.30a) was found to account for less than 2% of the total disappearance of m/z 28: therefore, it appears that proton-transfer isomerisation (if it occurs here) does not also involve H/D scrambling in the collision complex.

The reaction of DCND$^+$ (generated by electron impact on DCN in the ion source) with HCN is observed to result in rapid H/D scrambling:

$$DCND^+ + HCN \rightarrow HCND^+ + DCN \qquad (5.31)$$

$k_{5.31} = 1.47 \times 10^{-9}$ cm^3 molec^{-1} s^{-1}.

The high efficiency of this process shows that this reaction is not greatly endothermic (that is, the differences in zero-point energy of the reactants and products only marginally favour the reactants over formation of products). In fact, $\Delta H_{5.31} \sim 4$ kJ mol^{-1} according to experimental,[284] calculated[285] and estimated[286] zero-point vibrational energies for the various reactants. An estimate for $\Delta H_{5.31} \leq 3.3$ kJ mol^{-1} can be obtained from the Arrhenius expression: this is in reasonable agreement with the value calculated from zero-point energies, considering that the calculated value is not of high accuracy. Note that the structure of the product ion is expected to be $HCND^+$ rather than $DCNH^+$ since a simple deuteron-transfer reaction to HCN is the most straightforward mechanism available.

The experiments described here do not conclusively answer the problem of whether HCN can convert HCN^+ to HNC^+: however, the studies to date suggest that such a process (if it occurs) is very inefficient in comparison with formation of $HCNH^+$ in the same reaction. For this reason, the product ratios reported in table 5.8 are not likely to be significantly in error due to such an isomerisation process.

Finally, the charge-transfer reaction involving CN^+ and CO (also listed in table 5.8) may help to refine the thermochemistry of CN· : this reaction is calculated to be 7 kJ mol^{-1} exothermic,[184] but the total uncertainties on this value are very large. The observation that this reaction does indeed proceed reasonably rapidly suggests that it is exothermic, which allows some reduction of the uncertainties of $\Delta H_f(CN^+)$ and $\Delta H_f(CN\cdot)$.

Section 5.2: CH_2N^+.

Hydrogen cyanide[287] and hydrogen isocyanide[288] are the first pair of isomers to be reported in the interstellar environment. Protonation of this pair of isomers yields three possible structures:

$$XH^+ + HCN \rightarrow HCNH^+ + X \quad (5.32a)$$

$$\rightarrow H_2CN^+ + X \quad (5.32b)$$

$$XH^+ + HNC \rightarrow HCNH^+ + X \quad (5.33a)$$

$$\rightarrow CNH_2^+ + X \quad (5.33b).$$

Ab initio calculations by Pearson and Schaefer[289] on the relative energies of H_2CN^+ and $HCNH^+$ (see **table 5.9**) indicated that $HCNH^+$ was the more stable of this pair of isomers and would therefore be the most likely form of CH_2N^+ to be produced by reactions in interstellar clouds. However, these authors cautioned, "... there is some uncertainty as to whether [$HCNH^+$] would be observable, even if a radioastronomer were to stumble upon its proper frequency ... the electric dipole moment ... is 0.63 debyes".

The proper frequency was stumbled upon by Ziurys and Turner,[294] who reported a detection of $HCNH^+$ in the giant molecular cloud Sgr B2, with a calculated abundance (relative to H_2) of 3×10^{-10}. CNH_2^+ has also been searched for, but not detected. Brown[295] has suggested that the reaction

$$C^+ + NH_3 \rightarrow CH_2N^+ + H\cdot \quad (5.34)$$

should preferentially produce the CNH_2^+ isomer, which should yield HNC rather than HCN upon dissociative recombination:

$$CNH_2^+ + e \rightarrow HNC + H\cdot \quad (5.35a)$$

$$\rightarrow CN\cdot + H_2 \quad (5.35b).$$

Schaefer[291,292] has countered that reaction (5.34) is very exothermic and should deposit sufficient internal energy in any CNH_2^+ product to effect the isomerisation of this ion to the more stable $HCNH^+$ isomer. If this isomerisation occurs, the HCN/HNC ratio is dependent principally upon the branching ratio of the dissociative recombination process

Table 5.9: Experimental and theoretical thermochemistry of CH_2N^+.

$\Delta H_f(HCNH^+)$ [a]	$\Delta H_f(H_2CN^+)$ [a]	$\Delta H_f(CNH_2^+)$ [a]	$\Delta H_f(TS)$ [a,b]	Reference
947	–	1109	–	c
947	1257	1165	1248	d
947	–	1175	–	e
947	1248	1140	1265	f
947	–	1114	–	g

Notes

a. Heats of formation are expressed in kJ mol^{-1}.
b. TS = transition state for the isomerisation $HCNH^+ \leftrightarrow CNH_2^+$.
c. Literature values.[184]
d. MP4SDTQ/6-311G(d,p)//MP2/6-31G(d) calculations,[285] adjusted to the accepted literature value for $\Delta H_f(HCNH^+)$.
e. MP2/6-31G**//4-31G+ZPVE calculations,[290] adjusted to the accepted literature value for $\Delta H_f(HCNH^+)$.
f. DZ SCF calculations,[291,292] adjusted to the accepted literature value for $\Delta H_f(HCNH^+)$.
g. SCF/6-31G** calculations,[293] adjusted to the accepted literature value for $\Delta H_f(HCNH^+)$.

$$HCNH^+ + e \rightarrow HCN + H\cdot \quad (5.36a)$$

$$\rightarrow HNC + H\cdot \quad (5.36b)$$

$$\rightarrow CN\cdot + H_2 \quad (5.36c).$$

One aspect of understanding the observed HCN/HNC abundances is, therefore, a knowledge of the reactivity of $HCNH^+$ and of CNH_2^+. A requirement for studying these isomers in the SIFT is that some diagnostic reagent be found to distinguish between them. This in turn requires that a satisfactory method can be found for generating a CH_2N^+ ion signal which contains some observable proportion of the CNH_2^+ isomer. As explained below, this proved not to be an easy task.

The experimental techniques unsuccessfully used to generate CNH_2^+ are summarised in **table 5.10**. Of these methods, only (i) and (vi) resulted in injection of satisfactorily large signals of CH_2N^+ at m/z 28 from the ion source, and the predominant isomer produced in these instances is expected to be $HCNH^+$.

Several of the methods employed the reaction of C^+ or CCl^+ with NH_3, in the hope that CNH_2^+ would be the major product. Of these methods, (iv), (v) and (viii) failed to produce substantial m/z 28 signals in the ion source: (ix) produced appreciable m/z 28, but this appeared, from its subsequent reactivity, to be almost entirely due to CO^+ from electron impact upon CO.

Methods (ii) and (iii) produced sizeable m/z 28 signals within the flow tube, but no reactivity conclusively due to CNH_2^+ was observed in these instances.

Production of CH_2N^+ from NH_3 within the flow tube was problematic, since optimum m/z 28 signals were obtained when only a small flow of NH_3 was

Table 5.10: Methods of CNH_2^+ generation employed unsuccessfully.

	Source cpds. [a]	Reaction(s) involved	Site [a,b]
i	HCN	$CHN^+ + HCN \rightarrow CH_2N^+ + CN\cdot$	IS
ii	CCl_4 (IS); NH_3 (FT)	$CCl^+ + NH_3 \rightarrow CH_2N^+ + HCl$	FT
iii	CO (IS); NH_3 (FT)	$C^+ + NH_3 \rightarrow CH_2N^+ + H\cdot$	FT
iv	CCl_4, NH_3 [c]	$CCl^+ + NH_3 \rightarrow CH_2N^+ + HCl$	IS
v	He, CCl4, NH_3 [d]	$CCl^+ + NH_3 \rightarrow CH_2N^+ + HCl$	IS
vi	HCN, H_2 [e]	$CHN^+ + HCN \rightarrow CH_2N^+ + CN\cdot$ $H_2^+(H_3^+) + HCN \rightarrow CH_2N^+ + H\cdot(H_2)$	IS
vii	CS_2 (IS); NH_3 (FT)	$C^+ + NH_3 \rightarrow CH_2N^+ + H\cdot$	FT
viii	He, C_2N_2, NH_3 [d]	$C^+ + NH_3 \rightarrow CH_2N^+ + H\cdot$	IS
ix	He, CO, NH_3 [f]	$C^+ + NH_3 \rightarrow CH_2N^+ + H\cdot$	IS
x	$C_5H_5NO_3$ [gh]	$e + C_5H_5NO_3 \rightarrow CH_2N^+ + 3CO + CH_3\cdot + 2e$	IS
xi	He, $C_5H_5NO_3$ [gh]	$e + C_5H_5NO_3 \rightarrow CH_2N^+ + 3CO + CH_3\cdot + 2e$	IS
xii	CCl_4, $C_5H_5NO_3$ [gj]	$e + C_5H_5NO_3 \rightarrow CH_2N^+ + 3CO + CH_3\cdot + 2e$	IS
xiii	$C_6H_5NH_2$	$e + C_6H_5NH_2 \rightarrow CH_2N^+ + C_5H_5\cdot + 2e$	IS
xiv	H_2NCN [k]	$e + H_2NCN \rightarrow CH_2N^+ + N + 2e$	IS
xv	He (IS), H_2NCN [l] (FT)	$He^+ + H_2NCN \rightarrow CH_2N^+ + N + He$	FT
xvi	C_2N_2 (IS), H_2 (FT)	$CN^+ + H_2 \rightarrow CHN^+ + H.$ $CHN^+ + H_2 \rightarrow CH_2N^+ + H.$	FT FT

Notes

a. IS = ion source; FT = flow tube. Unless specified, all reagents are added at the ion source.
b. Site of CH_2N^+ generation.
c. 1:1 mixture.
d. 10:1:1 mixture.
e. 1:10 mixture.
f. 30:1:2 mixture.
g.

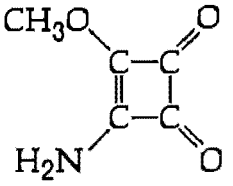

h. Introduced into source at T ~ 120°C.
j. A dilute solution of $C_5H_5NO_3$ in CCl_4.
k. Introduced entrained in helium or dissolved in CCl_4, $CHCl_3$ or tetrahydrofuran.
l. Dissolved in CCl_4.

established: under these conditions the signal detected due to the C^+ or CCl^+ primary ion was sizeable, and so CH_2N^+ production was occurring throughout the length of the flow tube from the point of NH_3 injection at portal 1 to the exit orifice. A titrating gas **X** could not be found which would apparently distinguish between $HCNH^+$ and CNH_2^+ without reacting also with C^+ or CCl^+, and under these conditions addition of a large flow of **X** would reduce the m/z 28 signal by approximately half due to removal of all C^+ or CCl^+ downstream of portal 2 by reaction with **X**. Identification of an additional decrease in m/z 28 due to the reaction of CNH_2^+ with **X** in a manner distinct from the reaction of $HCNH^+$ with **X** was, in these circumstances, not possible.

Method (**vii**) resulted in too small a signal of C^+ to be serviceable.

Methods (**x**), (**xi**) and (**xii**) attempted to exploit the demonstration, by Burgers et al,[296] that electron bombardment of the squaric acid derivative 1-methoxy 2-amino cyclobutenedione produces CNH_2^+, and not $HCNH^+$, at m/z 28. 1-methoxy 2-amino cyclobutenedione was prepared by the method of Cohen and Cohen[180] and its purity determined by ms, gc-ms and IR spectroscopy. For method (**x**) the crystalline solid was placed in a U-tube immediately upstream of the ion source and heated while a stream of argon was maintained through the tube to entrain the vapourised compound. For method (**xi**) the solid was stored in a glass bulb under helium and heated prior to injection into the ion source. For method (**xii**) the solid was dissolved (sparingly) in CCl_4 which was then vacuum-distilled and the resultant vapour was admitted to the ion source. In all these cases, heating of the glass vessel containing the compound resulted in the introduction of a reasonable pressure of $C_5H_5NO_3$ into the ion source, but

electron impact upon this vapour gave rise to much larger signals at m/z 27, 29 and 31 than at m/z 28. This is in disagreement with the observation by Burgers et al that a peak at m/z 28 due to CNH_2^+ dominated this region of the mass spectrum. In our experiment, it appeared that the peaks at m/z 27, 29 and 31 ($C_2H_3^+$, $C_2H_5^+$, CH_3O^+ ?) arose mainly from secondary reactions of ions produced within the ion source, since these signals diminished in intensity relative to m/z 28 as the pressure in the ion source was reduced. However, the m/z 28 signal did not exceed about 3 counts per second at any point over the whole range of pressures tested in our experiment: it was not felt to be worthwhile attempting to determine the isomeric purity of such a small signal, especially since the increased resolution required to remove the contaminant ion signals at m/z 27 and 29 would have resulted in a further signal attenuation. It appears that, though electron impact upon $C_5H_5NO_3$ at a pressure of approximately 10^{-7} Torr does produce large signals due to CNH_2^+ as shown by Burgers et al,[296] the higher operating pressure ($P > 10^{-4}$ Torr) required in the SIFT ion source to generate detectable signals results in the loss of most of the m/z 28 initially generated, due to secondary reactions.

Method (**xiii**) also attempted to favour CNH_2^+ formation by virtue of the structure of the source gas, aniline. However, injection of aniline into the ion source resulted in only a very small signal due to m/z 28, which we did not attempt to study further.

Methods (**xiv**) and (**xv**) attempted to favour CNH_2^+ formation from cyanamide, H_2NCN. The low-pressure mass spectrum of cyanamide[297] does feature a m/z 28 peak, which may well be CNH_2^+ on the basis of the parent neutral's structure.

However, none of the methods for introducing H_2NCN into the SIFT resulted in a usable m/z 28 ion signal. At 30°C, the vapour pressure of cyanamide is very low (~ 1 Torr) and so an attempt to add the vapour from solid cyanamide (stored under helium in a gas bulb) was not successful. Attempts with dissolved cyanamide were more successful - when CCl_4 was employed as the solvent, a sizeable m/z 42 signal could be obtained when the vapour was introduced into the ion source, and this appears a good method for studying the reactions of the cyanamide ion $CN_2H_2^+$. $CHCl_3$ and THF (tetrahydrofuran) were less useful solvents - although they dissolved cyanamide more readily, they also produced many unidentified ion signals in the mass range m/z 25 - 55: in the chloroform solution, these signals were most probably due to organic contaminants. The reaction of He^+ with cyanamide (introduced as the vapour from a saturated solution of H_2NCN in CCl_4) was also studied, in the hope that this might produce some m/z 28, but this did not eventuate - in this experiment, there was a background of ~ 10 counts per second at m/z 28 (most probably from the reaction of He^+ with an N_2 impurity within the tube), while complete reaction of He^+ with the added reactant gas did not produce any change at m/z 28, nor any observable signal at m/z 42.

Method (**xvi**) was studied in the hope that some observable fraction of the resulting CH_2N^+ signal might be CNH_2^+, the formation of which is energetically feasible:

$$CN^+ + H_2 \rightarrow HCN^+ + H\cdot \qquad [0.50] \qquad (5.37a)$$

$$\rightarrow HNC^+ + H\cdot \qquad [0.50] \qquad (5.37b)$$

$k_{5.37} = 1.1 \times 10^{-9}$ cm^3 molec^{-1} s^{-1}

$$HNC^+ + H_2 \rightarrow HCNH^+ + H\cdot \quad (5.38a)$$

$$\rightarrow CNH_2^+ + H\cdot \quad (5.38b)$$

$k_{5.38} = 7 \times 10^{-10}$ cm^3 molec^{-1} s^{-1}

$\Delta H_{5.38a} = -209$ kJ mol^{-1}

$\Delta H_{5.38b} = -47$ kJ mol^{-1}.

It might be expected that some of the HNC^+ produced in reaction (5.37b) can produce CNH_2^+, which should be left with insufficient energy to isomerise by unimolecular rearrangement since the calculated barrier is substantial. If CNH_2^+ is unreactive with H_2, addition of large flows of H_2 to the flow tube should result in complete conversion of CN^+ to CH_2N^+, containing a minority signal due to CNH_2^+ which should then undergo further reaction with an appropriate reagent. Unfortunately, this method too proved ineffective: no recognisable reaction was observed that might be due only to CNH_2^+ within this m/z 28 ion signal.

Reactions of CH_2N^+ which were studied to attempt to distinguish between $HCNH^+$ and CNH_2^+ are listed in **table 5.11**. Many of these reactions were selected in the hope that proton transfer would be observed due to the reaction of CNH_2^+, but not due to $HCNH^+$. This requires that the proton affinity of the neutral reactant be intermediate between PA (H<u>N</u>C) and PA(HC<u>N</u>), that is, 622 kJ mol^{-1} < PA(X) < 717 kJ mol^{-1}. The lower boundary condition here is necessarily vague because of the substantial uncertainty in $\Delta H_f(CNH_2^+)$, and a further uncertainty exists since a proton-transfer reaction involving isomerisation of the product neutral CHN can also be postulated:

$$CNH_2^+ + X \rightarrow XH^+ + HCN \quad (5.39a)$$

$$\rightarrow XH^+ + HNC \quad (5.39b)$$

$$\Delta H_{5.39a} = \Delta H_{5.39b} - 66 \text{ kJ mol}^{-1}.$$

If product channel (5.39a) is accessible to any proton transfer reactions under consideration, the range of compounds **X** which may have an appropriate PA to distinguish between CNH_2^+ and $HCNH^+$ is substantially increased (556 kJ mol^{-1} < PA(**X**) < 717 kJ mol^{-1}. It is not known if this channel is accessible. Another problem is isomerisation of the CH_2N^+ ions. Since, in the preceding section, HCN^+ is seen to be converted to HNC^+ by reactants with intermediate PA, it is entirely possible that a similar mechanism can also operate to efficiently convert CNH_2^+ to $HCNH^+$ by a two-step proton transfer process analogous to reaction

Table 5.11: Reactant gases **X** tested as titrants to distinguish between CNH_2^+ and $HCNH^+$.

X	Product channel sought	$-\Delta H_{CNH_2^+}$ [a]	$-\Delta H_{HCNH^+}$ [a]	Reaction seen?[b]
NO	$HNO^+ + HCN$ (HNC)	-25 (-91)	-186	N
CO	$HCO^+ + HCN$ (HNC)	38 (-28)	-123	N
C_2H_2	$C_2H_3^+ + HCN$ (HNC)	85 (19)	-76	A[c]
C_2N_2	$C_2N_2H^+ + HCN$ (HNC)	118 (52)	-43	N
C_2H_4	$C_2H_5^+ + HCN$ (HNC)	124 (58)	-37	A[c]
CS_2	$CS_2H^+ + HCN$ (HNC)	143 (77)	-18	N
CH_3Cl	$CH_3ClH^+ + HCN$ (HNC)	147 (81)	-14	N
N_2O	$HNCO^+ + N_2 + H\cdot$	-42	-204	N
SF_6	$SF_5^+ + HF + HCN$ (HNC)	-7 (-73)	-168	N
CF_4	$CF_3CNH^+ + HF$	106	-55	N
CH_4	$CH_5^+ + HCN$ (HNC)	-4 (-70)	-165	N
	$CH_3CNH^+ + H_2$	217	56	N
CCl_4	$CCl_3^+ + HCl + HCN$ (HNC)	137 (71)	-24	Y[c]

Notes

a. Reaction exothermicity, calculated using $\Delta H_f(CNH_2^+)$ = 1109 kJ mol^{-1}; ΔH_f(HNC) = 201 kJ mol^{-1}. Other energies are as tabulated by Lias et al,[184] except $\Delta H_f(SF_5^+)$ = 32 ± 6 kJ mol^{-1}.[298]

b. N = no reaction observed; A = adduct formation only observed; Y = reaction observed as shown.

c. See text for discussion.

(5.6). For this reason, proton affinity was not the only criterion by which appropriate reactant neutrals were selected. As with the reactions (5.7) - (5.10) which allowed discrimination of HCN^+ and HNC^+, special consideration was given to those reactions likely to result in rapid fragmentation of the initial collision complex: such reactivity should reduce the possibility for proton-transfer-based isomerisation of the CH_2N^+ ions concerned. This was the rationale behind the selection of SF_6 and CCl_4. Additionally, attention was given to reactions which might be exothermic for both ions but which required substantial rearrangement, as in the proposed reactions of CH_4, N_2O and CF_4. As Table 5.11 shows, none of these reactions allowed discrimination of CNH_2^+ and $HCNH^+$. **Table 5.12** shows the results for the reactivity observed. The rates observed for adduct formation with C_2H_2 and with C_2H_4 are in reasonable agreement with the rates observed for these processes by Herbst et al.[55] The product distribution for the reaction with CCl_4 is very surprising and will be discussed in some detail in the next section: suffice to say that the products observed appear due to $HCNH^+$ rather than to CNH_2^+, since CCl_3^+ was observed

Table 5.12: Reactions of $HCNH^+ + X$.

X	Products [a]		k_{obs} [a]	k_c [a]	$-\Delta H$ [a]
M	no reaction		<0.001	–	–
C_2H_4	$HCNH.C_2H_4^+$		0.07	1.29	–
C_2N_2	$HCNH.C_2N_2^+$		0.02	1.23	–
CCl_4	$CCl_3^+ + HCl + HCN$	[0.88]	0.80	1.56	-24
	$CCl_3CNH^+ + HCl$	[0.12]			66

Notes

a. See footnotes (a) - (c) for table (5.2), (b) for table (5.6).

b. M = CO, NO, CS_2, CF_4, SF_6, NO_2, CH_4, C_2H_2, CH_3Cl.

to be the major product of the reaction for all methods of CH_2N^+ formation and CNH_2^+ is not expected to dominate the m/z 28 ion signal in all of these methods.

The inability to observe any evidence for the existence of CNH_2^+, in the experiments described here, does not allow us to resolve what is actually happening. Two possibilities exist: either that in no instance have the techniques detailed in table 5.10 produced sufficient CNH_2^+ to detect, or that CNH_2^+ has been produced in some instances but not detected because of the unsuitability of the reactions detailed in table 5.11. I shall now examine these options in turn.

It seems likely that, given the energetic parameters detailed in table 5.9, some of the methods employed should produce some CNH_2^+: this ion exists in a deep potential well and has a very substantial barrier to isomerisation. The situation is complicated by the uncertainty in the heats of formation of the ion and its transition state to isomerisation, and by the very low efficiencies of the formation processes in some instances. For example, the attempt to generate CNH_2^+ from H_2NCN requires, to be successful, a C≡N bond to be broken during electron impact ionisation. In many instances, the yields of m/z 28 were too low for any study of the reactivity of this ion to be worthwhile: this does not indicate that these methods did not produce CNH_2^+, or that a substantially enhanced signal might not be obtained by a slight refinement in technique. Further attempts to generate CNH_2^+ by these or similar methods, using similar or modified equipment, therefore seem justified.

It is quite possible that the reactions detailed in table 5.11 are unable to distinguish CNH_2^+ and $HCNH^+$, because these ions do not react with any observable differences. For example, in our study of CHN^+ chemistry, the means of distinguishing between the HCN^+ and HNC^+ isomers remained elusive until an appropriate titrant (CF_4) was found. A mechanism involving proton-transfer isomerisation of CNH_2^+ to $HCNH^+$ would, as has been explained earlier, help to account for the inability to detect CNH_2^+ using reagents such as CO, CS_2 and CH_3Cl. Note that, if CNH_2^+ is converted to $HCNH^+$ by reaction with CO, then CNH_2^+ cannot have much influence on the observed interstellar abundances of HCN and HNC, since rapid isomerisation by CO represents a more efficient loss mechanism for CNH_2^+ than does dissociative recombination with an electron. This proposed isomerisation is highly speculative, and given the uncertainty in $\Delta H_f(CNH_2^+)$ ($\sim \pm 40$ kJ mol^{-1}) might be exothermic for both channels (5.40a) and (5.40b), for channel (5.40a) only, or for neither:

$$CNH_2^+ + CO \rightarrow (HNC\cdots OCH^+) \qquad (5.40a)$$

$$\rightarrow (HCN\cdots OCH^+) \qquad (5.40b)$$

$\Delta H_{5.40a} = 28$ kJ mol^{-1}

$\Delta H_{5.40b} = -38$ kJ mol^{-1}

$$(CHN\cdots OCH^+) \rightarrow HCNH^+ + CO \qquad (5.41).$$

The formula CHN is used in reaction (5.41) to denote that this reaction may occur for both HCN and HNC. The quoted values $\Delta H_{5.40a}$ and $\Delta H_{5.40b}$ relate to the heats of formation of HCN/HNC and HCO^+ at infinite separation, and may very well not relate closely to the heat of formation of the collision complex formed.

Channel (5.40b), although favoured upon the basis of enthalpy values, may not be practical given the greater degree of rearrangement required - migration of both H atoms is necessary for this channel to occur. An ab initio study would help resolve whether either of the reaction channels (5.40a) or (5.40b) are accessible to reactants under interstellar conditions.

Given the results obtained in this study, it is difficult to assert with confidence what chemistry is occurring here. The strong possibility that isomerisation of CNH_2^+ may be the dominant reaction channel for the reaction of this ion with many neutral reagents deserves further study: similar isomerisation has been observed now for HCN^+/HNC^+, HCO^+/HOC^+ [166,206] and $HNNO^+/NNOH^+$ [262,263] as has been discussed in the preceding section. The prospect for such isomerisation in this system should be seriously considered since both CNH_2^+ and $HCNH^+$ have been widely invoked as important ions in interstellar synthesis.

Section 5.3: Does a fast reaction have to be exothermic?

The reaction of HCN^+ with CF_4 (see section 5.1)

$$HCN^+ + CF_4 \rightarrow CF_3^+ + HF + CN\cdot \qquad (5.7)$$

$$k_{5.7} = 1.15 \times 10^{-9}\ cm^3\ molec^{-1}\ s^{-1}$$

is of interest not only because it distinguishes between HCN^+ and HNC^+ by virtue of its reactivity, but also because it occurs rapidly despite its apparent endothermicity. Tabulated heats of formation for the reactants and products are[184]

$$\Delta H_f(HCN^+) = 1447 \pm 10 \text{ kJ mol}^{-1}$$
$$\Delta H_f(CF_4) = -934.5 \pm 0.4 \text{ kJ mol}^{-1}$$
$$\Delta H_f(CF_3^+) = 399.0 \pm 5 \text{ kJ mol}^{-1}\ ^{299}$$
$$\Delta H_f(HF) = -272.5 \pm 0.8 \text{ kJ mol}^{-1}$$
$$\Delta H_f(CN\cdot) = 435.1 \pm 10 \text{ kJ mol}^{-1}.$$

Using these values, the calculated enthalpy of reaction is $\Delta H_{5.7} = + 49.1 \pm 26.2$ kJ mol^{-1}. The large uncertainty in this value can be considerably reduced: the main contributions to this uncertainty arise from the tabulated uncertainty in $\Delta H_f(HCN^+)$ and $\Delta H_f(CN\cdot)$. In fact the appearance potentials $AP(HCN^+/HCN)$ and $AP(H^+ + CN\cdot/HCN)$ are each known with much higher precision than $\pm$ 10 kJ mol^{-1}: this uncertainty arises from the heat of formation of HCN itself. Using these appearance potentials[300,301] and considering the process

$$HCN^+ \rightarrow H^+ + CN\cdot \qquad (5.42)$$
$$\Delta H_{5.42} = +521 \pm 2 \text{ kJ mol}^{-1},$$

the enthalpy for reaction (5.7) can be recalculated:

$$\Delta H_{5.7} = \Delta H_{5.42} + \Delta H_f(CF_3^+) + \Delta H_f(HF) - \Delta H_f(CF_4) - \Delta H_f(H^+)$$
$$\therefore \quad \Delta H_{5.7} = +52 \pm 8 \text{ kJ mol}^{-1}.$$

From these values, reaction (5.7) is apparently very endothermic. Such an endothermic reaction should not occur at the collision rate, since not all collisions of reactants will feature sufficient internal energy to overcome such an enthalpy barrier. Ferguson and co-workers[302,303] have argued that, clearly, the reaction is instead exothermic: this requires that one of the tabulated enthalpy values is dramatically incorrect. The heats of formation of CF_4, HF and H^+ have all been determined to high accuracy and are not open to question; similarly, $AP(HCN^+/HCN)$ and $AP(H^+ + CN\cdot/HCN)$ have been very precisely determined. The only thermochemical value in doubt is thus $\Delta H_f(CF_3^+)$.

There is considerable evidence that the tabulated heat of formation of CF_3^+ is too high. The earliest determination of this quantity, by photoionisation of CF_4, gave $AP(CF_3^+/CF_4) = 15.30$ eV which corresponds to $\Delta H_f(CF_3^+) = 463$ kJ mol^{-1}.[304] However, CF_3^+ in this instance is produced via dissociation of the unstable ion CF_4^+:

$$CF_4^+ \rightarrow CF_3^+ + F\cdot \qquad (5.43).$$

Since CF_4^+ is unstable with respect to $CF_3^+ + F\cdot$, the appearance potential for CF_3^+/CF_4 can only provide an upper limit to $\Delta H_f(CF_3^+)$. Other experiments indicate that this upper limit is an electron volt or more too high. Langford et al[305] performed charge-stripping experiments on CF_3^+ produced by electron bombardment upon a variety of source gases including CF_4. In these experiments, highly-accelerated reactant ions were allowed to collide with gas molecules which effected ionisation:

$$CF_3^+ + X \rightarrow CF_3^{2+} + X + e \qquad (5.44).$$

By measuring accurately the amount of translational energy lost, the energy required to further ionise CF_3^+ could be determined. Langford et al found that charge-stripping of CF_3^+ from CF_3Cl, CF_3Br, C_2F_6, C_2F_5H, CF_3CH_3 and CF_2HCFH_2 gave no evidence for population of excited states of CF_3^+, but that charge-stripping of the CF_3^+ produced from CF_4 did show such evidence. They concluded that CF_3^+ produced from CF_4 is initially vibrationally excited by ~ 0.5 eV and that this vibrational excitation is long-lived: this can be compared to the suggestion by Fisher et al[306] that ionisation of CF_4 produces pyramidal CF_3^+, which subseqently relaxes to the planar CF_3^+ ground state.

Tichy et al[307] have studied the reaction

$$HCl^+ + CF_4 \rightarrow CF_3^+ + HF + Cl. \qquad (5.45)$$

$$k_{5.45} = 1.0 \times 10^{-10} \text{ cm}^3 \text{ molec}^{-1} \text{ s}^{-1}$$

which is very similar to reaction (5.7) except that it does not occur at the collision rate. Upon the basis of this reaction, they concluded that the correct 'adiabatic' appearance potential $AP_A(CF_3^+/CF_4)$ [where the adiabatic potential is that for production of ground-state products from ground-state reactants: it should be distinguished from the 'vertical' appearance potential, which may be influenced by Franck-Condon effects] could not exceed 14.23 eV, which requires $\Delta H_f(CF_3^+) \leq$ 364 kJ mol^{-1}. The displacement between the vertical and adiabatic potentials is known as the kinetic shift. Vertical potentials, obtained from photoionisation and similar techniques, can be significantly higher than adiabatic potentials.

Methods such as photoionisation occur on too short a timescale to permit rearrangement of the product to its ground-state geometry: if this geometry differs significantly from that of the reactant, the potential thus obtained will not relate well to the heat of formation of the product in its ground state.

Babcock and Streit[308] have investigated the equilibrium

$$CF_3^+ + SF_6 \rightleftharpoons SF_5^+ + CF_4 \qquad (5.46)$$

in a flow-tube experiment: they determined $K_{5.46} \sim (5.9 \pm 0.9) \times 10^3$, from which they derived $AP_A(CF_3^+/CF_4) - AP_A(SF_5^+/SF_6) = 0.17$ eV. The heat of formation of SF_5^+ is also very much lower than its vertical appearance potential $AP_V(SF_5^+/SF_6) = 15.33 \pm 0.3$ eV would suggest, as reaction studies by Tichy et al[303,307] and double-charge-transfer experiments by Langford et al[309] have shown: the currently-accepted value for the adiabatic potential is $AP_A(SF_5^+/SF_6) = 13.65$ eV. This should, in conjunction with the equilibrium reaction (5.46), yield a value of $\Delta H_f(CF_3^+)$: however, subsequent studies by Fisher and Armentrout[310] have shown the results of Babcock and Streit to be in error. There is no accurately determined value of $K_{5.46}$ - therefore, determination of $AP_A(SF_5^+/SF_6)$ cannot provide an accurate indication of $AP_A(CF_3^+/CF_4)$. Notwithstanding this, there is still a large amount of evidence which demonstrates that $\Delta H_f(CF_3^+)$ is substantially below the currently tabulated value.

If reaction (5.7) is, as Ferguson claims, exothermic,[302] then an upper limit of $\Delta H_f(CF_3^+) < 347$ kJ mol^{-1} can be ascribed. This is lower than any other value yet determined for this heat of formation.

An alternative proposal is that reaction (5.7) is endothermic but exergonic: that is, the enthalpy change ΔH is positive while the free energy change ΔG for the reaction is negative. This can be so if the reaction is "entropy-driven" by virtue of the formation of three products from only two reactants - for such reactions the entropic contribution ($-T\Delta S$) to ΔG can amount to ~ 20 kJ mol^{-1} at 300 K, so a reaction which is endothermic by less than this can still proceed efficiently if 'assisted' by the change in entropy.

The rôle of entropy in ion-molecule reactions is still a subject of debate.[189,311] Traditionally, the enthalpy change ΔH has been considered as the deciding factor in ion-molecule reactions: convention holds that if ΔH is positive for a reaction, then this reaction will have less than unit efficiency. Henchman[311] has suggested that this perspective arose from the tendency to regard ion-molecule reactions observed in an experiment as 'single-collision' events in which a loss of energy is not permissible, with energy equating to enthalpy. In addition, the much more widespread tabulation of ionic heats of formation, than of free energies of formation of ions, has favoured the use of ΔH rather than ΔG in interpretation of ion-molecule reactions.

There are now several ion-molecule reaction studies which very strongly suggest the involvement of entropy in reaction rate enhancement or inhibition. Henchman et al[312-314] have studied systems such as $H^+(D^+) + H_2(D_2)$ and $CH_4^+(CD_4^+) + CH_4(CD_4)$ in a VT-SIFT, over appreciable temperature ranges. The observed variation in the equilibrium constant K with T for these reactions is clearly characteristic of a temperature-dependent change in the entropy of reaction. Mautner[189,315] has studied many proton-transfer equilibria in HP-MS

experiments. For some such systems, K displays a clear temperature dependence consistent with entropy changes due to changing symmetry, ring opening and closing, etc. King et al[316] have studied, in a SIFT, the reaction

$$CH_3ONO + F^- \rightarrow NO^- + HF + H_2CO \quad [0.18] \quad (5.47a)$$

$$\rightarrow NO.HF^- + H_2CO \quad [0.03] \quad (5.47b)$$

$$\rightarrow NO_2^- + CH_3F \quad [0.79] \quad (5.47c)$$

$k_{5.47} = 2.1 \times 10^{-9}$ cm^3 molec^{-1} s^{-1}

$\Delta H_{5.47a} = +25$ kJ mol^{-1}

$\Delta G_{5.47a} < 0$ kJ mol^{-1},

for which channel (5.47a) proceeds efficiently despite its endothermicity. This reaction closely parallels reaction (5.7) - if the latter reaction is entropy-driven. A problem connected with the reported occurrence of reaction (5.47a) is that this channel is not directly observable because the NO^- ion is not stable, rapidly undergoing detachment:

$$NO^- + He \rightarrow e + NO + He \quad (5.48).$$

In the study by King et al, this channel was deduced as a product channel by the assumption that the ratio of products for channels (5.47a) and (5.47b) was equal to the ratio of the analogous product channels (5.49a) and (5.49b)[316]

$$F^- + XCH_2ONO \rightarrow NO^- + HF + XCHO \quad [0.85] \quad (5.49a)$$

$$\rightarrow NO.HF^- + XCHO \quad [0.15] \quad (5.49b)$$

$k_{5.49} = 3.1 \times 10^{-9}$ cm^3 molec^{-1} s^{-1}

where X = $(CH_3)_3C$. This reaction presents a more convincing case for the existence of the endothermic, entropy-driven channel (5.49a) ($\Delta H_{5.49a}$ = +29 kJ mol^{-1}), since the only product channel seen accounts for only 15% of the F^- lost through reaction: however, the uncertainties in $\Delta H_{5.49a}$ will be larger owing to the greater complexity of the reactants and products. The uncertainties in product ratios and thermodynamic quantities relevant to channels (5.47a) and (5.49a) appear sufficiently large to make questionable the claim that these reactions are entropy-driven.

Mautner and Tsang[189] present a model for 'intrinsically fast' entropy-driven reactions (that is, in the absence of activation energy barriers and involving merely the formation of a single collision complex) of the form

$$A^+ + B \underset{k_b}{\overset{k_c}{\rightleftharpoons}} (AB^+)^{\ddagger} \underset{k_{c'}}{\overset{k_p}{\rightleftharpoons}} C^+ + D \qquad (5.50).$$

If $A^+ + B$ and $C^+ + D$ are the only possible product channels accessible from the collision complex $(AB^+)^{\ddagger}$, then the forward and reverse rate coefficients for the reaction

$$A^+ + B \rightarrow C^+ + D \qquad (5.51)$$

can be defined in terms of the fraction of $(A^+ + B)$ collisions producing $(C^+ + D)$ and vice versa:

$$k_f = k_c \frac{k_p}{k_p + k_b} \qquad \{5.xii\}$$

and $$k_r = k_{c'} \frac{k_b}{k_p + k_b} \qquad \{5.xiii\}.$$

By application of the definition of the equilibrium constant $K_{5.51}$

$$K_{5.51} = \frac{k_f}{k_r} \qquad \{5.xiv\},$$

Mautner and Tsang[189] show that the reaction efficiency r_f - that is, the fraction of $A^+ + B$ collisions which result in the successful production of $C^+ + D$ - has the relation

$$r_f = \frac{K}{K + k_c/k_{c'}} \qquad \{5.xv\}$$

which simplifies to

$$r_f = \frac{K}{K + 1} \qquad \{5.xvi\}$$

with the approximation that $k_c \approx k_{c'}$.

A problem in attempting to describe reaction (5.7), and similar reactions, as entropy-driven is the possible confusion between thermodynamic and kinetic effects. A common view of entropy in chemical systems is as a measure of disorder or probability: by extension of such a view, a system which is initially in

a condition of order will move naturally to a condition of greater disorder insofar as this is compatible with a low expenditure of energy. Thus, an equilibrium involving two reactants and three products will naturally favour the formation of three products (despite a minor endothermicity) because of the much greater probability of a bimolecular collision of the two reactants than the required termolecular collision of the three products. In terms of the model outlined above, this corresponds to an extreme case where $k_c >> k_{c'}$, since $k_{c'}$ must represent the effective collision rate for the termolecular process $C^+ + D + E$. This event is more properly regarded as a close succession of two bimolecular collisions, involving a model of the form

$$C^+ + D + E \underset{k_2}{\overset{k_{c''}}{\rightleftharpoons}} (CD^+)^\dagger + E \underset{k_1}{\overset{k_{c'}}{\rightleftharpoons}} (AB^+)^\ddagger \underset{k_c}{\overset{k_b}{\rightleftharpoons}} A^+ + B \qquad (5.52).$$

In this model (for which A^+ and B appear as products as shown here, rather than as reactants in reaction (5.50)) the rate law for removal of C^+ by reaction is

$$\frac{-d[C^+]}{dt} = k_{c''}[C^+][D][E]\frac{k_{c'}}{k_2 + k_{c'}[E]}\frac{k_b}{k_1 + k_b} - k_c[A^+][B]\frac{k_1}{k_1 + k_b}\frac{k_2}{k_2 + k_{c'}[E]} \qquad \{5.xvii\}.$$

In the case where the concentrations of the reactants C^+, D and E are in vast excess to the concentrations of the products A^+ and B, this expression can be simplified to

$$\frac{-d[C^+]}{dt} = k_{c''}[C^+][D][E]\frac{k_{c'}}{k_2 + k_{c'}[E]}\frac{k_b}{k_1 + k_b} \qquad \{5.xviii\}.$$

This simplification approximates to the situation in a SIFT experiment, where the occurrence of the reverse reaction is generally negligible because of the extremely low concentrations of the products. The rate coefficient for reaction of C^+ with D and E can now be expressed as

$$k_f = k_{c''}\frac{k_{c'}}{k_2 + k_{c'}[E]}\frac{k_b}{k_1 + k_b} \qquad \{5.xix\},$$

while the rate coefficient k_r for reaction of A^+ with B has the form

$$k_r = k_c\frac{k_1}{k_1 + k_b}\frac{k_2}{k_2 + k_{c'}[E]} \qquad \{5.xx\}.$$

If it is assumed that $k_2 >> k_{c'}[E]$- that is, that dissociation of the complex $(CD^+)^\dagger$ is much more probable than the formation of $(AB^+)^\ddagger$ by the collision of $(CD^+)^\dagger$ with E - then

$$k_f \approx k_{c'}\frac{k_{c'}}{k_2}\frac{k_b}{k_1 + k_b} \qquad \{5.xxi\}$$

and

$$k_r \approx k_c\frac{k_1}{k_1 + k_b} \qquad \{5.xxii\}.$$

Using the terminology of Mautner and Tsang,[189] the efficiency r_r (which defines the fraction of $A^+ + B$ collisions which successfully form $C^+ + D + E$) is

$$r_r \approx \frac{k_r}{k_c} = \frac{k_1}{k_1 + k_b} \qquad \{5.xxiii\}.$$

Similarly, the efficiency r_f can be defined as the fraction of $C^+ + D + E$ collisions resulting in formation of $A^+ + B$:

$$r_f \approx \frac{k_f}{k_c'' (k_c'/k_2)} = \frac{k_b}{k_1 + k_b} \qquad \{5.xxiv\}.$$

This method of expression is, however, misleading. r_f and r_r have similar forms, but it must be remembered that r_f denotes the efficiency of a termolecular process while r_r refers to the reverse, bimolecular process. An alternative expression, r_f', can be derived. This quantity denotes the efficiency of $C^+ + D$ collisions - that is, the fraction of $C^+ + D$ collisions which result in $A^+ + B$ formation:

$$r_f' \approx \frac{k_f [E]}{k_c''} = \frac{k_c' [E]}{k_2} \frac{k_b}{k_1 + k_b} \qquad \{5.xxv\}$$

Now, $r_f + r_r < 1$ and $r_f << r_r$ for $k_b \sim k_1$ (providing $k_c' [E] << k_2$, which holds if the concentration of E is negligible - as in, for example, our SIFT studies of reaction (5.7)). This model shows that the rate of conversion of $A^+ + B$ to $C^+ + D + E$ can greatly exceed the rate of the opposite process while still proceeding on only a small fraction of $A^+ + B$ collisions (those in which the reactants have sufficient energy to overcome the reaction endothermicity). This yields a system in which $K_{5,51}$ favours formation of the three particles $C^+ + D + E$ in spite of the low efficiency of this process.

This model of the 'entropy-driven' system is contested by Mautner, who claims that K in this case does not relate to the relative probabilities of collision in the two opposing directions, but to the likely disproportionation of the collision complex $(AB^+)‡$. In the instances where an ion-molecule reaction is seen as being entropy-driven, the entropy change is rationalised by Mautner in terms of a density-of-states argument. A reaction may be endothermic but still efficient provided that the density of states for products is large in comparison to the available density of states for reactants. This situation can occur, for example, when symmetry factors limit the available density of states for reactants. In the case of a reaction such as (5.7) where a change in the number of particles occurs due to reaction, it is argued that the available density of states for products will be large because of the larger number of permutations available for energy dispersal within three particles. **Figure 5.4** illustrates this concept. For such a reaction to occur on every collision, the endothermicity must be exceeded by the thermal energy of the reactants, and the products will be internally cold.

An approximate value for the thermal energy available in reaction (5.7) can be easily calculated. Using $E = nRT/2$ as the total quantity of thermal energy distributed among the n modes accessible, and $T = 300$ K, it becomes necessary to determine n. Each reactant has three translational degrees of freedom: but in a collision, one reactant can be considered as fixed (both reactants must occupy the same position, essentially, for a collision to occur) so the total number of accessible translational modes is three. HCN^+ is linear and has two rotational modes; CF_4 has three, so there are five accessible rotational modes. Several vibrational modes exist for each reactant, but the lowest vibrational frequency of HCN^+ is at $\nu = 712$ cm^{-1},[284] while the smallest vibrational frequency of CF_4 is $\nu =$

437 cm^{-1};[317] these frequencies are too large for these levels to be substantially populated at T = 300 K, so the vibrationally excited population of reactants is too small for these vibrational modes to contribute significantly to the available thermal energy. No electronic levels are low enough to be worth consideration, so n= 8. There is thus a total of 10 kJ mol^{-1} thermal energy available for reaction (5.7): therefore, this reaction cannot feasibly be endothermic to a greater extent than this. If all of this thermal energy is expended in driving this reaction, the products will have an effective internal temperature of zero - although, in a SIFT experiment, thermalisation following reaction would occur owing to repeated collision with bath gas molecules.

Figure 5.4: A diagram illustrating the model of Mautner,[189] which states that endothermic reactions can occur rapidly if they are entropy-driven. In this model, the endothermicity is exceeded by the available thermal energy (the dotted line in this diagram), and the 3-product channel is favoured by a greater density of available rovibrational states than the 2-reactant channel.

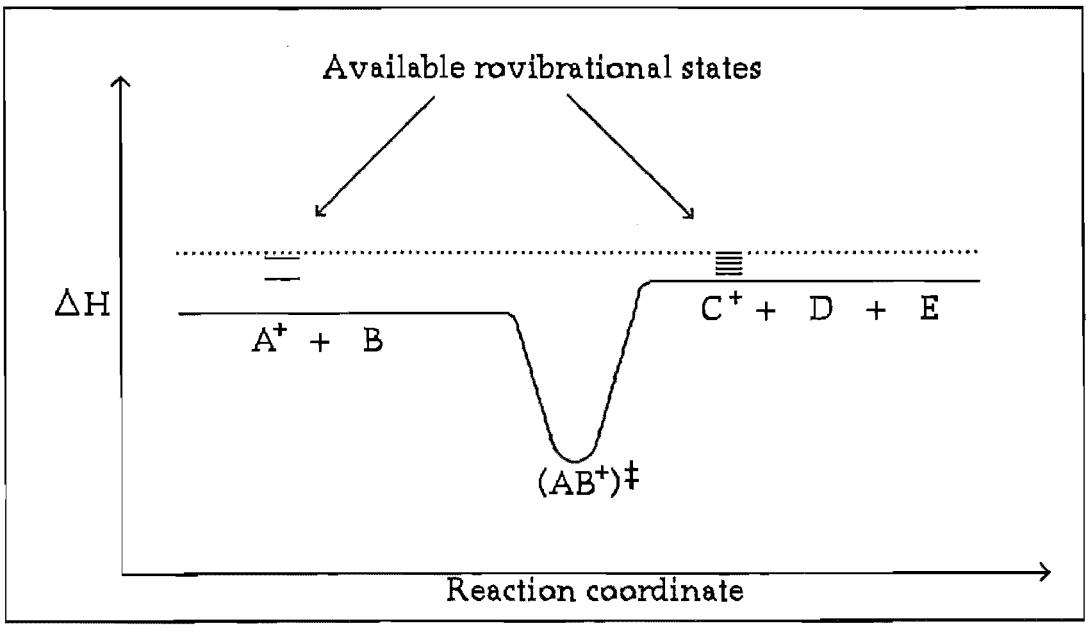

There is some experimental evidence to support the notion that reaction (5.7) is endothermic. We have studied the reaction

$$CF_3^+ + C_2H_4 \rightarrow C_2H_3^+ + CF_3H \quad [0.25] \quad (5.53a)$$

$$\rightarrow C_3F_2H_3^+ + HF \quad [0.75] \quad (5.53b)$$

$k_{5.53} = 1.0 \times 10^{-9}$ cm^3 molec^{-1} s^{-1}

$\Delta H_{5.53a} < 0$ kJ mol^{-1},

for which the product channel (5.53a) is clearly exothermic from the observation of a rate coefficient close to the collision rate. We were initially concerned that this product channel might have arisen through a substantial population of vibrationally excited CF_3^+, but this possibility was eliminated after using CF_3Br instead of CF_4 as a source gas (Langford et al[305] have determined that CF_4 produces excited-state CF_3^+ while CF_3Br does not) and additionally using N_2 as a quenching gas added upstream of the C_2H_4. Using the following tabulated heats of formation[184]

$\Delta H_f(C_2H_4) = 52.2 \pm 1$ kJ mol^{-1}

$\Delta H_f(C_2H_3^+) = 1112 \pm 4$ kJ mol^{-1}

$\Delta H_f(CF_3H) = -695 \pm 8$ kJ mol^{-1},

a lower limit of $\Delta H_f(CF_3^+) > 352$ kJ mol^{-1} is required if channel (5.53a) is to be exothermic. This is in conflict with the $\Delta H_f(CF_3^+)$ required for the exothermicity of reaction (5.7): thus, it appears that one of these reactions must be endothermic. Since the expected $T\Delta S_{5.53a}$ is negligible, reaction (5.7) must be an endothermic process.

The determination that reaction (5.7) is not exothermic does not, however, demonstrate that this reaction is driven by entropy in the style proposed by Mautner. Ferguson[302] has speculated that the apparent generation of three products is illusory: if one of the products was a weakly-bound cluster ion such as $CF_3.HF^+$, this ion might well be too fragile to survive the acceleration induced by electrostatic focussing prior to mass selection and detection. This proposal is related, by the principle of microscopic reversibility, to the model (5.52) in which the reaction $C^+ + D + E$ is viewed as two successive bimolecular collisions: if the fragmentation of $(AB^+)^‡$ occurs as two successive fragmentations, one of which is not necessarily spontaneous, then there is no immediate entropy gain accessible to the collision complex. Fisher and Armentrout[310] have also considered this proposal, and favour the formation of $CF_3.CN^+$ or $CF_3.HF^+$, or of the van der Waal's complex [FH···CN] as the neutral product in reaction (5.7). They estimate a binding energy for this neutral complex of ~ 14 kJ mol^{-1} by analogy with the binding energy of the HF dimer: under these criteria, the exothermicity of the reaction of HCN^+ with CF_4 requires an upper limit to $\Delta H_f(CF_3^+)$ of 361 kJ mol^{-1} (for production of FH···CN; a higher limit is obtained if $CF_3.CN^+$ or $CF_3.HF^+$ is formed) which would resolve the discrepancy apparent in the occurrence of reactions (5.7) and (5.53a). In the absence of a detailed study of the binding energy of such a complex as that formed in reactions (5.7) and (5.47a), this possibility cannot be dismissed.

It is of interest also to note the similarity of the reaction

$$HCNH^+ + CCl_4 \rightarrow CCl_3^+ + HCN + HCl \quad [0.88] \qquad (5.54a)$$
$$\rightarrow CCl_3CNH^+ + HCl \quad [0.12] \qquad (5.54b)$$

$k_{5.54} = 8.0 \times 10^{-10}$ cm^3 $molec^{-1}$ s^{-1}

$\Delta H_{5.54a} = +24$ kJ mol^{-1}

to reaction (5.7). This reaction was studied as part of our unsuccessful foray into CNH_2^+ chemistry (see the preceding section): channel (5.54a) is, as can be seen, substantially endothermic according to the available thermochemical data. This indicates either

(i). that this channel (which is an appreciable product channel of a fast reaction, and therefore exergonic) is driven by entropy changes in the same manner as reaction (5.7),

(ii). that the formation of a van der Waal's complex (HCN···HCl) with sufficient binding energy drives the reaction, or

(iii). that the thermochemical information is incorrect. The latter rationalisation most readily requires a lower value of $\Delta H_f(CCl_3^+)$, which has been determined from ICR and FA bracketing:[318]

$$H_3O^+ + CFCl_3 \rightarrow CCl_3^+ + HF + H_2O \qquad (5.55)$$

$$\text{sec-}C_3H_7^+ + CFCl_3 \not\rightarrow CCl_3^+ + C_3H_7F \qquad (5.56)$$

$$k_{5.56} < 1.0 \times 10^{-12}\ cm^3\ molec^{-1}\ s^{-1}.$$

If $\Delta H_f(CCl_3^+)$ had been determined in the same manner as $\Delta H_f(CF_3^+)$, - that is, by appearance potentials from photoionisation methods - it might be expected to be too high for similar reasons. Note, however, that in this case the upper limit for $\Delta H_f(CCl_3^+)$ is obtained from the occurrence of an ion-molecule reaction (5.55) in a flowing-afterglow apparatus, which should therefore give a value appropriate to the truly thermalised CCl_3^+ ion. An additional complicating factor is that reaction (5.55) is also of the '2→3' form of reactions (5.7), (5.47a) and (5.54a), which (if the entropy-driven argument is to be heeded) might rather be

expected in this instance to yield an underestimate of $\Delta H_f(CCl_3^+)$. Further studies involving CCl_3^+ ions might help resolve this issue.

CHAPTER 6.

ION-MOLECULE CHEMISTRY OF ACRYLONITRILE, CH_2CHCN.

Section 6.1: Introduction.

Acrylonitrile, CH_2CHCN, is structurally closely related to $H—(C{\equiv}C)_n—C{\equiv}N$, the cyanopolyynes, which form a prominent series of interstellar molecules. The interstellar chemistry of the cyanopolyynes has been extensively studied[64,167,205,214,255,265,267] and discussed,[27,39,40,99,224,238] but the interstellar chemistry of acrylonitrile has to date received little attention.

Acrylonitrile was first detected in the dense cloud TMC-1 by Matthews and Sears[319] in 1982. Herbst[54] has suggested that acrylonitrile is formed in such clouds as a result of the radiative association process

$$HCNH^+ + C_2H_2 \rightarrow C_3H_4N^+ + h\nu \qquad (6.1)$$

for which a rate coefficient $k_{6.1} = 2 \times 10^{-12}$ cm^3 molec^{-1} s^{-1} at 10 K has been estimated.[54] A possible additional pathway involves the reaction of hydrocarbon ions with nitrogen atoms[27,150]

$$C_nH_m^+ + N \rightarrow C_nH_{m-x}N^+ + xH \qquad (6.2).$$

Very few such reactions have yet been studied experimentally,[320-322] and none of those studied to date provides a useful method of generating interstellar CH_2CHCN. Millar and Nejad[323] suggested that reactions of N atoms with hydrocarbon radicals and molecules might provide a route to the formation of cyanopolyynes and related species, but this reaction type may feature activation energy barriers[324] and would, in consequence, be prohibitively inefficient under interstellar conditions.

Acrylonitrile has also been proposed as a likely trace constituent of the atmosphere of Titan,[325,326] as well as of other planetary atmospheres,[327] though it has not yet been detected in such environments. The proposed atmospheric synthesis of acrylonitrile involves a termolecular association of $HCNH^+$ and C_2H_2, analogous to reaction (6.1).[326,328] Abundances of acrylonitrile in the atmospheres of the outer planets will necessarily be low because of photodissociation and the high condensation point for such compounds: some support for the formation of nitriles, in Titan's atmosphere at least, is seen in the observation of cyanoacetylene by Kunde et al.[194]

The present chapter reports results for some ion-molecule reactions relating to the interstellar chemistry of acrylonitrile.

The ions $C_3H_2N^+$ and $C_3H_3N^+$ were produced in the ion source by electron impact upon a dilute solution (1:20) of acrylonitrile in helium, since it was found that the ion signal was unstable against fluctuations in size when pure acrylonitrile was used as the source gas. $C_3H_4N^+$ was generated by electron bombardment upon a dilute solution (1:10) of acrylonitrile in hydrogen:

$$H_2^+ + C_2H_3CN \rightarrow CH_2CHCNH^+ + H\cdot \quad (6.3)$$

$$H_3^+ + C_2H_3CN \rightarrow CH_2CHCNH^+ + H_2 \quad (6.4)$$

$$C_3H_3N^+ + H_2 \rightarrow CH_2CHCNH^+ + H\cdot \quad (6.5)$$

$$C_3H_2N^+ + C_2H_3CN \rightarrow CH_2CHCNH^+ + C_3HN \quad (6.6)$$

$\Delta H_{6.3} = -534$ kJ mol^{-1}

$\Delta H_{6.4} = -371$ kJ mol^{-1}

$\Delta H_{6.5} = -99$ kJ mol^{-1}

$\Delta H_{6.6} = -41$ kJ mol^{-1}.

Reaction (6.3) has not been studied to date; results for reactions (6.4), (6.5) and (6.6) are described within this chapter.

Acrylonitrile was also used as a dilute solution in helium for the studies of reactions of various ions with acrylonitrile, since the rate coefficients observed for these reactions were almost invariably too rapid to acquire satisfactorily accurate measurements from pure acrylonitrile used as a neutral reactant.

Section 6.2: Reactions of $C_3H_3N^+$.

The reactions of $C_3H_3N^+$ with various neutrals are summarised in **table 6.1**.

In the context of interstellar cloud chemistry, $C_3H_3N^+$ may be formed by cosmic-ray ionization, cosmic-ray-induced photoionization, electron bombardment or chemical ionization of acrylonitrile. $C_3H_3N^+$ has been reported as the major

product (80%), at a pressure of 0.30 Torr, of the reaction of $C_2H_2^+$ with HCN:[166,267] $k_{obs} = 3.7 \times 10^{-10}$ cm^3 molec^{-1} s^{-1} at 305K. Adduct formation in this instance is ascribed to termolecular association: under interstellar conditions, the analogous

Table 6.1: Reactions of $C_3H_3N^+ + X$.

X	Products [a]		k_{obs} [a]	k_c [a]	-ΔH [a]
H_2	$C_3H_4N^+ + H\cdot$		0.0012	1.50	99
CO	$C_3H_3N^+.CO$		0.007	0.79	–
N_2	none		<0.0005	0.73	–
CH_4	$CH_2CNH^+ + C_2H_4$ [e]	[0.70]	0.026	1.08	106
	$C_3H_4N^+ + CH_3\cdot$ [e]	[0.25]			97
	$C_4H_6N^+ + H\cdot$	[0.05]			–
H_2O	$C_2H_4O^+ + HCN$ [e]	[0.68]	0.21	2.42	–
	(or $H_2NCO^+ + C_2H_3\cdot$)				–
	$C_3H_4NO^+ + H\cdot$	[0.31]			–
	$C_3H_3N^+.OH_2$	[0.01]			–
NH_3	$NH_3^+ + CH_2CHCN$	[0.66]	1.9	2.18	73
	$NH_4^+ + C_3H_2N\cdot$	[0.34]			–
C_2H_2	$C_3H_3^+ + CH_2CN\cdot$ [e]	[0.08]	0.93	1.02	145 [f]
	$C_4H_4^+ + HCN$ [e]	[0.55]			–
	(or $HC_3NH^+ + C_2H_3\cdot$)				72
	$HC_5NH^+ + H_2 + H\cdot$	[0.21]			–
	$C_5H_4N^+ + H\cdot$	[0.16]			–
HCN	$C_4HN_2^+ + H_2 + H\cdot$	[0.09]	0.19	3.28	–
	$C_4H_2N_2^+ + H_2$	[0.38]			–
	$C_4H_3N_2^+ + H\cdot$	[0.20]			–
	$C_4H_4N_2^+$	[0.33]			–
CH_2CHCN	$C_3H_3N^+.CH_2CHCN$		2.0	3.62	–

Notes

a. Product channels reported in brackets, where more than one product was detected.
b. Observed rate coefficient, in units of 10^{-9} cm^3 molec^{-1} s^{-1}.
c. Calculated ADO collision rate coefficient, using the theory of Su and Chesnavich.[172]
d. Reaction exothermicity in units of kJ mol^{-1}. Taken from the tabulation of Lias et al,[184] unless otherwise stated.
e. See text for discussion of ion identification.
f. Calculated assuming a protonated cyclopropenylidene structure for $C_3H_3^+$.

radiative association reaction could occur. $C_3H_3N^+$ has also been reported as a minor product of the reaction of C_3H^+ with NH_3,[329-331] although this may not represent an efficient method of $C_3H_3N^+$ production depending upon the low-temperature reactivity of C_3H^+ with H_2 and other cloud species more abundant than NH_3.

The reaction of $C_3H_3N^+$ with H_2, which occurs via H-atom abstraction, is very slow. The product ion is presumed to be protonated acrylonitrile, in accordance with the calculations of Heerma et al[332] which establish $H_2C{=}CH{-}C{=}NH^+ \leftrightarrow H_2C{=}CH{-}C{\equiv}NH^+$ as the most stable $C_3H_4N^+$ isomer. The slow rate observed for this exothermic channel suggests that $C_3H_3N^+$ will be totally unreactive with H_2 under cold cloud conditions, although the low rate in this instance is not necessarily a consequence of an activation energy barrier. Atom abstraction reactions are generally fast if exothermic;[333] a dramatic exception is

$$NH_3^+ + H_2 \rightarrow NH_4^+ + H\cdot \qquad (6.7)$$

$$\Delta H_{6.3} = -86 \text{ kJmol}^{-1}.$$

This reaction occurs very slowly at room temperature ($k_{6.7} \sim 10^{-12}$ cm^3 molec^{-1} s^{-1} at 300K)[333] but proceeds much more rapidly at low temperature. The mechanism invoked to explain this behaviour involves formation of a weakly-bound complex prior to rearrangement to products. At elevated temperature, complex fragmentation occurs more rapidly than complex rearrangement, explaining the large negative temperature dependence seen for reaction (6.7) below 80K. A similar mechanism, to explain an even more marked negative temperature dependence, has been proposed for the reaction[334,335]

$$O_2^+ + CH_4 \rightarrow CH_3O_2^+ + H \qquad (6.8).$$

In the face of such counterexamples, and in the absence of a study of the temperature dependence of the reaction of $C_3H_3N^+$ with H_2 (the current version of the Canterbury SIFT permitting only room-temperature study of reactions), it is not possible to state that this reaction will necessarily be slow at low cloud temperatures. If the reaction is slow, then reaction of $C_3H_3N^+$ with other neutrals will be of some relevance in modelling of cloud chemistry.

The reaction of $C_3H_3N^+$ with CH_4 yields primary products at m/z 41, 54 and 68 as shown in table 6.1. The product ion at m/z 41 can be $C_3H_5^+$ or $C_2H_3N^+$ on the basis of its mass: however, all channels involving $C_3H_5^+$ are endothermic by at least 136 kJmol^{-1}, while channels involving CH_3CN^+ and CH_3NC^+ are also endothermic to a similar extent upon the basis of tabulated heats of formation.[184] The products are thus designated as $CH_2CNH^+ + C_2H_4$, since this is the only exothermic channel evident. The product ion at m/z 54 is protonated acrylonitrile, $C_3H_4N^+$: the other possible structure, $C_4H_6^+$, is rejected since all channels yielding $C_4H_6^+$ are very substantially endothermic. The product ion at m/z 68 is $C_4H_6N^+$. The structure of this $C_4H_6N^+$ ion cannot be reliably determined upon the basis of heats of formation. Production of the branched structure $(CH_3)_2CCN^+$ is endothermic by 15 kJmol^{-1}, but could well be exothermic within the combined uncertainties of the ΔH_f values used.[184] The formation of a cyclic isomer is also an exothermic channel, two such isomers (protonated pyrrole, and protonated cyclopropylcarbonitrile, c-$C_3H_5CNH^+$) having been reported.[184]

Identification of the main product of the reaction with H_2O is again difficult. The major product at m/z 42 can be either $C_2H_4O^+$ or CH_2NO^+, with the most exothermic possibility being the formation of $CH_2CHOH^+ + HCN$ (ΔH = -103 kJ mol^{-1}). Formation of H_2NCO^+ is possible (ΔH = -30 kJ mol^{-1}) but unlikely in view of the low exothermicity and the substantial degree of rearrangement required. The other product channels are adduct formation with, and without, the loss of H·.

For the fast reaction with NH_3, charge transfer and proton transfer compete. The presence of the latter channel establishes $PA(C_3H_2N) < PA(NH_3)$, corresponding to $\Delta H_f(C_3H_2N) < 561$ $kJmol^{-1}$. This is in comfortable agreement with $\Delta H_f(CH_2CHCN)$ = 184 kJ mol^{-1} and the expected value for $D(H—C_3H_2N)$, since $D(H—C_2H_3)$ = 213.1 kJ mol^{-1}.

The reaction with C_2H_2 proceeds at the collision rate, with several product channels. The major channel at m/z 52 is probably H-atom transfer to yield protonated cyanoacetylene (HC_3NH^+) and C_2H_3 (ΔH = -72 kJ mol^{-1}), although formation of $C_4H_4^+ + HCN$ is exothermic also for both linear and cyclic isomers of $C_4H_4^+$. The product ion at m/z 39 is identified as $C_3H_3^+ + CH_2CN$, since all channels to $C_2HN^+ + C_3H_4$ are endothermic. $C_3H_3^+$ produced in this reaction is most probably the cyclopropenylidenium cation, although a less exothermic channel to a linear isomer exists also. The minor channel at m/z 76 is very interesting, since this ion, $C_5H_2N^+$, may well be protonated cyanodiacetylene (HC_5NH^+). Alternative structures for this ion are less likely, since HC_5NH^+ is the protonated form of a known compound while other structures must represent linear ions with unsatisfied valences or cyclic ions with high strain due

to their extreme unsaturation. The cyclic structure with the lowest ring strain would be a structure related to pyridine. Bews and Glidewell[337] have calculated the heats of formation of six isomeric $C_5H_2N^+$ pyridine analogues: $\Delta H_f \geq 1777$ kJ mol^{-1} for all of these isomers. Given the accuracy of these calculations (agreement for the ΔH_f values calculated for ions in this study, where experimental values exist, is within ± 100 kJ mol^{-1} in all instances), such a cyclic structure for the ion formed in this reaction can be ruled out as endothermic. The study of Bews and Glidewell does not include N-protonated ions, but it seems intuitively unlikely that an N-protonated cyclic ion would have a heat of formation sufficiently far below those of the isomers covered by the study to permit generation of such an ion in the reaction considered here. The existence of the m/z 52 product channel thus establishes $\Delta H_f(HC_5NH^+) < 1247$ $kJmol^{-1}$, and would also yield a lower limit to the proton affinity of HC_5N except that, to date, no experimental value exists for $\Delta H_f(HC_5N)$. A theoretical calculation[336] using a STO-3G basis set yields an atomisation energy for HC_5N of 26.49 eV, corresponding to $\Delta H_f(HC_5N) = 1718$ kJ mol^{-1}: but since the same analysis drastically underestimates the atomisation energies for HCN and C_2H_2, this value for $\Delta H_f(HC_5N)$ is clearly far too high. The fourth channel evident for this reaction is formation of $C_5H_4N^+$, for which both linear and cyclic structures are energetically feasible: $\Delta H_f(C_5H_4N^+) < 1247$ kJ mol^{-1}, within the range of values given for pyridine-like $C_5H_4N^+$ ions.[337]

The reaction with HCN results in adduct formation with varying degrees of hydrogen loss, as listed in table 6.1. This reaction is evidently exothermic in view of the multiplicity of product channels observed, yet occurs at substantially below the calculated collision rate.

The reaction with CH_2CHCN is fast and results solely in adduct formation.

The exact structure of the $C_3H_3N^+$ ion exploited in these reactions is unknown. A CCCN skeletal structure is assumed, in view of its formation from acrylonitrile, and $\Delta H_f(C_3H_3N^+)$ = 1237 kJ mol^{-1} is assumed in accordance with IP(CH_2CHCN).[184,338] Several isomeric forms of $C_3H_3N^+$ probably exist as stable ionic structures: Heerma et al[332] postulate the existence of at least six stable $C_3H_4N^+$ isomers, and experiments on the Canterbury SIFT have demonstrated isomerism in a number of systems involving CN-containing ions (see chapters 4 & 5).[166,241,279,280,339] In view of these considerations, and of the highly energetic method of $C_3H_3N^+$ production, the isomeric purity of the reactant ion signal at m/z 53 cannot be certain: however, none of the reactions listed in table 6.1 gave any evidence to support the presence of multiple isomers in the reactant ion signal. It can also be assumed that the reactant ion signal was free of any effects from vibrational excitation: it would be unprecedented for an ion containing more than four atoms[226] to exhibit any metastable vibrational excitation.

Section 6.3: Reactions of $C_3H_4N^+$, $C_3H_2N^+$ and HC_3N^+.

In interstellar chemistry, $C_3H_4N^+$ can arise via protonation of CH_2CHCN as well as by the reactions detailed in section 6.1. $C_3H_4N^+$ is the ion which is central to acrylonitrile production in clouds:

$$CH_2CHCNH^+ + X \rightarrow C_2H_3CN + XH^+ \quad (6.9)$$

$$CH_2CHCNH^+ + e \rightarrow C_2H_3CN + H\cdot \quad (6.10)$$

$\Delta H_{6.10} = -518$ kJ mol^{-1}.

Dissociative recombination (6.10) may also lead to other products, for example $C_3H_2N\cdot + H_2$.

The reactions of $C_3H_4N^+$ with various neutrals are summarised in **table 6.2.**

Table 6.2: Reactions of $C_3H_4N^+ + X$.

X	Products [a]	k_{obs} [a]	k_c [a]	$-\Delta H$ [a]
H_2	none	< 0.0005	1.50	–
CO	none	< 0.0005	0.79	–
N_2	none	<0.0005	0.72	–
O_2	none	<0.0005	0.65	–
CH_4	none	< 0.0005	1.07	–
H_2O	$CH_2CHCN.OH_2^+ + H\cdot$	0.018	2.42	–
NH_3	$NH_4^+ + C_3H_3N$	1.7	2.18	60
C_2H_2	none? [b]	< 0.01	1.02	–
HCN	$CH_2CHCN.H.NCH^+$	0.034	3.27	–
CH_2CHCN	$(CH_2CHCN)_2H^+$	1.30	3.60	–

Notes

a. See footnotes (a-d) for table (6.1).
b. See text for discussion.

$C_3H_4N^+$ is substantially less reactive than $C_3H_3N^+$, exhibiting no reaction with H_2, CO, N_2, CH_4 or O_2, and slow adduct-forming reactions with HCN and H_2O. A reaction with C_2H_2 is possible, but the reaction (if it occurs) is very slow: products from such a reaction could not be detected due to the multiplicity of products formed by the rapid reaction of a small contaminant signal at m/z 53 ($C_3H_3N^+$) with C_2H_2, with additional products from secondary reactions in evidence also. Proton transfer is the only channel seen for the rapid reaction with NH_3. Adduct formation is the only channel seen for the reaction with the parent neutral, acrylonitrile.

Attempts were made to identify the $C_3H_4N^+$, generated in the manner described here, as protonated acrylonitrile on the basis of the known proton affinity of acrylonitrile. Staley et al[232] established $PA(CH_2CHCN)$ = 790.0 kJ mol^{-1} by ICR bracketing using 1,3-dioxolane, C_2H_5CHO and CH_3CN. Lias et al[185] adjusted this value to 794.0 kJ mol^{-1}, in good agreement with the value derived from a calculation by Heerma et al[332] of $\Delta H_f(CH_2CHCNH^+)$ = 925 kJ mol^{-1} which establishes this as the lowest-energy $C_3H_4N^+$ isomer.

Unfortunately, attempts to use proton-transfer bracketing techniques to characterise the m/z 54 ion signal were thwarted by the occurrence of competing adduct formation in the reactions between $C_3H_4N^+$ and toluene ($PA(C_6H_5CH_3)$ = 794.0 kJ mol^{-1})[185] and $C_3H_4N^+$ and CH_3CN ($PA(CH_3CN)$ = 788 kJ mol^{-1}).[185] These reagents were chosen on the basis of their PA values, which are close to the literature value (794 kJ mol^{-1}) for acrylonitrile. Proton transfer was observed as a minor channel in each of these reactions (less than 5% for $C_3H_4N^+ + CH_3CN$)

but in view of the competing adduction processes it was not felt useful to quantify the product distributions for these reactions.

Some studies were also made of the reactivity of $C_3H_2N^+$ with various neutrals: these results are presented in **table 6.3.**

Table 6.3: Reactions of $C_3H_2N^+$ + X.

X	Products[a]		k_{obs}[a]	k_c[a]	$-\Delta H$[a]
H_2	none		<0.0005	1.50	–
CO	none		<0.001	0.79	–
N_2	none		<0.0005	0.73	–
CH_4	none		<0.005	1.08	–
H_2O	none		<0.05	2.42	–
C_2H_2	none		<0.01	1.02	–
HCN	$C_3H_2N.HCN^+$		0.06	3.28	–
CH_2CHCN	$CH_2CHCNH^+ + HC_3N$[b] $C_5H_4N^+ + HCN$	[0.81] [0.19]	1.6	3.6	41[c] –
CH_3NO_2	$CH_3NO_2H^+ + HC_3N$ $C_3H_2N.CH_3NO_2^+$	[0.60] [0.40]	1.2[b]	2.7	-1 –
CH_3NO_2	$CH_3NO_2H^+ + HC_3N$ $C_3H_2N.CH_3NO_2^+$	[0.60] [0.40]	1.37[d]	2.7	-1 –

Notes

a. See footnotes (a-d) for table (6.1).
b. Results obtained for $C_3H_2N^+$ generated by electron impact upon CH_2CHCN.
c. Calculated assuming a protonated cyanacetylene structure for $C_3H_2N^+$; see text for discussion.
d. Results obtained for $C_3H_2N^+$ generated by electron impact upon a HC_3N / H_2 mixture (1:30).

HC_3NH^+ is the precursor ion to the prominent interstellar species HC_3N, and should also be detectable within dense clouds although attempts at its detection have to date proved fruitless.[39,40] Many interstellar pathways to HC_3NH^+ exist,[182] and its reactivity (with reference especially to proton transfer) has been previously studied in SIFT instruments by bracketing[205] and by determination of proton-transfer equilibrium constants.[167,267]

A small signal at m/z 52, due to $C_3H_2N^+$, was present in all cases when the reactions of $C_3H_3N^+$ were being studied. In consequence, it was necessary to study the reactivity of this m/z 52 ion to ensure that it was not giving rise to any signals ascribed to $C_3H_3N^+$ + **X** reaction products, and to determine also whether the $C_3H_2N^+$ ion signal was protonated cyanoacetylene. This possibility was strongly suggested by the reaction

$$C_3H_2N^+ + C_2H_3CN \rightarrow C_3H_4N^+ + C_3HN \quad [0.81] \quad (6.6a)$$

$$\rightarrow C_5H_4N^+ + CHN \quad [0.19] \quad (6.6b)$$

for which $k_{6.6} = 1.6 \times 10^{-9}$ cm^3 molec^{-1} s^{-1} was found. The presence of channel (6.6a) as the major product channel is consistent with rapid proton transfer from HC_3N to acrylonitrile (ΔH = -41 kJ mol^{-1}).[184] Channel (6.6b) requires $\Delta H_f(C_5H_4N^+) < 1177$ kJ mol^{-1}, a lower value than the upper limit for $C_5H_4N^+$ production from the reaction of $C_3H_3N^+$ with C_2H_2 (see table 6.1). The structure of the $C_5H_4N^+$ ion produced in this reaction is not known.

$C_3H_2N^+$ was not reactive with most of the neutral reagents tested: for **X** = H_2, CO, N_2, CH_4, H_2O, HCN and C_2H_2, $C_3H_2N^+$ was unreactive or exhibited

$k_{obs}(C_3H_2N^+) < 0.1\ k_{obs}(C_3H_3N^+)$, while for **X** = NH_3, proton transfer was the only product channel observed:

$$C_3H_2N^+ + NH_3 \rightarrow NH_4^+ + HC_3N \qquad (6.11),$$

with $k_{6.11} = 2.0 \times 10^{-9}$ cm^3 molec^{-1} s^{-1}. Adduct formation was observed to occur in the slow reaction with HCN; adduct formation may also be occurring with C_2H_2, although an upper limit of $k < 10^{-11}$ cm^3 molec^{-1} s^{-1} was assigned for this reaction. The $C_3H_2N^+$ ion was also seen to react with CH_3NO_2:

$$C_3H_2N^+ + CH_3NO_2 \rightarrow CH_3NO_2H^+ + HC_3N \quad [0.60] \quad (6.12a)$$

$$\rightarrow CH_3NO_2.H.NC_3H^+ \quad [0.40] \quad (6.12b),$$

with $k_{6.12} = 1.2 \times 10^{-9}$ cm^3 molec^{-1} s^{-1}. The product ratio determined here may be mildly distorted due to mass discrimination effects. Nevertheless, the observed product ratio is in excellent agreement with that observed for the reaction of protonated cyanoacetylene with nitromethane;[167] the rate coefficient observed is somewhat lower than the value of 1.8×10^{-9} cm^3 molec^{-1} s^{-1} reported by Knight et al for reaction (6.12) using protonated cyanoacetylene, but in very good agreement with the value of $k_{6.12} = 1.37 \times 10^{-9}$ cm^3 molec^{-1} s^{-1} obtained when we repeated Knight's measurement using HC_3N / H_2 as the source gas. The agreement between these two values, which are significantly below the collision rate expected for reaction (6.12), indicates that $C_3H_2N^+$ generated by electron ıpact upon acrylonitrile has the same structure as protonated cyanoacetylene.

Ions at the neighbouring masses, m/z 51 (HC_3N^+) and 53 ($C_3H_3N^+$), were also present when $C_3H_2N^+$ was injected to study the reaction with CH_3NO_2. By varying the mass setting on the upstream mass spectrometer, the ratios of the reactant ion signals at m/z 51, 52 and 53 could be altered, and thus it was possible to assign products also for the reactions of C_3HN^+ and $C_3H_3N^+$ with CH_3NO_2:

$$C_3HN^+ + CH_3NO_2 \rightarrow CH_3NO^+ + HC_3NO \qquad (6.13)$$

$$C_3H_3N^+ + CH_3NO_2 \rightarrow C_4H_6N^+ + NO_2 \qquad (6.14)$$

$k_{6.13} = 1.9 \times 10^{-9}$ cm^3 molec^{-1} s^{-1}

$k_{6.14} = 1.0 \times 10^{-9}$ cm^3 molec^{-1} s^{-1}.

A secondary product peak at m/z 76, especially prominent when m/z 51 was the largest reactant ion signal, was attributed to the reaction

$$CH_3NO^+ + CH_3NO_2 \rightarrow (CH_3)_2NO_2^+ + NO \qquad (6.15)$$

for which a rate determination was not attempted (although the reaction appeared to occur rapidly).

Although not directly related to the ion-molecule chemistry of acrylonitrile, some further reactions of HC_3N^+ with prominent interstellar neutrals were also studied. These reactions have not been included in previous investigations of cyanoacetylene ion-molecule chemistry:[64,167,205,214,255,265,267] since HC_3N^+ displays little reactivity with H_2, these reactions (which are presented in **table 6.4**) are likely to be important as loss processes of HC_3N^+ within interstellar clouds.

The reaction with CH_4 shows some parallels with the reaction of $C_3H_3N^+$ with methane: channels involving H-atom abstraction and formation of CH_2CNH^+ appear common to both ions, although the ion at m/z 41 can also be $CH_2CHCH_2^+$ since this channel is slightly exothermic also. A channel at m/z 40 is attributed to $C_3H_4^+$, since production of any ion of the form C_2H_2N+ is endothermic. The structure of the $C_3H_4^+$ product is not known: several possible structures exist, each of which corresponds to an exothermic channel.

The reaction with C_2H_2 displays adduct formation and a small charge-transfer channel in addition to a larger channel producing $C_4H_2^+$: this reaction has already been discussed in section 4.2.

Table 6.4: Reactions of $HC_3N^+ + X$.

X	Products [a]		k_{obs} [a]	k_c [a]	-ΔH [a]
CH_4	$C_3H_4^+ + HCN$	[0.11]	0.83	1.1	– [b]
	$CH_2CHCH_2^+ + CN\cdot$	[0.56]			18
	(or $CH_2CNH^+ + C_2H_2$)				168
	$HC_3NH^+ + CH_3\cdot$	[0.35]			126
C_2H_2	$C_2H_2^+ + HC_3N$	[0.05]	1.3	1.1	23
	$C_4H_2^+ + HCN$	[0.60]			145
	$HC_3N.C_2H_2^+$	[0.30]			–
CO	$HC_3N.CO^+$		0.055	0.80	–
NH_3	$NH_3^+ + HC_3N$		1.7	2.2	143
HCN	$HCNH^+ + C_3N\cdot$	[0.32]	1.32	3.3	33
	$C_4N_2H^+ + H\cdot$	[0.17]			< 143 [c]
	$HC_3N.HCN^+$	[0.51]			–

Notes

a. See footnotes (a) - (d) for table (6.1).
b. See text for discussion.
c. Calculated assuming a structure $NCCCCNH^+$ for the product ion (see section 4.3).

Charge-transfer (which occurs rapidly) is the only product channel seen with NH_3. The apparent absence of proton transfer (ΔH = -170 kJ mol^{-1}) as a competing product channel in this reaction is surprising, given the usual rapidity of proton transfer when exothermic.

The reaction with HCN exhibits adduct formation, proton transfer, and production of a $C_4N_2H^+$ ion: this ion may have the same structure as the protonated dicyanoacetylene species seen in several reactions of the $C_4N_2^+$ ion investigated in section 4.3.

All of these reactions occur rapidly at 300 K: they are likely to represent efficient reactions under interstellar conditions also, and should thus be considered in models of cyanopolyyne chemistry. The adduct formation channel evident with CO, although inefficient as a termolecular association process at 0.3 Torr, is likely also (as a radiative association process) to be of some significance to the loss of HC_3N^+ within clouds.

Section 6.4: Reactions of various ions with acrylonitrile.

Reactions of several ions with acrylonitrile are displayed in **table 6.5**.

Although a detailed survey of ions of astrophysical interest was not attempted, many of the reactions detailed in table 6.5 are of relevance to interstellar

Table 6.5: Reactions of $X^+ + CH_2CHCN$.

X^+	Products [a]		k_{obs} [a]	k_c [a]	$-\Delta H$ [a]
H_3^+	$CH_2CHCNH^+ + H_2$		9.9	11.1	370
He^+	$C_2H_2^+ + HCN + He$ [b]	[0.33]	10.5	9.6	1093
	$C_2H_3^+ + CN\cdot + He$	[0.05]			1009
	(or $CHN^+ + C_2H_2 + He$)				–
	$c\text{-}C_3H_3^+ + N\cdot + He$ [b]	[0.05]			477
	$HC_3N^+ + H_2 + He$	[0.29]			1082
	$C_3H_2N^+ + H\cdot + He$	[0.12]			1211 [c]
	$CH_2CHCN^+ + He$	[0.16]			1319
C^+	$C_3H_2^+ + HCN$ [b]	[0.24]	4.1	6.0	–
	$c\text{-}C_3H_3^+ + CN\cdot$ [b]	[0.44]			676
	$C_4H_2N^+ + H\cdot$	[0.29]			–
	$C_4H_3N^+$	[0.03]			–
N^+	$C_2H_2^+ + HNCN\cdot$ [d]	[0.20]	4.3	5.6	–
	$CHN^+ + CH_2CN\cdot$	[0.07]			–
	(or $C_2H_3^+ + N_2 + C$)				230
	$C_3H_2^+ + N_2 + H\cdot$ [b]	[0.48]			–
	$C_3H_2N^+ + NH$	[0.10]			555 [c]
	$CH_2CHCN^+ + N\cdot$	[0.15]			349
N_2^+	$C_2H_2^+ + HCN + N_2$	[0.57]	4.4	4.4	224
	$CHN^+ + N_2 + C_2H_2$	[0.08]			–
	(or $C_2H_3^+ + N_2 + CN\cdot$)				140
	$C_3H_2N^+ + N_2 + H.$	[0.26]			341 [c]
	$CH_2CHCN^+ + N_2$	[0.09]			450
Ar^+	$C_2H_2^+ + HCN + Ar$	[0.46]	3.1	3.9	242
	$CH_2CHCN^+ + Ar$	[0.54]			468
CH_3^+	$c\text{-}C_3H_3^+ + CH_2NH$ [b]	[0.15]	4.4	5.5	67
	$C_3H_2N^+ + CH_4$	[0.29]			224 [c]
	$CH_2CHCN.CH_3^+$	[0.56]			–
C_2H^+	$C_3H_2N^+ + C_2H_2$		4.8	4.4	532 [c]
	(or $C_4H_4^+ + CN\cdot$)				–
$C_2H_2^+$	$c\text{-}C_3H_3^+ + C_2H_2N\cdot$ [b]	[0.15]	4.3	4.4	192
	$CH_2CHCN^+ + C_2H_2$	[0.55]			47
	$CH_2CHCNH^+ + C_2H\cdot$	[0.15]			27
	$CH_2CHCN.C_2H_2^+$	[0.15]			–
$C_2H_3^+$	products [b]		4.4	4.4	–
$c\text{-}C_3H_2^+$	products [b]		4.5	3.9	–

(table 6.5 cont'd)

l-$C_3H_2^+$	products [b]		4.5	3.9	–
c-$C_3H_3^+$	$CH_2CHCN.C_3H_3^+$		0.11	3.9	–
l-$C_3H_3^+$	products [b]		4.0	3.9	–
CO^+	$C_2H_2^+ + HCN + CO$ [b]	[0.65]	4.1	4.4	114
	$CH_2CHCN^+ + CO$	[0.35]			340
CN^+	c-$C_3H_3^+ + N_2 + C$ [b]	[0.16]	4.5	4.4	187
	$CH_2CHCN^+ + CN\cdot$	[0.75]			307
	(or $C_2N_2H^+ + C_2H_2$)				586 [e]
	$CH_2CHCN.CN^+$	[0.09]			–
HCN^+	products [b]		4.6	4.4	–
HNC^+	products [b]		4.6	4.4	–
$HCNH^+$	$CH_2CHCNH^+ + HCN$		4.5	4.4	77
CCN^+	$C_3H_3^+ + C_2N_2$ [b]		3.6	3.9	–
CNC^+	$C_3H_3^+ + C_2N_2$ [b]		3.6	3.9	–
HC_2N^+	$CH_2CHCNH^+ + C_2N\cdot$	[0.70]	2.9	3.9	239
	$C_4H_3N^+ + HCN$	[0.15]			f
	(or $C_3HN_2^+ + C_2H_3\cdot$)				g
	$CH_2CHCN.C_2HN^+$	[0.15]			–

Notes

a. See footnotes (a) - (d) for table (6.1).
b. See text for discussion.
c. Calculated assuming a structure $HCCCNH^+$ for $C_3H_2N^+$.
d. Neutral products not established. The exothermicity of this product channel requires $\Delta H_f(HNCN\cdot) < 731$ kJ mol^{-1}, consistent with an upper limit of $\Delta H_f(HNCN\cdot) < 471$ kJ mol^{-1} upon the evidence of the product channel $HNC^+ + N_2O \rightarrow NO^+ + HNCN\cdot$ (see chapter 5). Alternatively, the neutrals here may be $HCN + N\cdot$ ($\Delta H = -123$ kJ mol^{-1}) or $CH\cdot + N_2$ ($\Delta H = -135$ kJ mol^{-1}).
e. Calculated using a value $\Delta H_f(C_2N_2H^+) = 1165$ kJ mol^{-1} (see chapter 3).
f. The exothermicity of this product channel requires $\Delta H_f(C_4H_3N^+) < 1580$ kJ mol^{-1}.
g. The exothermicity of this product channel requires $\Delta H_f(C_3HN_2^+) < 1450$ kJ mol^{-1}.

---

chemistry, since the ions H_3^+, He^+, C^+, CH_3^+, $C_2H_3^+$, $C_3H_2^+$, $C_3H_3^+$, N^+, $HCNH^+$ and CNC^+ are all unreactive (or react only slowly) with H_2. All of the ions studied,

except c-$C_3H_3^+$, were observed to react very rapidly ($k > 2.5 \times 10^{-9}$ cm^3 $molec^{-1}$ s^{-1}) with CH_2CHCN.

Where applicable, reactivity of the ions concerned is compared to their reactivity with other CN-containing neutrals such as HCN and C_2N_2.

He^+, N_2^+, CO^+, Ar^+. For these ions the major products from reaction with acrylonitrile were at m/z 26 and m/z 53. For **X** = N_2^+, CO^+, Ar^+, production of $CN^+ + C_2H_3\cdot + \mathbf{X}$ is endothermic and so the product ion at m/z 26 for these reactions is clearly $C_2H_2^+$; for He^+, production of CN^+ is energetically possible but $C_2H_2^+$ production is more likely upon energetic grounds and by analogy with the reactions of N_2^+, CO^+ and Ar^+. Attempts were made to distinguish between CN^+ and $C_2H_2^+$ upon the basis of the reactivity of these ions with CH_2CHCN, but it was not possible to positively identify the m/z 26 ion product for the reaction of He^+. Other fragmentary ions were produced in the reactions of He^+ and N_2^+: these include c-$C_3H_3^+$ (identified by its lack of reactivity with CH_2CHCN) and $C_3H_2N^+$, presumably protonated cyanoacetylene. The production in these reactions of protonated cyclopropenylidene, and HC_3NH^+, is of interest because these ions are integral to ion-molecule models of interstellar chemistry. Furthermore, He^+ reacts only slowly with H_2 and thus its reaction with acrylonitrile should be considered in such models.

The multiplicity of fragmentary products seen in these reactions suggests that these reactions occur by a mechanism of dissociative charge transfer. Charge transfer in all these instances is highly exothermic, and collisional stabilisation of the charge-transfer product may be in competition with unimolecular

dissociation of the initial, highly excited, product. The greatest multiplicity of product channels is seen in the reaction with He^+, corresponding to the very high exothermicity of charge-transfer in this instance. Reaction of He^+ with HCN and HC_3N also results in several fragmentation products,[167,341] whereas N_2^+ is observed[167,214,341] to undergo only charge-transfer with HCN and HC_3N.

C^+, N^+, CN^+. These ions all generated product ions at m/z 38 and/or m/z 39. Possible product ions at m/z 38 are c-$C_3H_2^+$, l-$C_3H_2^+$, CCN^+ and CNC^+; possible products at m/z 39 are c-$C_3H_3^+$, l-$C_3H_3^+$, $HCCN^+$ and $HCNC^+$. In all these instances, production of cyano-containing ions could be eliminated on energetic grounds or upon the basis of the reactivity of these product ions with acrylonitrile. The major product channel for the reaction of CN^+ with acrylonitrile, at m/z 53, is probably charge-transfer: it should be noted, however, that production of $C_2N_2H^+$ (protonated dicyanogen) requires only a slight degree of rearrangement and is more exothermic. Adduct formation was a minor channel for the reactions of C^+ and CN^+.

A parallel is evident between the reaction of C^+ with acrylonitrile, and those of C^+ with HCN, HC_3N and C_2N_2: in the latter reactions, as with CH_2CHCN, loss of H· and of CN· are the dominant product channels observed.[149,167,214,225,238,247,343] Similarly, the occurrence of charge-transfer as the major product channel for the reactions of CN^+ + HCN, HC_3N, CD_3CN and C_2N_2 [214,246,247,344] mirrors the tendency observed in the reaction of CN^+ with acrylonitrile. There are fewer similarities evident in the case of the reaction of N^+: a wider range of product channels in the reaction with CH_2CHCN, in comparison with the reactions[167,247]

$N^+ + HC_3N$	$\rightarrow$	$C_3H^+ + N_2$	[0.50]	(6.16a)
	$\rightarrow$	$HC_3N^+ + N\cdot$	[0.50]	(6.16b)
$N^+ + C_2N_2$	$\rightarrow$	$C_2N^+ + N_2$	[0.70]	(6.17a)
	$\rightarrow$	$C_2N_2^+ + N\cdot$	[0.30]	(6.17b),

probably reflects the greater structural complexity of the acrylonitrile molecule.

H_3^+, $C_2H_3^+$, $HCNH^+$. Proton transfer was the major channel evident in these reactions, which is consistent with the proton affinity of acrylonitrile ($PA(CH_2CHCN)$ = 794 kJ mol^{-1}). In the case of $C_2H_3^+$, some adduct formation (~ 20%) was also seen: a rigorous product analysis for this reaction was not attempted since we were unable to produce an adequately large, clean signal of $C_2H_3^+$.

HCN^+, HNC^+. These ions were injected together from the ion source, using HCN as a source gas. Under these conditions, HCN^+ accounts for ~ 70% of the m/z 27 ion signal.[279] No attempt was made in this instance to distinguish between the reactivity of HCN^+ and of HNC^+ with CH_2CHCN - the intent was, rather, to ascertain differences in the reactivity of CHN^+ and $C_2H_3^+$ with CH_2CHCN, so that product ions at m/z 27 could be characterised. The product channels observed for reaction of CHN^+ with acrylonitrile were at m/z 53 (60%) and m/z 54 (40%), corresponding to charge-transfer and proton-transfer respectively (these are also the only product channels seen in the reactions of CHN^+ with HCN and HC_3N).

As it happened, the reactions of He^+, N^+ and N_2^+ produced too little m/z 27 ($\leq$ 8% of total products) to be able to distinguish between $C_2H_3^+$ and CHN^+ in these instances.

CH_3^+. The major product observed for this reaction was the adduct. The other products were identified as the protonated forms of cyclopropenylidene and cyanoacetylene. In view of the lack of reactivity of CH_3^+ with H_2 and with CO, this reaction represents an important loss process for CH_2CHCN within interstellar clouds: although the minor products suggest that c-C_3H_2 and HC_3N will be eventual products of such reaction, it is possible also that radiative association may be more prominent under interstellar conditions.[60]

Association is also observed as the dominant channel for the reactions of CH_3^+ with HCN, CH_3CN and HC_3N, even at the low pressures pertinent to ICR experiments.[60,63] This indicates that CH_3^+ forms very long-lived and stable collision complexes with CN-containing compounds.

C_2H^+, $C_2H_2^+$. These ions were produced from electron impact upon C_2H_2. The sole product channel observed for the reaction of C_2H^+, at m/z 52, is presumed to be hydride transfer ($\rightarrow$ HC_3NH^+ + C_2H_2) since the alternative, production of $C_4H_4^+$ + CN·, is substantially less exothermic and requires more rearrangement. Charge-transfer is the major product from $C_2H_2^+$; other product channels are at m/z 39 (c-$C_3H_3^+$, identified by its lack of reactivity with CH_2CHCN) and at m/z 54, corresponding to proton transfer.

$C_3H_2^+$, $C_3H_3^+$. These ions were produced by electron bombardment upon propyne, CH_3CCH. Smith and Adams[345] have shown that electron impact upon propyne produces ~80% of $C_3H_2^+$, and ~35% of $C_3H_3^+$, in the higher-energy linear forms: the cyclic isomers account for the remainder. In the present studies, reactions of $C_3H_2^+$ and $C_3H_3^+$ were investigated to aid identification of m/z 38 and m/z 39 products from other reactions with acrylonitrile. No attempt was made to distinguish between the cyclic and linear forms of $C_3H_2^+$. Adduct formation was the dominant channel seen for all of the reactive ions: the reaction profile for m/z 39 with acrylonitrile displayed distinct curvature (see **figure 6.1**), indicating a difference in reactivity of the two isomers of $C_3H_3^+$. The more reactive ion, which accounted for ~30% of the m/z 39 ion signal, is identified as l-$C_3H_3^+$, since it could be removed by addition of C_2H_2 (see **figure 6.2**): the reactivity of the m/z 39 ion remaining was consistent with its reactivity in the absence of C_2H_2. The cyclic isomer reacted on only a few percent of collisions, exhibiting only adduct formation. The absence of proton transfer from c-$C_3H_3^+$ to CH_2CHCN suggests that PA(c-C_3H_2) exceeds 794 kJ mol^{-1}, the proton affinity of CH_2CHCN: PA(c-C_3H_2) has not been determined, but a value PA(c-C_3H_2) > 794 kJ mol^{-1} is in agreement with the findings of Smyth et al,[346] who studied the reactions of $C_3H_3^+$ with several hydrocarbons in an ICR experiment.

A minor product at m/z 54, corresponding to proton transfer, was in evidence in our experiments: we were unable to determine whether it arose from c-$C_3H_2^+$, l-$C_3H_2^+$ or l-$C_3H_3^+$ since we could not inject m/z 39 from propyne without some contamination from m/z 38, and vice versa. This peak at m/z 54 was not in evidence when C_2H_2 was added to remove l-$C_3H_3^+$ (and also $C_3H_2^+$, since both isomers are reactive with acetylene), so the possibility of proton transfer from c-$C_3H_3^+$ can be eliminated.

Figure 6.1: Experimental decay curves observed for the reaction of $C_3H_3^+$ with CH_2CHCN. (a). Graph over the entire flow range. (b). Graph highlighting the initial decay at low CH_2CHCN flows. The curvature evident in these graphs indicates that two isomers of $C_3H_3^+$ react at distinctly different rates with CH_2CHCN: the solid curve fitted to the experimental data points describes the sum of two exponential terms, yielding $k = 3.97 \times 10^{-9}$ cm^3 molec^{-1} s^{-1} for the more reactive $C_3H_3^+$ isomer (which accounts for 29% of the m/z 39 ion signal in this graph) and $k = 1.10 \times 10^{-10}$ cm^3 molec^{-1} s^{-1} for the less reactive isomer.

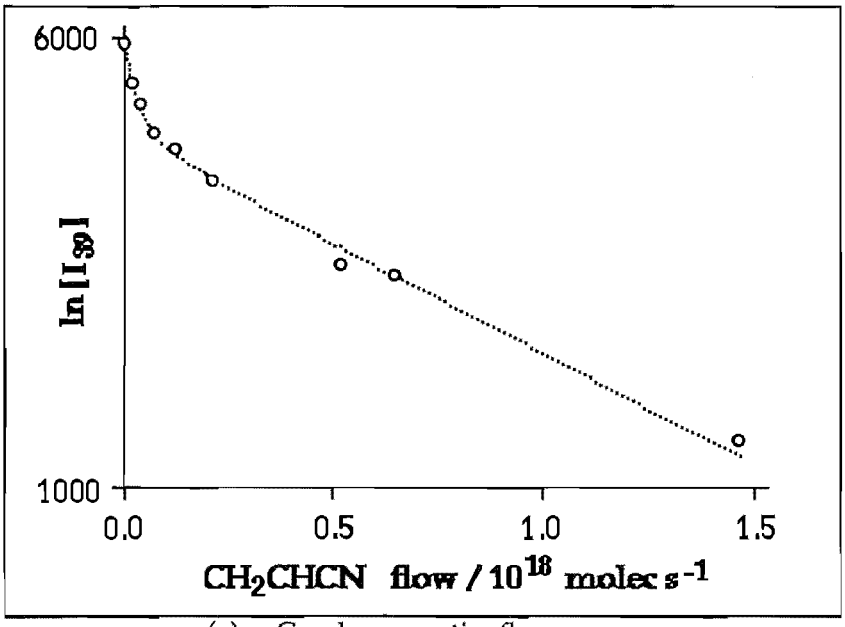

(a). Graph over entire flow range.

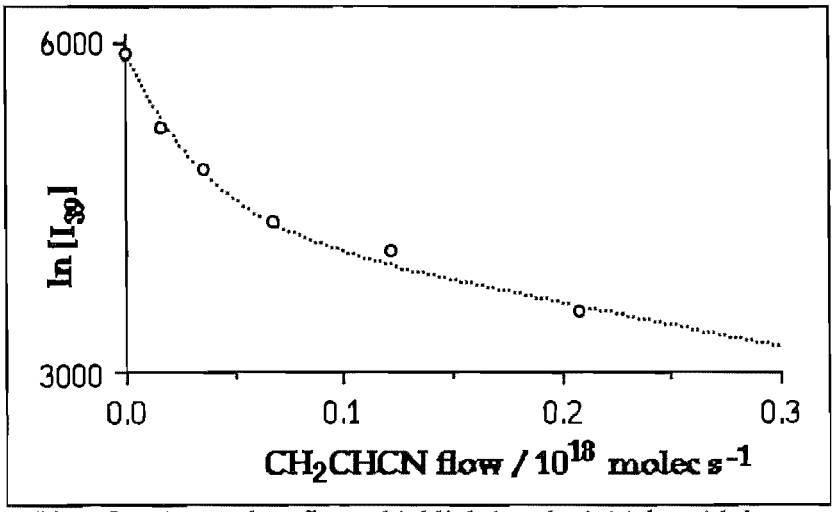

(b). Graph over low flows, highlighting the initial rapid decay.

C_2N^+, HC_2N^+. The reactions of these ions were studied so that products at m/z 38 (39) could be identified as $C_3H_{2(3)}^+$ or $(H)C_2N^+$.

CCN^+ and CNC^+ were produced by electron impact upon C_2N_2: we have previously shown[241] that this technique produces approximately 20% CCN^+ : 80% CNC^+. The only product seen (for reaction of both isomers of C_2N^+ with acrylonitrile) was at m/z 39, which was observed to react further with acrylonitrile to form an adduct at m/z 92. We suppose the product ions at m/z 39 to be a mixture of l-$C_3H_3^+$ and c-$C_3H_3^+$, since these channels are more exothermic than production of HC_2N^+ and since generation of $C_3H_3^+$ would be accompanied by C_2N_2 formation, in keeping with the reactions

Figure 6.2: Experimental decay curve observed for the reaction of $C_3H_3^+$ with CH_2CHCN (added at port 2), subsequent to the addition of a large flow of C_2H_2 at port 1. C_2H_2 reacts rapidly with l-$C_3H_3^+$ but is unreactive with c-$C_3H_3^+$: thus, this graph indicates the reaction due to c-$C_3H_3^+$ with acrylonitrile. The slope from this graph gives $k = (1.014 \pm 0.025) \times 10^{-10}$ cm^3 $molec^{-1}$ s^{-1} for this reaction, in excellent agreement with the rate coefficient determined for the reaction of the less reactive $C_3H_3^+$ isomer in the graph in figure 6.1.

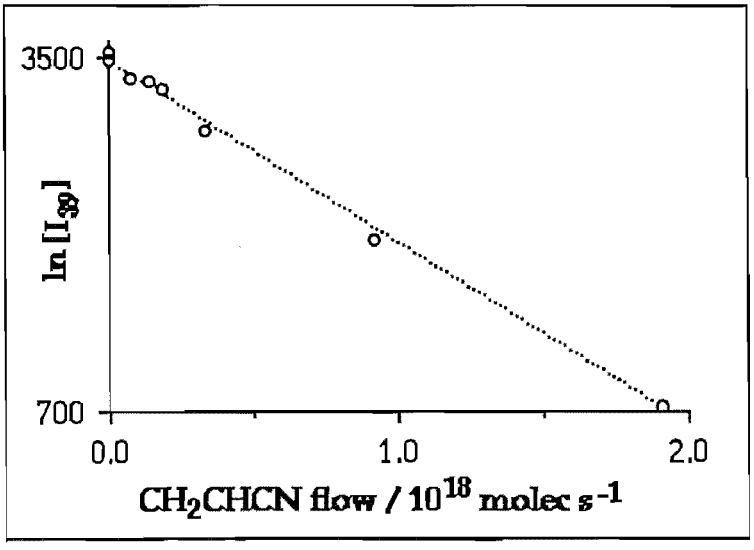

$$C_2N^+ + CH_3CN \rightarrow C_2H_3^+ + C_2N_2 \quad (6.18)$$

$$C_2N^+ + HC_3N \rightarrow C_3H^+ + C_2N_2 \quad (6.19).$$

HC_2N^+ was generated from a 5% mixture of C_2N_2 in H_2. The major product channel seen was proton transfer, with adduct formation also in evidence.

$HCNC^+$ was produced from methyl isocyanide, CH_3NC. Only a very small ion signal at m/z 39 could be obtained, and the isomeric nature of this ion could not be established. A rate coefficient for the reaction of $HCNC^+$ with CH_2CHCN could not be reliably obtained in view of the signal size and since m/z 39 was also the sole product from the contaminating signal at m/z 38. However, a lower limit of $k \geq 1.5 \times 10^{-9}$ cm^3 $molec^{-1}$ s^{-1} suggests that this isomer reacts rapidly, probably at the collision rate, with CH_2CHCN.

Section 6.5: Production of CH_2CHCN and cyanopolyynes in interstellar clouds.

Few of the reactions listed in tables 6.1 to 6.5 shed any light on the processes involved in acrylonitrile formation in interstellar clouds, beyond demonstrating that protonated acrylonitrile $C_3H_4N^+$ (which is the likely main precursor ion to acrylonitrile in the interstellar environment) is unreactive with the predominant interstellar species. In an effort to explore an additional possible pathway to CH_2CHCN production, the reactions of N^+ with C_2H_2 and CH_3CCH

were studied: the reactions of N^+ with alkynes represent an ion-molecule reaction class not previously investigated, and alkynes and their derivatives are prominent interstellar cloud constituents.

$N^+ + C_2H_2$	$\rightarrow$	$C_2H_2^+ + N\cdot$	[0.65]	(6.20a)
	$\rightarrow$	$CH_2N^+ + C$	[0.19]	(6.20b)
	$\rightarrow$	$C_2N^+ + H_2$	[0.09]	(6.20c)
	$\rightarrow$	$HC_2N^+ + H.$	[0.07]	(6.20d)

$k_{6.20} = 1.5 \times 10^{-9}$ cm^3 molec^{-1} s^{-1}

$N^+ + CH_3CCH$	$\rightarrow$	$C_2H_2^+ + HCN + H\cdot$	[0.20]	(6.21a)
	$\rightarrow$	$C_3H_3^+ + NH$	[0.47]	(6.21b)
	$\rightarrow$	$C_3H_4^+ + N\cdot$	[0.32]	(6.21c)
	$\rightarrow$	$C_3HN^+ + H_2 + H\cdot$	[0.01]	(6.21d)

$k_{6.21} = 1.4 \times 10^{-9}$ cm^3 molec^{-1} s^{-1}.

The products reported here are those calculated as the most exothermic product channels corresponding to the product ion masses: in the reaction of propyne, product channels to $CN^+ + C_2H_4$ and to $HC_2N^+ + CH_3\cdot$ are possible also but are less exothermic than the products assigned for channels (6.21a) and (6.21b), respectively. Charge transfer is a prominent channel for each reaction. None of the major product channels suggest any promise for CH_2CHCN synthesis by such reactions, although the appearance of a very small C_3HN^+ channel (6.21d) for the reaction with propyne is of interest since this ion could be ionized cyanoacetylene.

On the topic of HC_3N production, Turner has commented[18,39,347] that the non-detection[39,40] of the HC_3NH^+ ion in interstellar sources such as TMC-1 and Sagittarius B2 indicates a flaw in the ion-molecule modelling of cyanopolyyne synthesis in these sources. A discrepancy in the abundances of HCN and HC_3N is apparent relative to their protonated ions, since $HCNH^+$ is seen to be very abundant while HC_3NH^+ is, at present, below the detection limit. Given the broadly similar processes for interconversion of HC_nN and HC_nNH^+ for any **n**, and the broadly similar formation and destruction processes for these species, the ratio of HC_nNH^+ to HC_nN should, Turner argues, be essentially independent of the carbon skeleton length **n** - and yet this ratio is much larger for **n**=1 than for **n**=3. Turner interprets this in terms of a possible grain-surface process whereby HCN is absorbed and undergoes processing to form HC_3N which is then, in some manner, desorbed. It should be noted, however, that since HC_3N has a dipole moment larger than HCN, it is more likely to adhere strongly to dust grains. It is difficult to postulate a method of efficiently desorbing[83] HC_3N from grain surfaces, and thus this mechanism seems more likely to result in HC_3N depletion than in its formation.

It should also be noted that the products of the crucial dissociative recombination reactions

$$HCNH^+ + e \rightarrow \text{products} \qquad (6.22)$$

$$HC_3NH^+ + e \rightarrow \text{products} \qquad (6.23)$$

have not been determined: if reaction (6.22) were found to produce mainly $CN\cdot + H_2$, while reaction (6.23) yielded predominantly $HC_3N + H\cdot$, the discrepancy

detailed above would be resolved. Turner argues that reactions (6.22) and (6.23) should both produce predominantly C_nHN, in accordance with the Bates theory of dissociative recombination:[82] however, recent experiments on the dissociative recombination of H_3O^+ [85]

$$H_3O^+ + e \rightarrow H_2O + H\cdot \quad (6.24a)$$

$$\rightarrow OH\cdot + H_2 \quad (6.24b)$$

$$\rightarrow OH\cdot + H\cdot + H\cdot \quad (6.24c)$$

$$\rightarrow O + H_2 + H\cdot \quad (6.24d)$$

have indicated that a major product is OH·, in apparent conflict with the Bates theory which holds that only one existing bond should be broken in the recombination event. Further work on the products of dissociative recombination reactions is needed to adequately test the theories of Bates and others, with regard to dissociative recombination product channels.

A further point to note is that, while the reactions of HCN^+ and HNC^+ with H_2 are rapid at room temperature,[279,280,340,343] the reaction of HC_3N^+ with H_2 is very slow:[167,267] if this reaction possesses an activation barrier it will not occur at interstellar temperatures, and thus charge-transfer from HC_3N^+ to various neutrals could constitute a method of HC_3N production not available in the analogous case of HCN production, thus permitting resolution (if these charge-transfer processes occurred efficiently enough) of the apparent discrepancy in HC_nN/HC_nNH^+ observed abundances. An example is seen in the reaction of HC_3N^+ with NH_3, featured in table 6.4.

This point is of some relevance to acrylonitrile formation, if the reaction of $C_3H_3N^+$ with H_2 is prohibitively slow under interstellar conditions (as suggested by the room temperature measurements reported here). Charge transfer processes, for example involving NH_3 (see table 6.1), could well represent a significant source of interstellar CH_2CHCN, though this would naturally depend on the abundance of the $C_3H_3N^+$ ion. Reactions producing $C_3H_3N^+$, which may be of interstellar significance and which do not require CH_2CHCN as a precursor, are the association of $C_2H_2^+$ with HCN[166,267] and the reaction of C_3H^+ with NH_3:[329-331]

$$C_2H_2^+ + HCN \rightarrow CH_2N^+ + C_2H\cdot \quad [0.05] \quad (6.25a)$$

$$\rightarrow C_3H_2N^+ + H\cdot \quad [0.15] \quad (6.25b)$$

$$\rightarrow C_3H_3N^+ \quad [0.80] \quad (6.25c)$$

$k_{6.25} = 3.7 \times 10^{-10}$ cm^3 molec^{-1} s^{-1}

$$C_3H^+ + NH_3 \rightarrow NH_3^+ + C_3H\cdot \quad [0.25] \quad (6.26a)$$

$$\rightarrow NH_4^+ + C_3 \quad [0.40] \quad (6.26b)$$

$$\rightarrow CH_2N^+ + C_2H_2 \quad [0.20] \quad (6.26c)$$

$$\rightarrow C_3H_3N^+ + H\cdot \quad [0.15] \quad (6.26d)$$

$k_{6.26} = 1.7 \times 10^{-9}$ cm^3 molec^{-1} s^{-1}.

These and other processes (such as radiative association of CH_2N^+ and $C_2H\cdot$) can be considered likely sources of interstellar $C_3H_3N^+$.

To some extent, the arguments detailed above are of secondary importance in resolving Turner's discrepancy. Very recently, Herbst and Leung[42] have

considered the reactions of CN· radicals with unsaturated hydrocarbons in the context of interstellar synthesis. These reactions are known to occur rapidly at room temperature[348] and are thought to lack activation energy barriers, so they should also occur rapidly under interstellar conditions. If this is so, then this accounts for the apparent discrepancy in HC_nN/HC_nNH^+ ratios, since HC_3NH^+ is not necessarily the major source of HC_3N if the reaction

$$CN\cdot + C_2H_2 \rightarrow HC_3N + H\cdot \qquad (6.27)$$

proceeds at a significant rate within cold clouds. Similarly, the reaction

$$CN\cdot + C_2H_4 \rightarrow CH_2CHCN + H\cdot \qquad (6.28)$$

$$k_{6.28} = 2.1 \times 10^{-10}\ cm^3\ molec^{-1}\ s^{-1}\ (@\ 300\ K)$$

could well represent the dominant source of acrylonitrile if this reaction proceeds efficiently, and if acrylonitrile represents a significant product channel: products for this reaction have yet to be determined.[42]

Another possible source of organic nitriles is from reaction of hydrocarbon radicals with HCN

$$C_2H\cdot + HCN \rightarrow HC_3N + H\cdot \qquad (6.29)$$

$$k_{6.29} = 2.2 \times 10^{-12}\ cm^3\ molec^{-1}\ s^{-1}\ (@\ 300\ K)[43]$$

$$C_2H_3\cdot + HCN \rightarrow CH_2CHCN + H\cdot \qquad (6.30)$$

$$\Delta H_{6.30} = 1.6 \pm 15\ kJ\ mol^{-1},$$

although it appears from the low rate observed for reaction (6.29) that this reaction is inhibited by a sizeable activation barrier. Nevertheless, reaction (6.29) has been considered as a significant source of HC_3N within shocked clouds and circumstellar shells.[43] Reaction (6.30), which has not yet been studied experimentally, is of doubtful significance in acrylonitrile synthesis: even if this reaction lacks an activation barrier, it may well be endothermic.

It is of interest to note also that Brown et al (1990) have very recently proposed a greater importance for reactions of the type

$$C_nH_2 + N\cdot \rightarrow HC_nN + H\cdot \qquad (6.31)$$

in the synthesis of cyanopolyynes, if hot-ion hydrogen atom abstraction reactions between $C_nH_2^+$ and H_2 are considered. Brown et al. argue that hot-ion reactions can produce greater abundances of $C_nH_3^+$ ions than most ion-molecule models normally consider, resulting in higher abundances of C_nH_2 hydrocarbons from dissociative recombination of $C_nH_3^+$. These authors have commented that reactions such as (6.31) can help account for observed cyanopolyyne abundances, and the production of cyanopolyynes in this fashion (since HC_nNH^+ is not involved as a precursor) can also be invoked to explain Turner's observational discrepancy regarding HC_nNH^+/HC_nN abundances. Note that reactions of the type (6.31) are unlikely to influence the acrylonitrile abundance, since production of acrylonitrile in an analogous fashion would require the reactions

$$CH_3CCH + N\cdot \rightarrow CH_2CHCN + H\cdot \qquad (6.32)$$

$$\Delta H_{6.32} = -257 \text{ kJ mol}^{-1}$$

and/or

$$CH_2CCH_2 + N\cdot \rightarrow CH_2CHCN + H\cdot \qquad (6.33)$$

$\Delta H_{6.33} = -261$ kJ mol^{-1}.

An increase in the interstellar abundance of C_3H_4 owing to hot-ion reactions, in the manner described by Brown et al, requires the successive occurrence of three endothermic or barrier-inhibited reactions:

$$C_3H_2^+ + H_2 \rightarrow C_3H_3^+ + H\cdot \qquad (6.34)$$

$\Delta H_{6.34} \sim 0$ kJ mol^{-1}

$$C_3H_3^+ + H_2 \rightarrow C_3H_4^+ + H\cdot \qquad (6.35)$$

$\Delta H_{6.35} = 165$ kJ mol^{-1}

$$C_3H_4^+ + H_2 \rightarrow C_3H_5^+ + H\cdot \qquad (6.36)$$

$\Delta H_{6.36} = 38$ kJ mol^{-1}.

These endothermicities relate to formation and reaction of the lowest-energy linear isomer of $C_3H_n^+$. The insurmountable endothermicities of the latter two reactions indicate that hot-ion reactions cannot directly affect the C_3H_4 abundance, and thus these reactions cannot directly affect the acrylonitrile abundance either.

CHAPTER 7.

REACTIONS OF $H_nC_3O^+$ AND THE ION-MOLECULE CHEMISTRY OF C_3O_2.

Section 7.1: Introduction.

Tricarbon monoxide (:C=C=C=O) and propynal are among the largest oxygen-containing molecules to have yet been detected within interstellar clouds. C_3O, whose microwave spectrum was observed in the laboratory by Brown et al,[349] was subsequently detected in TMC-1 in 1984.[350,351] Propynal was also first detected in this source.[352] The presence of these molecules in such a cold, quiescent environment implies a gas-phase process for their production, in the absence of effective grain-surface processing.

For C_3O, Matthews et al[350] proposed the reaction

$$C_3H_2^+ + O \rightarrow C_3HO^+ + H\cdot \qquad (7.1)$$

followed by dissociative recombination

$$C_3HO^+ + e \rightarrow C_3O + H\cdot \qquad (7.2),$$

with the main loss mechanisms being charge transfer and proton transfer from reactions with positive ions. Brown et al[351] suggested

$$C_4 + O \rightarrow C_3O + C \qquad (7.3)$$

and the sequence

$$C_3O^+ + H_2 \rightarrow C_3HO^+ + H\cdot \qquad (7.4)$$

$$C_3HO^+ + H_2 \rightarrow C_3H_2O^+ + H\cdot \qquad (7.5)$$

$$C_3H_2O^+ + H_2 \rightarrow C_3H_3O^+ + H\cdot \qquad (7.6)$$

$$C_3H_3O^+ + e \rightarrow C_3O + H_2 + H\cdot \qquad (7.7).$$

Herbst et al[353] have suggested that the radiative association processes

$$C_2H_2^+ + CO \rightarrow C_3H_2O^+ + h\nu \qquad (7.8)$$

$$C_2H_3^+ + CO \rightarrow C_3H_3O^+ + h\nu \qquad (7.9)$$

are the major sources of C_3O: these reactions have been estimated[354] to occur with effective bimolecular rate coefficients of $k_{7.8} \sim 10^{-12}$ cm^3 molec^{-1} s^{-1} and $k_{7.9} \sim 10^{-11}$ cm^3 molec^{-1} s^{-1} at 10 K, upon the basis of their observed rates for termolecular association.[141] Herbst et al[353] note also that reactions of C_3H^+ with oxygen-containing neutrals also yield C_3HO^+ as products,[329-331,355] but consider such reactions as being less important due to the presumed rapid depletion[356] of C_3H^+ by reaction with H_2 at interstellar temperatures. A contribution to the interstellar C_3O abundance has also been suggested from the reaction sequence

$$C_3H_2^+ + CO \rightarrow C_4H_2O^+ + h\nu \quad (7.10)$$

$$C_4H_2O^+ + e \rightarrow C_3O + CH_2 \quad (7.11).$$

The radiative association reaction (7.10) is presumed to be fast as the analogous termolecular association is also fast ($k_{7.10} = 2 \times 10^{-26}$ cm^6 molec^{-2} s^{-1}, @ 80 K);[353] the product distribution of the dissociative recombination (7.11) is unknown. Formation of C_3O by reaction (7.11) is disfavoured as a major product channel according to the dissociative recombination theories of Herbst,[69] and Green and Herbst,[83] who consider that breaking of a multiple bond is unlikely to compete with single-bond cleavage. Bates, however, considers that breakage of a multiple bond can occur during dissociative recombination.[82] The feasibility of reaction (7.11) as a source of interstellar C_3O cannot be assessed until considerably more is known of the product distributions of dissociative recombination reactions.

Reactions (7.8) and (7.9) have also been considered by Nejad and Millar[100] in the chemistry of the circumstellar shell of IRC+10216 as a source of C_3O in this object, although a detection of circumstellar C_3O has yet to be reported.

Three C_3H_2O isomers, propynal (HC≡C–CHO), propadienone ($H_2C=C=C=O$) and cyclopropenone have been proposed as potential interstellar molecules. To date, only propynal has been detected within interstellar clouds.

Propynal is though to be formed principally by the dissociative recombination of $C_3H_3O^+$,[352,357] although the product distribution for this reaction is not known. Most theories of dissociative recombination favour cleavage of one bond only,

indicating a bias towards C_3H_2O formation. Irvine et al[352] have searched TMC-1 unsuccessfully for propadienone ($H_2C=C=C=O$), and argue that the apparent absence of this molecule indicates that it is not formed by dissociative recombination of $C_3H_3O^+$. Adams et al[357] support this proposal, suggesting that propadienone is not formed because interstellar $C_3H_3O^+$ does not have two hydrogens on the terminal carbon atom. This suggestion seems at variance with the theoretical and experimental findings of Holmes et al,[358] who determined the lowest-energy isomer of $C_3H_3O^+$ to be protonated propadienone, $[H_2C=CH—C=O]^+$ with other isomers having a calculated heat of formation at least 100 kJ mol^{-1} greater than this form. Furthermore, this lowest-energy isomer would appear to be the predominant product of reaction (7.9), which is the principal source of $C_3H_3O^+$ within models of cloud chemistry. Guillemin et al[359] propose that the isomer cyclopropenone may also be detectable within clouds, following an earlier unsuccessful search for this species:[360] the three isomers propynal, cyclopropenone and propadienone have similar heats of formation, so production of all three isomers within clouds should be at least energetically feasible.

Adams et al[357] have also considered the formation of larger analogues of C_nO and C_nH_2O in interstellar clouds, by virtue of the general class of radiative association reactions

$$C_{n-1}H_m^+ + CO \rightarrow C_nH_mO^+ + h\nu \qquad (7.12)$$

followed by dissociative recombination. The termolecular association processes related to reaction (7.12) have been studied by Giles et al[226] and mostly proceed

rapidly for $m \leq 2$: hydrocarbon ions having $n > 1$ and $m = 2$ or 3 are considered to be relatively abundant in interstellar clouds, by virtue of their unreactivity with H_2. These considerations suggest that C_nO and C_nH_2O may form an abundant class of interstellar molecules: Adams et al[357] propose that C_4O, C_5O, C_6O and C_7O should be observable in TMC-1, once their microwave spectra have been determined. To this end, Brown et al[361] and DeFrees and McLean[362] have recently calculated the rotational constants of C_5O; Ewing[363] has calculated the structures of C_4O and C_6O, finding that even-n C_nO species (over the short series from n = 3 to 6) are substantially less stable against fragmentation to products than are odd-n C_nO. This suggests that C_5O is a more likely candidate for interstellar detection than C_4O and C_6O.

The present chapter reports some results for reactions of the "C_3O precursor" ions $C_3H_{1\text{-}3}O^+$ with prominent interstellar molecules, as well as some reactions of the ions C_3O^+ and $C_3O_2^+$. The interstellar implications of these results are discussed.

Section 7.2: The ion-molecule chemistry of $H_nC_3O^+$ (n = 1 to 3).

C_3HO^+ and $C_3H_2O^+$ were generated in the ion source by electron bombardment upon fumaroyl dichloride, (1).

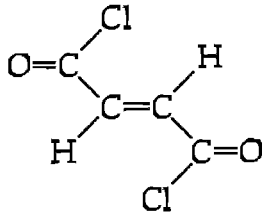

(1).

$C_3H_3O^+$ was produced by electron bombardment upon acrylic anhydride, (2).

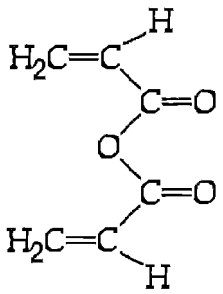

(2).

The mass spectra obtained when injecting at m/z 53, 54 and 55 for these three ions are tabulated in **table 7.1.** As can be seen from this table, the attainable signal for $C_3H_3O^+$ was much larger than for C_3HO^+ and $C_3H_2O^+$, most probably because only one bond of (2) needs to be broken to produce $C_3H_3O^+$; production of the other ions from (1) requires the breakage of two or three bonds and is hence less probable. None of the ions could be injected without contamination. C_3HO^+ could not be injected without contamination by sizeable signals at m/z 52 and / or m/z 54. $C_3H_2O^+$ and $C_3H_3O^+$ could be injected with only minor contamination from neighbouring ion masses, but contamination from $C_2H_n^+$ arising from the breakup process

$$C_3H_nO^+ \rightarrow C_2H_n^+ + CO \qquad (7.13)$$

$$\Delta H_{7.13} = +611 \text{ kJ mol}^{-1} \text{ (n=1)}$$

$$\Delta H_{7.13} = +242 \text{ kJ mol}^{-1} \text{ (n=2)}$$

$$\Delta H_{7.13} = +250 \text{ kJ mol}^{-1} \text{ (n=3)}$$

accounted for a significant fraction of the total reactant ion signal. In some instances, products initially attributed to reactions of $C_3H_nO^+$ were later discovered to arise from these breakup ions. The lack of breakup of C_3HO^+ can

Table 7.1: Mass spectra obtained under optimal conditions for injecting the ions $C_3H_nO^+$ ($n = 1 \rightarrow 3$).

		m/z	I/Imax [a]	Ion formula
i.	C_3HO^+ [b]	24	0.4	C_2^+
		25	0.8	C_2H^+
		26	3.9	$C_2H_2^+$
		27	<0.1	–
		46	<0.1	–
		47	0.3	$C^{35}Cl^+$
		48	2.5	C_4^+
		49	5.6	$C^{37}Cl^+$; C_4H^+
		50	2.2	$C_4H_2^+$
		51	2.1	$O^{35}Cl^+$?
		52	23.0	C_3O^+
		53 [c]	100	C_3HO^+
		54	7.7	$C_3H_2O^+$; $^{12}C_2{}^{13}CHO^+$
		55	<0.1	–
ii.	$C_3H_2O^+$ [b]	25	1.5	C_2H^+
		26	23.2	$C_2H_2^+$
		27	1.1	$C_2H_3^+$; $^{12}C^{13}CH_2^+$
		28	0.4	CO^+
		52	<0.1	–
		53	4.5	C_3HO^+
		54 [d]	100	$C_3H_2O^+$
		55	12.0	$C_3H_3O^+$; $^{12}C_2{}^{13}CH_2O^+$
		56	3.0	$C_2O_2^+$?
		57	<0.1	–
iii.	$C_3H_3O^+$ [e]	25	0.1	C_2H^+
		26	<0.1	–
		27	5.0	$C_2H_3^+$
		28	0.1	$^{12}C^{13}CH_3^+$; CO^+
		53	2.5	C_3HO^+
		54	0.4	$C_3H_2O^+$
		55 [f]	100	$C_3H_3O^+$
		56	2.9	$^{12}C_2{}^{13}CH_3O^+$

Notes

a. Ion signal, expressed as a percentage of the maximum peak height, using the mean value from 3 ten-second counts.

b. Derived by electron bombardment (50V electron energy) upon fumaroyl dichloride.

c. m/z 53 (71.2 counts per second) accounts for 66.8% of the total reactant ion signal. This spectrum was obtained with a setting of m/z 50.5 on the upstream QMS.

d. m/z 54 (77.8 counts per second) accounts for 68.6% of the total reactant ion signal. This spectrum was obtained using a setting of m/z 56.6 on the upstream QMS.

e. Derived by electron bombardment (30V electron energy) upon acrylic anhydride.

f. m/z 55 (2389.0 counts per second) accounts for 90.1% of the total reactant ion signal. This spectrum was obtained using a setting of m/z 56.2 on the upstream QMS.

be easily understood in terms of the much higher amounts of kinetic energy to drive reaction (7.13) in this case. Examination of the mass spectrum for $C_3H_3O^+$ also suggests that C_3HO^+ in this spectrum arises principally from the breakup process

$$C_3H_3O^+ \rightarrow C_3HO^+ + H_2 \qquad (7.14)$$

$$\Delta H_{7.14} = +220 \text{ kJ mol}^{-1}$$

rather than from insufficient mass resolution, since the signal at the intermediate mass (m/z 54) is very much smaller.

The ions C_3HO^+, $C_3H_2O^+$ and $C_3H_3O^+$ generated by the above techniques are all assumed to exist as the lowest-energy isomers listed in the tabulation of Lias et al.[184] The heats of formation of $C_3H_nO^+$ isomers, and related species, are detailed in **table 7.2.**

Only one form of C_3HO^+, $HCCCO^+$, has been reported to date: the equivalence of this ion with C_3HO^+ generated from fumaroyl dichloride can be reasonably assumed given the lack of rearrangement required to produce $HCCCO^+$ from the parent compound.

Several structures of $C_3H_2O^+$ have been reported[367-369] and proposed;[368] of those for which the appearance potentials have been experimentally determined, the isomer $H_2C{=}C{=}C{=}O^+$ (corresponding to ionized propadienone) has substantially the lowest heat of formation. This isomer can be formed by a 1,2 hydrogen shift during electron-impact ionization of fumaroyl dichloride. Schaefer[292] has noted

Table 7.2: Thermochemistry of $C_3H_nO^+$ (n = 0 → 3) and $C_3O_2^+$, and related neutrals.

Compound	ΔH_f [a]	Method [b]	Reference
·C=C=C=O$^+$	>1252	R	c
	1393	MNDO	364
:C=C=C=O	282	MO	365
	326	PA	366
	390	MO	363
HC=C–C=O$^+$	971	AP	367
HC=C=C=O·	<299	R	c
H_2C=C=C=O$^+$	975	IP	367
HC=CH–CO$^+$	996	MO [d]	368
HC=CH—C=O$^+$	1052	IP	367
	1089	MO [d]	368
HC≡C–C–OH$^+$	1120	MO [d]	368
HC≡C–CHO$^+$	1157	IP	369
	1216	MO [d]	368
H_2C=C=C=O	95	EST	184
HC≡C–CHO	115	EST	184
HC=CH—C=O	138±8	EST	184
HC=CH–CO	251	MO [e]	368
H_2C=CH–CO$^+$	749	MNDO	358
	751	AP	370
HC≡C–CH=OH$^+$	833	EST	370
	920	MNDO [f]	358
HC=CH—C=OH$^+$	858	EST	370
	866	MNDO [f]	358
H_2C=C=C=COH$^+$	882	EST	370
	977	MNDO [f]	358
HC≡C–CH_2O^+	950	AP	371
O=C=C=C=O$^+$	832	MNDO	364
	929	IP	372,373
O=C=C=C=O	-94±2		374

(table 7.2 cont'd)

Notes

a. Heat of formation in kJ mol^{-1}. Values which are underlined denote the ΔH_f, and the ion / neutral structure, assumed in the present work.

b. AP = appearance potential determination; EST = estimated value; IP = ionization potential determination; MNDO = ab initio MNDO calculation; MO = ab initio MO calculation; PA = theoretical proton affinity determination; R = reaction study.

c. This work.

d. referenced to $\Delta H_f(H_2CCCO^+)$.

e. referenced to $\Delta H_f(H_2CCCO)$.

f. referenced to $\Delta H_f(H_2CCHCO^+)$.

---

that such 1,2 shifts are facile in energised species such as ions produced by bombardment of high-energy electrons: an example of such a 1,2 shift is in the isomerisation of HCN^+ to HNC^+ (see chapter 5). Bouchoux et al[368] have proposed that the ion $HC{=}CH{-}CO^+$ is also a stable isomer of $C_3H_2O^+$, with a heat of formation only 21 kJ mol^{-1} higher than $\Delta H_f(H_2CCCO^+)$ according to ab initio calculations. The $HCCHCO^+$ ion can be formed without rearrangement from fumaroyl dichloride, and so it is also a likely component of the m/z 54 ion signal: the ratio of these two isomeric forms will depend upon their actual relative energies as well as on the height of the isomerisation barrier (as has been discussed at length for the case of C_2N^+ isomerisation, in chapter 4). In our studies of C_3HO^+ and of $C_3H_2O^+$ reactivity, no evidence was found for the existence of more than one isomer of each ion mass in the flow tube.

The lowest energy isomer of $C_3H_3O^+$, $H_2C{=}CH{-}CO^+$, can be generated without rearrangement by cleavage of the $H_2CCHC(O){-}OC(O)CHCH_2$ bond in acrylic anhydride. For this reason, and since $\Delta H_f(H_2CCHCO^+)$ is 199 kJ mol^{-1} lower in energy than the next lowest-energy isomer, the contribution from higher-energy isomeric forms in the m/z 55 ion signal is expected to be minimal.

The reactions of $C_3H_nO^+$ with various neutrals are summarised in **tables 7.3, 7.4** and **7.5.** It is immediately apparent from these tables that all of these ions are remarkably unreactive.

C_3HO^+ was seen to react only with NH_3, HCN and CH_3CCH. Adduct formation was a significant channel in the reaction with NH_3 and the sole product in the (very slow) reaction with HCN.

Table 7.3: Reactions of C_3HO^+ + **X**.

X	Products [a]		k_{obs} [b]	k_c [c]	$-\Delta H$ [d]
H_2	no reaction		<0.0005	–	–
CO	no reaction		<0.001	–	–
N_2	no reaction		<0.001	–	–
O_2	no reaction		<0.001	–	–
CH_4	no reaction		<0.001	–	–
NH_3	$CH_3CO^+ + HCN$ $C_3HO.NH_3^+$	[0.55] [0.45]	0.21	2.20	137 [e] –
H_2O	no reaction		<0.01	2.4	–
C_2H_2	no reaction		<0.001	-	–
HCN	$C_3HO.HCN^+$		0.004	3.28	–
CH_3CCH	$C_5H_5^+ + CO$ (or $C_4HO^+ + C_2H_4$)		0.92	1.40	– [f] – [g]

Notes

a. Product channels reported in brackets, where more than one product was detected.
b. Observed rate coefficient, in units of 10^{-9} cm^3 $molec^{-1}$ s^{-1}.
c. Calculated ADO collision rate coefficient, using the theory of Su and Chesnavich.[172]
d. Reaction exothermicity in units of kJ mol^{-1}. Taken from the tabulation of Lias et al,[184] unless otherwise stated.
e. Production of CH_2COH^+ is endothermic by 13 kJ mol^{-1}.
f. Formation of several $C_5H_5^+$ isomers is energetically possible.
g. This product channel requires $\Delta H_f(C_4HO^+) < 1105$ kJ mol^{-1}.

The occurrence of a significant product signal at m/z 18 in the reaction with NH_3 was initially attributed to proton transfer from C_3HO^+, in disagreement with Botschwina's[366] calculation of $PA(C_3O)$ which indicates that such a proton

Table 7.4: Reactions of $C_3H_2O^+ + X$.

X	Products [a]		k_{obs} [a]	k_c [a]	$-\Delta H$ [a]
H_2	no reaction		<0.0005	–	–
CO	no reaction		<0.001	–	–
N_2	no reaction		<0.001	–	–
O_2	$CHO^+ + C_2HO_2\cdot$	[0.60]	0.036	0.66	– [b]
	$C_2H_2O^+ + CO_2$	[0.40]			489 [c]
CH_4	no reaction		<0.001	–	–
NH_3	$NH_4^+ + C_3HO\cdot$		1.3	2.19	– [d]
H_2O	no reaction		<0.01	2.4	–
HCN	$C_3H_2O.HCN^+$		0.19	3.27	–
C_2H_2	$C_5O^+ + 2H_2$	[0.28]	0.43	1.02	– [e]
	$C_5HO^+ + H_2 + H\cdot$	[0.57]			– [f]
	$C_5H_2O^+ + H_2$	[0.15]			– [g]
CH_3C_2H	$C_5H_6^+ + CO$	[0.32]	1.2	1.39	– [h]
	(or $C_4H_2O^+ + C_2H_4$)				– [i]
	$C_5H_2O^+ + CH_4$	[0.21]			>33 [j]
	$C_3H_2O.CH_3C_2H^+$	[0.47]			–

Notes

a. See footnotes (a) - (d) for table (7.3).

b. The observation of this channel requires $\Delta H_f(C_2HO_2\cdot) < 149$ kJ mol^{-1} for production of $HCO^+ + C_2HO_2\cdot$. Alternatively, $-\Delta H = 215$ kJ mol^{-1} for production of $HCO^+ + HCO\cdot + CO$.

c. Calculated for production of H_2CCO^+. $-\Delta H = 336$ kJ mol^{-1} for production of $HCCOH^+ + CO_2$.

d. Proton-transfer in this instance is only exothermic if $\Delta H_f(C_3HO\cdot) < 299$ kJ mol^{-1}.

e. Requires $\Delta H_f(C_5O^+) < 1203$ kJ mol^{-1}.

f. Requires $\Delta H_f(C_5HO^+) < 985$ kJ mol^{-1}.

g. Requires $\Delta H_f(C_5H_2O^+) < 1203$ kJ mol^{-1}.

h. Calculated for ionized cyclopentadiene, c-$C_5H_6^+$, but production of several other $C_5H_6^+$ species is exothermic also.

i. Requires $\Delta H_f(C_4H_2O^+) < 1109$ kJ mol^{-1}.

j. Calculated using $\Delta H_f(C_5H_2O^+) < 1203$ kJ mol^{-1}.

transfer reaction is endothermic by approximately 30 kJ mol^{-1}. Subsequently, this reaction was re-examined to reveal that the signal at m/z 18 arose, at low flows, via a side reaction involving a contaminant ion at m/z 52 (C_3O^+) or 54 ($C_3H_2O^+$). NH_4^+ also dominated the product distribution at high flows, indicating that C_3HO^+ was responsible for its formation via a secondary reaction: the most likely explanation is that CH_3CO^+ undergoes rapid proton transfer to NH_3, and this accounts for the observed loss of CH_3CO^+ with increasing flow of NH_3.

Table 7.5: Reactions of $C_3H_3O^+ + X$.

X	Products[a]		k_{obs}[a]	k_c[a]	$-\Delta H$[a]
H_2	no reaction		<0.0005	–	–
CO	no reaction		<0.001	–	–
N_2	no reaction		<0.001	–	–
O_2	no reaction		<0.001	–	–
CH_4	no reaction		<0.001	–	–
NH_3	$C_3H_3O.NH_3^+$		0.021	2.19	–
H_2O	no reaction		<0.01	2.4	–
C_2H_2	no reaction		<0.001	–	–
HCN	$C_3H_3O.HCN^+$		0.002	3.27	–
CH_3C_2H	$C_5H_3O^+ + CH_4$	[0.16]	0.068	1.39	b
	$C_3H_3O.CH_3C_2H^+$	[0.84]			–

Notes

a. See footnotes (a) - (d) for table (7.3).

b. Requires $\Delta H_f(C_5H_3O^+) < 1012$ kJ mol^{-1}.

The absence of any apparent reaction between C_3HO^+ and H_2, CO or N_2 indicates that C_3HO^+ is likely to be persistent within interstellar clouds: in particular, the lack of reaction with H_2 suggests that C_3O cannot arise via the mechanism of Brown et al[351] which supposes that stepwise H-atom abstraction in reactions (7.4)-(7.6) precedes dissociative recombination to C_3O. The low upper limit, $k_{7.5} \leq 5.0 \times 10^{-13}$ cm^3 $molec^{-1}$ s^{-1}, suggests that C_3HO^+ is not involved in the production of C_3H_2O isomers within the interstellar environment. The radiative association process

$$C_3HO^+ + H_2 \rightarrow C_3H_3O^+ + h\nu \qquad (7.15)$$

is unlikely to be fast as the termolecular association channel is not observed for this reaction. Similarly, the absence of any apparent association between C_3HO^+ and CO indicates that the neutral species O=C=C=C=C=O (which might have been expected to result from from dissociative recombination following such an association process) cannot be formed in this manner. The absence of any visible reaction with H_2O and C_2H_2, as well as the very slow rate coefficient observed for the reaction with HCN, underlines the lack of reactivity of the C_3HO^+ ion.

$C_3H_2O^+$ is a somewhat more reactive species, although only the reactions with NH_3 and CH_3CCH proceeded at more than half the collision rate. As with C_3HO^+, the absence of reactivity with H_2, CO and N_2 indicates that $C_3H_2O^+$ will have a long lifetime within clouds: also, since $C_3H_2O^+$ does not appear to react via H-atom abstraction, it is unlikely to play a significant part in C_3H_2O formation.

The reactions with acetylene and propyne indicate that such reactions between $C_3H_2O^+$ and interstellar alkynes may be significant in terms of the synthesis of larger species. These reactions clearly produce precursors to C_5O (although not, apparently, to C_5H_2O - unless $C_5H_2O^+$ reacts further with H_2); the product at m/z 66, from reaction with CH_3CCH, is uncertain. This ion is either $C_5H_6^+$ or $C_4H_2O^+$: several possible channels to $C_5H_6^+$ isomers are exothermic, while production of $C_4H_2O^+$ by an exothermic channel requires $\Delta H_f(C_4H_2O^+) < 1109$ kJ mol^{-1} (which seems plausible). The ion at m/z 78 is identified as $C_5H_2O^+$ since formation of each known $C_6H_6^+$ isomer is endothermic (by ≥ 63 kJ mol^{-1}), and the possibility of some unknown $C_6H_6^+$ product having lower energy seems remote.

The occurrence of proton transfer to NH_3 establishes $\Delta H_f(C_3HO\cdot) < 299$ kJ mol^{-1}: no other measurement of this quantity has been previously reported.

$C_3H_3O^+$ was observed to display very little reactivity with any of the neutrals (see table 7.5), indicating its probable persistence in interstellar clouds. Reaction occurred only with NH_3, HCN and CH_3CCH, did not exceed 5% of the collision rate in any of these cases, and involved adduct formation as the major (or only) product channel in these reactions. In the reaction with CH_3CCH, which was the only case in which a product channel other than adduct formation was evident, the 16% channel at m/z 79 was identified as formation of $C_5H_3O^+$ (ion structure not known) + CH_4 since all channels leading to formation of $C_6H_7^+ + O$ are exothermic by >166 kJ mol^{-1}.[184]

Although the $C_3H_nO^+$ ions are clearly sufficiently unreactive with the predominant interstellar neutrals for these ions to persist within cold clouds,

their significance with respect to C_3O and C_3H_2O production cannot be accurately determined since their dissociative recombination chemistry is not known. The possible consequences of dissociative recombination of the $C_3H_nO^+$ ions, using a simple model allowing breakage of only one or two bonds of the parent ion without subsequent rearrangement, are summarised in **table 7.6.**

Table 7.6: Possible consequences of dissociative recombination of $C_3H_nO^+$.

Reaction	Products	-ΔH [a]
$H–C=C=C=O^+ + e$	$:C_3O + H\cdot$	427
	$C_2O + CH\cdot$	b
	$CO + C_2H\cdot$	517
	$O + C_3H\cdot$	c
$H_2C=C=C=O^+ + e$	$HC_3O\cdot + H\cdot$	>458
	$:C_3O + H_2$	649
	$C_2O + CH_2$	d
	$CO + H_2C=C:$	689 [e]
	$O + H_2C=C=C:$	189 [f]
$H_2C=CH–C=O^+ + e$	$H_2C=C=C=O + H\cdot$	438
	$\cdot HC=CH–C=O\cdot + H\cdot$	282
	$HC_3O\cdot + H_2$	>452
	$:C_3O + H_2 + H\cdot$	207
	$HC_2O\cdot + CH_2$	184
	$C_2O + CH_2 + H\cdot$	g
	$CO + C_2H_3\cdot$	596
	$O + C_3H_3\cdot$	159 [h]

Notes

a. Exothermicity in kJ mol^{-1}.

b. Not known. The exothermicity of this channel requires $\Delta H_f(C_2O) < 375$ kJ mol^{-1}.

c. Not known. The exothermicity of this channel requires $\Delta H_f(C_3H\cdot) < 722$ kJ mol^{-1}.

d. The exothermicity of this channel requires $\Delta H_f(C_2O) < 585$ kJ mol^{-1}.

e. Calculated using $\Delta H_f(H_2CC) = 397$ kJ mol^{-1}, from reference 375.

f. Calculated using $\Delta H_f(H_2CCC) = 544$ kJ mol^{-1}, from reference 376.

g Unlikely. The exothermicity of this channel requires $\Delta H_f(C_2O) < 143$ kJ mol^{-1}.

h. -ΔH for formation of linear $C_3H_3\cdot$.

C_3HO^+ cannot produce C_3H_2O, so all dissociative recombination channels not leading to C_3O are best regarded as destruction channels for tricarbon monoxide. The most exothermic channel is dissociation to the ethynyl radical and carbon monoxide: the enthalpy of reaction for other channels, apart from production of $C_3O + H\cdot$, is not known and the other channels may well be endothermic. Since C_3HO^+ is so unreactive, it is likely that the interstellar chemistry of C_3O and C_3HO^+ is very tightly coupled. C_3O produces HC_3O^+ upon protonation (virtually all H-bearing ions should serve to protonate C_3O, given the high value of $PA(C_3O) = 885$ kJ mol^{-1} calculated by Botschwina[366]) and upon ionization:

$$C_3O + h\nu \rightarrow C_3O^+ + H_2 \qquad (7.16)$$

$$C_3O^+ + H_2 \rightarrow C_3HO^+ + H\cdot \qquad (7.17)$$

C_3HO^+ can arise through other reactions not involving C_3O, as has been discussed in section 7.1, but these reactions are not likely to be as significant in determining the C_3HO^+ abundance as will be protonation of C_3O. C_3HO^+, therefore, probably serves mainly to recycle C_3O rather than to produce it. Given the high dipole moment which Botschwina[366] has determined for this ion, the high $PA(C_3O)$, and the probable long lifetime of C_3HO^+ within clouds, an interstellar search for protonated tricarbon monoxide appears justified.

$C_3H_2O^+$ can recombine to form $HC_3O\cdot$ and C_3O, but not C_3H_2O. (Radiative recombination processes have very low efficiencies.) As Herbst et al[353] have suggested, $C_3H_2O^+$ is likely to be a major ion precursor of C_3O by virtue of the efficient association reaction, (7.8), between $C_2H_2^+$ and CO.

$C_3H_3O^+$ can produce C_3O, $HC_3O\cdot$ and C_3H_2O upon recombination. A major channel competing with these possible products is likely to be CO + $C_2H_3\cdot$, which appears to be the most exothermic channel. Herbst et al[353] contend, on the basis of interstellar detection of propynal (HCCCHO) but not of propadienone (H_2CCCO), that propynal is a major product of this recombination process. A possible mechanism to account for the observation of propynal but not propadienone would require initial production of the biradical HC=CH–CO rather than the more stable $H_2C=C=C=O$, followed by a 1,2 hydrogen shift to yield propynal - though such a shift could, of course, also yield propadienone unless precluded by some energetic constraint. No information is available concerning the barriers to 1,2 hydrogen shifts in this system, although Kaneti et al[377] have determined that considerable barriers exist for another rearrangement of propynal:

$$HC{\equiv}C{-}CHO \quad \leftrightarrow \quad :C{=}CH{-}CHO \qquad (7.18).$$

An alternative hypothesis to explain the presence of propynal and the apparent absence of propadienone is that propynal is less reactive in the interstellar environment than is propadienone, the abundance of propadienone being maintained below the observational limit by, say, a rapid reaction with an abundant interstellar radical such as CN· or OH·.

Further reactions of the $C_3H_nO^+$ ions (especially $C_3H_2O^+$, which appears the most reactive) with higher alkynes such as C_4H_2 and CH_3C_4H may represent a source of higher-order interstellar C_nO and C_nH_2O molecules, as indicated by the reactions

of these ions with CH_3CCH. A further investigation of $C_3H_nO^+$ reactivity with hydrocarbons thus seems warranted.

Section 7.3: Ion-molecule chemistry of C_3O_2.

Electron impact upon carbon suboxide was used to generate the ions C_3O^+ and $C_3O_2^+$. The mass spectrum obtained by 50 V electron bombardment upon C_3O_2 is tabulated in **table 7.7**. Peaks due to CO_2^+, CO^+ and C^+ are attributed (in part) to a large CO_2 impurity, which was not eliminated from the C_3O_2 sample prepared.

The heats of formation of C_3O and C_3O^+ have not yet been determined experimentally. Brown and Rice[365] have performed MP3/6-31G* calculations upon the stability of C_3O relative to dissociation to the fragments C_2 + CO: their calculations yield an estimate of $\Delta H_f^\circ(C_3O)$ = 282 kJ mol^{-1}. Ewing[363] has used MP4/DZP//HF/DZP calculations to determine C_3O's stability in a similar manner, calculating $\Delta H_f(C_3O)$ = 390 kJ mol^{-1}. Botschwina[366] has performed detailed ab initio calculations upon C_3O and HC_3O^+: these calculations yield $PA(C_3O)$ = 885 ± 5 kJ mol^{-1}. Terlouw et al[367] have determined $\Delta H(HC_3O^+)$ = 971 ± 5 kJ mol^{-1} from the experimental appearance potential for this ion. These values permit calculation of $\Delta H_f(C_3O)$ = 326 ± 10 kJ mol^{-1}, a value which lies between the other theoretical values. McElvany et al[364] have performed MNDO calculations on the species C_n^+, C_nH^+, $C_nH_2^+$, C_nO^+ and $C_nO_2^+$ for n = 3 → 9. Their calculated value for C_3O^+ is $\Delta H_f(C_3O^+)$ = 1393 kJ mol^{-1}, with a substantial uncertainty: they calculate also $\Delta H_f(C_3^+)$ = 1979 kJ mol^{-1} and $\Delta H_f(C_3O_2^+)$ =

832 kJ mol^{-1}, which differ appreciably from the experimental literature values of $\Delta H_f(C_3^+)$ = 2004 kJ mol^{-1} and $\Delta H_f(C_3O_2^+)$ = 929 kJ mol^{-1}.

Table 7.7: Mass spectrum obtained by electron impact ionisation (50V electron energy) of C_3O_2.

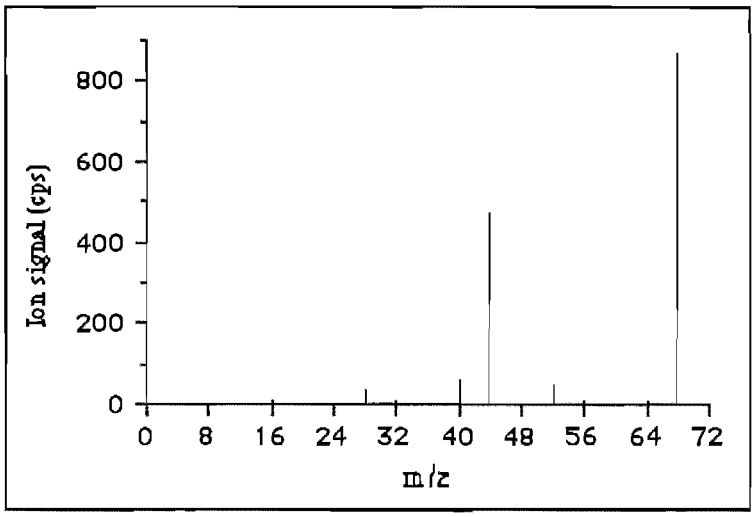

m/z	I/Imax [a]	Ion formula
12	0.1	C^+
16	0.8	O^+
24	0.3	C_2^+
28	3.8	CO^+
32	0.5	O_2^+
36	0.3	C_3^+
40	6.7	C_2O^+
44	54.4 [b]	CO_2^+
48	<0.1	C_4^+
52	5.0	C_3O^+
56	0.8	$C_2O_2^+$
60	<0.1	C_5^+
64	0.6	O_4^+; C_4O^+
68	100.0 [c]	$C_3O_2^+$

Notes

a. Ion signal, expressed as a percentage of the m/z 68 peak height, using the mean value from 3 ten-second counts.

b. Attributed principally to a large CO_2 impurity: the signals at m/z 12, 16 and 28 may also contain some contribution from CO_2 dissociative ionisation products.

c. 867 counts per second was obtained for m/z 68 in this experiment.

Thermochemical values for reactions of C_3O^+ presented here (see **table 7.8**) are calculated using $\Delta H_f(C_3O) = 326 \pm 10$ kJ mol^{-1} as described above, and $\Delta H_f(C_3O^+) > 1252$ kJ mol^{-1} based upon the observed occurrence of the rapid reaction

$$C_3O^+ + H_2O \rightarrow HC_3O^+ + OH\cdot \qquad (7.19)$$

$k_{7.19} = 5.0 \times 10^{-10}$ cm^3 molec^{-1} s^{-1}.

Table 7.8: Reactions of $C_3O^+ + X$.

X	Products[a]		k_{obs}[a]	k_c[a]	$-\Delta H$[a]
H_2	$C_3HO^+ + H\cdot$		0.8	1.50	> 63
CO	$C_3O.CO^+$		0.072	0.79	–
N_2	no reaction		<0.001	0.73	–
O_2	$CO^+ + 2CO$	[0.20]	0.22	0.67	> 232
	$C_3O_2^+ + O$	[0.80]			> 74
CH_4	$C_3HO^+ + CH_3\cdot$		0.83	1.08	> 60
NH_3	$C_3HO^+ + NH_2\cdot$[b]		1.9	2.20	> 46
	$C_3O.NH_3^+$				–
H_2O	$C_3HO^+ + OH\cdot$		0.50	2.44	> 0
C_2H_2	$C_4H_2^+ + CO$	[0.45]	1.08	1.03	> 69
	$C_3O.C_2H_2^+$	[0.55]			–
HCN	$HC_3N^+ + CO$[b]		2.9	3.30	> 24
	$C_3O.CN^+ + H\cdot$				–
CO_2	no reaction		<0.001	0.78	–

Notes

a. See footnotes (a) - (d) for table (7.3).

b. Product ratio not determined. See text for discussion.

Accurate product distributions for the reactions of C_3O^+ with NH_3 and HCN could not be determined under the experimental conditions. The occurrence of two major product channels in each of these reactions, with one channel leading to formation of a product ion at m/z 51 (HC_3N^+) or m/z 53 (HC_3O^+), meant that a higher resolution was required to satisfactorily resolve the m/z 52 ion signal from this product ion: under these conditions, signals at m/z 52 (C_3O^+) were too small (~ 5 cps) and too erratic to permit determination of the relative proportions of the two product channels concerned. In the case of the reaction with NH_3, H-atom transfer appeared to be the major channel (~75% of products), while for the reaction with HCN, both product channels observed appeared to be of comparable size.

The main product channels observed in the reactions of C_3O^+ are atom-transfer and adduct formation. Hydrogen atom transfer, to form HC_3O^+, was observed as the major or only product channel for the rapid reactions with H_2, CH_4, NH_3 and H_2O. Adduct formation was observed as a minor channel in the reactions with NH_3 and C_2H_2, and as the only channel in the slow reaction with CO. The most interesting reactions, from a mechanistic point of view, are those in which rearrangement or substantial fragmentation has occurred, as in the reactions with C_2H_2, HCN and O_2:

$$C_3O^+ + C_2H_2 \rightarrow C_4H_2^+ + CO \quad [0.45] \quad (7.20a)$$

$$\rightarrow C_3O.C_2H_2^+ \quad [0.55] \quad (7.20b)$$

$\Delta H_{7.20a} < -69$ kJ mol^{-1}

$k_{7.20} = 1.08 \times 10^{-9}$ cm^3 molec^{-1} s^{-1}

$$C_3O^+ + HCN \rightarrow HC_3N^+ + CO \quad (7.21a)$$

$$\rightarrow C_3O.CN^+ + H\cdot \quad (7.21b)$$

$\Delta H_{7.21a} < -24$ kJ mol^{-1}

$k_{7.21} = 2.9 \times 10^{-9}$ cm^3 molec^{-1} s^{-1}

$$C_3O^+ + O_2 \rightarrow CO^+ + CO + CO \quad [0.20] \quad (7.22a)$$

$$\rightarrow C_3O_2^+ + O \quad [0.80] \quad (7.22b)$$

$\Delta H_{7.22a} < -232$ kJ mol^{-1}

$\Delta H_{7.22b} < -74$ kJ mol^{-1}

$k_{7.22} = 2.2 \times 10^{-10}$ cm^3 molec^{-1} s^{-1}.

The reaction with O_2 has also been studied by McElvany et al[364] using a Fourier Transform ICR technique. They observed only channel (7.22b), for which they reported a rate coefficient $k_{7.22} = 1.3 \times 10^{-10}$ cm^3 molec^{-1} s^{-1}. The occurrence of channel (7.22b) in the SIFT experiment suggests that dissociation of a weakly-bound collision complex is responsible for this channel. McElvany et al[364] have proposed that reaction (7.22) occurs as a complexation of O_2 at the carbene end of C_3O^+, followed by loss of an oxygen atom:

$$OCCC^+: + O_2 \rightarrow OC_3O_2^+ \rightarrow OC_3O^+ + O.$$

Partial collisional stabilisation of the $(C_3O_3)^+$ complex would increase the complex lifetime and allow a greater degree of rearrangement. A longer complex lifetime would, therefore, be expected to be accompanied by an increase in the more exothermic channel (7.22a) which requires a greater degree of rearrangement.

The occurrence of channels (7.20a) and (7.21a) also suggests a mechanism involving dissociation of a weakly-bound collision complex. If the reactions of C_3O^+ are viewed as carbene-insertion reactions by analogy to the reactivity of $:C_3H^+$ and $:C4N^+$,[271,329-331] then those reactions of C_3O^+ involving H-atom transfer will have a mechanism which features carbene insertion into the H–X σ bond:

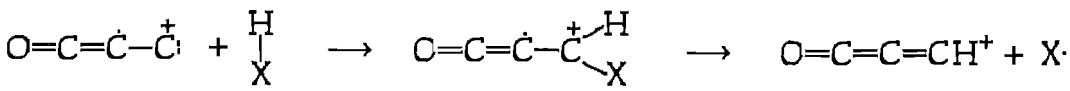

This product channel (loss of X from the collision complex) is not evident in the reactions with C_2H_2 or HCN, where H-atom transfer is not so energetically favourable: for the product channels

$$C_3O^+ + C_2H_2 \rightarrow HC_3O^+ + C_2H\cdot \qquad (7.20c)$$

$$C_3O^+ + HCN \rightarrow HC_3O^+ + CN\cdot \qquad (7.21c)$$

the calculated upper limits to the enthalpy of reaction are $\Delta H_{7.20c} < +19$ kJ mol^{-1} and $\Delta H_{7.21c} < +56$ kJ mol^{-1}. These channels may be endothermic: they are certainly less energetically feasible than H-atom transfer for H_2, CH_4, NH_3 and H_2O. A possible additional factor is that the lifetime of the collision complex formed with C_2H_2 or HCN is longer than that of the complex formed with the lighter reactants H_2, CH_4, NH_3 or H_2O, thus permitting the more exothermic channel (rearrangement accompanied by loss of CO) to dominate.

Although these reactions with HCN and C_2H_2 appear mechanistically interesting, the very rapid reaction of C_3O^+ with H_2 ensures that C_3O^+ will not have a

sufficiently long lifetime in interstellar clouds to make its reactivity with other cloud constituents significant.

$C_3O_2^+$ (see **table 7.9**) appeared to be less reactive than C_3O^+. Of the neutrals employed in our study, only NH_3 and C_2H_2 displayed collision-rate reactions with $C_3O_2^+$:

$$C_3O_2^+ + NH_3 \rightarrow NH_3^+ + C_3O_2 \quad [0.75] \quad (7.23a)$$

$$\rightarrow C_2H_2O^+ + HNCO \quad [0.25] \quad (7.23b)$$

$\Delta H_{7.23a} = -43$ kJ mol^{-1}

$\Delta H_{7.23b} = -108$ kJ mol^{-1}

$k_{7.23} = 2.0 \times 10^{-9}$ cm^3 molec^{-1} s^{-1}

$$C_3O_2^+ + C_2H_2 \rightarrow C_4H_2O^+ + CO \quad (7.24)$$

$k_{7.24} = 1.2 \times 10^{-9}$ cm^3 molec^{-1} s^{-1}.

Channel (7.24) requires a degree of rearrangement, but less than is evident in channel (7.23b): the rapidity of these reactions, and the extent of rearrangement evident, argues for the involvement of a 'tight' collision complex in these reactions. The existence of channel (7.23b) as a substantial product channel of a fast reaction requires that the products have the structure $HC{\equiv}COH^+ + HNCO$. All other possible channels involving production of m/z 42 (e.g. $H_2CCO^+ + HNCO$, $CNO^+ + C_2H_3O$, $C_2H_2O^+ + HCNO$) are substantially endothermic.

The reaction with O_2 also displays fragmentation and rearrangement:

$$C_3O_2^+ + O_2 \rightarrow CO^+ + CO + CO_2 \quad [0.09] \quad (7.25a)$$

$$\rightarrow CO_2^+ + CO + CO \quad [0.76] \quad (7.25b)$$

$$\rightarrow C_2O_2^+ + CO_2 \quad [0.15] \quad (7.25c)$$

$k_{7.25} = 1.2 \times 10^{-10}$ cm^3 molec^{-1} s^{-1}.

These product channels can be interpreted by a mechanism involving formation of the collision complex $(C_3O_4)^+$ followed by rearrangement and loss of the stable neutrals CO and/or CO_2.

Table 7.9: Reactions of $C_3O_2^+$ + X.

X	Products[a]		k_{obs}[a]	k_c[a]	$-\Delta H$[a]
H_2	no reaction		<0.0001	1.49	–
CH_4	$C_3O_2H^+ + CH_3\cdot$		0.3	1.05	b
NH_3	$NH_3^+ + C_3O_2$	[0.75]	2.0	2.12	43
	$C_2H_2O^+ + HNCO$	[0.25]			109[c]
H_2O	$C_3O_2.H_2O^+$		0.001	1.97	–
N_2	no reaction		<0.001	0.70	–
O_2	$CO^+ + CO + CO_2$	[0.09]	0.12	0.63	194
	$CO_2^+ + 2CO$	[0.76]			215
	$C_2O_2^+ + CO_2$	[0.15]			288[d]
CO	no reaction		<0.001	0.76	–
C_2H_2	$C_4H_2O^+ + CO$		1.2	0.99	e
HCN	$C_3O_2.HCN^+$		0.015	3.16	–
CO_2	no reaction		<0.001	0.74	–

Notes

a. See footnotes (a) - (d) for table (7.3).

b. This channel yields $\Delta H_f(C_3O_2H^+) < 709$ kJ mol^{-1}; $PA(C_3O_2) > 727$ kJ mol^{-1}.

c. Calculated for the products $H_2C{=}CO^+ + HNCO$. Production of $HC{\equiv}COH^+$ is 44 kJ mol^{-1} endothermic; production of HCNO is 214 kJ mol^{-1} endothermic.

d. Calculated using $D(OC.CO^+) = 22.4 \pm 1.0$ kCal mol^{-1}.[378]

e. This channel yields $\Delta H_f(C_4H_2O^+) < 1268$ kJ mol^{-1}.

In view of the lack of reactivity with H_2 and CO, the reaction with O_2 (which may be the major oxygen-containing species within clouds, excepting CO) may be the dominant loss process for any interstellar $C_3O_2^+$: note that this reaction serves to reduce the molecular complexity of the ion, thus suggesting that $C_3O_2^+$ cannot aid in the synthesis of more complex cloud constituents.

CHAPTER 8.

A CONSIDERATION OF RADICAL-H_2 REACTIONS IN INTERSTELLAR SYNTHESIS.

Section 8.1: Introduction.

Processes involved in interstellar synthesis are most commonly characterised by a lack of activation energy or of endothermicity, since under interstellar conditions the only processes which can occur without hindrance are exothermic reactions lacking energetic barriers. Ion-molecule reactions most usually adhere to this criterion, but certain categories of neutral-neutral reactions may also be of interstellar relevance. A recent review by Smith[32] distinguishes four types of bimolecular neutral reactions: molecule-molecule, radical-saturated molecule, radical-unsaturated molecule, and radical-radical, as characterised by reactions (8.1) to (8.4).

$$H_2 + D_2 \rightarrow HD + HD \qquad (8.1)$$

$E_a > 250$ kJ mol^{-1}

$$OH\cdot + H_2 \rightarrow H_2O + H\cdot \qquad (8.2)$$

$E_a = 17.5$ kJ mol^{-1}

$$OH\cdot + CO \rightarrow CO_2 + H\cdot \qquad (8.3)$$

$E_a \sim 0$ kJ mol^{-1}

$$OH\cdot + O \rightarrow O_2 + H\cdot \qquad (8.4)$$

$E_a = -100$ kJ mol^{-1}.

The occurrence of a negative activation energy for the biradical reaction of O + OH·, as determined from studies of the dependence of reaction rate on temperature, implies that these reactions are not well explained in terms of an Arrhenius rate law. Biradical reactions are, however, usually fast and usually exhibit a negative temperature dependence, both factors underlying their importance in interstellar synthesis. In this context, the prospect for radiative association between interstellar free radicals has been explored.[379]

Radical-unsaturated molecule reactions such as reaction (8.3) may also lack activation energy barriers, but may be slow nevertheless, since the transition state to product formation is 'tighter' than in the instance of radical-radical reactions. Only a narrow channel (on the potential energy surface describing the bimolecular interaction) may lead to product formation, and so these types of reaction are less efficient than radical-radical processes. However, as discussed in section (6.5), such reactions are also important in interstellar chemistry.

Reactions of types (8.1) and (8.2) are so hindered by activation energy barriers that they have been considered of no interstellar relevance[32] except in the case of shock chemistry, where very high prevailing temperatures permit such reactions to occur rapidly. I propose that under some conditions, reactions of type (8.2) may be significant in the chemistry of cold, dark clouds in the absence of shock effects. This may be compared with the suggestion[41,86,87] that endothermic ion-

molecule reactions may serve a useful purpose in the interstellar synthesis of ammonia:

$$He^+ + N_2 \rightarrow (N_2^+)^{\#} + He \quad (1.16a)$$

$$(N_2^+)^{\#} \rightarrow (N^+)^* + N\cdot \quad (1.16b)$$

$$(N^+)_{fast} + H_2 \rightarrow NH^+ + H\cdot \quad (1.17a)$$

$$\rightarrow N^+ + (H_2)_{fast} \quad (1.17b)$$

Formation of NH^+ by the endothermic reaction (1.17a) avoids a bottleneck in the synthesis of NH_3.[41,86]

Section 8.2: General considerations.

The occurrence, within cold dense interstellar clouds, of reactions of the type

$$X + AB \rightarrow XA + B \quad (8.5),$$

where the translational energy $E_{T(X)}$ of the radical X is sufficient to overcome the activation energy E_a, has not previously been explored in models of cloud chemistry. The factors relevant to the efficiency and importance of these reactions will now be considered.

Under the conditions prevailing within cold molecular clouds, AB is most likely to be H_2 or He, with a translational energy appropriate to the background temperature of the cloud (typically T ~ 20 K). Only collisions between X and H_2 are likely to be of any interest in terms of chemistry resulting from

translationally excited X, since H_2 is so much more abundant than any other reactant molecule of interest (CO, the next most abundant interstellar molecule, typically has an abundance $n(CO) \leq 10^{-4}\, n(H_2)$). Collisions with atoms such as H· and He are not, in this context, chemically interesting: these collisions will serve only to cool the translationally excited reactant X, as will unreactive collisions involving H_2. Since H_2 is the only reactant molecule that need be considered, and since H-atom abstraction is the only product channel feasible for such a reaction, reaction (8.5) may be rewritten:

$$X + H_2 \rightarrow XH + H\cdot \qquad (8.6).$$

Reaction (8.6) will only occur if a collision features sufficient energy to exceed the activation energy barrier E_a. The major source of such energy is the translational excitation of the fragment X: since the H_2 'target' is expected to be thermalised at T ~ 20 K, the contribution from translational and internal excitation of H_2 is very small. Similarly, the contribution from internal excitation of X is negligible. If X is produced by a dissociative recombination process

$$XY^+ + e \rightarrow X + Y \qquad (8.7),$$

then in a cold cloud with a particle density of $n(H_2) \sim 10^3$ cm^{-3}, the timescale for a possible collision will, on the average, exceed the time required for any vibrational, rotational or electronic de-excitation. In any case, the rates of many reactions of type (8.6) are not significantly affected by internal excitation of X - as in, for example, the case where X = OH·.[98,380,381] However, it must not be assumed that $E_{T(X)}$ must merely exceed E_a for reaction (8.6) to occur. The

collision energy E_{cm} will depend upon the relative velocities of X and H_2 in a collision, and it is this collision energy which governs the consequences of the collision: for the occurrence of any possible reaction, E_{cm} must exceed E_a.

E_{cm} can be calculated from $E_{T(X)}$ by consideration of the collision (8.6) in the centre-of-mass frame of reference (c.m.). If V is the velocity of X relative to H_2, then

$$E_{cm} = \tfrac{1}{2}\mu V^2 \qquad \{8.i\}$$

where μ is the reduced mass:

$$\mu = \frac{m_X\, m_{H_2}}{m_X + m_{H_2}} \qquad \{8.ii\}.$$

In keeping with the approximation commonly adopted in the mathematical treatment of trajectories in molecular beam experiments,[382] it is assumed that if $V_{H_2} << V_X$, then $V \sim V_X$. By this assumption,

$$E_{cm} = \tfrac{1}{2}\mu V_X^2 \qquad \{8.iii\},$$

and since $E_{T(X)} = \tfrac{1}{2} m_X V_X^2$,

$$E_{cm} = \frac{\mu}{m_X} E_{T(X)} \qquad \{8.iv\};$$

$$\therefore \quad E_{cm} = \frac{m_{H_2}}{m_{H_2} + m_X} E_{T(X)} \qquad \{8.v\}.$$

Thus $E_{T(X)}$ must exceed E_a by a factor $F = \dfrac{m_X + m_{H_2}}{m_{H_2}}$, for reaction (8.6) to have any possibility of occurrence. Because H_2 has such a low molecular mass, this factor F is typically large: for example, for X = OH·, F = 9.5. OH· is one of the lightest fragment radicals for which the hydrogen-abstraction reaction (8.6) is exothermic ($\Delta H_{8.6}$ = -67 kJ mol^{-1}) and accompanied by a comparatively low activation energy

barrier (E_a = 17.5 kJ mol^{-1}):[32,383] thus, for most other such reactions within interstellar clouds, F will be larger than for this reaction. This indicates that, while reactions of type (8.6) may be inhibited by a barrier of only 10 or 20 kJ mol^{-1} (see **table 8.1**), they will not occur under the conditions described unless $E_{T(X)}$ exceeds 100 or 200 kJ mol^{-1}.

Table 8.1: Energy parameters for reactions of the type $AH_n + H_2 \rightarrow AH_{n+1} + H\cdot$, for species of potential relevance to interstellar cloud chemistry.

AH_n	$-\Delta H$ [a]	E_a [b]	References
C	-97.1		
CH·	-12.2		
CH_2	26.2	23.9	384
CH_3·	2.3	44 ± 2	385-388
NH_2·	16.6	54	389
O	-7.8 ± 1.2		
OH·	62.8	17.5	32,383
Si	-145 ± 16		
SiH·	-130 ± 16		
SiH_2	-132 ± 14		
SiH_3·	-50 ± 6		
S	-80.3		
SH·	-58.2		
C_2	49 ± 4	? [c]	–
C_2H·	119 ± 5	5 ± 5	390
C_2H_3·	-4.9 ± 5	21.4	391
C_2H_5·	-16.0		
CN·	82	9.3 ± 1	195,392-394
HCO·	371.5	? [c]	–
C_3N·	60	? [c]	–

Notes

a. Reaction exothermicity in kJ mol^{-1}, using values obtained from reference 184.
b. Activation energy in kJ mol^{-1}, using values obtained from the references shown. Activation energies are not listed for those reactions which are endothermic.
c. This quantity has not been determined.

The effect of unreactive collisions, with H_2 and with He, should also be considered. If the X/H_2 collision is considered as one between smooth elastic spheres, then the fraction, f, of translational energy lost from X per collision is:[58,90]

$$f = \frac{8}{3}\frac{m_X m_{H_2}}{(m_X + m_{H_2})^2}\left(\frac{T_X - T_{H_2}}{T_X}\right) \qquad \{8.vi\}.$$

T_X is the effective translational temperature of the fragment X; in most instances, if X has sufficient translational energy to overcome E_a then $T_X >> T_{H_2}$ (T_{H_2} ~ 20 K), and so the expression can be approximated by

$$f' = \frac{8}{3}\frac{m_X m_{H_2}}{(m_X + m_{H_2})^2} \qquad \{8.vii\}.$$

In this manner, if a fragment X is produced by dissociative recombination of XY^+ and then collides (unreactively) with n molecules of H_2, $E_{T(X)} = (1 - f')^n E_{T(X)(init.)}$. For X = OH·, f' = 0.251: an OH· radical produced by dissociative recombination will lose one quarter of its translational energy upon each unreactive collision with H_2 (for collision with He, f' = 0.411). Thus, if $E_{T(X)}$ is not vastly in excess of that required to overcome E_a, comparatively few unreactive collisions are required to quench X so as to prevent any subsequent reaction with H_2. Since reactive collision of X with H_2 is not expected to approach unit efficiency, reactions of type (8.6) represent an inefficient source of XH - however, if no other source of XH exists, such reactions may be important nevertheless.

Having determined the translational threshold for occurrence of reaction (8.6), we must next study the dissociative recombination process (8.7) to determine

whether this threshold can be met by the energy release of such recombination processes. For the dissociative recombination of a thermalised ion XY^+ with a thermalised electron (at T ~ 20 K), the reactants have negligible translational energy, and so any translational energy residing in the product fragments must result from the exothermicity of reaction (8.7). Since the reactants can, to a good approximation, be considered 'at rest', the product fragments are required by conservation of linear momentum to have zero net linear momentum also: thus, $m_X V_X = -m_Y V_Y$. The translational energy of X can thus be expressed as a function of the total translational energy release:

since $$E_{T(total)} = \tfrac{1}{2} m_X V_X^2 + \tfrac{1}{2} m_Y V_Y^2 \qquad \{8.viii\},$$

and since $$V_Y = \frac{-m_X V_X}{m_Y} \qquad \{8.ix\},$$

$$E_{T(X)} = \frac{m_Y}{m_X + m_Y} E_{T(Total)} \qquad \{8.x\}.$$

The total translational energy release will depend upon the distribution of energy released by recombination:

$$-\Delta H_{8.7} = E_{T(Total)} + E_R' + E_V' + E_E' \qquad \{8.xi\},$$

where E_R', E_V', and E_E' represent the energy released as rotational, vibrational and electronic excitation of the product fragments. Very little is yet known about the distribution of energy in dissociative recombination reactions: theoretical treatments of these reactions[52,82] suggest that translational excitation of the products accounts for a considerable fraction of the reaction exothermicity. In the extreme case, where there is negligible internal excitation, $-\Delta H_{8.7} = E_{T(total)}$ and thus $E_{T(X)} = -\frac{m_Y}{m_X + m_Y} \Delta H_{8.7}$. In these circumstances the threshold for reaction (8.6) becomes

$$-\Delta H_{8.7} > \frac{m_X + m_Y}{m_Y}\frac{m_X + m_{H_2}}{m_{H_2}}E_a \qquad \{8.xii\}:$$

that is, dissociative recombination processes whose exothermicity does not exceed this threshold cannot produce fragments X with sufficient translational energy to permit the occurrence of reaction (8.6).

It should be noted, in relation to the above formula for the threshold, that dissociative recombination reactions of the types

$$XH^+ + e \rightarrow X + H\cdot \qquad (8.8)$$

and

$$XH_2^+ + e \rightarrow X + H_2 \qquad (8.9)$$

will impart most of the translational energy released to the light $H\cdot/H_2$ fragment. Therefore, $E_{T(total)}$ for such recombinations must be very large to permit the occurrence of a subsequent reaction (8.6) with even a modest activation barrier.

These factors will now be considered more specifically for the interstellar occurrence of reaction (8.6) with X = OH·, that is,

$$OH\cdot + H_2 \rightarrow H_2O + H\cdot \qquad (8.10).$$

Section 8.3: Reaction between OH· and H_2, for OH· produced by the dissociative recombination of H_3O^+.

Very few experimental determinations of dissociative recombination product channels have yet been performed. The reaction

$$H_3O^+ + e \rightarrow H_2O + H\cdot \quad (8.11a)$$

$$\rightarrow OH\cdot + H_2 \quad (8.11b)$$

$$\rightarrow OH\cdot + H\cdot + H\cdot \quad (8.11c)$$

$$\rightarrow O + H_2 + H\cdot \quad (8.11d)$$

has recently been investigated by Herd et al[85] in a FALP apparatus, using laser-induced fluorescence to determine the yield of OH· produced. Channels (8.11b) and (8.11c) account for (65 ± 15%) of H_3O^+ recombinations: unfortunately, since OH· is the only neutral product yet detected in such experiments, the efficiency of any of these channels cannot be readily assessed. Herd et al contend that channel (8.11b) accounts for most of the OH· produced, in accordance with Bates[52] who considers that this channel represents a favourable crossing of potentials in the recombination process. Bates also suggests that the H_2 product of this recombination will be vibrationally excited in accordance with the Franck-Condon principle, since the H–H separation in H_3O^+ is significantly greater than in ground-state H_2. Consideration of the Franck-Condon factors involved indicates that the degree of vibrational excitation of H_2 is likely to be between 2.0 and 3.4 eV : the remainder of the energy released by recombination, which Bates describes as the 'partial exothermicity' of the reaction, is 2.2 to 3.6 eV. Most of

this partial exothermicity must appear as translational energy of the products.[52] This is in accordance with the experimental results, which indicate that 46% of all H_3O^+ recombinations (and, therefore, 70% of recombinations yielding OH·) produce OH· in the ground vibrational state. It is reasonable to assume that the degree of rotational excitation of products is also slight.

If it is assumed that channel (8.11b) is the dominant product channel for recombination of H_3O^+, and that the energy released by neutralisation is partitioned only into H_2 vibration and product translation, can the OH· produced by channel (8.11b) react with H_2 via reaction (8.10) to produce H_2O, under conditions in cold interstellar clouds ?

The relevant parameters are

$$\Delta H_{8.11b} = -552 \text{ kJ mol}^{-1};$$

$$E_{V'} > 190 \text{ kJ mol}^{-1} (\equiv 2.0 \text{ eV}),$$

$$\therefore \quad E_{T(Total)} < 362 \text{ kJ mol}^{-1}.$$

$$m_X = 17.0 \text{ g mol}^{-1};$$

$$m_Y = 2.0 \text{ g mol}^{-1};$$

$$E_a = 17.5 \text{ kJ mol}^{-1}.$$

Calculation of the threshold for the occurrence of reaction (8.10), according to the expression derived earlier, gives a value of $E_{T(Total)} > 1579$ kJ mol^{-1}. This required translational energy release is vastly in excess of the maximum possible energy release. The possibility of additional vibrational, rotational or electronic excitation of OH· during the recombination process (8.11), or OH· production by channel (8.11c), further reduces the total available translational energy, and

therefore OH· produced by reaction (8.11) cannot possibly undergo further reaction with H_2 under the conditions considered here.

Section 8.4: Reaction between OH· and H_2, for OH· produced from dissociative recombination of $HOCO^+$.

The reaction

$$HOCO^+ + e \rightarrow OH\cdot + CO \quad [0.34] \quad (8.12a)$$

$$\rightarrow H\cdot + CO_2 \quad (8.12b)$$

$$\rightarrow H\cdot + O + CO \quad (8.12c)$$

$\Delta H_{8.12a} = -670$ kJ mol^{-1},

has also been studied recently by the FALP-LIF technique.[84,85] Channel (8.12a) produces two molecular fragments of comparable mass, and thus the threshold for the possibility of reaction (8.10) occurring subsequently for OH· produced by this channel should be lower than in the case of H_3O^+ recombination described above.

The distribution of energy in reaction (8.12a) is not known, but an analogy may be made with the photodissociation of HONO, which is isoelectronic with $HOCO^+$.[395,396]

$$HONO + h\nu \rightarrow HONO(\tilde{A}) \rightarrow OH + NO \quad (8.13)$$

$\Delta H_{8.13} = -123$ kJ mol^{-1}.

The energy distribution of reaction (8.13) has been extensively studied: approximately 46% of the total available energy appears as translational excitation of OH· ($E_{T(OH)}$ ~ 57 kJ mol^{-1}), implying that virtually three-quarters of the available energy is manifested as recoil energy of the products. Although reaction (8.13) is substantially less exothermic than reaction (8.12a), it is probable that rapid recombination of $HOCO^+ + e$ would manifest a similarly large fraction of its exothermicity as recoil energy. The observed distribution of translational and rotational energies in reaction (8.13) is consistent with the impulse model of Tuck,[397] and by analogy, the energy distribution of reaction (8.12a) can be partially predicted in this manner. Tuck's impulse model considers that the energy released by dissociation acts directly along the axis of the bond undergoing cleavage. By this model,

$$E_{T(OH)} : E_{T(CO)} : E_{R(OH)} : E_{R(CO)} =$$
$$m_C m_O m_{CO} : m_C m_O m_{OH} : m_C m_{CO} m_H \sin^2\theta : m_O m_{OH} m_O \sin^2\Phi.$$

Using $\theta = 119°$ and $\Phi = 174°$ (see **table 8.2**), the fraction of the available energy channelled into each of these modes is

$$E_{T(OH)} : E_{T(CO)} : E_{R(OH)} : E_{R(CO)} = 0.6008 : 0.3649 : 0.0290 : 0.0053.$$

This model does not account for possible vibrational and electronic excitation of the products OH· and CO. Vibrational excitation is expected to be slight (since r(O–H) and r(C=O) in $HOCO^+$ are very close to the ground-state internuclear separations of 0.97 and 1.128 Å, for OH· and CO respectively). This is supported by the observation that 50% of the OH· produced by channel (8.12a) is in the ground vibrational state.[84,85] Electronic excitation of the CO is not energetically possible, but production of electronically excited OH· ($A\ ^2\Sigma^+$) can occur. Indeed,

Adams et al have reported[84] detection of weak optical emissions due to OH· $A\ ^2\Sigma \rightarrow X\ ^2\Pi$ transitions in a HCO_2^+/e plasma, but believe that much of the OH· produced is in the ground electronic state ($X\ ^2\Pi$).

If OH· is produced in the ground electronic state ($X\ ^2\Pi$) and if vibrational excitation is considered negligible, $E_{T(Total)}$ = 647 kJ mol^{-1}; for production of OH· ($A\ ^2\Sigma^+$), $E_{T(Total)}$ = 243 kJ mol^{-1}. Can reaction (8.10) occur for OH· so produced ?

Using m_X = 17.0 g mol^{-1} and m_Y = 28.0 g mol^{-1}, the threshold for possibility of reaction (8.10) is $E_{T(Total)} > 267$ kJ mol^{-1}. Therefore, OH· ($X\ ^2\Pi$) produced by channel (8.12a) has ample energy to permit hydrogen-atom abstraction from H_2, although it appears that electronically-excited OH· ($A\ ^2\Sigma^+$) lacks just sufficient translational energy to drive reaction (8.10).

Table 8.2: Calculated geometry of $HOCO^+$.

r(H–O) [a]	r(O–C) [a]	r(C=O) [a]	θ [b]	Φ [b]	source
1.0082	1.2973	1.1542	111.9	171.8	c
0.987	1.224	1.121	117.2	180.0	d
1.000	1.246	1.171	127.8	171.6	e
0.986	1.237	1.135	118.0	174.5	f
0.9874	1.2161	1.1298	119.34	173.64	g
0.972	1.220	1.111	119.7	174.0	h

Notes

a. Bond length in angstroms.
b. Bond angles in degrees. θ is the angle ∠(HOC), Φ is the angle ∠(OCO).
c. STO-3G calculations, reference 398.
d. SCF/CI calculations, reference 399.
e. RMP2/4-31G calculations, reference 400.
f. CISD+Q calculations, reference 401.
g. Empirically corrected MP2/6-31G(d) calculations, reference 402.
h. MC SCF/6-31G* calculations, reference 403.

Having postulated that reaction (8.10) might occur for OH· (X $^2\Pi$) from the dissociative recombination of $HOCO^+$, it becomes desirable to estimate in some manner the efficiency of this process. While a detailed assessment of the reaction efficiency is beyond the scope of this present work, it is certainly possible to gain an approximate value of the efficiency. For OH· (X $^2\Pi$) produced by channel (8.12a),

$$E_{T(Total)} = 647 \text{ kJ mol}^{-1}$$

if vibrational excitation is neglected as discussed above;

$$\therefore \quad E_{cm} = 42.4 \text{ kJ mol}^{-1}$$

for the first OH· + H_2 collision following dissociative recombination. Schatz[381] has calculated the reactive cross-section for reaction (8.10) as a function of translational, rotational and vibrational energy. The calculated reactive cross-section for internally cold (v=0, j=0) reactants can be used to determine the efficiency of each collision with H_2, if the collision cross-section is known. The hard-sphere estimate of the collision cross-section, Q_{tot}, for reaction (8.10) is 30 Å^2. This value has been used in **table 8.3**, which shows the cumulative fraction of OH· (X $^2\Pi$) lost to reaction (8.10) after n+1 collisions with H_2. These figures show that ~ 6% of the OH· (X $^2\Pi$) radicals react on the first collision, ~ 4% react on the second collision and less than 2% react on the third collision. There is very little additional possibility for reaction after the third collision, since E_{cm} rapidly drops below E_a after this.

This calculation demonstrates that approximately 10% of OH· (X $^2\Pi$) radicals from $HOCO^+$ recombination should be converted to H_2O by reaction (8.10), under conditions pertaining to cold quiescent interstellar clouds.

Section 8.5: Discussion.

The possible formation of H_2O by reaction (8.10) is astrophysically significant. Millar et al[404] have modelled the consequences of changing **p**, the fraction of H_3O^+ recombinations which produce OH·. They find that if **p** = 0, then H_2O becomes the predominant oxygen-containing species (with the exception of CO); however, if **p** > 0.1, then O_2 predominates over H_2O owing to the rapidity of reaction (8.4), between OH· and O. Experimentally, **p** = 0.65 ± 0.15.[85] This suggests that O_2 will have a higher abundance than H_2O, and H_2O is in fact observed to be localised in small regions of dense clouds whereas the ion H_3O^+ is widespread.[405]

Table 8.3: Calculated cumulative efficiency of reaction (8.10), for OH· (X $^2\Pi$) from dissociative recombination of $HOCO^+$.

n [a]	E_{cm} [b]	Q_r [c]	P_r [d]	P_{nr} [e]
0	42.4	1.7	0.06	0.94
1	31.8	1.1	0.09	0.91
2	23.8	0.6	0.11	0.89
3	17.8	<0.1	0.11	0.89
4	13.3	0	0.11	0.89

Notes

a. Number of collisions (with H_2) elapsed since the dissociative recombination event.
b. Centre-of-mass collision energy, in kJ mol^{-1}.
c. Calculated reaction cross section, in $Å^2$, from reference 381.
d. Cumulative fraction of OH· radicals lost through reaction (8.10), calculated from Q_r using a hard-sphere collision cross-section Q_{tot} = 30 $Å^2$.
e. Fraction of OH· radicals remaining.

Nevertheless, the dissociative recombination of $HOCO^+$ should produce OH· with ample energy to drive reaction (8.10). This suggests a further connection between the abundances of the oxygen-containing species. If reaction (8.3), involving CO_2 formation from OH· and CO, has negligible activation energy then this reaction will compete with reaction (8.4) as a primary destruction mechanism for (cold) OH·. If the CO abundance significantly exceeds that of atomic oxygen, reaction (8.3) may dominate over reaction (8.4): n(CO)/n(O) will depend upon the overall C/O abundance ratio within the cloud (a parameter which is uncertain), the local density and the cloud age (bimolecular reactions will remove O more efficiently than CO). In dense regions especially, CO is likely to have a higher abundance than O, favouring CO_2 formation via reaction (8.3). Protonation of CO_2, followed by dissociative recombination, should yield OH· capable of H_2O formation as shown here, and this may help account for the observation of H_2O within denser regions of clouds.[405]

The H_3O^+ and $HOCO^+$ abundances within Sgr B2 (the only interstellar source for which abundances of both ions have been reported) are similar: $n(H_3O^+) \sim 10^{-9}$ $n(H_2)$[406] and $n(HOCO^+) > 10^{-10}$ $n(H_2)$.[407] The results of Herd et al[85] indicate that $[34 \pm 8]$% of $HOCO^+$ recombinations produce OH·. The estimation reported here suggests that, in the absence of electronic excitation of the OH· product, ~ 10% of these radicals can produce H_2O via reaction (8.10), leading to an effective branching ratio of ~ 3% efficiency of H_2O formation by $HOCO^+$ recombination. A maximum of $[35 \pm 15]$% of H_3O^+ recombinations may yield H_2O - although Herd et al[85] indicate that the H_3O^+ recombinations not yielding OH· may very likely produce O + H_2 + H· by predissociation of vibrationally excited OH· ($A\ ^2\Sigma^+$). Since the abundances of the $HOCO^+$ and H_3O^+ ions are comparable, and since the

calculated efficiency of H_2O formation from $HOCO^+$ recombination is so low (~ 3%), dissociative recombination of $HOCO^+$ is unlikely to have a major effect on the production of H_2O in the interstellar environment unless H_3O^+ recombination is also a very inefficient source of H_2O.

A possible experiment to test the production of H_2O from $HOCO^+$ dissociative recombination would be one analogous to the FALP-LIF experiments of Smith and co-workers,[84,85] but employing H_2 as a buffer gas in the place of helium. The rate for reaction (8.10) is comparatively insensitive to the rotational and vibrational state of OH·,[380,381] so an apparent reduction in the product channel (8.12a), in excess of that expected for OH· + H_2 at room temperature, would indicate the rapid occurrence of this reaction due either to translational or to electronic excitation. An additional test would be to see whether the fraction of H_3O^+ recombination channels yielding OH·, in a similar experiment with H_2 buffer gas, was similarly reduced: as described above, OH· produced from reactions (8.11b) and (8.11c) should lack sufficient translational excitation to allow reaction (8.10) to proceed rapidly.

It is of some interest to note the parallel which exists between the occurrence of reaction (8.10) under the conditions described here, and the conditions within shocked regions of diffuse interstellar clouds. The present scenario describes the reaction of translationally excited, internally cold OH· with cold H_2. Within shocked diffuse clouds the same reactants are expected to be translationally hot (as a result of the shock, for which an effective temperature T ~ 2000 K → 5000 K may be appropriate) but internally cooled: OH·, since it possesses a large dipole moment, will radiate away any vibrational or rotational energy,[95] and H_2 will

radiate vibrational or rotational energy by electric quadrupole transitions,[98] and diffuse clouds are usually of sufficient transparency to render re-absorption unlikely. In effect, therefore, the only difference between the occurrence of reaction (8.10) within dense clouds (following dissociative recombination of the $OH\cdot$ precursor) and within shocked diffuse clouds is in the translational energy of the hydrogen molecule. Both scenarios suggest analogy with molecular beam techniques, in which reactants are supersonically cooled with respect to vibration and rotation: it seems likely that such beam experiments could help verify the efficiencies of the reactions concerned.

The application of this hypothesis of translationally-driven interstellar reactions, to other products of dissociative recombination reactions, is uncertain. Observed interstellar ions are typically small - $HOCO^+$ is the largest yet observed, on the basis of molecular weight - and the possibility exists that neutral-neutral processes may be more important than ion-molecule reactions in determining the abundances of larger molecules such as cyanopolyynes. Activation barriers for many radical-H_2 reactions of possible interstellar significance are undetermined or uncertain. In addition, too little is known concerning the product distributions of other dissociative recombination reactions of interstellar relevance. Further experimental work is required to at least establish which theories are able to satisfactorily account for the products observed. For these reasons, discussions concerning the subsequent reactivity of recombination products of other large ions seem unproductive.

CHAPTER 9.

A COMPARISON OF THE REACTIVITIES OF UNSATURATED, LINEAR $C_4H_n^+$, $C_3H_nN^+$, AND $C_3H_nO^+$ IONS.

Section 9.1: Introduction.

Giles et al[226] have determined that, as a general rule for the ions $C_nH_m^+$ ($n = 4 \rightarrow 6$; $m = 0 \rightarrow 6$), only those ions having $m \leq 1$ react with H_2. Similarly, ions with $m \leq 1$ were observed to be more reactive with CO than their more highly hydrogenated counterparts. Bohme et al[355] have explored the reactivity of C_n^+ ($n = 1 \rightarrow 6$) and C_nH^+ ($n = 2 \rightarrow 5$) with CO, and observe a similar pattern of reactivity. The reactions of C_n^+ ($n = 3 \rightarrow 19$) with D_2 and O_2 have been studied by McElvany et al,[364] who observed that $C_nD_2^+$ did not react further with D_2. These authors have interpreted their observations via a model involving linear carbon-chain ions $:C=(C{=}C)_x{=}C:^+$ which have carbene character at the terminal C atoms.

H-atom abstraction from H_2 is calculated to be exothermic only for reaction at these termini, since this does not involve disruption of the cumulene-type bonding of the carbon chain. Similarly, association with CO is more efficient if

the ion concerned features such carbene moieties, since these lone pairs can add directly to the CO molecule.

Bohme and co-workers[245,271,329-331,408] have also explored the reactivity of the ions C_3H^+, C_2N^+ and C_4N^+: many reactions of these ions can be accounted for by their carbene character. Bohme's results are applicable to ions of the type C_nN^+ (where n is even) or C_nH^+ (where n is odd), since for these ions resonance forms can be drawn which illustrate the partial localisation of the cationic charge upon the terminal (carbene) carbon atom: for example,

$$:\overset{+}{C}-(C\equiv C)_x-C\equiv N: \text{ and } :\overset{+}{C}-(C\equiv C)_x-C\equiv C-H.$$

Bohme et al have not considered ions such as C_3N^+ to be potential carbene cations: such ions have no possible resonance structure featuring a positive charge upon the carbene carbon. However, Parent[269,270] has performed MNDO calculations upon several C_nN^+ ($n = 4 \rightarrow 8$) ions: these calculations indicate that all these ions have some carbene character. Parent's studies[269,270] also include experimental results for the reactions of these C_nN^+ ions with methane: some product channels in these reactions are attributed to the presence of carbene character. This suggests that the absence of charge upon the terminal carbon atom is not, in itself, an impediment to carbene reactivity in ion-molecule reactions.

In the studies described in chapters 4, 6, and 7, similar patterns of reactivity were observed for $C_3H_nN^+$ and $C_3H_nO^+$ ions. This chapter thus describes a comparison between the reactivities of these types of ions.

Section 9.2: Discussion.

Rate coefficients for reactions of the ions concerned with H_2, CO, C_2H_2 and HCN are summarised in **table 9.1**: these neutrals have been selected since results for the series $C_4H_n^+$ (n = 0 → 4) are available, whereas reactions of these ions with other neutrals have not, in general, been studied. (The units used in this table are 10^{-10} cm^3 $molec^{-1}$ s^{-1} rather than 10^{-9} cm^3 $molec^{-1}$ s^{-1}, to amplify differences in reactivity.)

Table 9.1: A comparison of $C_4H_n^+$, $C_3H_nN^+$ and $C_3H_nO^+$ reactivities.

Reactant	H_2 [a]	CO [a]	C_2H_2 [a]	HCN [a]
C_4^+	0.96 [b,c]	4.5 [b]*	15 [d]	28 [d]
C_4H^+	1.5 [b]	4.7 [b]*	15 [d]	17 [d]
$C_4H_2^+$	<0.005 [b]	0.32 [b]*	1.4 [d]	<0.2 [d]
$C_4H_3^+$	<0.005 [b]	0.013 [b]*	2.4 [d]	<0.5 [d]
$C_4H_4^+$	<0.005 [b]	<0.005 [b]	1.2 [d]	<0.3 [d]
C_3N^+	8.1	5.4*	10.2	22
C_3HN^+	0.012	0.56*	13	13
$C_3H_2N^+$	<0.005	<0.01	<0.1	0.6*
$C_3H_3N^+$	0.01	0.07*	9.3	1.9
$C_3H_4N^+$	<0.005	<0.005	<0.1	0.34*
C_3O^+	8.0	0.72*	10.8	29
C_3HO^+	<0.005	<0.01	<0.01	0.04*
$C_3H_2O^+$	<0.005	<0.01	4.3	1.9*
$C_3H_3O^+$	<0.005	<0.01	<0.01	0.02*

Notes

a. Rate coefficient in units of 10^{-10} cm^3 $molec^{-1}$ s^{-1}. An asterisk indicates that the only reactive channel observed is association.
b. Reference 226.
c. at 300 K; $k = 4.1 \times 10^{-10}$ cm^3 $molec^{-1}$ s^{-1} at 80K.
d. Reference 225.

General trends evident in these data are:

(i). Ions lacking terminal carbon atoms do not react rapidly with H_2.

(ii). Ions lacking teminal carbon atoms do not undergo efficient association with CO.

(iii). The radical cations C_3HN^+, $C_3H_3N^+$ and $C_3H_2O^+$ are substantially more reactive than the non-radical cations $C_3H_2N^+$, $C_3H_4N^+$, C_3HO^+ and $C_3H_3O^+$.

(iv). For the $C_4H_n^+$ ions, radical cations are no more reactive than non-radical cations.

H-atom abstraction is predicted to be exothermic for the reactions of HC_3N^+, $C_3H_3N^+$ and $C_3H_2O^+$; however, these reactions occur very slowly at room temperature. The failure of the reaction

$$C_3H_2O^+ + H_2 \rightarrow C_3H_3O^+ + H\cdot \qquad (9.1)$$

$$\Delta H_{9.1} = -8 \text{ kJ mol}^{-1}$$

to proceed at a measurable rate may indicate that this reaction is endothermic: alternatively, in keeping with the low reactivity of HC_3N^+ and $C_3H_3N^+$ with H_2, reaction (9.1) may just be slow. An exothermic reaction may be slow due to an activation energy barrier (accompanied by a positive temperature dependence) or the formation of a weakly-bound collision complex which has a shorter lifetime than the time required for reaction to occur (often diagnosed by a negative temperature dependence: the reaction between C_4^+ and H_2 appears to involve such a mechanism). A study of the variation of the rate of reaction (9.1) with

temperature, or with effective centre-of-mass energy, might indicate which of these factors is at work in this reaction.

The resonance forms most likely to contribute to the electronic structures of the ions $C_3H_nN^+$ and $C_3H_nO^+$ are shown in **figures 9.1** and **9.2**. These figures indicate that, as with the carbon cluster ions and their reaction products,[355,364] only the terminal carbon atoms in these ions can possess significant carbene character, and only those ions with terminal carbon atoms have any resonance forms in which carbene character is evident (with the exception of HC_3O^+, for which one carbene form seems plausible). Other ions can be drawn in such a way that carbene character is present - for example, HC_3N^+ can be drawn as the structures $H–\overset{+}{\dot{C}}–\ddot{C}–C{\equiv}N:$ and $H–\ddot{C}–\overset{+}{\dot{C}}=C=\dot{N}:$, but these forms are not expected to

---

Figure 9.1: Resonance forms of the ions $C_3H_nN^+$ ($n = 0 \rightarrow 4$).

(n = 0) $\overset{+}{\dot{C}}{\equiv}C–C{\equiv}N:$ $\leftrightarrow$ $:C=\overset{+}{\dot{C}}–C{\equiv}N:$ $\leftrightarrow$ $:C=C=C=\ddot{\dot{N}}^+$

(n = 1) $H–C{\equiv}C–C{\equiv}\dot{N}^+$ $\leftrightarrow$ $H–C{\equiv}C–\overset{+}{\dot{C}}=\dot{N}:$ $\leftrightarrow$ $H–C{\equiv}C–\dot{C}=\dot{N}^+$

$\leftrightarrow$ $H–\overset{+}{\dot{C}}=C=C=\dot{N}:$ $\leftrightarrow$ $H–\dot{C}=C=C=\ddot{\dot{N}}^+$ $\leftrightarrow$ $H–\overset{+}{\dot{C}}=\dot{C}–C{\equiv}N:$

$\leftrightarrow$ $H–\dot{C}=\overset{+}{\dot{C}}–C{\equiv}N:$

(n = 2) $H–C{\equiv}C–C{\equiv}\overset{+}{\dot{N}}–H$ $\leftrightarrow$ $H–\overset{+}{\dot{C}}=C=C=\ddot{\dot{N}}–H$

(n = 3) $H_2C=CH–C{\equiv}\dot{N}^+$ $\leftrightarrow$ $H_2C=CH–\dot{C}=\ddot{\dot{N}}^+$ $\leftrightarrow$ $H_2C=CH–\overset{+}{\dot{C}}=\dot{N}:$

$\leftrightarrow$ $H_2\overset{+}{\dot{C}}–CH–C{\equiv}N:$ $\leftrightarrow$ $H_2\dot{C}–\overset{+}{\dot{C}}H–C{\equiv}N:$ $\leftrightarrow$ $H_2\dot{C}–CH=C=\ddot{\dot{N}}^+$

(n = 4) $H_2C=CH–C{\equiv}\overset{+}{\dot{N}}–H$ $\leftrightarrow$ $H_2C=CH–\overset{+}{\dot{C}}=\ddot{\dot{N}}–H$ $\leftrightarrow$ $H_2\overset{+}{\dot{C}}–CH=C=\ddot{\dot{N}}–H$

contribute significantly to the character of the ion under thermal conditions, since they require the excitation of two π electrons into a non-bonding orbital. This is expensive in terms of energy requirements, and de-excitation is likely to be facile since the positive charge in these forms is localised on the neighbouring C atom, inviting the re-formation of the missing π bond:

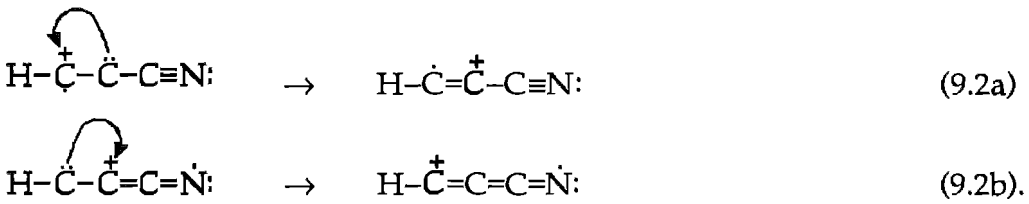

(9.2a)

(9.2b).

Figure 9.2: Resonance forms of the ions $C_3H_nO^+$ (n = 0 → 3).

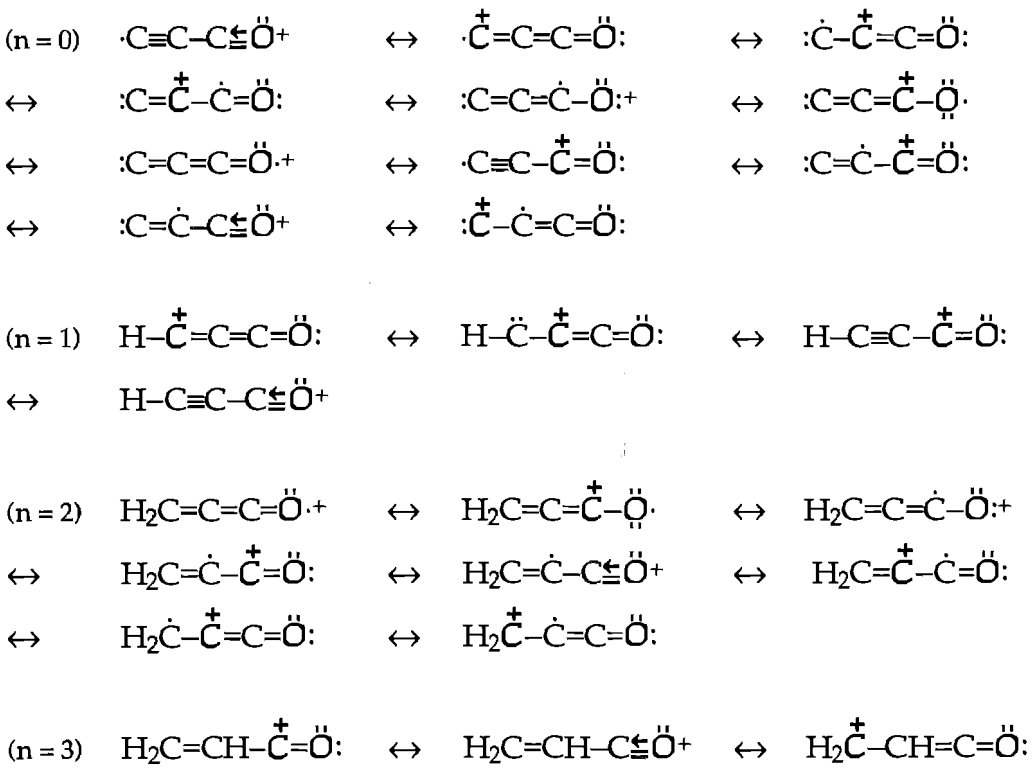

In addition to those structures shown in figure 9.1, the diradical resonance forms $\cdot C{\equiv}C{-}C{\equiv}\overset{+}{N}\cdot$, $\cdot C{\equiv}C{-}\overset{+}{C}{=}\ddot{N}\cdot$ and $\cdot\overset{+}{C}{=}C{=}C{=}\ddot{N}\cdot$ may also contribute to the reactivity of the C_3N^+ ion: Harland and Maclagan[259] have calculated that the lowest-lying triplet state of $CCCN^+$ is only 4 kJ mol^{-1} above the ground (singlet) state, although this energy difference neglects the effect of vibrational and rotational internal energy. When vibrational and rotational effects are considered, the triplet state is 28 kJ mol^{-1} above the singlet state at 298K.[259]

In table 9.1, only the ions with terminal C atoms react rapidly with H_2. The reactivity of the $C_3H_nN^+$ and $C_3H_nO^+$ ions with H_2 can thus be rationalised as occurring most efficiently via a mechanism of carbene insertion into the H-H bond: such a mechanism also accounts for the observed trends in hydrocarbon ion reactivity with H_2.[226,364] Similarly, the trend in $C_3H_nN^+$ / $C_3H_nO^+$ reactivity with CO can be explained by a carbene model: carbene addition to CO is seen to occur efficiently according to the results in table 9.1. An alternative and more mechanistic viewpoint is that the ions having carbene character form more stable and hence longer-lived 'tight' collision complexes with CO, increasing the probability of collisional stabilisation before complex fragmentation can occur.

Ions with carbene character may react with HCN and with C_2H_2 via C–H bond insertion or via carbene addition to the C≡C or C≡N groups. Either mechanism permits the formation of a cyclic reactive intermediate. Such an intermediate has been invoked by Bohme[29,271,329] to explain the observed products from reactions of the carbene ions C_3H^+ and C_4N^+ with the neutrals CH_4, NH_3, H_2O and H_2S, and the formation of a cyclic reactive intermediate may explain the loss of CO in several reactions of C_3O^+. C_3O^+ also has parallels with the reactivity of

C_3H^+ and C_4N^+ (see **figure 9.3**) since product channels common to reaction with CH_4, NH_3 and H_2O differ from those seen in the reactions with HCN and C_2H_2. In common with the C_3H^+ and C_4N^+ reactions depicted in figure 9.3, the reactions of C_3O^+ are better described by a mechanism involving carbene X–H bond insertion than by a scheme involving addition to the C≡X group. The loss of CO as the dominant product channel of the reactions with HCN and C_2H_2 is more conveniently explained by formation of the cyclic intermediate

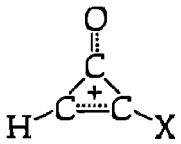

(X = C_2H, CN)

resulting from C-H bond insertion than by formation of the structure

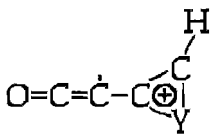

(Y = CH, N)

which would result from carbene attack at the triple bond: loss of CO from the latter structure would give a cyclic product ion

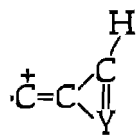

(Y = CH, N)

as the initial product. The heats of formation of these cyclic ions are not known: they are likely to have considerably higher ΔH_f than the linear ions $HCCCCH^+$ and $HCCCN^+$, and thus it is quite possible that the production of the above cyclic product ions is endothermic in these reactions.

Figure 9.3: A comparison of the reactivity of C_3O^+ with the carbene cations C_3H^+ and C_4N^+. The reactions shown do not completely describe the reactivity of these cations: reaction types shown are, rather, those which are most effectively described in terms of a carbene σ bond insertion mechanism.

(a). Reaction channels observed for reaction of C_3H^+, C_4N^+ (R = H,CN) with the neutral H-X.[271,329-331]

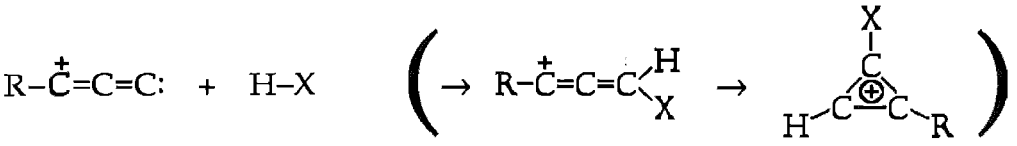

(i). X = CH_3, NH_2, OH, SH.

→ H–C≡C–R + :CX^+

(ii). X = CN, C_2H, C_3N; (X = H, R = H)

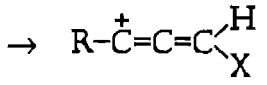

(iii). (R = CN). X = H, CH_3, C_2H, C_4H, NH_2, SH.

→ X–$\overset{+}{C}$=C=C: + H–R

(b). Reaction channels observed for reaction of C_3O^+ with the neutral H-X.

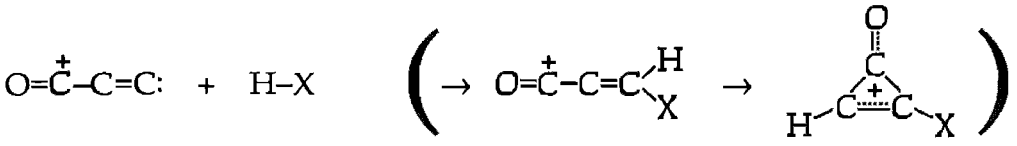

(i). X = H, CH_3, NH_2, OH.

→ O=C=C=CH^+ + X

(ii). X = C_2H, NH_2.

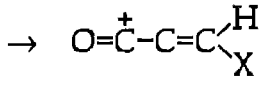

(iii). X = C_2H, CN.

→ X–C≡C–H^+ + CO

The reaction products from C_3N^+ can also be explained in terms of carbene reaction mechanisms. The most commonly observed product channels with neutrals of the type H–X are H-atom abstraction (seen with X = H, CH_3, OH, CN), X-group abstraction (seen with X = CH_3, C_2H, OH) and adduct formation (seen with X = H, C_2H, CN, and with the neutrals N_2, CO and C_2N_2). Carbene H–X insertion followed by X loss can adequately account for production of $HCCCN^+$ in several reactions (the formation of this isomer is assumed: no other C_3HN^+ isomers have been reported in the literature). Alternatively, a simple one-step abstraction mechanism can account for $HCCCN^+$ production. O-atom abstraction in the reactions with O_2 and CO_2 can satisfactorily be attributed to carbene reactivity

$$:N{\equiv}C{-}\overset{+}{C}{=}C: \;+\; :\ddot{O}{=}X \;\rightarrow\; :N{\equiv}C{-}\overset{+}{C}{=}C{=}\ddot{O}: \;+\; :X \qquad (9.3);$$

similarly, such double-bond formation might also account for the adduct formation observed with the normally unreactive neutral N_2:

$$:N{\equiv}C{-}\overset{+}{C}{=}C: \;+\; :N{\equiv}N: \rightarrow \;:N{\equiv}C{-}\overset{+}{C}{=}C{=}N{-}\ddot{N}: \qquad (9.4).$$

Several canonical forms of this possible structure for the adduct ion can be drawn. The formation of $HCNH^+$ in the reactions with H_2O and NH_3 cannot easily be explained by a mechanism involving carbene insertion or addition reactions, without the occurrence of substantial rearrangement within the collision complex. These reactions might more satisfactorily be interpreted in terms of nitrene reactivity (a nitrene is a univalent nitrogen with four nonbonding electrons), although a degree of rearrangement is still required.

However, the canonical forms of C_3N^+ displayed in figure 9.1 suggest that C_3N^+ does not possess significant classical nitrene character.

HCN and C_2H_2 are more reactive neutrals than H_2 or CO (as is evident from the large rates observed for their reactions with many ions),[182] so it is reasonable that ions without carbene character may also undergo reasonably rapid reaction with these neutrals. Table 9.1 indicates that reactions of C_3H_nN/O^+ ions with HCN and C_2H_2 are reasonably rapid ($k > 1.0 \times 10^{-10}$ cm^3 $molec^{-1}$ s^{-1}) if the ions possess terminal C atoms, or are radicals. Ions which do not fulfil either of these criteria are not observed to react significantly with C_2H_2 or with HCN, although a slow association channel may be evident. This pattern of reactivity is not reflected in the reactions of $C_4H_n^+$ with these neutrals, however: in these reactions only the ions featuring terminal C atoms are observed to react rapidly with HCN, and rates for reaction with C_2H_2 are also substantially lower for $n \geq 2$ than for $n = 0$ or 1. A possible explanation for this difference is that the reactions of these hydrocarbon ions with C_2H_2 and HCN have only been studied using the ICR technique, and thus channels which require a degree of rearrangement would be expected to occur with reduced efficiency under conditions which are less conducive to the formation of reasonably long-lived collision complexes. A SIFT study of these reactions would hopefully resolve this issue.

Finally, the observation that the most reactive polyatomic carbon-containing ions are highly unsaturated linear ions with terminal C atoms seems very relevant to the chemical evolution of cold interstellar clouds. The abundance of highly unsaturated linear molecules in these clouds, the relative scarcity of double bonds as opposed to alternating single and triple bonds, and the complete

absence of branched-chain compounds are all observational constraints which suggest that the production of highly unsaturated compounds is somehow kinetically favoured (although it should be noted that observations of interstellar molecules are biased towards the detection of linear, unsaturated species since these have the simplest rotational spectra): the rather sketchy exploration of ion reactivity in this chapter supports the notion that ion-molecule reactions can account for the higher efficiency of production of these very unsaturated compounds.

CHAPTER 10.

A SUMMARY.

Section 10.1: Overall conclusions.

Thermochemical values determined in the present work are summarised in **table 10.1.**

The proton affinities of C_2N_2 and C_4H_2 were determined by measurement of the reaction rates for proton transfer between bases of similar PA (CH_3Cl and C_2H_4 with C_2N_2, and BrCN and CH_3NO_2 with C_4H_2). The value of $PA(C_2N_2)$ (674 kJ mol^{-1}) thus obtained is in very good agreement with previous determinations, but our value of $PA(C_4H_2)$ (741 kJ mol^{-1}, which is supported by several other studies) is in serious disagreement with the accepted literature value of this quantity.

Studies of the reactivity of the CCN^+ and CNC^+ isomers, produced by a variety of techniques, have established that the higher-energy CCN^+ isomer is more reactive with a variety of neutral reagents. This finding is in keeping with the study of C_2N^+ reactivity performed independently by Bohme et al.[245] The isomeric ratio CCN^+:CNC^+ (~1:4), for C_2N^+ produced by electron impact ionisation upon each of several source gases within the SIFT ion source, is very close to the calculated ratio of rovibrational states for CCN^+:CNC^+ at the saddle-point energy (using parameters calculated by DeFrees and MacLean[241]): this close

similarity in values is explained in terms of the competition between unimolecular rearrangement (isomerisation) and bimolecular collisional deexcitation of the C_2N^+ ions. At low pressures, the rate of isomerisation is fast compared to the rate of quenching and so the observed isomeric ratio should adhere closely to the density-of-states ratio at the saddle-point energy. For C_2N^+

Table 10.1: Thermodynamic quantities determined in the present work.

Quantity	Value	Comments	Chapter
$PA(CH_3Cl)$	673 ± 4 kJ mol^{-1}	referenced to $PA(C_2H_4)$	3
$PA(C_2N_2)$	674 ± 4 kJ mol^{-1}	referenced to $PA(C_2H_4)$	3
PA(BrCN)	747 ± 4 kJ mol^{-1}	referenced to $PA(CH_3NO_2)$ [a]	3
$PA(C_4H_2)$	741 ± 6 kJ mol^{-1}	referenced to $PA(CH_3NO_2)$ [a]	3
$\Delta H_f(C_2O)$	≤ 661 kJ mol^{-1}	from reaction $CCCN^+ + H_2O$	4
$\Delta H_f(C_3NO^+)$ [b]	≤ 1567 kJ mol^{-1}	from reaction $CCCN^+ + CO_2$	4
$\Delta H_f(HNC^+)$	≤ 1373 kJ mol^{-1}	from $HCN^+ + CO \rightarrow HNC^+ + CO$	5
PA(CN)	≥ 595 kJ mol^{-1}	from $HCN^+ + CO \rightarrow HNC^+ + CO$	5
$\Delta H_f(HNCN\cdot)$	≤ 471 kJ mol^{-1}	from reaction $HNC^+ + N_2O$	5
$\Delta H_f(C_5H_2N^+)$ [c]	≤ 1247 kJ mol^{-1}	from reaction $C_3H_3N^+ + C_2H_2$	6
$\Delta H_f(C_3H_2N\cdot)$ [d]	≤ 561 kJ mol^{-1}	from reaction $C_3H_3N^+ + NH_3$	6
$\Delta H_f(C_5H_4N^+)$ [d]	≤ 1177 kJ mol^{-1}	from reaction $HC_3NH^+ + CH_2CHCN$	6
$\Delta H_f(C_3O^+)$ [e]	≥ 1252 kJ mol^{-1}	from reaction $C_3O^+ + H_2O$	7
$\Delta H_f(C_3HO\cdot)$ [f]	≤ 299 kJ mol^{-1}	from reaction $C_3H_2O^+ + NH_3$	7
$\Delta H_f(C_4H_2O^+)$ [d]	≤ 1268 kJ mol^{-1}	from reaction $C_3O_2^+ + C_2H_2$	7
$\Delta H_f(C_5O^+)$ [g]	≤ 1203 kJ mol^{-1}	from reaction $C_3H_2O^+ + C_2H_2$	7
$\Delta H_f(C_5HO^+)$ [h]	≤ 985 kJ mol^{-1}	from reaction $C_3H_2O^+ + C_2H_2$	7
$\Delta H_f(C_5H_2O^+)$ [d]	≤ 1203 kJ mol^{-1}	from reaction $C_3H_2O^+ + C_2H_2$	7
$\Delta H_f(C_5H_3O^+)$ [d]	≤ 1012 kJ mol^{-1}	from reaction $C_3H_2O^+ + CH_3CCH$	7
$\Delta H_f(C_3HO_2^+)$ [i]	≤ 709 kJ mol^{-1}	from reaction $C_3O_2^+ + CH_4$	7
$PA(C_3O_2)$	≥ 727 kJ mol^{-1}	from reaction $C_3O_2^+ + CH_4$	7

Notes

a. assuming a ± 2 kJ mol^{-1} uncertainty in $PA(CH_3NO_2)$.
b. $NCCCO^+$ is the most probable structure of this ion.
c. $HCCCCCNH^+$ is the structure ascribed to this ion.
d. The structure of this species is not known.
e. $CCCO^+$ is the most probable structure of this ion.
f. HCCCO· is the structure ascribed to this species.
g. $CCCCCO^+$ is the structure ascribed to this ion.
h. $HCCCCCO^+$ is the structure ascribed to this ion.
i. $OCCCOH^+$ is the structure ascribed to this ion.

produced by the reaction of C^+ with C_2N_2, ~10% of the C_2N^+ produced is the higher-energy isomer. Production of CCN^+ from ground-state C^+ is endothermic, but can be accounted for if some fraction of the C^+ undergoing reaction is metastably excited.

In contrast to the observation that the higher-energy isomer of C_2N^+ is the more reactive form, extensive studies of C_3N^+ reactivity have established that the lowest-energy isomer ($CCCN^+$) is substantially more reactive than a higher-energy form (which we believe to be a cyclic isomer, in accordance with the theoretical and experimental study by Harland and Maclagan).[259] The most abundant form of C_3N^+ (which accounts for at least 90% of the C_3N^+ ion signal formed by electron impact upon HC_3N or upon C_4N_2) is seen to react much more rapidly with several neutral reagents than does a less abundant isomer. The most abundant isomer is $CCCN^+$ since this is the ion structure most likely to arise from electron impact upon HCCCN or NCCCCN. This isomer is the lowest-energy form of C_3N^+ according to Maclagan's calculations,[259] and according also to the observation that the predominant C_3N^+ ion formed by several chemical ionisation reactions (within the flow tube) has identical reactivity to $CCCN^+$: the C_3N^+ product of these chemical ionisation reactions is not constrained to have the $CCCN^+$ structure, and the fact that this isomer predominates for C_3N^+ formed in this fashion indicates that $CCCN^+$ is the lowest-energy isomer. The lack of reactivity of c-C_3N^+ is not completely understood, but indicates that there may be substantial activation energy barriers inhibiting many reactions of this ion.

CHN^+ produced by electron impact ionisation upon HCN produces HCN^+ and HNC^+ in a ratio of approximately 3:1. Many previous theoretical and experimental studies have demonstrated that HCN^+ is the higher-energy isomer: our studies of CHN^+ reactivity unearthed two reactions in which HCN^+ was converted to HNC^+, which we explain by a mechanism involving forth-and-back proton transfer. Isomerisation of HCN^+ to HNC^+ in this manner is expected to be the dominant product channel for all bimolecular reactions $HCN^+ + X$ for which $518 < PA(X) < 595$ kJ mol^{-1}, these limits representing the values for PA(C<u>N</u>) and PA(<u>C</u>N) respectively.

Isomerism was investigated in the CH_2N^+ system, but was not detected. The absence of any evidence of the higher-energy isomer, CNH_2^+, demonstrates either that none of the diagnostic reactions employed in this study succeed in distinguishing CNH_2^+ from $HCNH^+$, or that none of the ion generation techniques produce substantial amounts of CH_2N^+ in the CNH_2^+ form. An explanation for the possible failure of some diagnostic reactions is that they serve to isomerise CNH_2^+ to $HCNH^+$, by a forth-and-back mechanism such as was used to explain the isomerisation of HCN^+ to HNC^+. Further studies on this system will be required to resolve these issues.

Reactions of HCN^+ with CF_4, and $HCNH^+$ with CCl_4, exhibit product channels in apparent conflict with literature values for the heats of formation of reactants and products in these systems.[184] These observations can be rationalised (i) by the assumption that the literature values for the heats of formation of CF_3^+ and of CCl_3^+ are in error, (ii) by the assumption that these two reactions may represent 'entropy-driven' processes - that is, they are endothermic but exergonic,

or (iii) by the assumption that weakly-bound van der Waal's complexes are formed in these reactions, rather than the ionic and neutral products assigned in the present work. Further studies are required to determine which of these cases applies to each of these reactions.

The ions $C_3H_3N^+$ and $C_3H_4N^+$ derived from acrylonitrile were seen to have an interesting and varied ion-molecule chemistry in the laboratory. An equally varied chemistry in interstellar clouds is expected providing that both species are unreactive with H_2 as suggested by our SIFT studies: if this is so, then their reactions with trace cloud components will be of significance to models of interstellar chemistry.

Ion-molecule reactions of acrylonitrile were seen to produce HC_3NH^+ and HC_5NH^+, suggesting at least a tenuous link between the cloud chemistry of acrylonitrile and that of the cyanopolyynes. In this regard, several reactions of HC_3N^+ and HC_3NH^+ were also studied, with some parallels evident between the reactivity of HC_3N^+ and $C_3H_3N^+$, and between HC_3NH^+ and $C_3H_4N^+$. Production of protonated cyclopropenylidene in several reactions is also of interest for ion-molecule models of cloud chemistry.

Studies on the reactivity of the ions $C_3H_nO^+$ (n=1 to 3), undertaken as part of an investigation into the interstellar chemistry of ions related to C_3O and HC_3HO, indicated that these three ions are remarkably unreactive with the most abundant interstellar molecules. This observation supports the notion that dissociative recombination of these ions should provide an efficient source of tricarbon monoxide and propynal within dense interstellar clouds.

The rôle of translationally excited OH· (produced by dissociative recombination of H_3O^+ and $HOCO^+$) within dense interstellar clouds was evaluated, with results which can be extended to reactions of any translationally excited radicals within cold clouds. This translational energy is very inefficient in promoting chemical processes within cold interstellar clouds, because the chemically interesting fragments (i.e., those heavier than H· or H_2) of dissociative recombination reactions possess little of the total translational energy released by recombination. In addition, the centre-of-mass collision energy for collision of such a fragment with a cold H_2 molecule is very much less than the fragment's translational energy, and this collision energy is not likely to exceed the activation energy barrier for a radical-H_2 reaction. In consequence, the translational energy released by recombination of most positive ions is able only to be thermalised by collision. Possible exceptions to this rule are when the dissociative recombination yields two molecular fragments of comparable mass - for example, the production of OH· + CO from $HOCO^+ + e$. The dissociative recombination of $HOCO^+$ should thus have an effect on the production of H_2O in cold clouds, although this effect is likely to be slight when compared to the dominant H_2O production processes.

Reactions of the ions $C_3H_nN^+$ (n = 0 - 4) and $C_3H_nO^+$ (n = 0 - 3) were compared to the reactions of $C_4H_n^+$ (n = 0 -4) with H_2, CO, C_2H_2 and HCN. These studies showed that ions containing bare terminal carbon atoms were substantially more reactive than ions lacking bare terminal carbon atoms, in keeping with a model explaining such differences in reactivity by the presence of carbene character in ions featuring bare terminal C atoms. For the ion series $C_3H_nN^+$ and $C_3H_nO^+$,

radical ions were also found to be more reactive than non-radical ions, although this pattern of reactivity was not apparent in the reported reactions of $C_4H_n^+$.

Section 10.2: Suggestions for further work.

Modifications to the Canterbury SIFT in the near future should allow further exploration of many facets of the present work.

The first such modification, the inclusion of a drift region in the SIFT, will permit a more detailed study of energetics of several types of processes. Drift experiments could determine the barriers to isomerisation for the isomeric systems C_2N^+, C_3N^+ and CHN^+. Acceleration of the reactant ions by application of a voltage gradient should result in the internal partitioning of energy in the reactant ions sufficient to overcome such isomerisation barriers; two thresholds should be apparent. The first threshold arises when the higher-energy isomer possesses sufficient internal energy to isomerise, resulting in severe depletion of this higher-energy isomer; the second threshold arises when the lower-energy isomer has sufficient energy to isomerise, resulting in the production of an equilibrium in which the isomeric ratio reflects the density-of-states ratio at this barrier height. Care with such experiments would be necessary to ensure that the titration reaction used to identify the isomeric ratio is able to distinguish between the drift-accelerated isomers, whose reactivity will differ from that exhibited by the thermalised isomers.

Another application of the drift technique which should prove useful is in the examination of H-atom abstraction reactions from H_2. Brown et al[41] have postulated that such reactions are inhibited by a slight barrier, and many such reactions reported in the present work are observed to occur slowly if at all despite their exothermicity. An exploration of the energetic factors involved would help in the modelling of such reactions as they relate to the chemical evolution of interstellar clouds. Of the reactant ions studied in the present work, c-C_3N^+, HC_3N^+, HC_3NH^+, $C_3H_3N^+$, C_3HO^+, $C_3H_2O^+$, $C_3H_3O^+$, $C_3O_2^+$ and $C_4N_2^+$ were found to react very slowly (if at all) with H_2 at room temperature. A study of these reactions in a SIFDT apparatus is recommended. A study of these reactions at varying temperatures, especially below 300 K, should also prove helpful in examining the possible reactivity of these ions under interstellar conditions. The addition of a variable-temperature jacket, permitting the study of reactions over the temperature range 80 K - 550 K, is planned for the Canterbury SIFT.

Further examinations of the isomeric systems $CCCN^+$/ c-C_3N^+ and $HCNH^+/CNH_2^+$ are also recommended. It is desirable to find a source gas giving a sufficiently pure signal of c-C_3N^+ to permit determination of the product channels for reactions of this ion: as suggested in chapter 4, a cyclic compound such as azetidine may be a suitable source gas. Additional studies of the CH_2N^+ system may reveal the reactivity of the proposed interstellar ion CNH_2^+. Efforts in this direction should involve the study of further CH_2N^+ generating methods and diagnostic reactions.

SIFT study of the reactions of $C_4H_n^+$ (n = 0 - 4) with HCN and C_2H_2 is relevant to the comparison of $C_4H_n^+$, $C_3H_nN^+$ and $C_3H_nO^+$ reactivity outlined in chapter 9. These $C_4H_n^+$ reactions have only been studied using the ICR technique and thus product channels involving association, or rearrangement of partially stabilised collision complexes, might not have been apparent in these ICR studies.

Recent reports suggest that radical-molecule processes are a major source of interstellar nitriles such as acrylonitrile, but further work is necessary on such reactions to determine whether they do indeed lack activation energy barriers. Similarly, further experimental investigations, and refinement of theoretical treatments of such processes as dissociative recombination and radiative association, will reduce current uncertainties concerning the relationship between CH_2CHCN and the $C_3H_nN^+$ ions which can be generated from acrylonitrile.

Some preliminary efforts to study ion-atom reactions (of X^+ with $H\cdot$, O, $N\cdot$, and ultimately C) were made during the present work, using a microwave discharge to dissociate reactant molecules. The results of these studies were inconclusive and are therefore not presented here, but further studies of such ion-atom reactions would be of great significance in the modelling of interstellar chemistry, especially since neutrals such as $H\cdot$, O and C are expected to be relatively abundant within interstellar clouds. In particular, the reaction

$$H_3^+ + C \rightarrow CH^+ + H_2 \qquad (10.1)$$

$$\Delta H_{10.1} = -101 \text{ kJ mol}^{-1}$$

is very important in models of interstellar chemistry, since C is about as abundant as CO within some cloud regions.[409-411] This reaction, which is presumed to occur rapidly, is a major loss process for H_3^+ and an important step in the synthesis of the methyl ion CH_3^+: an experimental study of this reaction would be very valuable.

Studies of reactions of many ions with O would also be useful, since atomic oxygen is thought to be responsible for the destruction of several reactive species within interstellar clouds and as such may limit the developing molecular complexity.

A refinement of the dissociative technique employed for ion-atom reactions would also allow study of ion-radical reactions of interest in interstellar cloud modelling: the reactions of ions with radicals such as $CN\cdot$, $OH\cdot$, $CH_3\cdot$ and $C_2H\cdot$ have not been studied experimentally.

A study of the reaction of H_2 with $OH\cdot$ produced from dissociative recombination of $HOCO^+$ would assist in testing the hypothesis, presented in chapter 8, that such reactions may be of relevance to interstellar chemistry. Such verification is likely to be difficult, however, in view of the low efficiency predicted for the production of H_2O by reaction following $HOCO^+$ recombination, and SIFT studies are not likely to be of much assistance in this endeavour. Experiments using a FALP-LIF apparatus may be more helpful in this respect, as discussed in chapter 8.

REFERENCES.

1. Dyson J.E., Williams D.A.
"The Physics of the Interstellar Medium".
(Manchester University Press, Manchester. 1980).

2. Zeilik M., Smith E.v.P.
"Introductory Astronomy and Astrophysics".
(Saunders College Publishing, Philadelphia, 1987).

3. Smith D., Adams N.G.
J. Chem. Soc. Far. Trans. 2 **85** (1989) 1613
A brief review of interstellar ion chemistry.

4. Irvine W.M., Avery L.W., Friberg P., Matthews H.E., Ziurys L.M.
Astro. Lett. & Commun. **26** (1988) 167
Newly detected molecules in dense interstellar clouds.

5. Kroto H.W.
Phil. Trans. R. Soc. Lond. A **325** (1988) 405
The chemistry of the interstellar medium.

6. Grim R.J.A., Greenberg J.M.
Astrophys. J. **321** (1987) L91
Ions in grain mantles: the 4.62 micron absorption by OCN^- in W33A.

7. Saito S., Yamamoto S., Irvine W.M., Ziurys L.M., Suzuki H.,Ohishi M, Kaifu N.
Astrophys. J. **334** (1988) L113
Laboratory detection of a new interstellar free radical $CH_2CN(^2B_1)$.

8. Adams N.G., Smith D.
Contemp. Phys. **29** (1989) 559
Ionic reactions in atmospheric, interstellar and laboratory plasmas.

9. Dalgarno A.
New Scientist **126 no. 1722** (1990) 61
The molecules of outer space.

10. Dickman R.L., Snell R.L., Young J.S. (eds.)
"Molecular Clouds in the Milky Way and External Galaxies. Proceedings of a symposium held at the University of Massachusetts in Amherst, November 2-4, 1987".
Lecture Notes in Physics vol. **315**
(Springer-Verlag, Berlin Heidelberg. 1988.)

11. Herbst E.
in "Interstellar Processes", p. 611
Hollenbach D.J., Thronson H.A.,Jr. (eds).
(Reidel, Dordrecht, the Netherlands. 1987)
Gas phase chemical processes in molecular clouds.

12. Herbst E.
in "Rate Coefficients in Astrochemistry", p. 239
Millar T.J., Williams D.A. (eds).
(Kluwer Academic Publishers, Dordrecht, the Netherlands. 1988).
Dense interstellar cloud chemistry.

13. Herbst E.
Angew. Chem. Int. Ed. Engl. **29** (1990) 595
The chemistry of interstellar space.

14. Millar T.J., Williams D.A. (eds).
"Rate Coefficients in Astrochemistry (Proceedings of a conference held at UMIST, Manchester, U.K. September 21-24, 1987)"
(Kluwer Academic Publishers, Dordrecht, the Netherlands. 1988).

15. Newman A.R.
Analyt. Chem. **62** (1990) 671A
Molecular chemistry to the stars.

16. Smith D.
Phil. Trans. R. Soc. Lond. A **323** (1987) 269
Interstellar molecules.

17. Smith D.
Phil. Trans. R. Soc. Lond. A **324** (1988) 257
Formation and destruction of molecular ions in interstellar clouds.

18. Turner B.E.
Space Sci. Rev. **51** (1989) 235
Recent progress in astrochemistry.

19. Winnewisser G., Armstrong J.T. (eds)
"The Physics and Chemistry of Interstellar Molecular Clouds (mm and sub-mm observations in astrophysics)"
Lecture Notes in Physics vol. **331**.
(Springer-Verlag, Berlin Heidelberg. 1989).

20. Winnewisser G., Herbst E.
in "Organic Geo- and Cosmochemistry", p.119
Topics in Current Chemistry vol. **139**.
(Springer-Verlag, Berlin Heidelberg. 1987)
Organic molecules in space.

21. Black J.H.
Adv. At. Mol. Phys. **25** (1988) 477
The abundances and excitation of interstellar molecules.

22. Shu F.H., Lizano S.
Astrophys. Lett. & Commun. **26** (1988) 217
The evolution of molecular clouds.

23. Langer W.D., Graedel T.E.
Astrophys. J. Suppl. Ser. **69** (1989) 241
Ion-molecule chemistry of dense interstellar clouds: nitrogen-, oxygen-, and carbon-bearing molecule abundances and isotopic ratios.

24. Swade D.A.
Astrophys. J. **345** (1989) 828
The physics and chemistry of the L134N molecular core.

25. Bailey M.E., Williams D.A. (eds).
Dust in the Universe.
(Cambridge University Press, 1988).

26. Greenberg J.M., Zhao N., Hage J.
Ann. Phys. Fr. **14** (1989) 103
Chemical evolution of interstellar dust, comets and the origins of life.

27. Herbst E., Leung C.M.
Astrophys. J. Suppl. Ser. **69** (1989) 271
Gas-phase production of complex hydrocarbons, cyanopolyynes, and related compounds in dense interstellar clouds.

28. Williams D.A.
in "Rate Coefficients in Astrochemistry", p. 281
Millar T.J., Williams D.A. (eds).
(Kluwer Academic Publishers, Dordrecht, the Netherlands. 1988).
Dynamical models of the chemistry in interstellar clouds.

29. Bohme D.K.
in "Structure / Reactivity and Thermochemistry of Ions", p. 219
Ausloos P., Lias S.G. (eds).
(Reidel, Dordrecht, the Netherlands. 1987).
Growing molecules with ion/molecule reactions.

30. DePuy C.H.
Pure Appl. Chem. **61** (1989) 693
Interstellar organic chemistry and other applications of gas phase ion molecule chemistry.

31. Bates D.R., Herbst E.
in "Rate Coefficients in Astrochemistry", p. 17
Millar T.J., Williams D.A. (eds).
(Kluwer Academic Publishers, Dordrecht, the Netherlands. 1988).
Radiative association.

32. Smith I.W.M.
in "Rate Coefficients in Astrochemistry", p. 103
Millar T.J., Williams D.A. (eds).
(Kluwer Academic Publishers, Dordrecht, the Netherlands. 1988).
Experimental measurements of the rate constants for neutral-neutral reactions.

33. Brown P.D.
Mon. Not. Roy. Astron. Soc. **243** (1990) 65
The grain-surface formation of complex molecules.

34. Millar T.J.
Mon. Not. Roy. Astron. Soc. **199** (1982) 309
Dense cloud chemistry - 1. Direct and indirect effects of grain surface reactions.

35. Irvine W.M., Friberg P., Kaifu N., Kawaguchi K., Kitamura Y., Matthews H.E., Minh Y., Saito S., Ukita N., Yamamoto S.
Astrophys. J. **342** (1989) 871
Observations of some oxygen-containing and sulfur-containing organic molecules in cold dark clouds.

36. Nejad L.A.M., Williams D.A., Charnley S.B.
Mon. Not. Roy. Astron. Soc. **246** (1990) 183
Dynamical models of molecular clouds: nitrogen chemistry.

37. Pineau des Forêts G., Roueff E., Flower D.R.
Mon. Not. Roy. Astron. Soc. **244** (1990) 668
The formation of nitrogen-bearing species in dark interstellar clouds.

38. Turner B.E.
in "Physics and Chemistry of Small Clusters", p. 915
NATO ASI Ser, Ser. B Phys. vol. **158.**
Jena P., Rao BK., Khanna S.N. (eds). (Plenum Press, New York. 1987).
Current views on astrochemistry.

39. Turner B.E., Amano T., Feldman P.A.
Astrophys. J. **349** (1990) 376
Searches for the protonated interstellar species HC_3NH^+, CH_3CNH^+, and $HOCS^+$: implications for ion-molecule chemistry.

40. Amano T., Saito S., Yamamoto S., Kawaguchi K., Suzuki H., Ohishi M., Kaifu N.
Astrophys. J. **351** (1990) 500
Search for HC_3NH^+: the upper limit of the column density in TMC-1.

41. Brown R.D., Cragg D.M., Bettens R.P.A.
Mon. Not. Roy. Astron. Soc. **245** (1990) 623
Interstellar chemistry: hot ion reactions.

42. Herbst E., Leung C.M.
Astron. Astrophys. **233** (1990) 177
The gas phase production of CH_2CN and other organo-nitrogen species in dense interstellar clouds.

43. Howe D.A., Millar T.J.
Mon. Not. Roy. Astron. Soc. **244** (1990) 444
The formation of carbon chain molecules in IRC+ 10216.

44. Watson W.D.
Astrophys. J. **188** (1974) 35
Ion-molecule reactions, molecule formation, and hydrogen-isotope exchange in dense interstellar clouds.

45. Brown R.D., Rice E.
Phil. Trans. R. Soc. Lond. A **303** (1981) 523
Interstellar deuterium chemistry.

46. Henchman M.J., Paulson J.F., Smith D., Adams N.G., Lindinger W.
in "Rate Coefficients in Astrochemistry", p. 201
Millar T.J., Williams D.A. (eds).
(Kluwer Academic Publishers, Dordrecht, the Netherlands. 1988).
Chemical pathways for deuterium fractionation in interstellar molecules.

47. Brown P.D., Charnley S.B.
Mon. Not. Roy. Astron. Soc. **244** (1990) 432
Chemical models of interstellar gas-grain processes - I. Modelling and the effect of accretion on gas abundances and mantle composition in dense clouds.

48. Dalgarno A., Oppenheimer M., Berry R.S.
Astrophys. J. **183** (1973) L21
Chemiionisation in interstellar clouds.

49. Spitzer L., Jr., Tomasko M.G.
Astrophys. J. **152** (1968) 971
Heating of HI regions by energetic particles.

50. Solomon P.M., Werner M.W.
Astrophys. J. **165** (1971) 41
Low-energy cosmic rays and the abundance of atomic hydrogen in dark clouds.

51. MacGregor M., Berry R.S.
J. Phys. B: Atom. Molec. Phys. **6** (1973) 181
Formation of HCO^+ by the associative ionisation of CH + O.

52. Bates D.R.
Astrophys. J. **344** (1989) 531
Dissociative recombination of polyatomic ions: curve crossing.

53. Williams D.A.
Astrophys. Lett. **10** (1971) 17
Association reactions.

54. Herbst E.
Astrophys. J. **291** (1985) 226
An update of and suggested increase in calculated radiative association rate coefficients.

55. Herbst E., Adams N.G., McIntosh B.J., Smith D.
J. Chem. Soc. Far. Trans. 2 **85** (1989) 1655
Association reactions: theoretical shortcomings.

56. Barlow S.E., Dunn G.H., Schauer M.
Phys. Rev. Lett. **52** (1984) 902
Radiative association of CH_3^+ and H_2 at 13K.

57. Bates D.R.
Astrophys. J. **312** (1987) 363
Rate of $CH_3^+ + H_2 \rightarrow CH_5^+ + h\nu$ and role of electronic transitions in other radiative association processes.

58. Bates D.R.
Phys. Rev. A **34** (1987) 1878
Interpretation of the measured rate of radiative association of CH_3^+ and H_2.

59. Gerlich D., Kaefer G.
Astrophys. J. **347** (1989) 849
Ion trap studies of association processes in collisions of CH_3^+ and CD_3^+ with n-H_2, p-H_2, D_2, and He at 80 K.

60. Herbst E., McEwan M.J.
Astron. Astrophys. **229** (1990) 201
How efficient is radiative association between large species? The case of $CH_3^+ + CH_3CN$.

61. McEwan M.J., Anicich V.G., Huntress W.T., Jr., Kemper P.R., Bowers M.T.
Chem. Phys. Lett. **75** (1980) 278
A low pressure study of the reaction $CH_3^+ + HCN \rightarrow CH_3.HCN^+$. A case for radiative association.

62. McEwan M.J., Denison A.B., Anicich V.G., Huntress W.T., Jr.
Int. J. Mass Spectrom. Ion Proc. **81** (1987) 247
Association reactions at low pressure. 1. Collision-stabilized association below 1 micron.

63. McEwan M.J., Denison A.B., Huntress W.T., Jr., Anicich V.G., Snodgrass J., Bowers M.T.
J. Phys. Chem. **93** (1989) 4064
Association reactions at low pressure. 2. The CH_3^+ / CH_3CN system.

64. Sen A.D., Huntress W.T., Anicich V.G., McEwan M.J., Denison A.B.
J. Chem. Phys. (1990) Submitted.
Association reactions at low pressure. 4. The HC_3N^+/HC_3N system.

65. Smith S.C., McEwan M.J., Gilbert R.G.
J. Chem. Phys. **90** (1989) 1630
The pressure dependence of ion-molecule association rate coefficients.

66. Smith S.C., Wilson P.F., Sudkeow P., Maclagan R.G.A.R., McEwan M.J., Anicich V.G., Huntress W.T.
J. Chem. Phys. (1991) Submitted.
An RRKM model for competition between binary reactions and association in the CH_3^+/CH_3CN system.

67. Adams N.G., Smith D.
in "Rate Coefficients in Astrochemistry", p. 173
Millar T.J., Williams D.A. (eds).
(Kluwer Academic Publishers, Dordrecht, the Netherlands. 1988).
Laboratory studies of dissociative recombination and mutual neutralisation and their relevance to interstellar chemistry.

68. Bates D.R., Herbst E.
in "Rate Coefficients in Astrochemistry", p. 41
Millar T.J., Williams D.A. (eds).
(Kluwer Academic Publishers, Dordrecht, the Netherlands. 1988).
Dissociative recombination: polyatomic positive ion reactions with electrons and negative ions.

69. Herbst E.
Astrophys. J. **222** (1978) 508
What are the products of polyatomic ion-electron dissociative recombination reactions?

70. Mitchell J.B.A., Guberman S.L. (eds).
"Dissociative Recombination: Theory, Experiment and Applications".
(World Scientific, Singapore. 1989).

71. Oppenheimer M., Dalgarno A.
Astrophys. J. **192** (1974) 29
The fractional ionization in dense interstellar clouds.

72. Bardsley J.N., Biondi M.A.
Adv. At. Mol. Phys. **6** (1970) 1
Dissociative recombination.

73. Adams N.G., Smith D., Alge E.
J. Chem. Phys. **81** (1984) 1778
Measurement of dissociative recombination coefficients of H_3^+, HCO^+, N_2H^+, and CH_5^+ at 95 and 300 K using the FALP apparatus.

74. Mul P.M., McGowan J.W.
Astrophys. J. **237** (1980) 749
Dissociative recombination of C_2^+, C_2H^+,$C_2H_2^+$ and $C_2H_3^+$.

75. Amano T.
J. Chem. Phys. **92** (1990) 6492
The dissociative recombination rate coefficients of H_3^+, HN_2^+, and HCO^+.

76. Leu M.T., Biondi M.A., Johnsen R.
Phys. Rev. A **8** (1973) 413
Measurement of recombination of electrons with H_3^+ and H_5^+ ions.

77. Macdonald J.A., Biondi M.A., Johnsen R.
Planet. Space Sci. **32** (1984) 651
Recombination of electrons with H_3^+ and H_5^+ ions.

78. Auerbach D., Cacak R., Caudano R., Gaily T.D., Keyser C.J., McGowan J.W., Mitchell J.B.A., Wilk S.F.J.
J. Phys. B **10** (1977) 3797
Merged electron-ion beam experiments. I. Method and measurements of (e - H_2^+) and (e - H_3^+) dissociative-recombination cross sections.

79. McGowan J.W., Mul P.M., D'Angelo V.S., Mitchell J.B.A., Defrance P., Froelich H.R.
Phys. Rev. Lett. **42** (1979) 373
Energy dependence of dissociative recombination below 0.08 eV measured with (electron-ion) merged beam technique.

80. Black J.H., van Dishoeck E.F., Willner S.P., Woods R.C.
Astrophys. J. **358** (1990) 459
Interstellar abundance lines toward NGC 2264 and AFGL 2591: abundances of H_2, H_3^+, and CO.

81. Marquette J.B., Rebrion C., Rowe B.R.
Astron. Astrophys. **213** (1989) L29
Proton transfer reactions of H_3^+ with molecular neutrals at 30 K.

82. Bates D.R.
Astrophys. J. **306** (1986) L45
Products of dissociative recombination of polyatomic ions.

83. Green S., Herbst E.
Astrophys. J. **229** (1979) 121
Metastable isomers: a new class of interstellar molecules.

84. Adams N.G., Herd C.R., Smith D.
J.Chem. Phys. **91** (1989) 963
Development of the flowing afterglow / Langmuir probe technique for studying the neutral products of dissociative recombination using spectroscopic techniques: OH production in the $HCO_2^+ + e$ reaction.

85. Herd C.R., Adams N.G., Smith D.
Astrophys. J. **349** (1990) 388
OH production in the dissociative recombination of H_3O^+, HCO_2^+, and N_2OH^+: comparison with theory and interstellar implications.

86. Adams N.G., Smith D., Millar T.J.
Mon. Not. Roy. Astron. Soc. **211** (1984) 857
The importance of kinetically excited ions in the synthesis of interstellar molecules.

87. Luine J.A., Dunn G.H.
Astrophys. J. **299** (1985) L67
Ion-molecule reaction probabilities near 10K.

88. Lepp S., Dalgarno A.
Astrophys. J. **324** (1988) 553
Polycyclic aromatic hydrocarbons in interstellar chemistry.

89. Omont A.
Astron. Astrophys. **164** (1986) 159
Physics and chemistry of interstellar polycyclic aromatic molecules.

90. Cravath A.M.
Phys. Rev. **36** (1930) 248
The rate at which ions lose energy in elastic collisions.

91. Sternberg A., Dalgarno A., Lepp S.
Astrophys. J. **320** (1987) 676
Cosmic-ray induced photodestruction of interstellar molecules in dense clouds.

92. Aannestad P.A.
Astrophys. J. Suppl. Ser. **25** (1973) 223
Molecule formation. II. In interstellar shock waves.

93. Flower D.R.
J. Phys. B. **22** (1989) 2319
Atomic and molecular processes in interstellar shocks.

94. Flower D.R., Heck L., Pineau des Forêts G.
Mon. Not. Roy. Astron. Soc. **239** (1989) 741
Theoretical studies of interstellar molecular shocks - IX. The influence of PAH molecules on the ratio C / CO in dark clouds.

95. Graff M.M., Dalgarno A.
Astrophys. J. **317** (1987) 432
Oxygen chemistry of shocked interstellar clouds. II. Effects of nonthermal internal energy on chemical evolution.

96. Iglesias E.R., Silk J.
Astrophys. J. **226** (1978) 851
Nonequilibrium chemistry in shocked molecular clouds.

97. Leen T.M., Graff M.M.
Astrophys. J. **325** (1988) 411
Oxygen chemistry of shocked interstellar clouds. III. Sulfur and oxygen species in dense clouds.

98. Wagner A.F., Graff M.M.
Astrophys. J. **317** (1987) 423
Oxygen chemistry of shocked interstellar clouds. I. Rate constants for thermal and nonthermal internal energy distributions.

99. Jura M., Kroto H.
Astrophys. J. **351** (1990) 222
Dust around AFGL 2688, molecular shielding, and the production of carbon chain molecules.

100. Nejad L.A.M., Millar T.J.
Astron. Astrophys. **183** (1987) 279
Chemical modelling of molecular sources. V. IRC+10216.

101. Nejad L.A.M., Millar T.J.
Mon. Not. Roy. Astron. Soc. **230** (1988) 79
Chemical modelling of molecular sources - VI. Carbon-bearing molecules in oxygen-rich circumstellar envelopes.

102. Wlodek S., Bohme D.K.
J. Am. Chem. Soc. **110** (1988) 2396
Gas-phase reactions of Si^+ with ammonia and the amines $(CH_3)_xNH_{3-x}$ (x = 1-3): possible ion-molecule reaction pathways toward SiH, SiCH, SiNH, $SiCH_3$, $SiNCH_3$, and H_2SiNH.

103. Wlodek S., Bohme D.K.
J. Am. Chem. Soc. **111** (1989) 61
Gas phase reactions of Si^+ (^2P) with hydrogen cyanide, acetonitrile, cyanogen, and cyanoacetylene - comparisons with reactions of C^+ (^2P).

104. Wlodek S., Bohme D.K., Herbst E.
Mon. Not. Roy. Astron. Soc. **242** (1990) 674
The reaction between Si^+ and H_2O. Interstellar implications.

105. Wlodek S., Rodriquez C.F., Lien M.H., Hopkinson A.C., Bohme D.K.
Chem. Phys. Lett. **143** (1988) 385
The proton affinity of SiNH and its formation from $SiNH_2^+$ in the gas phase.

106. Bohme D.K.
Int. J. Mass Spec. Ion Proc. **100** (1990) 719
Chemistry initiated by atomic silicon ions in the gas phase: formation of silicon-bearing ions and molecules.

107. Flores J.R., Largo-Cabrerizo J.
Chem. Phys. Lett. **142** (1987) 159
A comparative ab initio study of the H_2SiN^+ and H_2CN^+.

108. Flores J.R., Largo-Cabrerizo J.
J. Molec. Struct. (Theochem) **183** (1989) 17
The $(SiNH_2)^+$ isomers as intermediates in the interstellar production of SiNH: an ab initio study.

109. Herbst E., Millar T.J., Wlodek S., Bohme D.K.
Astron. Astrophys. **222** (1989) 205
The chemistry of silicon in dense interstellar clouds.

110. Langer W.D., Glassgold A.E.
Astrophys. J. **352** (1990) 123
Silicon chemistry in interstellar clouds.

111. Maclagan R.G.A.R.
J. Phys. Chem. **94** (1990) 3373
A theoretical study of the proton affinities of some phosphorus compounds.

112. Smith D., McIntosh B.J., Adams N.G.
J. Chem. Phys. **90** (1989) 6213
A selected ion flow tube study of the reactions of the PH_n^+ ions (n = 0 to 4) with several molecular gases at 300 K.

113. Adams N.G., McIntosh B.J., Smith D.
Astron. Astrophys. **232** (1990) 443
Production of phosphorus-containing molecules in interstellar clouds.

114. Matthews H.E., MacLeod J.M., Broten N.W., Madden S.C., Friberg P.
Astrophys. J. **315** (1987) 646
Observations of OCS and a search for OC_3S in the interstellar medium.

115. Millar T.J., Herbst E.
Astron. Astrophys. **231** (1990) 466
Organo-sulphur chemistry in dense interstellar clouds.

116. Minh Y.C., Ziurys L.M., Irvine W.M., McGonagle D.
Astrophys. J. **360** (1990) 136
Observations of H_2S toward OMC-1.

117. Muramaki A.
Astrophys. J. **357** (1990) 288
A quantum chemical study on the linear C_2S and C_3S molecules.

118. Peeso D.J., Ewing D.W., Curtis T.T.
Chem. Phys. Lett. **166** (1990) 307
A theoretical study of C_2S and C_3S.

119. Balm S.P., Kroto H.W.
Mon. Not. Roy. Astron. Soc. **245** (1990) 193
Possible assignment of the 11.3 μm UIR feature to emission from carbonaceous microparticles with internal hydrogens.

120. Cossart-Magos C., Leach S.
Astron. Astrophys. **233** (1990) 559
Polycyclic aromatic hydrocarbons as carriers of the diffuse interstellar bands: rotational band contour tests.

121. Duley W.W., Jones A.P.
Astrophys. J. **351** (1990) L49
Simple linear polycyclic aromatic hydrocarbon molecules and infrared emission features: mothballs in the Orion Ridge?

122. Kroto H.W.
Ann. Phys. Fr. **14** (1989) 169
The role of linear and spheroïdal carbon molecules in interstellar grain formation.

123. Léger A., d'Hendecourt L.
Ann. Phys. Fr. **14** (1989) 181
Large aromatic molecules in the interstellar medium.

124. Somerville W.B., Bellis J.G.
Mon. Not. Roy. Astron. Soc. **240** (1989) 41P
An astronomical search for the molecule C_{60}.

125. Farrar J.M., Saunders W.H., Jr. (eds).
"Techniques for the Study of Ion-Molecule Reactions",
Techniques of Chemistry vol. **XX**.
(Wiley-Interscience, New York. 1988).

126. Kemper P.R., Bowers M.T.
in "Techniques for the Study of Ion-Molecule Reactions", p. 1.
Techniques of Chemistry vol. **XX**.
Farrar J.M., Saunders W.H., Jr. (eds).
(Wiley-Interscience, New York. 1988).
Ion cyclotron resonance spectrometry.

127. Rowe B.R.
in "Rate Coefficients in Astrochemistry", p. 135
Millar T.J., Williams D.A. (eds).
(Kluwer Academic Publishers, Dordrecht, the Netherlands. 1988).
Studies of ion-molecule reactions at $T < 80$ K.

128. Rowe B.R., Marquette J.B.
Int. J. Mass Spectrom. Ion Proc. **80** (1987) 239
CRESU studies of ion-molecule reactions.

129. Rowe B.R., Marquette J.-B., Rebrion C.
J. Chem. Soc. Far. Trans. 2 **85** (1989) 1631
Mass-selected ion-molecule reactions at very low temperatures. The CRESUS apparatus.

130. Smith D., Adams N.G., Miller T.M.
J. Chem. Phys. **69** (1978) 308
A laboratory study of the reactions of N^+, N_2^+, N_3^+, N_4^+, O^+, O_2^+, and NO^+ ions with several molecules at 300 K.

131. Hawley M., Mazely T.L., Randeniya L.K., Smith R.S., Zeng X.K., Smith M.A.
Int. J. Mass Spectrom. Ion Proc. **97** (1990) 55
A free jet flow reactor for ion/molecule reaction studies at very low energies.

132. Randeniya L.K., Smith M.A.
J. Phys. Chem. **94** (1990) 5205
Temperature dependence of the atomic three-body association reaction $Ar^+ + 2Ar \rightarrow Ar_2^+ + Ar$ below 3K.

133. Schauer M.M., Jefferts S.R., Barlow S.E., Dunn G.H.
J. Chem. Phys. **91** (1989) 4593
Reactions of H_2 with He^+ at temperatures below 40K.

134. Ferguson E.E., Fehsenfeld F.C., Dunkin D.B., Schmeltekopf A.L., Schiff H.I.
Planet. Space Sci. **12** (1964) 1169
Laboratory studies of helium ion loss processes of interest in the ionosphere.

135. Ferguson E.E., Fehsenfeld F.C., Schmeltekopf A.L.
Adv. At. Mol. Phys. **5** (1969) 1
Flowing afterglow measurements of ion-neutral reactions.

136. Schmeltekopf A.L., Broida H.P.
J. Chem. Phys. **39** (1963) 1261
Short-duration visible afterglow in helium.

137. Fehsenfeld F.C., Schmeltekopf A.L., Goldan P.D., Schiff H.I., Ferguson E.E.
J. Chem. Phys. **44** (1966) 4087
Thermal energy ion-neutral reaction rates. I. Some reactions of helium ions.

138. Graul S.T., Squires R.R.
Mass Spectrom. Rev. **7** (1988) 263
Advances in flow reactor techniques for the study of gas-phase ion chemistry.

139. Smith D., Adams N.G.
Adv. At. Mol. Phys. **24** (1988) 1
The selected ion flow tube (SIFT): studies of ion-neutral reactions.

140. Ferguson E.E.
Adv. At. Mol. Phys. **25** (1989) 61
Flow tube studies of ion-molecule reactions.

141. Smith D., Adams N.G.
in "Gas Phase Ion Chemistry", vol. **1** p. 1.
Bowers M.T. (ed).
(Academic Press, New York. 1979).
Recent advances in flow tubes: measurement of ion-molecule rate coefficients and product distributions.

142. Ferguson E.E.
in *NATO ASI Series, Series C* **193** (1987). p. 81
"Structure / Reactivity and Thermochemistry of Ions".
Ausloos P., Lias S.G. (eds).
Production, quenching and reaction of vibrationally excited ions in collisions with neutrals in drift tubes.

143. Adams N.G., Smith D.
Int. J. Mass Spectrom. Ion Phys. **21** (1976) 349
The selected ion flow tube (SIFT); a technique for studying ion-neutral reactions.

144. Dunkin D.B., Fehsenfeld F.C., Schmeltekopf A.L., Ferguson E.E.
J. Chem. Phys. **49** (1968) 1365
Ion-molecule reaction studies from 300° to 600°K in a temperature-controlled flowing afterglow system.

145. McFarland M., Albritton D.L., Fehsenfeld F.C., Ferguson E.E., Schmeltekopf A.L.
J. Chem. Phys. **59** (1973) 6610
Flow-drift technique for ion mobility and ion-molecule reaction rate constant measurements. I. Apparatus and mobility measurements.

146. Howorka F., Dotan I., Fehsenfeld F.C., Albritton D.L.
J. Chem. Phys. **73** (1980) 758
Kinetic energy dependence of the branching ratios of the reaction of N^+ ions with O_2.

147. Smith D., Adams N.G., Alge E.
Chem. Phys. Lett. **105** (1984) 317
Further studies of the $N_2^+ + N_2 \rightarrow N_4^+$ association reaction.

148. Clary D.C.
Mol. Phys. **54** (1985) 605
Calculations of rate constants for ion-molecule reactions using a combined capture and centrifugal sudden approximation.

149. Clary D.C., Smith D., Adams N.G.
Chem. Phys. Lett. **119** (1985) 320
Temperature dependence of rate coefficients for reactions of ions with dipolar molecules.

150. Herbst E., Leung C.M.
Astrophys. J. **310** (1986) 378
Effects of large rate coefficients for ion-polar neutral reactions on chemical models of dense interstellar clouds.

151. Smith D., Adams N.G.
in "Swarms of Ions and Electrons in Gases", p. 284.
Lindinger W., Märk T.D., Howorka F. (eds.)
(Springer-Verlag, Wien / New York. 1984)
Studies of plasma reaction processes using a flowing-afterglow / Langmuir probe apparatus.

152. Smith D., Adams N.G., Dean A.G., Church M.J.
J. Phys. D: Appl. Phys **8** (1975) 141
The application of Langmuir probes to the study of flowing afterglow plasmas.

153. Mott-Smith H.M., Langmuir I.
Phys. Rev. **28** (1926) 727
The theory of collectors in gaseous discharges.

154. Smith D., Adams N.G.
J. Chem. Soc. Far. Trans. 2 **83** (1987) 149
Ionic reactions in thermal plasmas.

155. Hamilton C.E., Duncan M.A., Zwier T.S., Weisshaar J.C., Ellison G.B., Bierbaum V.M., Leone S.R.
Chem. Phys. Lett. **94** (1983) 4
Product vibrational analysis of ion-molecule reactions by laser-induced fluorescence in a flowing afterglow: $O^- + HF \rightarrow OH\ (v = 0,1) + F^-$.

156. Jones M.E., Ellison G.B.
J. Am. Chem. Soc. **111** (1989) 1645
A gas-phase E2 reaction: methoxide ion and bromopropane.

157. Marinelli W.J., Morton T.H.
J. Am. Chem. Soc. **100** (1978) 3536
Neutral products from deprotonation of tertiary cations in the gas phase.

158. Smith M.A., Barkley R.M., Ellison G.B.
J. Am. Chem. Soc. **102** (1980) 6851
Neutral products of ion-molecule reactions.

159. Upschulte B.L., Shul R.J., Passarella R., Keesee R.G., Castleman A.W., Jr.
Int. J. Mass. Spec. Ion Proc. **75** (1987) 27
Diagnostics of flow tube techniques for ion / molecule reactions.

160. Adams N.G., Church M.J., Smith D.
J. Phys. D. **8** (1975) 1409
An experimental and theoretical investigation of the dynamics of a flowing afterglow plasma.

161. Bolden R.C., Hemsworth R.S., Shaw M.J., Twiddy N.D.
J. Phys. B. **3** (1970) 45
Measurement of thermal-energy ion-neutral reaction rate coefficients for rare-gas ions.

162. Glosik J., Raksit A.B., Lister D.G., Twiddy N.D., Adams N.G., Smith D.
J. Phys. B. **11** (1978) 3365
Measurement of the rates of reaction of the ground and metastable excited states of O_2^+, NO^+ and O^+ with atmospheric gases at thermal energy.

163. Upschulte B.L., Shul R.J., Passarella R., Keesee R.G., Castleman A.W., Jr.
Int. J. Mass. Spec. Ion Proc. **85** (1988) 277
Curvature in the plots for the determination of rate constants derived from fast-flow techniques.

164. Harland P.W., Kim N.D., Petrie S.A.H.
Aust. J. Chem. **42** (1989) 9
Kinetic and electron impact studies of the HCO+ / COH+ isomers.

165. DeFrees D.J.
in "Astrochemistry",
(120th Symposium of the International Astronomical Union, 1985).
Theoretical studies of interstellar isomers.

166. Knight J.S.
"Selected Ion Flow Tube Studies of some Gaseous Ion-Molecule Reactions"
(Ph. D. thesis, University of Canterbury, New Zealand. 1986)

167. Knight J.S., Freeman C.G., McEwan M.J., Adams N.G., Smith D.
Int. J. Mass Spectrom. Ion Proc. **67** (1985) 317
Selected-ion flow tube studies of HC_3N.

168. Dahl D.A., Delmore J.E.
SIMION PC/PS2 version 3.1.

169. McGilvery D.C.
Ph.D. Thesis, LaTrobe University, 1978

170. See appendix 1.

171. Knight J.S.
EXPON, adapted from HSFITTEM(SIMPLEX), Stock H.S., Harland P.W.

172. Su T., Chesnavich W.J.
J. Chem. Phys. **76** (1982) 5183
Parametrization of the ion - polar molecule collision rate constant by trajectory calculations.

173. Stock H.M.P.
J. Phys. B. **6** (1973) L86
A note on the theory of the flowing afterglow.

174. Farragher A.L.
Trans. Far. Soc. **66** (1970) 1411
Ion-molecule reaction rate studies in a flowing afterglow system.

175. Melville H.W., Gowenlock B.G.
"Experimental Methods in Gas Reactions".
(Macmillan & Co, London. 1964).

176. Miller F.A., Fateley W.G.
Spectrochim. Acta **20** (1964) 253
The infrared spectrum of carbon suboxide.

177. Kim H.H., Roebber J.L.
J. Chem. Phys. **44** (1966) 1709
Vacuum-ultraviolet absorption spectrum of carbon suboxide.

178. Durrant M.C., Kroto H.W., McNaughton D., Nixon J.F.
J. Mol. Spectrosc. **109** (1985) 8
The new molecule 1-cyano-4-phosphabutadiyne, N≡C–C≡C–C≡P, produced by copyrolysis of PCl_3 and $CH_3C{\equiv}C{-}C{\equiv}N$: detection and vibration-rotation analysis by microwave spectroscopy.

179. Khanna R.K., Perera-Jarmer M.A., Ospina M.J.
Spectrochim. Acta **43A** (1987) 421
Vibrational infrared and Raman spectra of dicyanoacetylene.

180. Cohen S., Cohen S.G.
J. Am. Chem. Soc. **88** (1966) 1533
Preparation and reactions of derivatives of squaric acid. Alkoxy-, hydroxy- and aminocyclobutenediones.

181. Brandsma L.
"Preparative Acetylenic Chemistry"
Studies in Organic Chemistry vol. **34**
(Elsevier, Amsterdam. 1988)

182. Anicich V.G., Huntress W.T., Jr.
Astrophys. J. Suppl. Ser. **62** (1986) 553
A survey of bimolecular ion-molecule reactions for use in modeling the chemistry of planetary atmospheres, cometary comae and interstellar clouds.

183. Ikezoe Y., Matsuoka S., Takabe M., Viggiano A.
"Gas Phase Ion-Molecule Reaction Rate Constants Through 1986".
(Ion Reaction Research Group of the Mass Spectroscopy Society of Japan. 1986).

184. Lias S.G., Bartmess J.E., Liebman J.F., Holmes J.L., Levin R.D., Mallard W.G.
J. Phys. Chem. Ref. Data **17** (1988) supplement no. 1
"Gas-Phase Ion and Neutral Thermochemistry".

185. Lias S.G., Liebman J.F., Levin R.D.
J. Phys. Chem. Ref. Data **13** (1984) 695
Estimated gas phase basicities and proton affinities of molecules; heats of formation of protonated molecules.

186. Weast R.C., Astle M.J., Beyer W.H. (eds).
"C.R.C. Handbook of Chemistry and Physics", vol. **64**
(C.R.C. Press, Boca Raton, Florida. 1983).

187. Atkins P.W.
"Physical Chemistry", 2nd edition.
(Oxford University Press, 1978)

188. Hirschfelder J.O., Curtiss C.F., Bird R.D.
"Molecular Theory of Gases and Liquids".
(Wiley & Sons, New York. 1954)

189. Meot-Ner (Mautner) M., Tsang W.
J. Am. Chem. Soc. **112** (1991) submitted.
Entropy-driven proton transfer reactions.

190. Wright L.G., McLuckey S.A., Cooks R.G., Wood K.V.
Int. J. Mass Spectrom. Ion Phys. **42** (1982) 115
Relative gas-phase acidities from triple quadrupole mass spectrometers.

191. Botschwina P., Sebald P.
Chem. Phys. **141** (1990) 311
Calculated spectroscopic properties for NCCN, CNCN, CNNC and $HNCCN^+$.

192. Gerry M.C.L., Stroh F., Winnewisser M.
J. Mol. Spectrosc. **140** (1990) 147
The microwave Fourier transform, millimeter-wave, and submillimeter-wave rotational spectra of isocyanogen, CNCN.

193. Crovisier J.
Astron. J. **90** (1985) 670
Searching for cometary parent molecules at radio wavelengths.

194. Kunde V.G., Aikin A.C., Hanel R.A., Jennings D.E., Maguire W.C., Samuelson R.E.
Nature **292** (1981) 686
C_4H_2, HC_3N and C_2N_2 in Titan's atmosphere.

195. Li X., Sayah N., Jackson W.M.
J. Chem. Phys. **81** (1984) 833
Laser measurements of the effects of vibrational energy on the reactions of CN.

196. Halpern J.B., Miller G.E., Okabe H.
Chem. Phys. Lett. **155** (1989) 347
The reaction of CN radicals with cyanoacetylene.

197. Baer T.
J. Am. Chem. Soc. **102** (1980) 2482
Gas-phase heats of formation of $C_2H_5^+$ and $C_3H_7^+$.

198. Rosenstock H.M., Buff R., Ferreira M.A.A., Lias S.G., Parr A.C., Stockbauer R.L., Holmes J.L.
J. Am. Chem. Soc. **104** (1982) 2337
Fragmentation mechanism and energetics of some alkyl halide ions.

199. Bohme D.K., Mackay G.I.
J. Am. Chem. Soc. **103** (1981) 2173
Gas-phase proton affinities for H_2O, C_2H_4, and C_2H_6.

200. Collyer S.M., McMahon T.B.
J. Phys. Chem. **87** (1983) 909
Proton affinity of water. A scale of gas-phase basicities including ethylene and water from ion cyclotron resonance proton transfer equilibrium measurements.

201. Corderman R.R., Beauchamp J.L.
Inorg. Chem. **17** (1978) 1585
Properties and reactions of phosphorus trifluoride in the gas phase by ion cyclotron resonance spectroscopy. Energetics of formation of PF_2^+, PF_4^+, HPF_3^+, and $CH_3PF_3^+$.

202. Beauchamp J.L., Holtz D., Woodgate S.D., Patt S.L.
J. Am. Chem. Soc. **94** (1972) 2798
Thermochemical properties and ion-molecule reactions of the alkyl halides in the gas phase by ion cyclotron resonance spectroscopy.

203. Petrie S.A.H., Freeman C.G., McEwan M.J., Meot-Ner (Mautner) M.
Int. J. Mass Spectrom. Ion Proc. **90** (1989) 241
The proton affinity of cyanogen and ion / molecule reactions of $C_2N_2^+$.

204. Deakyne C.A., Meot-Ner (Mautner) M., Buckley T.J., Metz R.
J. Chem. Phys. **86** (1987) 2334
Proton affinities of diacetylene, cyanoacetylene, and cyanogen.

205. Raksit A.B., Bohme D.K.
Int. J. Mass Spectrom. Ion Proc. **57** (1984) 211
Selected-ion flow tube methods applied to the bracketing of proton affinities. PA(C_2N_2) and PA(HC_3N).

206. Freeman C.G., Knight J.S., Love J.G., McEwan M.J.
Int. J. Mass Spectrom. Ion Proc. **80** (1987) 255
The reactivity of HOC^+ and the proton affinity of CO at O.

207. McEwan M.J., unpublished results.

208. Kim J.K., Anicich V.G., Huntress W.T., Jr.
J. Phys. Chem. **81** (1977) 1798
Product distributions and rate constants for the reactions of CH_3^+, CH_4^+, $C_2H_2^+$, $C_2H_3^+$, $C_2H_4^+$, $C_2H_5^+$, and $C_2H_6^+$ ions with CH_4, C_2H_2, C_2H_4, and C_2H_6.

209. Warneck P.
Ber. Bunsenges. Phys. Chem. **76** (1972) 428
Investigations of ion reactions using photoionization mass spectrometry. VI. Reactions in acetylene, ethylene, methane, and their mixtures.

210. Miasek P.G., Beauchamp J.L.
Int. J. Mass Spectrom. Ion Phys. **15** (1974) 49
A novel trapped-ion mass spectrometer for the study of ion-molecule reactions.

211. Fiaux A., Smith D.L., Futrell J.H.
Int. J. Mass Spectrom. Ion Phys. **25** (1977) 281
Ion-molecule reactions of CH_3^+, $C_2H_5^+$, $C_3H_5^+$ and $C_3H_7^+$ with unsaturated C_2, C_3 and C_4 hydrocarbons.

212. Lischka H., Köhler H.-J.
J. Am. Chem. Soc. **100** (1978) 5297
Structure and stability of the carbocations $C_2H_3^+$ and $C_2H_4X^+$, X = H, F, Cl, and CH_3. Ab initio investigation including electron correlation and a comparison with MINDO/3 results.

213. Dheandanoo S., Forte L., Fox A., Bohme D.K.
Can. J. Chem. **64** (1986) 641
Ion-molecule reactions with carbon chain molecules: reactions with diacetylene and the diacetylene cation.

214. Raksit A.B., Bohme D.K.
Can. J. Chem. **63** (1985) 854
Flow tube studies of reactions of selected ions with cyanoacetylene.

215. Freeman C.G., Harland P.W., McEwan M.J.
Chem. Phys. Lett. **64** (1979) 596
Thermal energy charge transfer reactions of acetone and biacetyl.

216. Freeman C.G., Harland P.W., McEwan M.J.
Chem. Phys. Lett. **66** (1979) 607
Thermal energy charge transfer reactions of acetone and biacetyl: errata.

217. Warnatz J., Bockhorn H., Moeser A., Wenz H.W.
in "19th Symposium (International) on Combustion", p. 197
(The Combustion Institute, Pittsburgh, Pa. 1982)
Experimental investigations and computational simulations of acetylene-oxygen flames from near stoichiometric to sooting conditions.

218. Keil D.G., Gill R.J., Olson D., Calcote H.F.
in "The Chemistry of Combustion Processes", p. 33
A.C.S. Symposium Series, vol. **249**
Sloane T.M. (ed.)
(American Chemical Society, Washington D.C. 1984)
Ion concentrations in premixed acetylene-oxygen flames near the soot threshold.

219. Raulin F.
Adv. Space Res. **7(5)** (1987) 71
Organic chemistry in the oceans of Titan.

220. Jones T.D., Lewis J.S.
Icarus **72** (1987) 381
Estimated impact shock production of N_2 and organic compounds on early Titan.

221. Pollack J.B., Rages K., Pope S.K., Tomasko M.G., Romani P.N.,Atreya S.K.
J. Geophys. Res. A **92** (1987) 15037
Nature for the stratospheric haze on Uranus: evidence for condensed hydrocarbons.

222. Romani P.N., Atreya S.K.
Icarus **74** (1988) 424
Methane photochemistry and haze production on Neptune.

223. MacLeod J.M., Avery L.W., Broten N.W.
Astrophys. J. **282** (1984) L89
The detection of interstellar methyldiacetylene (CH_3C_4H).

224. Herbst E.
Astrophys. J. Suppl. Ser. **53** (1983) 41
Ion-molecule syntheses of interstellar molecular hydrocarbons through C_4H: toward molecular complexity.

225. Anicich V.G., Huntress W.T., Jr., McEwan M.J.
J. Phys. Chem. **90** (1986) 2446
Ion-molecule reactions of hydrocarbon ions in C_2H_2 and HCN.

226. Giles K., Adams N.G., Smith D.
Int. J. Mass Spectrom. Ion Proc. **89** (1989) 303
A study of reactions of $C_nH_m^+$ ions (n = 4,5,6; m = 0 - 6) with H_2 and CO at 300 K and 80 K.

227. Knight J.S., Freeman C.G., McEwan M.J., Anicich V.G., Huntress W.T., Jr.
J. Phys. Chem. **91** (1987) 3899
A flow tube study of ion-molecule reactions of acetylene.

228. Anicich V.G., Blake G.A., Kim J.K., McEwan M.J., Huntress W.T., Jr.
J. Phys. Chem. **88** (1984) 4608
Ion-molecule reactions in unsaturated hydrocarbons: allene, propyne, diacetylene, and vinylacetylene.

229. Mackay G.I., Bohme D.K.
Int. J. Mass Spectrom. Ion Phys. **26** (1978) 327
Proton-transfer reactions in nitromethane at 297K.

230. Lias S.G., Shold D.M., Ausloos P.
J. Am. Chem. Soc. **102** (1980) 2540
Proton-transfer reactions involving alkyl ions and alkenes. Rate constants, isomerization processes, and the derivation of thermochemical data.

231. McAllister T., Pitman P.
Int. J. Mass Spectrom. Ion Phys. **19** (1976) 241
Ion-molecule reactions and proton affinities of methyl nitrite and nitromethane.

232. Staley R.H., Kleckner J.E., Beauchamp J.L.
J. Am. Chem. Soc. **98** (1976) 2081
Relationship between orbital ionization energies and molecular properties. Proton affinities and photoelectron spectra of nitriles.

233. Petrie S., Knight J.S., Freeman C.G., Maclagan R.G.A.R.,McEwan M.J., Sudkeaw P.
Int. J. Mass Spectrom. Ion Proc. (1991) In press.
The proton affinity and selected ion-molecule reactions of diacetylene.

234. Botschwina P., Schramm H., Sebald P.
Chem. Phys. Lett. **169** (1990) 121
A theoretical investigation of $H_2C_4H^+$ and the proton affinity of HC_4H.

235. Fowler P.W., Diercksen G.H.F.
Chem. Phys. Lett. **167** (1990) 105
Polarisabilities of triply bonded molecules: the 14- and 26-electron systems CN^-, N_2, HCN, C_2H_2, C_2N_2, HC_3N and C_4H_2.

236. Bohme D.K., Mackay G.I., Schiff H.I.
J. Chem. Phys. **73** (1980) 4976
Determination of proton affinities from the kinetics of proton transfer reactions. VII. The proton affinities of O_2, H_2, Kr, O, N_2, Xe, CO_2, CH_4, N_2O, and CO.

237. Haese N.N., Woods R.C.
Astrophys. J. **246** (1981) L51
On the possible selective formation of CNC^+ and CCN^+ in the interstellar reactions of C^+ with HCN and HNC.

238. Schiff H.I., Bohme D.K.
Astrophys. J. **232** (1979) 740
An ion-molecule scheme for the synthesis of hydrocarbon-chain and organonitrogen molecules in dense interstellar clouds.

239. Hopkinson A.C., unpublished data: cited in reference 237.

240. Yoshimine M., Kraemer W.P.
Chem. Phys. Lett. **90** (1982) 145
Theoretical microwave spectroscopic constants for CCN^+ and CNC^+.

241. Knight J.S., Petrie S.A.H., Freeman C.G., McEwan M.J, McLean A.D., DeFrees D.J.
J. Am. Chem. Soc. **110** (1988) 5286
Structural isomers of C_2N^+: a selected-ion flow tube study.

242. Dibeler V.H., Reese R.M., Franklin J.L.
J. Am. Chem. Soc. **83** (1961) 1813
Mass spectrometric study of cyanogen and cyanoacetylenes.

243. Smith O.I.
Int. J. Mass Spectrom. Ion Proc. **54** (1983) 55
Cross-section for formation of parent and fragment ions by electron impact from C_2N_2.

244. Harland P.W., McIntosh B.J.
Int. J. Mass Spectrom. Ion Proc. **67** (1985) 29
Enthalpies of formation of the isomeric ions H_xCCN^+ and H_xCNC^+ (x = 0 - 3) by "monochromatic" electron impact on C_2N_2, CH_3CN and CH_3NC.

245. Bohme D.K., Wlodek S., Raksit A.B., Schiff H.I., Mackay G.I., Keskinen K.J.
Int. J. Mass Spectrom. Ion Proc. **81** (1987) 123
Selected-ion flow tube studies of reactions of C_2N^+ ions derived from cyanogen by electron ionization.

246. McEwan M.J., Anicich V.G., Huntress W.T., Jr., Kemper P.R., Bowers M.T.
Int. J. Mass Spectrom. Ion Phys. **50** (1983) 179
Reactions of CN^+ and C_2N^+ ions.

247. Raksit A.B., Bohme D.K.
Int. J. Mass Spectrom. Ion Proc. **63** (1985) 217
Flow tube studies of reactions of cyanogen with ions selected from cyanogen.

248. Troe J.
J. Chem. Phys. **66** (1977) 4758
Theory of thermal unimolecular reactions at low pressures. II. Strong collision rate constants. Applications.

249. Forst W.
"Theory of Unimolecular Reactions".
(Academic Press, New York. 1973).

250. Daniel R.G., Keim E.R., Farrar J.M.
Astrophys. J. **303** (1986) 439
The reaction of C^+ with HCN: isomeric identity of the C_2N^+ product.

251. Wilson S., Green S.
Astrophys. J. **212** (1977) L87
Theoretical study of the butadiynyl and cyanoethynyl radicals: support for the identification of C_3N in IRC+10216.

252. Guélin M., Thaddeus P.
Astrophys. J. **212** (1977) L81
Tentative detection of the C_3N radical.

253. Friberg P., Hjalmarsson Å, Irvine W.M., Guélin M.
Astrophys. J. **241** (1980) L99
Interstellar C_3N: detection in Taurus dark clouds.

254. Wilson S.
Astrophys. J. **220** (1978) 363
Theoretical study of isocyanoacetylene and the isocyanoethynyl radical.

255. Halpern J.B., Miller G.E., Okabe H., Nottingham W.
J. Photochem. Photobiol. A. **42** (1988) 63
The UV photochemistry of cyanoacetylene.

256. Wilson P.F., unpublished results.

257. Wells B.A., unpublished results.

258. McEwan M.J., personal communication.

259. Harland P.W., Maclagan R.G.A.R.
J. Chem. Soc. Far. Trans. 2 **83** (1987) 2133
The structure and energetics of the C_3N^+ ion.

260. Moureu C., Bongrand J. Ch.
Annales de Chimie **14** (1920) 47
Le cyanoacétylène C^3NH.

261. Anicich V.G., unpublished results.

262. Jones T.T.C., Raouf A.S.M., Birkinshaw K., Twiddy N.D.
J. Phys. B. **14** (1981) 2713
Experimental evidence for the existence of states of HN_2O^+ with different reactivities.

263. Ferguson E.E.
Chem. Phys. Lett. **156** (1989) 319
Reactions of $NNOH^+$ and $HNNO^+$ ions with CH_4 and NO.

264. Mackay G.I., Vlachos G.D., Bohme D.K., Schiff H.I.
Int. J. Mass Spectrom. Ion Phys. **36** (1980) 259
Studies of reactions involving $C_2H_x^+$ ions with HCN using a modified selected ion flow tube.

265. Bohme D.K., Raksit A.B.
Mon. Not. Roy. Astron. Soc. **213** (1985) 717
New results for ion-molecule reactions of HC_3N in dense interstellar clouds.

266. Harland P.W.
Int. J. Mass Spectrom. Ion Proc. **70** (1986) 231
Appearance energies and enthalpies of formation from ionization of cyanoacetylene by "monochromatic" electron impact.

267. Knight J.S., Freeman C.G., McEwan M.J., Smith S.C., Adams N.G., Smith D.
Mon. Not. Roy. Astron. Soc. **219** (1986) 89
Production and loss of HC_3N in interstellar clouds: some relevant laboratory measurements.

268. Hendrickson J.B., Cram D.J., Hammond G.S.
"Organic Chemistry", 3rd edition.
(McGraw-Hill, New York. 1970).

269. Parent D.C.
Astrophys. J. **347** (1989) 1183
Reactions of C_nN^+ with methane and the implications for interstellar chemistry.

270. Parent D.C.
J. Am. Chem. Soc. **112** (1990) 5966
Reactions of the carbene ions C_nN^+ with labeled methane: mechanistic interpretation.

271. Bohme D.K., Wlodek S., Raksit A.B.
Can. J. Chem. **65** (1987) 1563
Selected-ion flow tube studies of reactions of the carbene cation $:C_4N^+$ and their implications for interstellar gas cloud chemistry.

272. Yung Y.L.
Icarus **72** (1987) 468
An update on nitrile photochemistry on Titan.

273. Prodnuk S.D., Depuy C.H., Bierbaum V.M.
Int. J. Mass Spectrom. Ion Proc. **100** (1990) 693
The heats of formation of cyclic and linear $C_3H_2^+$.

274. Inoue M., Cottin M.
Adv. Mass Spectrom. **3** (1966) 339
Réactions molécule-ion dans le cyanogène et l'acide cyanhydrique.

275. Bieri G., Jonsson B.-Ö.
Chem. Phys. Lett. **56** (1978) 446
HNC^+ radical cation studied by charge-exchange mass spectrometry.

276. von Niessen W., Cederbaum L.S., Domcke W., Diercksen G.H.F.
Molec. Phys. **32** (1976) 1057
Ionization potentials of HCN and HNC by a Green's function method.

277. Murrell J.N., Derzi A.Al.
J. Chem. Soc. Far. Trans. 2 **76** (1980) 319
Calculations on the ground states of HCN^+ and HNC^+.

278. Koch W., Frenking G., Schwarz H.
Naturwissenschaften **71** (1984) 473
On the barrier and nature of [1,2]-hydrogen migrations in HCN / HNC and their cation radicals.

279. Petrie S., Freeman C.G., Meot-Ner (Mautner) M., McEwan M.J., Ferguson E.E.
J. Am. Chem. Soc. **112** (1990) 7121
An experimental study of HCN^+ and HNC^+ ion chemistry.

280. Petrie S., Freeman C.G., McEwan M.J., Ferguson E.E.
Mon. Not. Roy. Astron. Soc. (1991) In press.
The ion chemistry of HNC^+/HCN^+ isomers: astrochemical implications.

281. Freeman C.G., unpublished results.

282. Exact value not quoted, since it depends upon the structure of the neutral products which cannot be determined experimentally.

283. Moore C.E.
"Atomic Energy Levels" (N.B.S. Circular 467)
(U.S. Department of Commerce, Washington D.C. 1971).

284. Herzberg G.
Molecular Spectra and Molecular Structure. II. Infrared and Raman Spectra of Polyatomic Molecules.
(Van Nostrand, New York, 1945).

285. DeFrees D.J., Binkley J.S., Frisch M.J., McLean A.D.
J. Chem. Phys. **85** (1986) 5194
Is N-protonated hydrogen isocyanide, H_2NC^+, an observable interstellar species?

286. Henchman M.J., Smith D., Adams N.G.
Int. J. Mass Spectrom. Ion Phys. **42** (1982) 25
Estimations of enthalpy changes in several ion-molecule reactions involving H-D exchange from zero-point energy considerations.

287. Snyder L.E., Buhl D.
Astrophys. J. **163** (1971) L47
Observations of radio emission from interstellar hydrogen cyanide.

288. Snyder L.E., Buhl D.
Ann. N.Y. Acad. Sci. **194** (1972) 17
Detection of several new interstellar molecules.

289. Pearson P.K., Schaefer H.F.
Astrophys. J. **192** (1974) 33
Some properties of H_2CN^+: a potentially important interstellar species.

290. Uggerud E., Schwarz H.
J. Am. Chem. Soc. **107** (1985) 5046
An ab initio molecular orbital study on rearangement / fragmentation processes of isomeric CH_3N^+.

291. Conrad M.P., Schaefer H.F., III
Nature **274** (1978) 456
Role of different isomers of the H_2CN^+ ion in the formation of interstellar HCN and HNC.

292. Schaefer H.F.
Acc. Chem. Res. **12** (1979) 288
The 1,2 hydrogen shift: a common vehicle for the disappearance of evanescent molecular species.

293. Ha T.-Y., Nguyen M.T.
Chem. Phys. Lett. **97** (1983) 503
An ab initio study of the formation and structure of $H_2CN^+ \cdot N_2$.

294. Ziurys L.M., Turner B.E.
Astrophys. J. **302** (1986) L31
$HCNH^+$: a new interstellar molecular ion.

295. Brown R.D.
Nature **270** (1977) 39
Deuterium enrichment in interstellar HCN and HNC.

296. Burgers P.C., Terlouw J.K., Weiske T., Schwarz H.
Chem. Phys. Lett. **132** (1986) 69
CNH_2^+: laboratory generation of a proposed interstellar species.

297. Mass Spectrometry Data Centre
"Eight Peak Index of Mass Spectra," vol. 1.
(Mass Spectrometry Data Centre, Reading, United Kingdom. 1974)

298. Sieck L.W., Ausloos P.J.
J. Chem. Phys. **93** (1990) 8374
The ionization energy of SF_5 and the SF_5-F bond dissociation energy.

299. Bombach R., Dannacher J., Stadelmann J.-P., Vogt J., Thorne L.R., Beauchamp J.L.
Chem. Phys. **66** (1982) 403
Photoelectron-photoion coincidence study of CF_3I. Implications for the CW IR laser multiphoton dissociation of CF_3I^+.

300. Berkowitz J., Chupka W.A., Walter T.A.
J. Chem. Phys. **50** (1969) 1497
Photoionization of HCN: the electron affinity and heat of formation of CN.

301. Dibeler V.H., Liston S.K.
J. Chem. Phys. **48** (1968) 4765
Mass-spectrometric study of photoionisation. IX. Hydrogen cyanide and acetonitrile.

302. Ferguson E.E.
(Unpublished manuscript).
Application of the 'adiabatic'nature of thermal energy ion-molecule reactions to thermochemistry, $\Delta H_f(SF_5^+)$ and $\Delta H_f(CF_3^+)$.

303. Tichy M., Javahery G., Twiddy N.D., Ferguson E.E.
Int. J. Mass Spectrom. Ion Proc. **97** (1990) 211
Selected ion flow drift tube studies of the reaction of HBr^+ with various neutral molecules.

304. Dibeler V.H., Mohler F.L.
J. Res. Natl. Bur. Stand. **40** (1948) 25
Dissociation of sulfur hexafluoride, carbon tetrafluoride, and silicon tetrafluoride by electron impact.

305. Langford M.L., Hamdan M., Harris F.M.
Int. J. Mass Spectrom. Ion Proc. **95** (1990) 243
Long-lived excited states of halocarbon cations identified in high-resolution charge-stripping experiments.

306. Fisher I.P., Homer J.B., Lossing F.P.
J. Am. Chem. Soc. **87** (1965) 957
Free radicals by mass spectrometry. XXXIII. Ionization potentials of CF_2, CF_3CF_2, CF_3CH_2, *n* -C_3F_7, and *i* -C_3F_7 radicals.

307. Tichy M., Javahery G., Twiddy N.D., Ferguson E.E.
Int. J. Mass Spectrom. Ion Proc. **79** (1987) 231
The thermal energy reactions $HCl^+ + SF_6 \rightarrow SF_5^+ + HF + Cl$ and $HCl^+ + CF_4 \rightarrow CF_3^+ + HF + Cl$.

308. Babcock L.M., Streit G.E.
J. Chem. Phys. **74** (1981) 5700
Ion-molecule reactions of SF_6: determination of $IP(SF_5)$, $AP(SF_5^+/SF_6)$, and $D(SF_5-F)$.

309. Langford M.L., Almeida D.P., Harris F.M.
Int. J. Mass Spectrom. Ion Proc. **98** (1990) 147
Measurement of single ionization energies or electron affinities of SF_n molecules (n = 1-5) using double-charge-transfer spectroscopy.

310. Fisher E.R., Armentrout P.B.
Int. J. Mass Spectrom. Ion Proc. **101** (1990) R1
The appearance energy of CF_3^+ from CF_4: ion/molecule reactions related to the thermochemistry of CF_4.

311. Henchman M.
in *NATO ASI Series, Series C* **193** (1987). p. 381
"Structure / Reactivity and Thermochemistry of Ions".
Ausloos P., Lias S.G. (eds).
Entropy-driven reactions. Summary of the panel discussion.

312. Henchman M.J., Adams N.G., Smith D.
J. Chem. Phys. **75** (1981) 1201
The isotope exchange reactions $H^+ + D_2 \leftrightarrow HD + D^+$ and $D^+ + H_2 \leftrightarrow HD + H^+$ in the temperature range 200-300 K.

313. Henchman M., Adams N.G., Smith D., Herman Z., Paulson J.F.
Int. J. Mass Spec. Ion Proc. **92** (1989) 15
The mechanism of the reaction $CH_4^+ + CH_4 \rightarrow CH_5^+ + CH_3$ as a function of energy - rate constants and product distributions for the reactions of $CH_4^+ + CD_4$ and $CD_4^+ + CH_4$ at 80 K and 300 K.

314. Adams N.G., Smith D., Henchman M.J.
Int. J. Mass Spectrom. Ion Phys. **42** (1982) 11
Isotope exchange in the reactions $H_3O^+ + D_2O$, $NH_4^+ + ND_3$, $CH_5^+ + CD_4$ and their mirror reactions at thermal energies.

315. Meot-Ner M., Hamlet P., Hunter E.P., Field F.H.
J. Am. Chem. Soc. **102** (1980) 6393
Internal and external solvation of polyfunctional ions.

316. King G.K., Maricq M.M., Bierbaum V.M., DePuy C.H.
J. Am. Chem. Soc. **103** (1981) 7133
Gas-phase reactions of negative ions with alkyl nitrites.

317. Bailey C.R., Hale J.B., Thompson J.W.
Proc. Roy. Soc. London **167 A** (1938) 555
The molecular structure of carbon and silicon tetrafluorides.

318. Lias S.G., Ausloos P.
Int. J. Mass Spectrom. Ion Phys. **23** (1977) 273
Ion-molecule reactions involving halomethyl ions; heats of formation of halomethyl ions.

319. Matthews H.E., Sears T.J.
Astrophys. J. **272** (1983) 149
The detection of vinyl cyanide in TMC-1.

320. Fehsenfeld F.C.
Astrophys. J. **209** (1976) 638
Ion reactions with atomic oxygen and atomic nitrogen of astrophysical importance.

321. Federer W., Villinger H., Lindinger W., Ferguson E.E.
Chem. Phys. Lett. **123** (1986) 12
Reactions of some hydrocarbon cations with nitrogen atoms.

322. Viggiano A.A., Howorka F., Albritton D.L., Fehsenfeld F.C., Adams N.G., Smith D.
Astrophys. J. **236** (1980) 492
Laboratory studies of some ion-atom reactions related to interstellar molecular synthesis.

323. Millar T.J., Nejad L.A.M.
Mon. Not. Roy. Astron. Soc. **217** (1985) 507
Chemical modelling of molecular sources - IV. Time-dependent chemistry of dark clouds.

324. Millar T.J., Leung C.M., Herbst E.
Astron. Astrophys. **183** (1987) 109
How abundant are complex interstellar molecules ?

325. Capone L.A., Prasad S.S., Huntress W.T., Whitten R.C., Dubach J., Santhanam K.
Nature **293** (1981) 45
Formation of organic molecules on Titan.

326. Cerceau F., Raulin F., Courtin R., Gautier D.
Icarus **62** (1985) 207
Infrared spectra of gaseous mononitriles: application to the atmosphere of Titan.

327. Bossard A., Mourey D., Raulin F.
Adv. Space Res. **3(9)** (1983) 39
The escape of molecular hydrogen and the synthesis of organic nitriles in planetary atmospheres.

328. McEwan M.J., Anicich V.G., Huntress W.T.
in "Interstellar Molecules", p. 299
(87th Symposium of the International Astronomical Union).
Andrews B.H. (ed.)
(Reidel, Dordrecht. 1980)
An ICR study of ion-molecule reactions in the C_2H_2/HCN system.

329. Bohme D.K., Raksit A.B., Fox A.
J. Am. Chem. Soc. **105** (1983) 5481
Carbene chemistry of cations: the chemistry of $:C_3H^+$ in the gas phase.

330. Rakshit A.B., Bohme D.K.
Int. J. Mass Spectrom. Ion Phys. **49** (1983) 275
The proton affinity of C_3 and heat of formation of C_3H^+.

331. Raksit A.B., Bohme D.K.
Int. J. Mass Spectrom. Ion Proc. **55** (1983/1984) 69
Studies of reactions of C_3H^+ ions in the gas phase at 296±2 K.

332. Heerma W., Sarneel M.M., Dijkstra G.
Org. Mass Spectrom. **21** (1986) 681
Structure and formation of gaseous $[C_3H_4N]^+$ ions.

333. Adams N.G., Smith D.
Int. J. Mass Spectrom. Ion Proc. **61** (1984) 133
A study of the reactions of $NH_3^{+\cdot}$ and $ND_3^{+\cdot}$ with H_2 and D_2 at several temperatures.

334. Adams N.G., Smith D., Ferguson E.E.
Int. J. Mass Spectrom. Ion Proc. **67** (1985) 67
Comparative effects of temperature and kinetic energy change on the reaction of O_2^+ with CH_4 and CD_4.

335. Rowe B.R., Dupeyrat G., Marquette J.B., Smith D., Adams N.G., Ferguson E.E.
J. Chem. Phys. **80** (1984) 241
The reaction $O_2^+ + CH_4 \rightarrow CH_3O_2^+ + H$ studied from 20 to 560 K in a supersonic jet and in a SIFT.

336. Boyd R.J., Jones W.E., Ling K.W.
Chem. Phys. **58** (1981) 203
Geometries, energies and polarities of cyanopolyynes.

337. Bews J.R., Glidewell C.
J. Molec. Struct. (THEOCHEM) **91** (1983) 353
Molecular fragmentations. Part XII. Mass spectral fragmentation of pyridine.

338. Ohno K., Matsumoto S., Imai K., Harada Y.
J. Phys. Chem. **88** (1984) 206
Penning ionization electron spectroscopy of nitriles.

339. Knight J.S., Freeman C.G., McEwan M.J.
J. Am. Chem. Soc. **108** (1986) 1405
Isomers of $C_2H_4N^+$ and the proton affinities of CH_3CN and CH_3NC.

340. Huntress W.T., Jr.
Astrophys. J. Suppl. Ser. **33** (1977) 495
Laboratory studies of bimolecular reactions of positive ions in interstellar clouds, in comets, and in planetary atmospheres of reducing composition.

341. McEwan M.J., Anicich V.G., Huntress W.T., Jr.
Int. J. Mass Spectrom. Ion Phys. **37** (1981) 273
An ICR investigation of ion-molecule reactions of HCN.

342. Anicich V.G., Huntress W.T., Jr., Futrell J.H.
Chem. Phys. Lett. **40** (1976) 233
Ion cyclotron resonance studies of some reactions of C^+ ions.

343. Liddy J.P., Freeman C.G., McEwan M.J.
Mon. Not. Roy. Astron. Soc. **180** (1977) 683
Laboratory investigation of some ion-molecule reactions related to cyanide chemistry in dense interstellar clouds.

344. Raksit A.B., Schiff H.I., Bohme D.K.
Int. J. Mass Spectrom. Ion Proc. **56** (1984) 321
A selected ion flow tube study of the kinetics of CN^+ reactions at 296±2K.

345. Smith D., Adams N.G.
Int. J. Mass Spectrom. Ion Proc. **76** (1987) 307
Cyclic and linear isomers of $C_3H_2^+$ and $C_3H_3^+$: the $C_3H^+ + H_2$ reaction.

346. Smyth K.C., Lias S.G., Ausloos P.
Combust. Sci. Tech. **28** (1982) 147
The ion-molecule chemistry of $C_3H_3^+$ and the implications for soot formation.

347. Turner B.E., Amano T., Lee S., Feldman P.A.
in "Molecular Clouds in the Milky Way and External Galaxies", p. 172
Lecture Notes in Physics vol. **315**
Dickman R.L., Snell R.L., Young J.S. (eds.)
(Springer-Verlag, Berlin Heidelberg. 1988.)
New observational tests of ion-molecule chemistry: HC_3NH^+ and PN.

348. Lichtin D.A., Lin M.C.
Chem. Phys. **96** (1985) 473
Kinetics of cyanogen radical reactions with selected molecules at room temperature.

349. Brown R.D., Eastwood F.W., Elmes P.S., Godfrey P.D.
J. Am. Chem. Soc. **105** (1983) 6496
Tricarbon monoxide.

350. Matthews H.E., Irvine W.M., Friberg P., Brown R.D., Godfrey P.D.
Nature **310** (1984) 125
A new interstellar molecule: tricarbon monoxide.

351. Brown R.D., Godfrey P.D., Cragg D.M., Rice E.H.N., Irvine W.M., Friberg P., Suzuki H., Ohishi M., Kaifu N., Morimoto M.
Astrophys. J. **297** (1985) 302
Tricarbon monoxide in TMC-1.

352. Irvine W.M., Brown R.D., Cragg D.M., Friberg P., Godfrey P.D., Kaifu N., Matthews H.E., Ohishi M., Suzuki H., Takeo H.
Astrophys. J. **335** (1988) L89
A new interstellar polyatomic molecule: detection of propynal in the cold cloud TMC-1.

353. Herbst E., Smith D., Adams N.G.
Astron. Astrophys. **138** (1984) L13
Ion-molecule synthesis of C_3O.

354. Smith D., Adams N.G., Alge E., Herbst E.
Astrophys. J. **272** (1983) 365
Association reactions of Na^+ and some implications for interstellar chemistry.

355. Bohme D.K., Wlodek S., Williams L., Forte L., Fox A.
J. Chem. Phys. **87** (1987) 6934
Laboratory measurements of gas-phase reactions of polyatomic carbon ions C_n^+ (n = 1-6) and C_nH^+ (n = 2-5) with carbon monoxide.

356. Herbst E., Adams N.G., Smith D.
Astrophys. J. **269** (1983) 329
Laboratory measurements of ion-molecule reactions pertaining to interstellar hydrocarbon synthesis.

357. Adams N.G., Smith D., Giles K., Herbst E.
Astron. Astrophys. **220** (1989) 269
The production of C_nO, HC_nO, and H_2C_nO molecules in dense interstellar clouds.

358. Holmes J.L., Terlouw J.K., Burgers P.C.
Org. Mass Spectrom. **15** (1980) 140
$[C_3H_3O]^+$ ions; reacting and non-reacting configurations.

359. Guillemin J.C., Wlodarczak G., Lopez J.C., Demaison J.
J. Mol. Spectrosc. **140** (1990) 190
Millimeter-wave spectrum of cyclopropenone, C_3H_2O.

360. Lovas F., Johnson D.R., Buhl D., Snyder L.E.
Astrophys. J. **209** (1976) 770
Millimeter emission lines in Orion A.

361. Brown R.D., McNaughton D., Dyall K.G.
Chem. Phys. **119** (1988) 189
Pentacarbon monoxide - a theoretical study.

362. DeFrees D.J., McLean A.D.
Chem. Phys. Lett. **158** (1989) 540
A priori predictions of the rotational constants for $HC_{13}N$, $HC_{15}N$, and C_5O.

363. Ewing D.W.
J. Am. Chem. Soc. **111** (1989) 8809
Theoretical study of C_4O and C_6O.

364. McElvany S.W., Dunlap B.I., O'Keefe A.
J. Chem. Phys. **86** (1987) 715
Ion molecule reactions of carbon cluster ions with D_2 and O_2.

365. Brown R.D., Rice E.H.N.
J. Am. Chem. Soc. **106** (1984) 6475
Tricarbon monoxide - a theoretical study.

366. Botschwina P.
J. Chem. Phys. **90** (1989) 4301
A theoretical investigation of the astrophysically important molecules C_3O and HC_3O^+.

367. Terlouw J.K., Holmes J.L., Lossing F.P.
Can. J. Chem. **61** (1983) 1722
Ionized ethylidene ketene and its homologue methylene ketene.

368. Bouchoux G., Hoppilliard Y., Flament J.-P., Terlouw J.K., van der Valk F.
J. Phys. Chem. **90** (1986) 1582
Experimental and theoretical study of $[C_3H_2O]^{+\cdot}$ cations. Evidence for the existence of stable $[CH{=}CH{-}CO]^{+\cdot}$ ions in the gas phase.

369. von Niessen W., Bieri G., Asbrink L.
J. Electron Spectrosc. Relat. Phenom. **21** (1980) 175
30.4 nm He(I) photoelectron spectra of organic molecules. Part III. Oxo-compounds (C,H,O).

370. Bouchoux G., Hoppilliard Y., Flament J.-P.
Org. Mass Spectrom. **20** (1985) 560
Structures and stabilities of $[C_3H_3O]^+$ ions in the gas phase: a molecular orbital study.

371. Lossing F.P., Holmes J.L.
J. Am. Chem. Soc. **106** (1984) 6917
Stabilization energy and ion size in carbocations in the gas phase.

372. Roebber J.L., Larrabee J.C., Huffman R.E.
J. Chem. Phys. **46** (1967) 4594
Vacuum-ultraviolet absorption spectrum of carbon suboxide.

373. Kim H.H., Roebber J.L.
J. Chem. Phys. **44** (1966) 1709
Vacuum-ultraviolet absorption spectrum of carbon suboxide.

374. Stull D.R., Prophet H.
"JANAF Thermochemical Tables"
(U.S. Government Printing Office, Washington D.C. 1971)

375. Binkley J.S.
J. Am. Chem. Soc. **106** (1984) 603
Theoretical study of the relative stabilities of C_2H_2 and Si_2H_2 conformers.

376. McAllister T., Nicholson A.J.C.
J. Chem. Soc. Far. Trans. 1 **77** (1981) 821
$C_3H_3^+$ in flames and the proton affinity of C_3H_2.

377. Kaneti J., Karpf M., Dreiding A.S.
Helv. Chim. Acta **65** (1982) 2517
On the mechanism of the a-alkynone cyclization: a theoretical study.

378. Linn S.H., Ono Y., Ng C.Y.
J. Chem. Phys. **74** (1981) 3342
Molecular beam photoionization study of CO, N_2, and NO dimers and clusters.

379. Smith I.W.M.
Chem. Phys. **131** (1989) 391
Radiative association in collisions between neutral free radicals.

380. Spencer J.E., Endo H., Glass G.P.
in "The Sixteenth Symposium (International) on Combustion", p. 829
(The Combustion Institute, Pittsburgh, Pennsylvania. 1977).
Reactions of vibrationally excited OH.

381. Schatz G.C.
J. Chem. Phys. **74** (1981) 1133
A quasiclassical trajectory study of reagent vibrational excitation effects in the $OH + H_2 \rightarrow H_2O + H$ reaction.

382. Chantry P.J.
J. Chem. Phys. **55** (1971) 2746
Doppler broadening in beam experiments.

383. Ravishankara A.R., Nicovich J.M., Thompson R.L., Tully F.P.
J. Phys. Chem. **85** (1981) 2498
Kinetic study of the reaction of OH with H_2 and D_2 from 250 to 1050K.

384. Lebrilla C.B., Maier W.F.
Chem. Phys. Lett. **105** (1984) 183
How facile is C-H abstraction? A semi-empirical study.

385. Whittle E., Steacie E.W.R.
J. Chem. Phys. **21** (1953) 993
The reactions of methyl radicals with the hydrogen isotopes.

386. Sepherad A., Marshall R.M., Purnell H.
J. Chem. Soc. Far. Trans. 1 **75** (1979) 835
Reaction between hydrogen atoms and methane.

387. Marshall R.M., Shankar G.
J. Chem. Soc. Far. Trans. 1 **77** (1981) 2271
Rate parameters for $CH_3 + H_2 \rightarrow CH_4 + H$ in the temperature range 584-671K.

388. Kerr J.A., Parsonage M.J.
"Evaluated kinetic data on gas phase hydrogen transfer reactions of methyl radicals".
(Butterworths, London. 1976)

389. Sutherland J.W., Michael J.V.
J. Chem. Phys. **88** (1988) 830
The kinetics and thermodynamics of the reaction $H + NH_3 \leftrightarrow NH_2 + H_2$ by the flash photolysis - shock tube technique: Determination of the equilibrium constant, the rate constant of the back reaction, and the enthalpy of formation of the amidogen radical.

390. Harding L.B., Schatz G.C., Chiles R.A.
J. Chem. Phys. **76** (1982) 5172
An ab initio determination of the rate constant for $H_2 + C_2H \rightarrow H + C_2H_2$.

391. Wessman M.A., Benson S.W.
J. Phys. Chem. **92** (1988) 4080
Rate parameters for the reactions of vinyl and butadienyl radicals with hydrogen and acetylene.

392. Albers E.A., Hoyermann K., Schacke H., Schmatjko K.J., Wagner H. Gg., Wolfrum J.
"15th Symposium (International) on Combustion", p. 765
(The Combustion Institute, Pittsburgh, Pa. 1975)
Absolute rate coefficients for the reaction of H-atoms with N_2O and some reactions of CN radicals.

393. Atakan B., Jacobs A., Wahl M., Weller R., Wolfrum J.
Chem. Phys. Lett. **154** (1989) 449
Kinetic studies of the gas-phase reactions of CN with O_2 and H_2 from 294 to 1000 K.

394. Wagner A.F., Bair R.A.
Int. J. Chem. Kinet. **18** (1986) 473
An ab initio determination of the rate constant for $H_2 + CN \rightarrow H + HCN$.

395. Vasudev R., Zare R.N., Dixon R.N.
Chem. Phys. Lett. **96** (1983) 399
Dynamics of photodissociation of HONO at 369 nm: motional anisotropy and internal state distribution of the OH fragment.

396. Vasudev R., Zare R.N., Dixon R.N.
J. Chem. Phys. **80** (1984) 4863
State-selected photodissociation dynamics: complete characterization of the OH fragment ejected by the HONO $\tilde{A}$ state.

397. Tuck A.F.
J. Chem. Soc. Far. Trans. 2 **73** (1977) 689
Molecular beam studies of ethyl nitrite photodissociation.

398. Cremaschi P., Simonetta M.
Theor. Chim. Acta **34** (1974) 175
A theoretical study of electrophilic aromatic substitution. 1. The electronic structure of NO_2^+.

399. Green S., Schor H., Siegbahn P., Thaddeus P.
Chem. Phys. **17** (1976) 479
Theoretical investigation of protonated carbon dioxide.

400. Seeger U., Seeger R., Pople J.A., von R. Scheler P.
Chem. Phys. Lett. **55** (1978) 399
Isomeric structures of protonated carbon dioxide.

401. DeFrees D.J., Loew G.H., McLean A.D.
Astrophys. J. **254** (1982) 405
The rotational spectra of $HOCO^+$, HOCN, HN_3, and HNCO from quantum mechanical calculations.

402. Frisch M.J., Schaefer H.F., Binkley J.S.
J. Phys. Chem. **89** (1985) 2192
Theoretical study of the structure and spectroscopic characteristics of protonated carbon dioxide.

403. Yu J.G., Fu X.Y., Liu R.Z., Yamashita K., Koga N., Morokuma K.
Chem. Phys. Lett. **125** (1986) 438
Theoretical study of structures and energies of $[HCOO]^+$ and $[COOH]^+$ and their rearrangement.

404. Millar T.J., DeFrees D.J., McLean A.D., Herbst E.
Astron. Astrophys. **194** (1988) 250
The sensitivity of gas-phase models of dense interstellar clouds to changes in dissociative recombination branching ratios.

405. Mitchell J.B.A., McGowan J.W.
in "Physics of Ion-Ion and Electron-Ion Collisions",p. 279
Brouillard F., McGowan J.W. (eds.)
(Plenum Press, New York. 1983).

406. Wootten A., Boulanger F., Bogey M., Combes F., Encrenaz P.J., Gerin M., Ziurys L.
Astron. Astrophys. **166** (1986) L15
A search for interstellar H_3O^+.

407. Thaddeus P., Guélin M., Linke R.A.
Astrophys. J. **246** (1981) L41
Three new 'nonterrestrial' molecules.

408. Bohme D.K.
Nature **319** (1986) 473
Ionic origins of carbenes in space.

409. Phillips T.G., Huggins P.J.
Astrophys. J. **251** (1981) 533
Abundance of atomic carbon (C I) in dense interstellar clouds.

410. Jaffe D.T., Harris A.I., Silber M., Genzel R., Betz A.L.
Astrophys. J. **290** (1985) L59
Detection of the 370 micron $^3P_2$ - $^3P_1$ fine-structure line of [C I].

411. Keene J., Blake G.A., Phillips T.G., Huggins P.J., Beichman C.A.
Astrophys. J. **299** (1985) 967
The abundance of atomic carbon near the ionization fronts in M17 and S140.

APPENDIX.

Computer programs.

Program "HELLO"

```
10      REM ** HELLO **
40      CD$ =  CHR$ (13) +  CHR$ (4)
50      PRINT  CHR$ (4);"PR#3"
55      TEXT
60      HOME : PRINT : VTAB (10): HTAB (10): PRINT "ENSURE YOUR PROGRAM DISC IS IN
        DRIVE 1"
70      HTAB (10): PRINT "AND YOUR DATA DISC IN DRIVE 2 BEFORE PROCEEDING"
80      PRINT : PRINT : HTAB (10): PRINT "(Press any key when ready)";: GET KI$
90      PRINT CD$;"RUN OPTIONS,D1"
```

Program "OPTIONS"

```
10      REM ** PROGRAM OPTIONS **
20      DIM OPST$(10)
30      CD$ =  CHR$ (13) +  CHR$ (4)
40      TEXT
50      PRINT  CHR$ (4);"PR#3"
90      OPST$(1) = "COLLATE DATA INTO DATA FILE": REM  to be replaced by automatic data
        collection option.
92      OPST$(2) = "RESET THE CURRENT FILENAMES"
94      OPST$(3) = "CALCULATE A RATE CONSTANT"
96      OPST$(4) = "CALCULATE TWO OR MORE RATE CONSTANTS"
98      OPST$(5) = "DISPLAY A PRODUCT RATIO"
100     OPST$(6) = "EXAMINE OR EDIT A FILE"
102     OPST$(7) = "MONITOR PRESSURE"
120     NC% = 8
125     OPST$(NC%) = "QUIT"
130     HOME : PRINT "MAKE A CHOICE:": PRINT "---- - ------": PRINT
140     FOR I = 1 TO NC%
150     HTAB (10): PRINT "(";I;"). ";OPST$(I): PRINT
160     NEXT
170     PRINT : PRINT "Enter an option (1-";NC%;"): ";
180     GET KI$:OP% =  ASC (KI$) - 48: IF OP% < 1 OR OP% > NC% GOTO 180
190     PRINT OP%;".  ";OPST$(OP%)
200     PRINT "Sure about that ? (Y/N): ";
201     GET KS$: IF KS$ < > "Y" AND KS$ < > "N" GOTO 201
203     PRINT KS$: IF KS$ = "N" GOTO 130
205     HOME
210     IF OP% = 1 THEN  PRINT CD$;"RUN MEANFLOWS,D1"
220     IF OP% = 2 THEN  PRINT CD$;"RUN SETFILES,D1"
230     IF OP% = 3 THEN  PRINT CD$;"RUN RASCAL,D1"
240     IF OP% = 4 THEN  PRINT CD$;"RUN MULE,D1"
250     IF OP% = 5 THEN  PRINT CD$;"RUN PROD RAT,D1"
260     IF OP% = 6 THEN  PRINT CD$;"RUN STUDYFILES,D1"
270     IF OP% = 7 THEN  PRINT CD$;"RUN PRESSMONITOR,D1"
490     PRINT
500     END
```

Program "MEANFLOWS"

```
100     GOSUB 1000
110     REM initialise program
200     GOSUB 2000
210     REM average flow measurements
300     GOSUB 3000
310     REM input ion counts
400     GOSUB 4000
410     REM write file
500     PRINT CD$;"RUN OPTIONS,D1"
600     END
1000    REM * INITIALISE PROGRAM *
1010    CD$ =  CHR$ (13) +  CHR$ (4)
1020    DIM FM(400): DIM X(40): DIM Y(40,6)
1030    TF% = 0:CF% = 1
1035    BLANK$ = "                    "
1040    PRINT  CHR$ (4);"PR#3"
1050    INPUT "ENTER RUN NUMBER ? (1-30): ";RN$:NM$ = "FLOWFILE" + RN$
1060    PRINT CD$;"OPEN ";NM$;",D2"
1070    PRINT CD$;"READ ";NM$
1080    INPUT NF%
1090    FOR I = 1 TO NF%
1100    INPUT FM(I)
1110    NEXT
1120    PRINT CD$;"CLOSE ";NM$
1200    FOR I = 1 TO 40
1210    X(I) = 0
1220    FOR J = 1 TO 6
1230    Y(I,J) = 0
1240    NEXT
1250    NEXT
1260    L$ = "L":M$ = "M":S$ = "S"
1270    HOME : PRINT "VOLUME SCALE FACTORS:": PRINT "------ ----- -------": PRINT :
        PRINT : PRINT
1300    INPUT "Smallest volume ? (cm^3): ";SV
1310    INPUT "Largest volume  ? (cm^3)  <0 to quit> : ";LV: IF LV < SV THEN L$    = "S"
1320    IF L$ = "S" THEN M$ = "S"
1330    IF M$ = "M" THEN  INPUT "Medium volume  ? (cm^3)  <0 to quit> : ";MV: IF MV < SV
        THEN M$ = "S"
1340    IF L$ = "L" THEN LS = LV / SV
1350    IF M$ = "M" THEN MS = MV / SV
1360    PRINT : PRINT : PRINT
1400    IF L$ = "L" THEN  PRINT "Large vol. scale factor  = "; INT (1000 * LS + 0.5) / 1000
1410    IF M$ = "M" THEN  PRINT "Medium vol. scale factor = "; INT (1000 * MS + 0.5) / 1000
1420    PRINT : PRINT : PRINT "Any changes ? (Y/N): ";
1430    GET KS$: IF KS$ <  > "Y" AND KS$ <  > "N" GOTO 1430
1440    PRINT KS$: IF KS$ = "Y" GOTO 1260
1500    RETURN
2000    REM * AVERAGE THE FLOW MEASUREMENTS *
2010    TF% = TF% + 1:HM% = 0:PF = 0
2020    HOME : PRINT "Flow #";TF%;":": PRINT "--------": PRINT
2030    FOR J = 1 TO (17 - HM%)
```

```
2040  IF CF% + J > NF% GOTO 2060
2050  VTAB (6 + HM% + J): PRINT CF% + J;".  ";FM(CF% + J)
2060  NEXT
2100  VTAB (HM% + 3): PRINT HM% + 1;".  ";FM(CF%);"          ";: POKE 1403,40: PRINT
      BLANK$;: POKE 1403,40: PRINT "Include this ? (Y/N): ";
2110  GET KS$: IF KS$ <  > "Y" AND KS$ <  > "N" GOTO 2110
2120  PRINT KS$: IF KS$ = "Y" THEN HM% = HM% + 1:PF = PF + FM(CF%)
2130  CF% = CF% + 1
2140  VTAB (HM% + 4): PRINT "More measurements for this flow ? (Y/N): ";
2150  GET KS$: IF KS$ <  > "Y" AND KS$ <  > "N" GOTO 2150
2160  PRINT KS$: IF KS$ = "Y" THEN  VTAB (HM% + 4): PRINT BLANK$;BLANK$
2200  FOR X = (HM% + 6) TO 23
2210  VTAB (X): PRINT BLANK$
2220  NEXT
2225  IF KS$ = "Y" GOTO 2030
2230  VTAB (HM% + 5)
2240  IF L$ = "S" AND M$ = "S" GOTO 2320
2250  PRINT : PRINT "Which neutral volume ? (L/";: IF M$ = "M" THEN  PRINT "M/";
2260  PRINT "S): ";
2270  GET KS$: IF KS$ <  > L$ AND KS$ <  > M$ AND KS$ <  > S$ GOTO 2270
2280  PRINT  KS$
2290  IF KS$ = "L" THEN PF = PF * LS
2300  IF KS$ = "M" THEN PF = PF * MS
2320  IF PF < 1E - 05 THEN X(TF%) = 0: GOTO 2350
2330  X(TF%) = PF / HM%:LX% = 3 -  INT ( LOG (X(TF%)) /  LOG (10))
2340  X(TF%) =  INT (X(TF%) * (10 ^ LX%) + 0.5) / (10 ^ LX%)
2350  PRINT : PRINT : PRINT "This flow value is ";X(TF%)
2400  PRINT : PRINT "More flows yet ? (Y/N): ";
2410  GET KS$: IF KS$ <  > "Y" AND KS$ <  > "N" GOTO 2410
2420  PRINT KS$: IF KS$ = "Y" GOTO 2010
2500  RETURN
3000  REM * INPUT ION SIGNALS *
3010  PTS = TF%
3020  HOME : PRINT "INPUT ION SIGNALS: ": PRINT "----- --- -------": PRINT
3030  PRINT "How many ion masses ? (1-6): ";
3040  GET KS$:MAX =  ASC (KS$) - 48: IF MAX < 1 OR MAX > 6 GOTO 3040
3050  PRINT  KS$
3060  FOR J = 1 TO MAX
3070  HOME : PRINT "ION #";J;":": PRINT "------": PRINT
3080  FOR I = 1 TO PTS
3090  PRINT I;".  "; INT (X(I) * 10000 + 0.5) / 10000;: POKE 1403,25
3100  INPUT "Count ?  ";Y(I,J)
3110  NEXT
3120  NEXT
3500  RETURN
4000  REM * WRITE DATA FILE *
4010  HOME : PRINT "WRITE DATA FILE: ": PRINT "----- ---- ----": PRINT
4020  INPUT "Filename ? <NONE to quit>:  ";SF$: IF SF$ = "N" OR SF$ = "NONE" THEN
      RETURN
4030  PRINT : PRINT : PRINT "Writing data file ";SF$;" now ..."
4040  PRINT  CD$;"OPEN  ";SF$;",D2"
4050  PRINT  CD$;"WRITE  ";SF$
4060  PRINT PTS
```

```
4070    PRINT MAX
4080    FOR I = 1 TO PTS
4090    FOR J = 1 TO MAX
4100    PRINT Y(I,J)
4110    PRINT X(I)
4120    NEXT
4130    NEXT
4140    PRINT CD$;"CLOSE ";SF$
4150    PRINT CD$;"OPEN FILENAMES,D2"
4160    PRINT CD$;"READ FILENAMES"
4170    INPUT DF$: INPUT FF$
4180    PRINT CD$;"CLOSE FILENAMES"
4200    PRINT CD$;"OPEN FILENAMES,D2"
4210    PRINT CD$;"WRITE FILENAMES"
4220    PRINT SF$
4230    PRINT FF$
4240    PRINT CD$;"CLOSE FILENAMES"
4300    PRINT CD$;"DELETE ";NM$;",D2"
4500    RETURN
```

Program "SETFILES"

```
10      REM ** PROGRAM SETFILES **
20      CD$ =  CHR$ (13) +  CHR$ (4)
30      PRINT  CHR$ (4);"PR#3"
40      PRINT CD$;"OPEN  FILENAMES,D2"
50      PRINT CD$;"READ  FILENAMES"
60      INPUT DF$
70      INPUT FF$
80      PRINT CD$;"CLOSE  FILENAMES"
90      TEXT : HOME : PRINT
100     VTAB (5): PRINT "THE CURRENT DATA FILENAME IS ";DF$
110     PRINT : PRINT "NEW DATA FILENAME ?": INPUT "('L' to leave unchanged):   ";ND$
120     IF ND$ <  > "L" THEN DF$ = ND$
130     VTAB (13): PRINT "THE CURRENT FORMAT FILENAME IS ";FF$
140     PRINT : PRINT "NEW FORMAT FILENAME ?": INPUT "('L' to leave unchanged):
          ";NF$
150     IF NF$ <  > "L" THEN FF$ = NF$
160     VTAB (21): PRINT "DATA FILE   = ";DF$: PRINT "FORMAT FILE = ";FF$
170     PRINT : PRINT "ANY CHANGES ? (Y/N): ";
180     GET NC$: IF NC$ <  > "Y" AND NC$ <  > "N" GOTO 180
190     PRINT NC$
200     IF NC$ = "Y" GOTO 90
210     HOME
300     PRINT CD$;"OPEN  FILENAMES,D2"
305     PRINT CD$;"WRITE  FILENAMES"
310     PRINT DF$
320     PRINT FF$
330     PRINT CD$;"CLOSE  FILENAMES"
350     PRINT CD$;"RUN  OPTIONS,D1"
360     END
```

Program "RASCAL"

```
10    REM ** PROGRAM RASCAL **
11    REM Last change in calibration: 3rd July 1989
15    PRINT  CHR$ (4);"BRUN LOMEM:": &  LOMEM: 2048
20    DIM  XP(25),YP(25,6),RCNC(25),Y(25)
25    DIM RV$(11): DIM QV(11): DIM TY%(11): DIM RG$(11): DIM VN$(11)
26    DIM  TS$(6)
30    CD$ =  CHR$ (13) +  CHR$ (4)
35    CC$ =  CHR$ (9)
60    FOR I = 1 TO 11:TY%(I) = 1: NEXT
70    TY%(2) = 2:TY%(8) = 2:TY%(10) = 2:TY%(11) = 2
75    PRINT CD$;"OPEN FILENAMES,D2": PRINT CD$;"READ FILENAMES": INPUT DF$:
      INPUT FF$: PRINT CD$;"CLOSE FILENAMES"
95    RF$ = "N":RC$ = "N"
97    PRINT  CHR$ (4);"PR#3"
100   GOSUB 1000
110   REM display menu
200   IF OP% = 1 THEN  GOSUB 2000
210   REM read data/format files
300   IF OP% = 2 THEN  GOSUB 3000
310   REM display / adjust data file
400   IF OP% = 3 THEN  GOSUB 4000
410   REM  display / adjust rate variables
500   IF OP% = 4 THEN  GOSUB 6000
510   REM calculate rate coefficient
600   IF OP% = 5 THEN  GOSUB 5000
610   REM draw log graph
700   IF OP% < > 6 GOTO 100
800   PRINT CD$;"RUN OPTIONS,D1"
1000  REM options menu
1010  TEXT : HOME
1015  TS$(1) = "Load data / format files":TS$(2) = "Display / edit data in memory":TS$(3) =
      "Display / adjust rate variables":TS$(4) = "Calculate rate constant":TS$(5) = "Display
      graph":TS$(6) = "Quit"
1020  PRINT "RATE CALCULATION:": PRINT "--- ----------": PRINT : PRINT "Make a
      choice:": PRINT "---- - ------": PRINT : FOR I = 1 TO 6: PRINT : POKE 1403,10: PRINT
      "(";I;").  ";TS$(I): NEXT : PRINT : PRINT "WHICH OPTION ? (1-6): ";
1030  GET KS$:OP% =  ASC (KS$) - 48: IF OP% < 1 OR OP% > 6 GOTO 1030
1040  PRINT OP%: PRINT : PRINT OP%;".  ";TS$(OP%): FOR I = 1 TO 6:TS$(I) = "": NEXT :
      RETURN
2000  REM load data file
2010  RC$ = "N": HOME : PRINT "READ DATA / RATE VARIABLE FILES:": PRINT "---- ----
      ---- -------- -----": PRINT : VTAB 7: PRINT "CURRENT DATA FILENAME IS: ";DF$:
      PRINT : PRINT "CHANGE THIS ? (Y/N): ";
2020  GET KS$: IF KS$ < > "Y" AND KS$ < > "N" THEN 2020
2030  PRINT KS$: IF KS$ = "Y" THEN  PRINT : INPUT "NEW FILENAME ? ... ";DF$
2040  PRINT : PRINT "READING YOUR DATA FILE ";DF$;" NOW ... ":YU% = 0
2050  PRINT CD$;"OPEN ";DF$;",D2": PRINT CD$;"READ ";DF$: INPUT PTS: INPUT MAX:
      FOR  I = 1 TO PTS: FOR J = 1 TO MAX: INPUT YP(I,J): INPUT XP(I): NEXT : NEXT : PRINT
      CD$;"CLOSE ";DF$
2060  FOR I = 1 TO PTS:Y(I) = 0: IF YP(I,1) >  = 1.0 THEN Y(I) =  LOG (YP(I,1))
2070  NEXT
```

```
2100  PRINT : PRINT : PRINT "READ RATE VARIABLES FILE ALSO ? (Y/N): ";
2110  GET KS$: IF KS$ < > "Y" AND KS$ < > "N" GOTO 2110
2120  PRINT KS$: IF KS$ = "N" THEN RETURN
2130  PRINT : PRINT "CURRENT RATE VARIABLES FILENAME IS ";FF$: PRINT : PRINT
      "CHANGE THIS ? (Y/N): ";
2140  GET KS$: IF KS$ < > "Y" AND KS$ < > "N" GOTO 2140
2150  PRINT KS$: IF KS$ = "Y" THEN PRINT : INPUT "NEW FILENAME ? ... ";FF$
2160  PRINT : PRINT "READING YOUR FILE ";FF$;" NOW ... ": PRINT CD$;"OPEN
      ";FF$;",D2": PRINT CD$;"READ ";FF$: FOR I = 1 TO 11: INPUT RV$(I):QV(I) = VAL
      (RV$(I))
2180  NEXT : PRINT CD$;"CLOSE ";FF$: HOME :RF$ = "Y": RETURN
3000  REM examine/edit data file
3005  HD$ = "EXAMINE DATA FILE":UD$ = "------- ---- ----"
3010  GOSUB 3600: REM display data file
3015  PRINT : POKE 1403,10: PRINT "(0). Quit": POKE 1403,10: PRINT "(1). Select ion signal
      for rate calculation": POKE 1403,10: PRINT "(2). Edit a data point": POKE 1403,10:
      PRINT "(3). Delete a row of data"
3020  POKE 1403,10: PRINT "(4). Add a data point": POKE 1403,10: PRINT "(5). Delete a
      column of data": PRINT
3025  PRINT "WHICH OPTION ? (0-5): ";
3030  GET KS$:WO% = ASC (KS$) - 48: IF WO% < 0 OR WO% > 5 THEN 3030
3032  IF WO% = 1 AND MAX < = 1 THEN 3030: REM don't need to choose ion signal if only one
      ion monitored
3035  PRINT WO%: IF WO% = 0 THEN RETURN
3040  ON WO% GOSUB 3100,3200,3300,3400,3500
3045  RC$ = "N": GOTO 3005
3090  RETURN
3100  REM choose ion signal for rate calculation
3110  HD$ = "SELECT ION SIGNAL FOR RATE CALCULATION:":UD$ = "------ --- ------ --- ----
      ----------": GOSUB 3600: PRINT : PRINT "Which ion signal Y ? (1-";MAX;"): ";
3120  GET KS$:YU% = ASC (KS$) - 48: IF YU% < 1 OR YU% > MAX GOTO 3120
3130  PRINT YU%: PRINT : PRINT " (Press any key to proceed): ";: GET KS$: FOR I = 1 TO
      PTS:Y(I) = 0: IF YP(I,YU%) > = 1 THEN Y(I) = LOG (YP(I,YU%))
3140  NEXT : RETURN
3200  REM Edit data point
3210  HD$ = "EDIT DATA POINT:":UD$ = "---- ---- -----": GOSUB 3600: PRINT : PRINT
      "Which point ? (0 - ";PTS;") ";: INPUT " <0 = esc>: ";WP: IF WP > PTS OR WP < = 0
      THEN RETURN
3220  PRINT : PRINT "Change X ? <";XP(WP);"> (Y/N): ";
3230  GET KS$: IF KS$ < > "Y" AND KS$ < > "N" GOTO 3230
3240  PRINT KS$: IF KS$ = "Y" THEN INPUT "Enter new value <-1 to escape>: ";X: IF X > -
      0.0001 THEN XP(WP) = X
3250  FOR J = 1 TO MAX: PRINT : PRINT "Change Y";J;" ? <";YP(WP,J);"> (Y/N): ";
3260  GET KS$: IF KS$ < > "Y" AND KS$ < > "N" GOTO 3260
3270  PRINT KS$: IF KS$ = "Y" THEN INPUT "Enter new value <-1 to escape>: ";Y: IF Y > -
      0.0001 THEN YP(WP,J) = Y
3280  NEXT : RETURN
3300  REM delete a data point
3310  HD$ = "DELETE DATA POINT:":UD$ = "------ ---- -----": GOSUB 3600: PRINT : PRINT
      "Which point ? (0 - ";PTS;") ";: INPUT "<0 = esc>: ";WP: IF WP > PTS OR WP < 1 THEN
      RETURN
3320  FOR I = WP TO PTS - 1:XP(I) = XP(I + 1):Y(I) = Y(I + 1): FOR J = 1 TO MAX:YP(I,J) = YP(I +
      1,J): NEXT : NEXT :PTS = PTS - 1: GOTO 3310
```

```
3400  REM add a data point
3410  HD$ = "ADD A DATA POINT":UD$ = "--- - ---- -----": GOSUB 3600: PRINT : INPUT
      "Enter X-value <-1 to escape>: ";X: IF X < - 0.0001 THEN  RETURN
3420  PTS = PTS + 1: IF PTS > 25 THEN  PRINT : PRINT "FILE EXCEEDS MAX. ALLOWABLE
      SIZE !!": PRINT "(Press any key to continue): ";: GET KS$:PTS = 25: RETURN
3430  XP(PTS) = X: PRINT : FOR J = 1 TO MAX: PRINT "Enter Y";J;: INPUT ": ";YP(PTS,J): NEXT :
      GOTO 3410
3500  IF MAX < = 1 THEN  RETURN : REM delete a column of data
3510  HD$ = "DELETE A COLUMN OF DATA:":UD$ = "------ - ------ -- ----": GOSUB 3600:
      PRINT : PRINT "Which data column ? (Y = 0 to ";MAX;: INPUT ")  <0 = esc>: ";WC%:
      PRINT : PRINT "Sure about that ? (Y/N): ";
3520  GET KS$: IF KS$ < > "Y" AND KS$ < > "N" GOTO 3520
3525  PRINT KS$: IF KS$ = "N" GOTO 3510
3526  IF WC% < = 0 OR WC% > MAX THEN  RETURN
3530  MAX = MAX - 1: FOR J = WC% TO MAX: FOR I = 1 TO PTS:YP(I,J) = YP(I,J + 1): NEXT :
      NEXT : IF YU% < = MAX THEN  RETURN
3540  YU% = MAX: FOR I = 1 TO PTS:Y(I) = 0: IF YP(I,YU%) > = 1 THEN Y(I) =  LOG
      (YP(I,YU%))
3550  NEXT : RETURN
3600  REM list data file contents
3605  ST = 1:FI = PTS: IF FI > 15 THEN FI = 15
3610  HOME : PRINT HD$: PRINT UD$: PRINT : PRINT "   X";: FOR J = 1 TO MAX: POKE
      1403,(10 * (J + 1)): PRINT " Y";J;: NEXT : PRINT : FOR I = ST TO FI:QX = 2 -  INT (( LOG (I) /
      LOG (10)) + 0.0001): POKE 1403,QX: PRINT I;".  ";XP(I);
3620  FOR J = 1 TO MAX: POKE 1403,(10 * (J + 1)): PRINT YP(I,J);: NEXT : PRINT : NEXT : IF FI >
      = PTS THEN  RETURN
3630  FI = PTS:ST = FI - 15: GET KS$: GOTO 3610
4000  REM setup rate variables
4002  VN$(1) = "Run number":RG$(1) = "(1-30)":VN$(2) = "Date":RG$(2) = "":VN$(3) = "Portal
      no. ":RG$(3) = "(1 - 2)":VN$(4) = "Neutral vol.":RG$(4) = "(100-9000)":VN$(5) = "T
      (degrees C)":RG$(5) = "(0 - 50)"
4004  VN$(6) = "Tube pressure":RG$(6) = "(0.1 - 1.0)":VN$(7) = "Tylan flow value":RG$(7) = "(1
       - 400)":VN$(8) = "Reaction title":RG$(8) = "":VN$(9) = "Ion mass (amu)":RG$(9) = "(1 -
      500)":VN$(10) = "Carrier gas":RG$(10) = "(H2/HE/N2/AR)"
4005  VN$(11) = "Comments":RG$(11) = "": IF RF$ = "Y" GOTO 4500: REM vbles already
      initialised; adjust
4010  HOME : PRINT "INITIALISE RATE VARIABLES:": PRINT "---------- ---- ---------": PRINT
      : FOR I = 1 TO 11:KS$ =  CHR$ (I + 64): PRINT KS$;".  ";VN$(I);"  ";RG$(I);: POKE 1403,40:
      INPUT ":  ";RV$(I):QV(I) =  VAL (RV$(I)): NEXT
4020  HOME : PRINT "RATE VARIABLES:": PRINT "---- ---------": PRINT : GOSUB 4800:
      PRINT : PRINT : PRINT "(Press any key to proceed): ";: GET KS$:RF$ = "Y": FOR I = 1 TO
      11:VN$(I) = "":RG$(I) = "": NEXT : RETURN
4500  REM adjust rate variables
4510  HOME : PRINT "EDIT RATE VARIABLES:": PRINT "---- ---- ---------": PRINT : GOSUB
      4800: PRINT : PRINT "Change which value ? (A-K) (N to quit): ";
4540  GET KS$:CV% =  ASC (KS$) - 64: IF CV% < 1 OR (CV% > 11 AND KS$ < > "N") GOTO
      4540
4550  PRINT KS$: IF KS$ < > "N" THEN  PRINT : PRINT KS$;".  ";VN$(CV%);"
      ";RG$(CV%);" <";RV$(CV%);: INPUT ">: ";RV$(CV%):QV(CV%) =  VAL (RV$(CV%)):
      GOTO 4510: REM redisplay
4560  FOR I = 1 TO 11:VN$(I) = "":RG$(I) = "": NEXT :RC$ = "N": RETURN
4800  FOR I = 1 TO 11:KS$ =  CHR$ (I + 64): PRINT KS$;".  ";VN$(I);: POKE 1403,22: PRINT " =
      ";RV$(I): NEXT : PRINT : RETURN : REM display rate variables
```

```
5000  REM setup log graph
5010  TEXT : HOME
5020  IF PTS < 1 THEN  PRINT : VTAB (11): HTAB (25): PRINT "PLEASE LOAD A DATA FILE
      !": HTAB (25): PRINT "(Press any key ...)";: GET KS$: RETURN
5030  PRINT "DRAW LOG GRAPH:": PRINT "---- --- -----": PRINT
5040  MX = 0:MY = O:MN = 20
5050  FOR I = 1 TO PTS
5060  IF MX < XP(I) THEN MX = XP(I)
5070  IF Y(I) < 0 GOTO 5100
5080  IF MY < Y(I) THEN MY = Y(I)
5090  IF MN > Y(I) THEN MN = Y(I)
5100  NEXT
5110  XS = 240 / MX
5120  YS = 160 / (MY - MN)
5300  GOSUB 9000
5310  REM draw graph
5400  PRINT : VTAB (11): PRINT "Dump graph on printer ? (Y/N): ";
5410  GET KS$: IF KS$ < > "Y" AND KS$ < > "N" GOTO 5410
5420  PRINT KS$
5430  IF KS$ = "N" GOTO 5500
5440  PRINT CD$;"PR#1"
5450  PRINT CHR$ (9);"G2"
5490  PRINT CD$;"PR#3"
5500  RETURN
6000  REM calculate rate constant
6010  HOME
6015  IF PTS < 1 THEN  PRINT : VTAB (12): POKE 1403,30: PRINT "LOAD SOME DATA !!":
      POKE 1403,30: PRINT "(Press any key...) ";: GET KS$: RETURN
6020  IF RF$ = "N" THEN  PRINT : VTAB (12): POKE 1403,25: PRINT "INITIALISE RATE
      VARIABLES !!": POKE 1403,25: PRINT "(Press any key ...) ";: GET KS$: RETURN
6025  RC$ = "Y": IF YU% = 0 THEN YU% = 1
6030  PRINT "RATE COEFFICIENT CALCULATION:": PRINT "---- ---------- ----------":
      PRINT
6050  GOSUB 7000: REM initialise constants & physical parameters
6060  GOSUB 7200: REM determine ion velocity IVEL
6070  GOSUB 7400: REM determine SLOPE ( d ln[ion]/d [react. neutral] ) by least-squares analysis
6080  GOSUB 7600: REM determine correction factor CTWO to compensate for off-axis ion
      diffusion
6090  GOSUB 7700: REM determine effective reaction distance ZEFF
6100  K =  - (SLOPE * IVEL) / (CTWO * ZEFF)
6110  GOSUB 8000: REM determine correction for non-uniform velocity profile
6120  GOSUB 8200: REM determine axial diffusion correction
6150  GOSUB 8600: REM package results for printout
6400  GOSUB 8800: REM display & print results
6500  RETURN
7000  REM initialise constants & parameters
7010  PI = 3.1415926:TUBERAD = 3.66:Z(1) = 70.9:Z(2) = 42.9:VELCRR = 4.0 / 3.0:JZERO = 2.405
7020  RU% =  INT (QV(1) + 0.5):DAY$ = RV$(2):PO% =  INT (QV(3) + 0.5):NVOL = QV(4):TGAS
      = QV(5) + 273.16:PBUFF = QV(6)
7030  TYFLOW = QV(7):TITLE$ = RV$(8):IMASS = QV(9):CARRIER$ = RV$(10):COMMENTS$
      = RV$(11)
7040  IF COMMENTS$ < > "" THEN COMMENTS$ = "(" + COMMENTS$ + ")"
```

```
7060  IF CARRIER$ < > "H2" AND CARRIER$ < > "N2" AND CARRIER$ < > "AR" THEN
      CARRIER$ = "HE"
7190  RETURN
7200  REM  DETERMINE ION VELOCITY VION
7210  IF CARRIER$ = "H2" THEN G1AS = 8.75E - 05:GMASS = 2.0159:POL = 0.79:F1LOWCRR =
      8.4:F2LOWCRR = 0.2968
7220  IF CARRIER$ = "HE" THEN G1AS = 1.94E - 04:GMASS = 4.0026:POL = 0.199:F1LOWCRR =
      11.7:F2LOWCRR = 0.4353
7230  IF CARRIER$ = "N2" THEN G1AS = 1.76E - 04:GMASS = 28.014:POL = 1.76:F1LOWCRR =
      9.703:F2LOWCRR = 1.0 / 1.754
7240  IF CARRIER$ = "AR" THEN G1AS = 2.217E - 04:GMASS = 39.948:POL = 1.60:F1LOWCRR =
      9.703:F2LOWCRR = 1.44 / 1.754
7310  QBUFF = F1LOWCRR + (TYFLOW * F2LOWCRR)
7320  VBUFF = (QBUFF / (PI * TUBERAD * TUBERAD)) * (760 / PBUFF) * (TGAS / 273.16)
7330  IVEL = VELCRR * VBUFF
7340  VISC = G1AS *  SQR (TGAS / 273.16)
7350  YMFP = 8.59 * VISC *  SQR (TGAS / GMASS)
7390  RETURN
7400  REM determine SLOPE
7405  BMEAN = 0
7410  FOR I = 1 TO PTS
7420  PREACT = (XP(I) * NVOL) / (VBUFF * PI * TUBERAD * TUBERAD)
7430  RCNC(I) = PREACT * (273.16 / TGAS) * 3.5351E + 16
7435  BMEAN = BMEAN + RCNC(I)
7440  NEXT
7445  BMEAN = BMEAN / PTS: REM average neutral reactant concn. during run
7450  REM least squares analysis
7460  A = 0:B = 0:C = 0:D = 0:E = 0:W1 = 0:W2 = 0:W3 = 0:SLOPE = 0:I1NTERCEPT = 0
7470  FOR I = 1 TO PTS
7475  RCNC(I) = RCNC(I) * 1E - 10
7480  A = A + RCNC(I):B = B + Y(I):C = C + RCNC(I) * RCNC(I):D = D + Y(I) * Y(I):E = E +
      RCNC(I) * Y(I)
7485  RCNC(I) = RCNC(I) * 1E + 10
7490  NEXT
7500  W1 = PTS * C - A * A:W2 = PTS * D - B * B:W3 = PTS * E - A * B
7510  SLOPE = (W3 / W1) * 1E - 10
7520  I1NTERCEPT = (B * C - A * E) / W1
7530  REM determine accuracy of fit
7540  ZAP = (PTS * D) - (B * B) - (W3 / W1 * W3):ZAP =  SQR (ZAP * ZAP):SIG =  SQR (ZAP):
      COMP = 2 * SIG / PTS:MIC = (PTS - 2.0) * W1:Z1 = SIG /  SQR (MIC):Z2 = SIG *  SQR (C) /
      SQR (PTS * MIC)
7550  S1 = - Z1 / SLOPE
7560  I2 = Z2 / I1NTERCEPT
7590  RETURN
7600  REM determine CTWO
7610  RMOB = (13.876 /  SQR (POL)) *  SQR ((IMASS + GMASS) / (IMASS * GMASS))
7650  DFFCO = (RMOB * 0.02354) * (760 / PBUFF) * (TGAS / 273.16)
7660  CTWO = 1 - 2 * ((DFFCO * JZERO / (TUBERAD * IVEL)) ^ 2) + 6 * ((DFFCO * JZERO /
      (TUBERAD * IVEL)) ^ 4)
7690  RETURN
7700  REM determine ZEFF
7760  ZEFF = Z(PO%) - (0.0 * PBUFF)
7790  RETURN
```

```
8000  REM  NON-UNIFORM VELOCITY CORRECTION
8010  W = 2 / (1 + (5.52 * YMFP / (PBUFF * TUBERAD)))
8020  BEE = 1 + (2.76 * YMFP / (PBUFF * TUBERAD))
8030  ELL = (0.25 - BEE) * (0.1 - 0.6 * BEE) - ((0.15 - 0.75 * BEE) ^ 2)
8040  EMM = 1.6 * BEE - 0.4
8050  ENN = 0.025 - 0.075 * BEE
8060  GAMMA = ( - 1 / (2 * ELL)) * (ENN - ((2 * EMM * ENN + 6.4 * ELL) / (2 *  SQR (EMM *
      EMM - 32 * ELL))))
8070  NUNVELCO = W / GAMMA
8080  K1 = K * NUNVELCO
8190  RETURN
8200  REM  AXIAL DIFFUSION
8210  DLTA = (1 / (2 * ELL)) * (EMM -  SQR (EMM * EMM - 32.0 * ELL))
8220  L2AMBDA = ((DLTA / (W * TUBERAD * TUBERAD)) + ((GAMMA / W) * K * BMEAN /
      DFFCO)) / VBUFF
8230  EPSIL = L2AMBDA * DFFCO * DFFCO / IVEL
8240  AXDFCO = 1 / (1 - EPSIL)
8250  K2 = K1 * AXDFCO
8260  K2 = K2 * 0.8186: REM Correction factor (3/7/89)
8390  RETURN
8600  REM package results for printout
8610  K2 = K2 * 1E15
8620  EK% =  - 15
8630  K2 = K2 / 10:EK% = EK% + 1: IF K2 >  = 10 GOTO 8630
8640  S1 =  INT (S1 * (K2 / 1E10) * 10000 + 0.5) / 10000:K2 =  INT (K2 * 1000 + 0.5) / 1000
8650  I2 =  INT (I2 * I1NTERCEPT * 10000 + 0.5) / 10000:I1NTERCEPT =  INT (I1NTERCEPT * 1000
      + 0.5) / 1000:I3 =  INT ( EXP (I1NTERCEPT) * 10 + 0.5) / 10
8660  I4 =  INT (( EXP (I1NTERCEPT - I2) -  EXP (I1NTERCEPT)) * 10 + 0.5) / 10
8670  I4 =  ABS (I4)
8790  RETURN
8800  REM ** DISPLAY RESULTS **
8805  HOME : PRINT "RATE COEFFICIENT:": PRINT "---- ----------": PRINT
8810  PRINT "k       = ";K: PRINT "k (corr)  = ";K2;"E";EK%: PRINT
8815  PRINT "Intercept = ";I1;" ln. counts ": PRINT "         = ";I3: PRINT : PRINT : PRINT
8820  PRINT "DO YOU WANT A PRINTOUT ? (Y/N): ";
8825  GET PT$: IF PT$ <  > "Y" AND PT$ <  > "N" GOTO 8825
8830  PRINT PT$: IF PT$ = "N" GOTO 8990
8850  HOME : PRINT  CHR$ (4);"PR#1": PRINT : PRINT "----------------------------------------
      ----------": PRINT : PRINT : PRINT "RATE COEFFICIENT:": PRINT
      "---- ----------":  PRINT
8855  PRINT TITLE$;"       m/z = ";IMASS
8860  PRINT "Date: ";DAY$;"       Run #";RU%;"       Data file ";DF$: PRINT COMMENTS$
8870  PRINT "T = "; INT (TGAS * 10 + 0.5) / 10;" K          P = "; INT (PBUFF * 10000 + 0.5) /
      10000;" Torr of ";CARRIER$;" (Tylan flow = "; INT (TYFLOW + 0.5);")"
8875  PRINT "Portal ";PO%;"          Neutral vol = "; INT (10 * NVOL + 0.5) / 10;" cm^3"
8878  PRINT "Corrected reaction distance = "; INT (ZEFF * 10 + 0.5) / 10;" cm"
8880  PRINT : PRINT "Neutral flow  |  Ion signal": PRINT "  (torr/s)    |      ": PRINT "----------
      -- | --------------"
8890  FOR I = 1 TO PTS
8895  PRINT " ";: HTAB (4): PRINT XP(I);: HTAB (16): PRINT "|     ";YP(I,YU%)
8900  NEXT
8910  PRINT : PRINT : PRINT "k       = ";K: PRINT "k (corr)  = (";K2;" +/- ";S1;")E";EK%;"cm^3
      molec^-1 s^-1": PRINT
```

```
8920  PRINT "Intercept = ";I1;" +/- ";I2;" ln. counts": PRINT "        = ";I3;" +/- ";I4;" ion counts"
8930  PRINT : PRINT : PRINT  CHR$ (4);"PR#3"
8990  RETURN
9000  REM graphics
9005  HOME
9010  PRINT  CHR$ (17);"e0"
9020  HGR2 : HCOLOR= 3
9030  HPLOT 20,3 TO 20,165 TO 262,165: HPLOT 18,5 TO 22,5: HPLOT 260,163 TO 260,167
9040  FOR I = 1 TO PTS:YC = 165 -  INT (YS * (Y(I) - MN) + 0.5):XC = 20 +  INT (XS * XP(I) + 0.5)
9050  HPLOT XC,YC - 2 TO XC,YC + 2: HPLOT XC - 2,YC TO XC + 2,YC: NEXT : REM setup
      coordinates of points
9070  IF RC$ <  > "Y" THEN  GET KS$: PRINT KS$: TEXT : PRINT  CHR$ (4);"PR#3": RETURN
9075  REM setup calculated decay curve
9080  XM = RCNC(1): FOR I = 1 TO PTS: IF RCNC(I) > XM THEN XM = RCNC(I)
9090  NEXT
9100  FOR I = 1 TO 48:DB = I * XM / 48.0:DA = I1NTERCEPT + SLOPE * DB:CD = 165 -  INT (YS *
      (DA - MN) + 0.5)
9110  XV = 20 + (5 * I): IF CD > 4 AND CD < 166 THEN  HPLOT XV,CD
9120  NEXT
9200  GET KS$: PRINT KS$: TEXT : PRINT  CHR$ (4);"PR#3"
9500  RETURN
```

Program "MULE"

```
1       REM ** PROGRAM MULE **
2       PRINT  CHR$ (4);"PR#3"
3       PRINT  CHR$ (4);"BRUN LOMEM:": &  LOMEM: 16384
4       CD$ =  CHR$ (13) +  CHR$ (4)
6       CC$ =  CHR$ (9)
7       POKE 7,0: POKE 8,0
8       GOSUB 9000: REM input default filenames
13      DIM  AX(50),AY(50),AZ(65): DIM  B(50),C(50),D(50),T(50): DIM
        A(20),S(20),V(20),X(20),Y(20),P(21,20)
17      HGR : HCOLOR= 1:X = 0:Y = 0: TEXT :XAXIS = 270:YAXIS = 180:BASE = 2
20      HOME : GOSUB 900: REM input data
25      GOSUB 1200: REM calculation of weights
30      HOME : GOSUB 1250: REM input of trial values
35      GOSUB 1600: REM loading of initial simplex points
40      GOSUB 1800: REM calculation of initial simplex values
45      GOSUB 2000: REM set expansion & contraction parameters
50      GOSUB 2200: REM find highest & lowest points and simplex centroid
55      GOSUB 2400: REM iteration to improve simplex
60      GOSUB 2800: REM check if minimum reached: if so, produce output; otherwise repeat
        iteration
65      IF C3 = 0 GOTO 50
70      GOSUB 3000
75      IF K$ = "D" GOTO 20
80      IF K$ = "T" GOTO 30
900     REM  INPUT OF DATA
901     JP = 0
910     HOME : PRINT "MULE: MULTIPLE EXPONENTIAL FITTING": PRINT "----  -------- -------
        ---- -------": PRINT : PRINT "LOAD DATA FILE:": PRINT : PRINT
920     PRINT "CURRENT DATA FILENAME IS ";DF$: PRINT : PRINT "CHANGE THIS ?
        (Y/N): ";
925     GET KS$: IF KS$ <  > "Y" AND KS$ <  > "N" THEN 925
930     PRINT KS$: IF KS$ <  > "Y" GOTO 940
935     PRINT : INPUT "ENTER NEW FILENAME (N=leave unchanged/NONE=escape): ";KS$
936     IF KS$ = "NONE" GOTO 1028
937     IF KS$ <  > "N" THEN DF$ = KS$
940     PRINT : PRINT : PRINT "PROCEED ? (Y/N): ";
945     GET KS$: IF KS$ <  > "Y" AND KS$ <  > "N" THEN 945
950     PRINT KS$: IF KS$ = "N" THEN 910
960     HOME : PRINT : VTAB (12): POKE 1403,20: PRINT "READING FILE ";DF$;" NOW ..."
1000    PRINT  CD$;"OPEN  ";DF$;",D2"
1007    PRINT CD$;"READ  ";DF$
1008    INPUT L
1009    INPUT M
1010    FOR A = 1 TO L
1011    INPUT C(A): INPUT T(A)
1015    NEXT
1016    PRINT  CD$;"CLOSE"
1018    GOSUB 18000: GOTO 1065
1028    I = 0
1029    I = I + 1
1030    INPUT "FLOW(TORR/S) ? ";T(I)
```

```
1035  IF T(I) < 0 THEN L = I - 1: GOSUB 18000:DF$ = "": HOME : GOTO 1065
1040  INPUT "ION COUNT    ? ";C(I)
1045  PRINT : GOTO 1029
1065  RETURN
1200  REM  CALCULATION OF WEIGHTS
1210  FOR I = 1 TO L:B(I) = 100 / D(I): NEXT : RETURN
1250  REM  INPUT OF TRIAL VALUES
1252  HOME :NF = 0: PRINT : PRINT
1255  PRINT "INPUT OF TRIAL VALUES:": PRINT "----- -- ----- ------": PRINT : PRINT
1260  PRINT "PRE-EXP(Ai) AS THE PRE-EXPONENTIAL FACTOR OF DECAY #i": PRINT :
      PRINT "SLOPE(Ki) AS THE RATE COEFF. (cm3/molec.s) OF DECAY #i"
1270  PRINT "STEP OF Ai & Ki AS A PERCENTAGE 1-25%; ie ENTER A VALUE IN THE
      RANGE 1-10": PRINT : PRINT "ENTER INTERCEPT AS 0 TO FINISH INPUT OF TRIAL
      RATE VARIABLES"
1400  PRINT : PRINT :PE = 1:I =  - 1
1425  I = I + 2: PRINT "ENTER TRIAL VALUES FOR DECAY #";PE: PRINT : PRINT : INPUT
      "PRE-EXP (Ai)   ?";A(I): IF A(I) = 0 GOTO 1452
1430  INPUT "SLOPE   (Ki)   ?";A(I + 1): INPUT "STEP OF Ai     ?";S(I): INPUT "STEP OF Ki
      ?";S(I + 1)
1440  PRINT :PE = PE + 1: GOTO 1425
1452  PRINT : INPUT "TORR/S TO MOLEC.S/CM3 CONVERSION VALUE  ?";CV
1455  M = I:N = I - 1: GOSUB 7000: GOSUB 8000:L1 = L - N: IF L1 <  = 0 THEN  PRINT
      "INSUFFICIENT DATA POINTS !!": PRINT
1490  RETURN
1600  GOSUB 6200: RETURN : REM loading of initial simplex points
1800  REM  CALCULATION OF INITIAL SIMPLEX VALUES
1805  FOR I = 1 TO M
1810  FOR J = 1 TO N:A(J) = P(I,J): NEXT
1820  GOSUB 6500: GOSUB 5200:Y(I) = X1
1830  NEXT
1840  RETURN
2000  A1 = 1:B1 = 0.5:G1 = 2:C1 = 0:C9 = 1E - 04: RETURN : REM set expansion & contraction
      parameters
2200  REM find highest & lowest points and simplex centroid
2210  C1 = C1 + 1:J1 = 1:K1 = 1
2220  FOR I = 2 TO M
2230  IF Y(I) >  = Y(J1) THEN J1 = I
2240  IF Y(I) <  = Y(K1) THEN K1 = I
2250  NEXT
2260  FOR J = 1 TO N:X(J) = 0
2270  FOR I = 1 TO M: IF I <  > J1 THEN X(J) = X(J) + P(I,J)
2280  NEXT
2290  X(J) = X(J) / N
2300  NEXT
2310  RETURN
2400  REM iteration to improve simplex
2410  FOR I = 1 TO N:V(I) = ((1 + A1) * X(I)) - (A1 * P(J1,I)): NEXT
2420  GOSUB 5600: GOSUB 5200:Y1 = X1: IF Y1 > Y(K1) GOTO 2485
2430  FOR I = 1 TO N:A(I) = ((G1 + 1) * V(I)) - (G1 * X(I)): NEXT
2440  GOSUB 5200:Y2 = X1: IF Y2 > Y(K1) GOTO 2520
2450  GOSUB 5800:Y(J1) = Y2: GOTO 2650
2485  J2 = 0
2490  FOR I = 1 TO M: IF I <  > J1 AND Y1 <  = Y(I) THEN J2 = J2 + 1
```

```
2500  NEXT
2510  IF J2 = 0 GOTO 2540
2520  GOSUB 5600: GOSUB 5800:Y(J1) = Y1: GOTO 2650
2540  IF Y1 < = Y(J1) THEN  GOSUB 5600: GOSUB 5800:Y(J1) = Y1
2550  FOR I = 1 TO N:A(I) = (B1 * P(J1,I)) + ((1 - B1) * X(I)): NEXT
2560  GOSUB 5200:Y1 = X1: IF Y1 < = Y(J1) THEN  GOSUB 5800:Y(J1) = Y1: GOTO 2650
2605  FOR I = 1 TO N:A(I) = P(K1,I): NEXT
2610  FOR I = 1 TO M
2620  FOR J = 1 TO N:P(I,J) = (P(I,J) + A(J)) / 2: NEXT
2630  NEXT
2640  GOSUB 1800
2650  RETURN
2800  REM  CHECK IF MINIMUM REACHED
2810  Y1 = Y(K1): GOSUB 5500: GOSUB 20000:NF = NF + 2: IF C1 < = 1 THEN Y5 = Y1:K8 = 0:Y4 =
      Y1:C3 = 0: GOTO 2950
2820  IF (R2 * 0.95 > Y(K1)) OR (R2 > R1) THEN C3 = 1: GOTO 2950
2830  IF C1 > 100 THEN C3 = 2: GOTO 2950
2840  IF  ABS (Y5 - Y1) > 0.01 THEN K8 = 0:Y5 = Y1: GOTO 2950
2850  K8 = K8 + 1: IF K8 > 6 THEN C3 = 3: GOTO 2950
2860  Y5 = Y1
2945  Y5 = Y1
2950  IF C3 = 1 THEN  INPUT "END OF ITERATION.  PRESS RETURN FOR OUTPUT MENU.";
      A$
2951  IF C3 = 2 THEN  INPUT "TOO MANY ITERATIONS.  PRESS RETURN FOR OUTPUT
      MENU";A$
2952  IF C3 = 3 THEN  INPUT "CHANGE DURING LAST ITERATION TOO SMALL.  PRESS
      RETURN FOR OUTPUT MENU";A$
2960  RETURN
3000  REM  OUTPUT OF RESULTS
3005  GOTO 3097
3010  GOSUB 2200: VTAB (9 + N): IF C3 > = 1 THEN  PRINT "ITERATION SUCCESSFUL"
3020  GOSUB 2200: VTAB (9 + N): IF C3 > 1 OR C3 < 3 THEN  PRINT "ITERATION
      SUCCESSFUL": GOTO 3079
3030  PRINT "ITERATION UNSUCCESSFUL": PRINT : PRINT : IF C3 = 2 THEN  PRINT "TOO
      MANY ITERATIONS REQUIRED"
3040  IF C3 = 3 THEN  PRINT "CHANGE DURING LAST ITERATION TOO SMALL"
3050  IF C3 = 4 THEN  PRINT "ZERO VALUE MISMATCH"
3060  IF C3 > 4 THEN  PRINT "REASON FOR FAILURE UNKNOWN"
3079  AS = C1 - 1: PRINT "NO. OF ITERATIONS = ";AS: PRINT : PRINT "IMPROVED FROM
      INITIAL FIT OF ";Y4: IF ZQ = 1 THEN  GOTO 3144
3097  GOSUB 9999: HOME : IF SS = 2 THEN  GOSUB 13000
3100  IF SS = 1 THEN  GOSUB 12000
3102  IF SS < 3 GOTO 3097
3104  GOTO 3247
3105  PRINT "ITERATED VALUES:": PRINT "-------- ------": PRINT : PRINT :EP = 0
3110  FOR I = 1 TO N STEP 2:EP = EP + 1:A(I) = P(K1,I):A(I + 1) = P(K1,I + 1): VTAB (6 + I): POKE
      1403,0: PRINT " (";EP;")  |";: POKE 1403,8: PRINT A(I);: POKE 1403,22: PRINT " | ";A(I + 1)
      / CV: NEXT
3120  VTAB (4): PRINT "DECAY | PRE-EXP FACTOR |    SLOPE": PRINT "      | (ION COUNTS)
      | (CM3/MOLEC.S)": PRINT "------|---------------|--------------": PRINT :ZQ = 1: GOTO
      3010
3144  PRINT : PRINT "THESE VALUES GIVE A FIT OF ";Y(K1): GOSUB 11000: IF PZ = 1 THEN
      HOME : GOTO 3105
```

```
3150  GOTO 3097
3170  HOME
3171  PRINT "DATA TABLE:": PRINT "---- -----": PRINT : PRINT "FLOW     FITTED CTS EXPTL
      CTS   WEIGHT": PRINT "-----------------------------------":JG = 0
3180  FOR J = 1 TO L: GOSUB 5400:A = 5:JG = JG + (Z - C(J)) * (Z - C(J)): VTAB (A + J): POKE
      1403,0: PRINT T(J);: POKE 1403,9: PRINT Z;: POKE 1403,15: PRINT "     ";C(J);: POKE
      1403,29: PRINT "  ";D(J);: POKE 1403,35: PRINT "  ": NEXT
3202  PRINT : PRINT : PRINT "FLOW IN TORR/S     RMS(diff) = "; SQR (JG / L):PRINT:PRINT:
      GOSUB 11000: IF PZ = 1 GOTO 3170
3210  GOTO 3097
3220  HOME : INPUT "ERROR !!!   PRESS RETURN ";A$
3247  HOME : PRINT : VTAB (10): POKE 1403,20: PRINT "1.   GENERATE MORE OUTPUT":
      PRINT : POKE 1403,20: PRINT "2.   SET NEW TRIAL VALUES": PRINT : POKE 1403,20:
      PRINT "3.   LOAD A NEW DATA FILE": PRINT : POKE 1403,20: PRINT "4.   QUIT"
3250  PRINT : PRINT : POKE 1403,20: PRINT "WHICH OPTION ? (1-4): ";
3255  GET KS$:OP% =  ASC (KS$) - 48: IF OP% < 1 OR OP% > 4 GOTO 3255
3260  PRINT OP%: PRINT : POKE 1403,20: PRINT "SURE ABOUT THAT ? (Y/N): ";
3265  GET KS$: IF KS$ <  > "Y" AND KS$ <  > "N" GOTO 3265
3270  PRINT KS$: IF KS$ = "N" GOTO 3247
3275  IF OP% = 1 GOTO 3097
3280  IF OP% = 2 THEN K$ = "T": RETURN
3285  IF OP% = 3 THEN K$ = "D": RETURN
3290  IF OP% = 4 THEN  PRINT CD$;"RUN OPTIONS,D1"
5200  REM calculation of simplex value
5210  X1 = 0
5220  FOR J = 1 TO L: GOSUB 5400:X1 = X1 + (Z - C(J)) * (Z - C(J)) * B(J): NEXT
5230  X1 =  SQR (X1 / L1): RETURN
5400  REM calculation of function
5410  Z = 0
5420  FOR K = 1 TO N STEP 2:Z = Z + (A(K) *  EXP (A(K + 1) * T(J))): NEXT
5430  RETURN
5500  REM  RMS
5510  Z5 = 0:X4 = 0:X6 = 0
5520  FOR K = 1 TO L:Z5 = 0
5530  FOR F = 1 TO N STEP 2:Z5 = Z5 + P(K1,F) *  EXP (T(K) * P(K1,F + 1)): NEXT
5540  X6 = X6 + C(K) * C(K):X4 = X4 + (Z5 - C(K)) * (Z5 - C(K)): NEXT
5550  R1 =  SQR (X4 / L):R2 =  SQR ( SQR (X6 / L)): RETURN
5600  FOR I = 1 TO N:A(I) = V(I): NEXT : RETURN : REM rearrangement of curve fitting
      parameters
5800  FOR I = 1 TO N:P(J1,I) = A(I): NEXT : RETURN : REM insertion into simplex of new values
5900  PRINT "** DATAFILE ";DF$;" **": PRINT : RETURN
6000  J1 = 0: IF I <  > 1 THEN J1 =  INT (10 *  RND (I + J)): IF J1 - 5 >  = 0 THEN J1 = 5 - J1
6010  RETURN : REM random no. generator for simplex loading
6100  XL = 0: REM sum Ai
6110  FOR K = 1 TO N STEP 2:XL = XL + A(K): NEXT : RETURN
6200  FOR I = 1 TO M: REM loading of ordered initial simplex
6210  FOR J = 1 TO N:P(I,J) = A(J): IF I <  > 1 AND I = J + 1 THEN P(I,J) = P(I,J) + S(J)
6220  NEXT
6230  NEXT : RETURN
6300  FOR A = 1 TO L: IF T(A) = 0 THEN XG = A: REM find C(I) at zero flow
6310  NEXT : RETURN
6400  FOR I = 1 TO M: REM lo ading of random initial simplex
6410  FOR J = 1 TO N: GOSUB 6000:P(I,J) = A(J) + (J1 * S(J)): NEXT
```

```
6420  NEXT : RETURN
6500  GOSUB 6300: GOSUB 6100:XF =  ABS (C(XG) - XL) * 2 / N: REM  improve Ai
6510  FOR K = 1 TO N STEP 2:A(K) = A(K) - XF: IF (C(XG) - XL) > 0 THEN A(K) = A(K) + XF
6520  NEXT : RETURN
6699  HOME
6700  PRINT "DATAFILE NAME: ";DF$: PRINT "-------- ----": PRINT : PRINT "INITIAL TRIAL
      VALUES": PRINT "------- ----- ------":PRINT : PRINT "DECAY | PRE-EXP FACTOR |
      SLOPE": PRINT "------|---------------|------------------": PRINT "     | VALUE  | STEP |
      VALUE   | STEP"
6710  PRINT "      |(ION CTS)|  (%) |(CM3/MOLEC.S)|  (%)": PRINT "------|---------|------|------
      -------|-----":EP = 0
6720  FOR I = 1 TO N STEP 2:EP = EP + 1: PRINT "     |       |     |          |": PRINT " (";EP;")
      |";W(I);: POKE 1403,15: PRINT " |  ";E(I);: POKE 1403,22: PRINT " | ";W(I + 1);: POKE
      1403,36: PRINT " |  ";E(I + 1): NEXT
6730  PRINT : PRINT "TORR/S TO MOLEC.S/CM3 CONVERSION VALUE IS ";CV:LL = 1:
      GOSUB 11000: HOME : IF PZ = 1 GOTO 6700
6740  RETURN
7000  PRINT : PRINT "DISPLAY AND/OR EDIT TRIAL VALUES ? (Y/N): ";: REM edit trial
      values
7010  GET A$: IF A$ < > "Y" AND A$ < > "N" GOTO 7010
7020  PRINT A$: IF A$ = "N" GOTO 7500: REM print all trial values
7040  HOME : PRINT ;: POKE 1403,25: PRINT "TRIAL VALUES: ": POKE 1403,25: PRINT "----- --
      ----":I = 4:K = 1:T = 0
7110  VTAB (4): POKE 1403,T + 5: PRINT "DECAY ";K:K = 2 * K - 1: POKE 1403,T + 10: PRINT
      "PRE-EXP Ai ";A(K): POKE 1403,T + 10: PRINT "SLOPE   Ki ";A(K + 1): POKE 1403,T + 10:
      PRINT "STEP OF Ai ";S(K): POKE 1403,T + 10: PRINT "STEP OF Ki ";S(K +  1)
7120  K = (K + 3) / 2: IF K > N / 2 GOTO 7200
7130  T = 0: IF  INT (K - K / 2) = K / 2 THEN T = 25
7140  IF  INT (K - K / 2) < > K / 2 THEN I = I + 6
7150  GOTO 7110
7200  VTAB (21): PRINT "TORR/S TO MOLEC.S/CM3 CONVERSION FACTOR IS ";CV: PRINT
      : PRINT "EDITING REQUIRED ? (Y/N): ";
7210  GET A$: IF A$ < > "Y" AND A$ < > "N" GOTO 7210
7220  PRINT A$: IF A$ = "N" GOTO 7500: REM edit
7230  PRINT "CONVERSION VALUE (0) OR WHICH DECAY ? (1-";N / 2;")";
7240  GET KS$:P =  ASC (KS$) - 48: IF P < 0 OR P > N / 2 GOTO 7240
7250  HOME : PRINT : PRINT "EDIT TRIAL VALUES:": PRINT "---- ----- ------": IF P = 0 GOTO
      450
7260  PRINT : PRINT "DECAY ";P:P = (P * 2) - 1
7300  VTAB (5): POKE 1403,10: PRINT "(1). PRE-EXP Ai: ";A(P): POKE 1403,10: PRINT "(2).
      SLOPE   Ki: ";A(P + 1): POKE 1403,10:PRINT "(3). STEP OF Ai: ";S(P): POKE 1403,10:
      PRINT "(4). STEP OF Ki: ";S(P + 1): PRINT : PRINT "WHICH VALUE ? <0 to quit>  (0-4):
      ";
7310  GET KS$:TG% =  ASC (KS$) - 48: IF TG% < 0 OR TG% > 4 GOTO 7310
7320  PRINT TG%: IF TG% = 0 GOTO 7040
7330  VTAB (12): IF TG% = 1 THEN  INPUT "PRE-EXP Ai ?";A(P)
7340  IF TG% = 2 THEN  INPUT "SLOPE   Ki ?";A(P + 1)
7350  IF TG% = 3 THEN  INPUT "STEP OF Ai ?";S(P)
7360  IF TG% = 4 THEN  INPUT "STEP OF Ki ?";S(P + 1)
7370  GOTO 7300
7450  VTAB (12): PRINT "CONVERSION VALUE = ";CV: PRINT : INPUT "CHANGE TO      ? "
      ;CV: GOTO 7030
```

```
7500  FOR I = 1 TO N STEP 2:E(I) = S(I):E(I + 1) = S(I + 1):W(I) = A(I):W(I + 1) = A(I + 1): NEXT :
      RETURN
8000  FOR I = 1 TO N STEP 2: PRINT :A(I + 1) = A(I + 1) * CV:S(I + 1) = S(I + 1) * A(I + 1) / 100:S(I)
      = S(I) * A(I) / 100: NEXT : RETURN
9000  PRINT CD$;"OPEN FILENAMES,D2": PRINT CD$;"READ FILENAMES": INPUT DF$:
      INPUT FF$: PRINT CD$;"CLOSE FILENAMES": RETURN
9999  LL = 2: HOME :NF = 0: PRINT : VTAB (6): POKE 1403,30: PRINT "OUTPUT MENU:": POKE
      1403,30: PRINT "------ ----": VTAB (12): POKE 1403,20: PRINT "1.  DISPLAY RESULTS":
      PRINT : POKE 1403,20: PRINT "2.  GENERATE GRAPHICS": PRINT : POKE 1403,20:
      PRINT "3.  QUIT OUTPUT": PRINT : PRINT
10010 POKE 1403,30: PRINT "WHICH OPTION ? (1-3): ";
10020 GET KS$:SS =  ASC (KS$) - 48: IF SS < 1 OR SS > 3 GOTO 10020
10030 PRINT SS: RETURN
11000 IF PZ = 1 THEN  PRINT  CHR$ (4);"PR#1": PRINT  CHR$ (9);"8S": PRINT  CHR$ (4);
      "PR#3":LK = 2:PZ = 2: RETURN
11010 PRINT : PRINT : PRINT "DUMP OUTPUT ? (Y/N): ";
11020 GET KS$: IF KS$ <  > "Y" AND KS$ <  > "N" GOTO 11020
11030 PRINT KS$: IF KS$ = "N" THEN LK = 2:PZ = 2: RETURN
11040 PZ = 1: RETURN
12000 REM display results
12010 PT$ = "N":PU$ = "N"
12020 IF PT$ <  > "Y" GOTO 12200
12030 HOME : PRINT "DATA FILE: ";DF$: PRINT "---- ----": PRINT
12040 PRINT " No  |  Flow  |  Ion Signal  | Weighting": PRINT "  | (Torr/s) |
      (Observed)  | (Calculated) |": PRINT "_____|_____|_____|
      _____|_____"
12050 JG = 0
12060 FOR J = 1 TO L: GOSUB 5400:JG = JG + (Z - C(J)) * (Z - C(J)): VTAB (6 + J): POKE 1403,2:
      PRINT J;: POKE 1403,7: PRINT "| ";T(J);: POKE 1403,22: PRINT "|  ";C(J);: POKE 1403,36:
      PRINT "|  ";Z;: POKE 1403,45: PRINT "  |";D(J)
12070 IF PU$ <  > "Y" AND (6 + J) > 23 THEN PU$ = "Y": PRINT  CHR$ (4);"PR#1": PRINT
      CHR$  (9);"8S"
12080 NEXT
12085 PRINT : PRINT "SQR(RMS(experimental)  = ";R2: PRINT "RMS(weighted difference) = ";
      Y(K1)
12090 IF PU$ <  > "Y" THEN PU$ = "Y": PRINT  CHR$ (4);"PR#1": PRINT  CHR$ (9);"8S"
12100 PRINT
12200 HOME : IF PT$ <  > "Y" THEN  PRINT : VTAB (7)
12210 FOR A = 1 TO N STEP 2: PRINT "DECAY #"; INT (A + 1.5) / 2;":": PRINT "----- --": PRINT :
      PRINT "Intercept = ";A(A);"  (initially ";W(A);", step ";S(A);" %)": PRINT "Slope  =
      ";A(A  + 1) / CV;"  (initially ";W(A + 1);", step ";S(A + 1);" %)": PRINT : NEXT
12220 IF PT$ = "Y" GOTO 12300
12230 PRINT : PRINT "DO YOU WANT A PRINTOUT ? (Y/N): ";
12240 GET PT$: IF PT$ <  > "Y" AND PT$ <  > "N" GOTO 12240
12250 PRINT PT$: IF PT$ = "Y" GOTO 12020
12300 IF PT$ = "Y" THEN  PRINT  CHR$ (4);"PR#3"
12400 HOME
12990 RETURN
13000 REM * GRAPHICS *
13005 GD$ = "N"
13010 TEXT : HOME : PRINT
13015 LC% = OP%
13020 VTAB (5): POKE 1403,15: PRINT "GRAPHICS:": VTAB (6): POKE 1403,15: PRINT "-------"
```

```
13030 VTAB (10): POKE 1403,15: PRINT "(1). GRAPH USING INITIAL TRIAL VALUES, FULL
      AXIS RANGE."
13040 VTAB (12): POKE 1403,15: PRINT "(2). GRAPH USING INITIAL TRIAL VALUES,
      HIGHER RESOLUTION."
13050 VTAB (14): POKE 1403,15: PRINT "(3). GRAPH USING ITERATED VALUES, FULL AXIS
      RANGE."
13060 VTAB (16): POKE 1403,15: PRINT "(4). GRAPH USING ITERATED VALUES, HIGHER
      RESOLUTION."
13065 VTAB (18): POKE 1403,15: PRINT "(5). DUMP GRAPH ON PRINTER."
13070 VTAB (20): POKE 1403,15: PRINT "(6). OUTPUT MENU."
13080 VTAB (23): POKE 1403,15: PRINT "WHICH OPTION ? (1-6): ";
13090 GET KS$:OP% = ASC (KS$) - 48: IF OP% < 1 OR OP% > 6 GOTO 13090
13100 PRINT KS$: IF OP% = 6 THEN RETURN
13105 IF OP% = 5 GOTO 14000: REM dump graph
13110 HOME : PRINT
13120 HV = 1:LV = 0: IF OP% < > 2 AND OP% < > 4 GOTO 13240
13130 VTAB (5): PRINT "ENTER THE UPPER AND LOWER BOUNDS OF THE X-AXIS (between
      0 & 1)"
13140 VTAB (10): INPUT "UPPER BOUND OF AXIS ? (0-1): ";HV
13150 IF HV < = 0 OR HV > 1 GOTO 13140
13160 VTAB (12): INPUT "LOWER BOUND OF AXIS ? (0-1): ";LV
13170 IF LV < 0 OR LV > = 1 GOTO 13160
13180 HOME : PRINT
13240 VTAB (11): POKE 1403,25: PRINT "***************": POKE 1403,25: PRINT "*             *":
      POKE 1403,25: PRINT "* CALCULATING *": POKE 1403,25: PRINT "*             *": POKE
      1403,25: PRINT "***************"
13250 FOR K = 1 TO N STEP 2
13260 WA(K) = A(K):WA(K + 1) = A(K + 1): IF OP% = 1 OR OP% = 2 THEN WA(K) =
      W(K):WA(K + 1) = W(K + 1) * CV
13270 NEXT
13280 KH = T(1):KL = T(1)
13300 FOR A = 2 TO L
13310 IF KH < T(A) THEN KH = T(A)
13320 IF KL > T(A) THEN KL = T(A)
13330 NEXT
13340 KH = (KH - KL) * HV:KL = (KH - KL) * LV:MH = 0:ML = 0
13350 FOR J = 1 TO N STEP 2
13360 MH = MH + WA(J) * EXP (WA(J + 1) * KL):ML = ML + WA(J) * EXP (WA(J + 1) * KH)
13370 NEXT
13380 FOR A = 1 TO L
13390 IF T(A) < KL OR T(A) > KH GOTO 13420
13400 IF MH < C(A) THEN MH = C(A)
13410 IF ML > C(A) THEN ML = C(A)
13420 NEXT
13430 FL = KH - KL:CL = LOG (MH) - LOG (ML)
13440 FOR A = 1 TO L
13450 KJ = ( LOG (C(A)) - LOG (MH)) * 154 / CL
13460 AY(A) = 1 + ABS ( INT (KJ)):AX(A) = 10 + ABS ( INT (T(A) * 250 / FL))
13470 NEXT
13480 PF = 0
13490 FOR K = 10 TO 260 STEP 4
13500 BY = 0:XZ = (K - 10) * FL / 250
13510 FOR I = 1 TO N STEP 2
```

```
13520  PO =  EXP (XZ * WA(I + 1)):AP = WA(I) * PO:BY = BY + AP
13530  NEXT
13540  ZZ =  LOG (MH) -  LOG (BY):PF = PF + 1:AZ(PF) = 1 +  INT (ZZ * 154 / CL)
13550  NEXT
13560  HGR : HCOLOR= 3: HPLOT 10,1 TO 10,155: HPLOT 10,155 TO 260,155
13570  FOR I = 1 TO L
13580  IF (AX(I) + 1 < 9) OR (AX(I) - 1 > 261) OR (AY(I) + 1 < 1) OR (AY(I) - 1 > 156) GOTO 13600
13590  HPLOT AX(I) - 1,AY(I) - 1 TO AX(I) - 1,AY(I) + 1 TO AX(I) + 1,AY(I) + 1 TO AX(I) +
       1,AY(I) - 1 TO AX(I) - 1,AY(I) - 1:HPLOT AX(I),AY(I)
13600  NEXT
13610  PF = 0
13620  FOR J = 10 TO 260 STEP 4
13630  PF = PF + 1:X = J:Y = AZ(PF): IF (Y <  = 155) AND (Y >  = 1) THEN  HPLOT X,Y
13640  NEXT
13650  IF OP% = 2 OR OP% = 4 THEN  PRINT : VTAB (22): PRINT "GRAPH FROM ";LV;" TO
       ";HV;" OF X-AXIS RANGE"
13660  VTAB (24): POKE 1403,20: PRINT "(Press any key to continue)";: GET KS$: PRINT KS$
13670  GD$ = "Y": GOTO 13010
14000  REM dump graph
14010  IF GD$ <  > "Y" THEN  PRINT : PRINT "NO GRAPH TO DUMP !": GET KS$: PRINT KS$:
       GOTO 13010
14050  PRINT  CD$;"PR#1"
14060  IF LC% = 1 OR LC% = 2 THEN  PRINT "GRAPH OF INITIAL VALUES:": PRINT "----- -- ---
       ----  ------"
14070  IF LC% = 3 OR LC% = 4 THEN  PRINT "GRAPH OF ITERATED VALUES:": PRINT "----- --
       --------  ------"
14080  PRINT : IF LC% = 2 OR LC% = 4 THEN  PRINT "from ";LV;" to ";HV;" of x-axis range."
14100  PRINT  CC$;"G"
14110  PRINT  CD$;"PR#3"
14120  GOTO 13010
15999  PRINT : PRINT
18000  REM  EDIT DATA FILE
18001  HOME : PRINT "      DATA TABLE OF ";DA$
18002  PRINT "         *************"
18003  PRINT "FLOW(TORR/S) ION COUNTS WEIGHTING"
18004  PRINT  "------------------------------"
18005  FOR K = 1 TO L
18006  D(K) =  SQR (C(K)) + 0.1 * T(K)
18007  NEXT K
18010  FOR A = 1 TO L
18015  VTAB (A + 5): PRINT "(";A;")"
18020  VTAB (A + 5): POKE 1403,5: PRINT T(A)
18030  VTAB (A + 5): POKE 1403,14: PRINT C(A)
18040  VTAB (A + 5): POKE 1403,23: PRINT D(A)
18050  NEXT A
18060  VTAB (L + 8): INPUT "EDITING REQUIRED ? (Y/N) ";A$
18070  IF A$ = "N" THEN  GOTO 18130
18080  VTAB (L + 10): INPUT "WHICH POINT ? ";DH
18085  IF (DH < 1) OR (DH > L) THEN  GOTO 18000
18090  INPUT "FLOW(TORR/S) ? ";T(DH)
18100  INPUT "ION COUNTS   ? ";C(DH)
18110  INPUT "WEIGHTING    ? ";D(DH)
18120  GOTO 18001
```

```
18130  HOME : RETURN
20000  REM  ITN OUTPUT
20010  IF NF > 1 THEN  GOTO 20060
20015  HOME
20020  PRINT  "SQR(RMS(exptl))=";R2
20030  VTAB (3): PRINT "ITN."
20031  ZY = 0:YZ = 0
20035  FOR K = 1 TO N STEP 2
20036  YZ = YZ + 1
20040  VTAB (3): POKE 1403,10 + ZY: PRINT "DECAY ";YZ
20050  ZY = ZY + 20
20055  NEXT K
20060  VTAB (1): POKE 1403,35: PRINT "RMS(wtd.diff.) =";Y(K1)
20070  VTAB (4 + NF): PRINT C1
20075  ZY = 0
20076  FOR I = 1 TO N STEP 2
20080  VTAB (5 + NF): POKE 1403,10 + ZY: PRINT P(K1,I + 1) / CV
20085  VTAB (4 + NF): POKE 1403,10 + ZY: PRINT P(K1,I)
20086  ZY = ZY + 20
20087  NEXT I
20090  IF NF = 16 THEN NF =  - 2
20100  RETURN
```

Program "PROD RAT"

```
10    REM ** PROGRAM PROD RAT **
20    DIM XP(25),YP(25,6),X(25),Y(25,6)
25    DIM TS$(4),ES$(5),SH$(6),TT(25)
30    CD$ = CHR$ (13) + CHR$ (4)
35    CC$ = CHR$ (9)
40    TS$(1) = "Load data file":TS$(2) = "Select from data in memory":TS$(3) = "Display
      product ratio graph":TS$(4) = "Quit"
50    ES$(0) = "Quit":ES$(1) = "Select ion signals for product distribution":ES$(2) = "Edit a data
      point":ES$(3) = "Delete a row of data":ES$(4) = "Add a data point":ES$(5) = "Delete a
      column of data"
75    PRINT CD$;"OPEN FILENAMES,D2": PRINT CD$;"READ FILENAMES": INPUT DF$:
      INPUT FF$: PRINT CD$;"CLOSE FILENAMES"
95    RF$ = "N":RC$ = "N"
97    PRINT  CHR$ (4);"PR#3"
100   GOSUB 1000
110   REM display menu
200   IF OP% = 1 THEN  GOSUB 2000
210   REM read data file
300   IF OP% = 2 THEN  GOSUB 3000
310   REM display / adjust data file
400   IF OP% = 3 THEN  GOSUB 4000
410   REM draw graph
500   IF OP% < > 4 GOTO 100
600   PRINT CD$;"RUN OPTIONS,D1"
1000  REM options menu
1010  TEXT : HOME
1020  PRINT "PRODUCT RATIO:": PRINT "------- -----": PRINT : PRINT "Make a choice:":
      PRINT "---- - ------": PRINT : FOR I = 1 TO 4: PRINT : POKE 1403,10: PRINT "(";I;").
      ";TS$(I): NEXT : PRINT : PRINT "WHICH OPTION   ? (1-4): ";
1030  GET KS$:OP% =  ASC (KS$) - 48: IF OP% < 1 OR OP% > 4 GOTO 1030
1040  PRINT OP%: RETURN
2000  REM load data file
2010  HOME : PRINT "READ DATA FILE:": PRINT "---- ---- ----": PRINT : VTAB 10: PRINT
      "CURRENT DATA FILENAME IS: ";DF$: PRINT: PRINT "CHANGE THIS ? (Y/N): ";
2020  GET KS$: IF KS$ < > "Y" AND KS$ < > "N" THEN 2020
2030  PRINT KS$: IF KS$ = "Y" THEN  PRINT : INPUT "NEW FILENAME ? ...      ";DF$
2040  PRINT : PRINT "READING YOUR DATA FILE ";DF$;" NOW ... ":YU% = 0
2050  PRINT CD$;"OPEN ";DF$;",D2": PRINT CD$;"READ ";DF$: INPUT PTS: INPUT MAX:
      FOR I = 1 TO PTS: FOR J = 1 TO MAX: INPUT YP(I,J): INPUT XP(I): NEXT : NEXT :
      PRINT CD$;"CLOSE ";DF$
2060  FOR J = 1 TO MAX:SH$(J) = "Y":MD(J) = 1: NEXT : GOSUB 6000
2070  RF$ = "Y"
2500  RETURN
3000  REM examine/edit data file
3002  IF RF$ < > "Y" THEN  RETURN
3005  HD$ = "EXAMINE DATA FILE":UD$ = "------- ---- ----"
3010  GOSUB 3600: REM display data file
3020  PRINT : FOR I = 0 TO 5: POKE 1403,10: PRINT "(";I;").  ";ES$(I): NEXT : PRINT : PRINT
      "WHICH OPTION ? (0-5): ";
3030  GET KS$:WO% =  ASC (KS$) - 48: IF WO% < 0 OR WO% > 5 THEN 3030
3035  PRINT WO%: IF WO% = 0 THEN  GOSUB 6000: RETURN
3040  ON WO% GOSUB 3100,3200,3300,3400,3500
3045  GOTO 3005
3090  RETURN
3100  REM choose ion signal for rate calculation
```

```
3110  HD$ = "SELECT PRODUCT IONS TO BE INCLUDED:":UD$ = "------ ------- ---- -- -- --------":
      GOSUB 3600: PRINT
3115  FOR I = 1 TO 6:MD(I) = 1: NEXT
3120  NP = 0: FOR J = 1 TO MAX: PRINT "Include Y";J;" ? (Y/N): ";
3130  GET SH$(J): IF SH$(J) < > "Y" AND SH$(J) < > "N" GOTO 3130
3135  IF SH$(J) = "Y" THEN NP = NP + 1
3140  PRINT SH$(J);: IF SH$(J) = "N" THEN  PRINT : GOTO 3170
3145  PRINT "   Mass disc. factor ? <default=1> (Y/N): ";
3150  GET K$: IF K$ < > "Y" AND K$ < > "N" GOTO 3150
3160  PRINT K$: IF K$ = "Y" THEN  INPUT "Enter mass discrimination factor <1 - 9.9>: ";MD(J)
3170  NEXT
3185  IF NP < 2 THEN  HOME : PRINT : VTAB 12: POKE 1403,20: PRINT "THAT'S NOT
      WORTH THE EFFORT !!": PRINT : POKE 1403,20: PRINT "(Press any key to continue)":
      GET KS$: RETURN
3190  RETURN
3200  REM Edit data point
3210  HD$ = "EDIT DATA POINT:":UD$ = "---- ---- -----": GOSUB 3600: PRINT : PRINT "Which
      point ? (0 - ";PTS;") ";: INPUT " <0 = esc>: ";WP: IF WP > PTS OR WP < = 0 THEN
      RETURN
3220  PRINT : PRINT "Change X ? <";XP(WP);">  (Y/N): ";
3230  GET KS$: IF KS$ < > "Y" AND KS$ < > "N" GOTO 3230
3240  PRINT KS$: IF KS$ = "Y" THEN  INPUT "Enter new value <-1 to escape>: ";X: IF X >  -
      0.0001 THEN XP(WP) = X
3250  FOR J = 1 TO MAX: PRINT : PRINT "Change Y";J;" ? <";YP(WP,J);">  (Y/N): ";
3260  GET KS$: IF KS$ < > "Y" AND KS$ < > "N" GOTO 3260
3270  PRINT KS$: IF KS$ = "Y" THEN  INPUT "Enter new value <-1 to escape>: ";Y: IF Y >  -
      0.0001 THEN YP(WP,J) = Y
3280  NEXT : RETURN
3300  REM delete a data point
3310  HD$ = "DELETE DATA POINT:":UD$ = "------ ---- -----": GOSUB 3600: PRINT : PRINT
      "Which point ? (0 - ";PTS;") ";: INPUT "<0 = esc>: ";WP: IF WP > PTS OR WP < 1 THEN
      RETURN
3320  FOR I = WP TO PTS - 1:XP(I) = XP(I + 1): FOR J = 1 TO MAX:YP(I,J) = YP(I + 1,J): NEXT :
      NEXT :PTS = PTS - 1: GOTO 3310
3400  REM add a data point
3410  HD$ = "ADD A DATA POINT":UD$ = "--- - ---- -----": GOSUB 3600: PRINT : INPUT "Enter
      X-value  <-1 to escape>: ";X: IF X < - 0.0001 THEN  RETURN
3420  PTS = PTS + 1: IF PTS > 25 THEN  PRINT : PRINT "FILE EXCEEDS MAX. ALLOWABLE
      SIZE !!": PRINT "(Press any key to continue): ";: GET KS$:PTS = 25: RETURN
3430  XP(PTS) = X: PRINT : FOR J = 1 TO MAX: PRINT "Enter Y";J;: INPUT ": ";YP(PTS,J): NEXT
      : GOTO 3410
3500  IF MAX < = 1 THEN  RETURN : REM delete a column of data
3510  HD$ = "DELETE A COLUMN OF DATA:":UD$ = "------ - ------ -- ----": GOSUB 3600: PRINT :
      PRINT "Which data column ? (Y = 0 to ";MAX;: INPUT ")  <0 = esc>: ";WC%: PRINT :
      PRINT "Sure about that ? (Y/N): ";
3520  GET KS$: IF KS$ < > "Y" AND KS$ < > "N" GOTO 3520
3525  PRINT KS$: IF KS$ = "N" GOTO 3510
3526  IF WC% < = 0 OR WC% > MAX THEN  RETURN
3530  MAX = MAX - 1: FOR J = WC% TO MAX:SH$(J) = SH$(J + 1): FOR I = 1 TO PTS:YP(I,J) =
      YP(I,J + 1): NEXT : NEXT : RETURN
3600  REM list data file contents
3605  ST = 1:FI = PTS: IF FI > 15 THEN FI = 15
3610  HOME : PRINT HD$: PRINT UD$: PRINT : PRINT "   X";: FOR J = 1 TO MAX: POKE
      1403,(10 * (J + 1)): PRINT " Y";J;: NEXT : PRINT: FOR I = ST TO FI:QX = 2 -  INT (( LOG (I) /
      LOG (10)) + 0.0001): POKE 1403,QX: PRINT I;". ";XP(I);
3620  FOR J = 1 TO MAX: POKE 1403,(10 * (J + 1)): PRINT YP(I,J);: NEXT : PRINT : NEXT : IF FI >
      = PTS THEN  RETURN
3630  FI = PTS:ST = FI - 15: GET KS$: GOTO 3610
```

```
4000  REM draw graph
4005  IF RF$ <  > "Y" THEN  RETURN
4010  HOME : PRINT  CHR$ (17);"e0": HGR2 : HCOLOR= 3
4020  HPLOT 30,4 TO 30,165 TO 271,165: FOR I = 5 TO 157 STEP 8: HPLOT 28,I TO 29,I: NEXT
4030  FOR I = 1 TO PTS: FOR J = 1 TO MAX: IF SH$(J) = "Y" THEN  ON J GOSUB 4200,4220,4240,
      4260,4280,4300
4040  NEXT : NEXT
4050  GET KS$: PRINT KS$: TEXT : PRINT  CHR$ (4);"PR#3"
4100  PRINT : VTAB (11): PRINT "Dump graph on printer ? (Y/N): ";
4110  GET KS$: IF KS$ <  > "Y" AND KS$ <  > "N" GOTO 4110
4120  PRINT KS$: IF KS$ = "N" THEN  RETURN
4130  PRINT CD$;"PR#1": PRINT  CHR$ (9);"G2": PRINT CD$;"PR#3": RETURN
4200  HPLOT X(I) - 2,Y(I,J) TO X(I) + 2,Y(I,J): RETURN
4220  HPLOT X(I) - 1,Y(I,J) TO X(I) + 1,Y(I,J): HPLOT X(I),Y(I,J) - 2 TO X(I),Y(I,J) + 2: RETURN
4240  HPLOT X(I) - 2,Y(I,J) - 1 TO X(I) + 1,Y(I,J) - 1: HPLOT X(I) - 1,Y(I,J) - 1 TO X(I) - 1,Y(I,J) + 2:
      HPLOT X(I) - 1,Y(I,J) + 1 TO X(I) + 2,Y(I,J) + 1: HPLOT X(I) + 1,Y(I,J) - 2 TO X(I) + 1,Y(I,J) + 1:
      RETURN
4260  HPLOT X(I) - 2,Y(I,J) - 1: HPLOT X(I) - 2,Y(I,J) + 1: HPLOT X(I) + 2,Y(I,J) - 1: HPLOT X(I) +
      2,Y(I,J) + 1: RETURN
4280  FOR X =  - 1 TO 1: HPLOT X(I) - 1,Y(I,J) + X TO X(I) + 1,Y(I,J) + X: NEXT : RETURN
4300  HPLOT X(I) - 1,Y(I,J) TO X(I) + 1,Y(I,J): HPLOT X(I) - 1,Y(I,J) - 2 TO X(I) - 1,Y(I,J) + 2: HPLOT
      X(I) + 1,Y(I,J) - 2 TO X(I) + 1,Y(I,J) + 2: RETURN
6000  REM calculate % of ion signal at each flow
6005  MX = 0
6010  FOR I = 1 TO PTS:TT(I) = 0: FOR J = 1 TO MAX: IF SH$(J) = "Y" THEN TT(I) = TT(I) +
      YP(I,J) * MD(J)
6015  NEXT : IF TT(I) < 1 THEN TT(I) = 1
6020  FOR J = 1 TO MAX: IF SH$(J) <  > "Y" GOTO 6040
6030  Y(I,J) = 165 -  INT (160 * YP(I,J) * MD(J) / TT(I) + 0.5)
6040  NEXT : IF XP(I) > MX THEN MX = XP(I)
6050  NEXT
6100  FOR I = 1 TO PTS:X(I) = 30 +  INT (240.0 * XP(I) / MX + 0.5): NEXT
6500  RETURN
```

Program "STUDYFILES"

```
10      REM ** PROGRAM STUDYFILES **
20      DIM XP(40): DIM YP(40,6): DIM RC$(20)
25      DIM VN$(12): DIM RG$(12): DIM TY(12): DIM VQ(12)
30      CD$ = CHR$ (13) + CHR$ (4)
40      TS$(1) = "LOAD A DATA FILE"
42      TS$(2) = "LOAD A FORMAT FILE"
44      TS$(3) = "DISPLAY FILE CONTENTS"
46      TS$(4) = "EDIT FILE CONTENTS"
48      TS$(5) = "SAVE A FILE"
50      TS$(6) = "RETURN TO MAIN MENU"
51      TS$(7) = "QUIT"
55      NC% = 7
60      GOSUB 9000
61      REM get default filenames
65      FOR I = 1 TO 12:TY(I) = 1: NEXT
70      TY(2) = 2:TY(8) = 2:TY(10) = 3:TY(11) = 2
80      FT$(1) = "N":FT$(2) = "N":FT$(3) = "N":MF$ = "N"
85      VN$(1) = "Run number":VN$(2) = "Date":VN$(3) = "Portal no.":VN$(4) = "Neutral vol."
86      RG$(1) = "(1 - 30)":RG$(2) = "":RG$(3) = "(1 - 2)":RG$(4) = "(100 - 9000)"
90      VN$(5) = "T (degrees C)":VN$(6) = "Tube pressure":VN$(7) = "Tylan flow value":VN$(8)
        = "Reaction title"
91      RG$(5) = "(0 - 50)":RG$(6) = "(0.1 - 1.0)":RG$(7) = "(1 - 400)":RG$(8) = ""
95      VN$(9) = "Ion mass (amu)":VN$(10) = "Carrier gas":VN$(11) = "Comments"
96      RG$(9) = "(1 - 500)":RG$(10) = "(H2/HE/N2/AR)":RG$(11) = ""
98      DS$(0) = "Escape":DS$(1) = "Edit a data point":DS$(2) = "Delete a row of data":DS$(3) =
        "Add a data point":DS$(4) = "Delete a column of data"
100     GOSUB 1000
110     REM get option desired
120     REM
200     IF OP% = 1 THEN  GOSUB 2000
210     REM load data file
220     REM
300     IF OP% = 2 THEN  GOSUB 3000
310     REM load format file
320     REM
600     IF OP% = 3 THEN  GOSUB 6000
610     REM examine file contents
620     REM
700     IF OP% = 4 THEN  GOSUB 7000
710     REM edit file contents
720     REM
800     IF OP% = 5 THEN  GOSUB 8000
810     REM save file
900     IF OP% = 6 THEN  PRINT CD$;"RUN OPTIONS,D1"
910     REM return to main menu
950     IF OP% < >NC% GOTO 100
990     END
1000    REM options menu
1010    HOME
1020    PRINT "STUDY FILES:": PRINT "----- -----": PRINT "Make a choice:": PRINT "---- - ------":
        PRINT
1030    FOR I = 1 TO NC%
1040    HTAB (10): PRINT "(";I;").  ";TS$(I)
1045    PRINT
1050    NEXT
```

```
1060  PRINT "WHICH OPTION ? (1-";NC%;"): ";
1070  GET OS$:OP% =  ASC (OS$) - 48: IF OP% < 1 OR OP% > NC% GOTO 1070
1075  PRINT OP%: PRINT
1080  PRINT OP%;".  ";TS$(OP%)
1500  RETURN
2000  REM load data file
2010  HOME : PRINT "LOAD DATA FILE:": PRINT "---- ---- ----": PRINT
2020  VTAB (6): PRINT "Current data filename is ";DF$
2030  PRINT : PRINT "Change this ? (Y/N): ";
2040  GET KS$: IF KS$ < > "Y" AND KS$ < > "N" THEN 2040
2050  PRINT KS$: IF KS$ = "N" THEN 2060
2052  PRINT : INPUT "New filename ? (N=no change / NONE=don't read): ";NF$
2054  IF NF$ = "" OR NF$ = "NONE" THEN  RETURN
2056  IF NF$ < > "N" THEN DF$ = NF$
2060  PRINT : PRINT "READING FILE ";DF$;" NOW ..."
2070  PRINT CD$;"OPEN ";DF$;",D2"
2080  PRINT CD$;"READ ";DF$
2090  INPUT PTS
2100  INPUT MAX
2110  FOR I = 1 TO PTS
2120  FOR J = 1 TO MAX
2130  INPUT YP(I,J): INPUT XP(I)
2140  NEXT
2150  NEXT
2160  PRINT CD$;"CLOSE ";DF$
2170  FT$(1) = "Y"
2200  IF FT$(2) = "Y" THEN MF$ = "Y"
2500  RETURN
3000  REM read format file
3010  HOME : PRINT "READ RATE VARIABLES FILE:": PRINT "---- ---- --------- ----": PRINT
3020  VTAB (7): PRINT "Current filename is ";FF$
3030  PRINT : PRINT "Change this ? (Y/N): ";
3040  GET KS$: IF KS$ < > "Y" AND KS$ < > "N" GOTO 3040
3050  PRINT KS$: IF KS$ = "N" GOTO 3100
3060  PRINT : INPUT "New filename ? (N=no change / NONE=don't read): ";NF$
3070  IF NF$ = "" OR NF$ = "NONE" THEN  RETURN
3080  IF NF$ < > "N" THEN FF$ = NF$
3100  PRINT : PRINT "READING FILE ";FF$;" NOW ...": PRINT
3110  PRINT CD$;"OPEN ";FF$;",D2"
3120  PRINT CD$;"READ ";FF$
3130  FOR I = 1 TO 11
3140  INPUT RC$(I):VQ(I) =  VAL (RC$(I))
3150  NEXT
3160  PRINT CD$;"CLOSE ";FF$
3200  FT$(2) = "Y"
3210  IF FT$(1) = "Y" THEN MF$ = "Y"
3500  RETURN
6000  REM examine file contents
6010  HOME : PRINT "DISPLAY A FILE:": PRINT "------ - ----": PRINT
6030  IF MF$ = "Y" GOTO 6100
6040  FOR I = 1 TO 2
6050  IF FT$(I) = "Y" THEN TF% = I
6060  NEXT
6070  GOTO 6130
6100  PRINT "Data or format file ? (D/F): ";
6105  GET KS$: IF KS$ < > "D" AND KS$ < > "F" GOTO 6105
6110  IF KS$ = "D" THEN TF% = 1
6115  IF KS$ = "F" THEN TF% = 2
```

```
6120    IF FT$(TF%) <  > "Y" THEN 6110
6125    PRINT KS$
6130    IF TF% = 1 THEN HD$ = "DATA FILE " + DF$:UL$ = "---- ----"
6135    IF TF% = 2 THEN HD$ = "FORMAT FILE " + FF$:UL$ = "------ ----"
6150    ON TF% GOSUB 6200,6400
6160    GET KS$
6180    RETURN
6200    REM display data file
6205    ST = 1:FI = PTS: IF FI > 15 THEN FI = 15
6210    HOME : PRINT HD$: PRINT UL$: PRINT
6220    PRINT "   X";
6230    FOR J = 1 TO MAX: POKE 1403,(10 * (J + 1)): PRINT " Y";J;: NEXT
6240    PRINT
6250    FOR I = ST TO FI
6260    QX = 2 -  INT ( LOG (I) /  LOG (10)): POKE 1403,QX: PRINT I;".  ";XP(I);
6270    FOR J = 1 TO MAX
6280    POKE 1403,(10 * (J + 1)): PRINT YP(I,J);:
6285    NEXT
6288    PRINT
6290    NEXT
6300    IF FI >  = PTS THEN 6350
6310    ST = ST + 15:FI = FI + 15: IF FI > PTS THEN FI = PTS:ST = PTS - 15
6320    GET KS$: GOTO 6210
6350    RETURN
6400    REM display rate vbles file
6410    HOME : PRINT HD$: PRINT UL$: PRINT
6420    FOR I = 1 TO 11
6430    I$ =  CHR$ (I + 64)
6440    PRINT "(";I$;"). ";VN$(I);: POKE 1403,30: PRINT ;" = ";
6450    PRINT RC$(I)
6470    NEXT
6550    RETURN
7000    REM edit file
7005    HOME : PRINT "EDIT A FILE:": PRINT "---- - ----": PRINT
7010    IF TF% = 1 OR TF% = 2 OR TF% = 3 GOTO 7050
7020    IF MF$ = "Y" GOTO 7040
7030    FOR I = 1 TO 3
7031    IF FT$(I) = "Y" THEN TF% = I
7032    NEXT
7033    GOTO 7050
7035    IF TF% < 1 THEN  HOME : PRINT : VTAB (11): POKE 1403,30: PRINT "LOAD A FILE
        FIRST !": PRINT "(Press any key to continue )": GET KS$: RETURN
7040    PRINT "Data or format file ? (D/F): ";
7041    GET KS$: IF KS$ <  > "D" AND KS$ <  > "F" GOTO 7041
7042    PRINT KS$
7043    IF KS$ = "F" THEN TF% = 2
7044    IF KS$ = "D" THEN TF% = 1
7045    IF FT$(TF%) <  > "Y" GOTO 7041
7050    ON TF% GOSUB 7100,7400
7060    RETURN
7100    REM edit data file
7110    HD$ = "EDIT DATA FILE " + DF$:UL$ = "---- ---- ----"
7120    GOSUB 6200: REM display data file
7125    PRINT
7130    FOR I = 0 TO 4: POKE 1403,10: PRINT I;".  ";DS$(I): NEXT
7135    PRINT : PRINT "WHICH OPTION ? (0-4): ";
7140    GET KS$:WO% =  ASC (KS$) - 48: IF WO% < 0 OR WO% > 4 THEN 7140
7150    PRINT KS$: IF WO% = 0 THEN  RETURN
```

```
7160  ON WO% GOSUB 7200,7260,7300,7360
7170  GOTO 7110
7180  RETURN
7200  REM edit data point
7210  HD$ = "EDIT DATA POINT":UL$ = "---- ---- -----": GOSUB 6200: REM display data file
7215  PRINT : PRINT "Which point ? (0-";PTS;") ";: INPUT "(0=esc): ";WP
7220  IF WP > PTS OR WP < = 0 THEN RETURN
7225  PRINT : PRINT "Change X ? <";XP(WP);"> (Y/N): ";
7228  GET KS$: IF KS$ < > "Y" AND KS$ < > "N" THEN 7228
7230  PRINT KS$: IF KS$ = "Y" THEN INPUT "Enter new value (-1 to escape): ";X: IF X > - 0.02
      THEN XP(WP) = X
7235  FOR J = 1 TO MAX
7238  PRINT : PRINT "Change Y";J;" ? <";YP(WP,J);"> (Y/N): ";
7240  GET KS$: IF KS$ < > "Y" AND KS$ < > "N" THEN 7240
7242  PRINT KS$: IF KS$ = "Y" THEN INPUT "Enter new value (-1 to escape): ";Y: IF Y > - 0.02
      THEN YP(WP,J) = Y
7245  NEXT
7250  RETURN
7260  REM delete data point
7265  HD$ = "DELETE DATA POINT":UL$ = "------ ---- -----": GOSUB 6200: REM display data file
7270  PRINT : PRINT "Which point ? (0-";PTS;") ";: INPUT "(0=esc): ";WP
7275  IF WP > PTS OR WP < 1 THEN 7298
7280  FOR I = WP TO PTS - 1
7282  XP(I) = XP(I + 1)
7285  FOR J = 1 TO MAX
7288  YP(I,J) = YP(I + 1,J)
7290  NEXT
7292  NEXT
7295  PTS = PTS - 1
7296  GOTO 7265
7298  RETURN
7300  REM add a data point
7305  HD$ = "ADD A DATA POINT":UL$ = "--- - ---- -----": GOSUB 6200: REM display data file
7310  PRINT : INPUT "Enter x-value (-1 to escape )";X
7315  IF X > = 0 THEN PTS = PTS + 1: IF PTS > 40 THEN PRINT : PRINT "FILE EXCEEDS MAX.
      ALLOWABLE SIZE!": PRINT "(Press any key to continue )";: GET KS$:PTS = 40: RETURN
7318  IF X < 0 THEN 7355
7320  XP(PTS) = X
7325  FOR J = 1 TO MAX
7330  PRINT "Enter Y";J;: INPUT " :";YP(PTS,J)
7335  NEXT
7355  RETURN
7360  REM delete a column of data
7365  HD$ = "DELETE A COLUMN OF DATA":UL$ = "------ - ------ -- ----": GOSUB 6200: REM
      display data file
7370  PRINT "Which data column ? (Y= 0 to ";MAX;") (0=esc): ";
7375  GET KS$:WC% = ASC (KS$) - 48: IF WC% < 0 OR WC% > MAX THEN 7375
7380  PRINT KS$: IF WC% = 0 THEN RETURN
7382  PRINT : PRINT "Sure about that ? (Y/N): ";
7385  GET KS$: IF KS$ < > "Y" AND KS$ < > "N" THEN 7385
7388  PRINT KS$: IF KS$ = "N" THEN RETURN
7389  MAX = MAX - 1: IF MAX < 1 THEN MAX = 1: RETURN
7390  FOR J = WC% TO MAX
7391  FOR I = 1 TO PTS
7392  YP(I,J) = YP(I,J + 1)
7393  NEXT
7394  NEXT
7395  RETURN
```

```
7400  REM edit rate variables file
7410  HD$ = "EDIT FORMAT FILE":UL$ = "---- ------ ----"
7420  GOSUB 6400: REM  display file
7430  PRINT : PRINT "EDIT WHICH ENTRY ?(A-K) (N = escape): ";
7440  GET WO$:WP% =  ASC (WO$) - 64: IF WP% < 1 OR (WP% > 11 AND WO$ < > "N")
      GOTO 7440
7450  PRINT WO$: IF WO$ = "N" THEN  RETURN
7460  ON TY(WP%) GOSUB 7500,7560,7620
7465  GOTO 7410
7470  RETURN
7500  REM edit numerical entries
7505  PRINT : PRINT WO$;".  ";VN$(WP%);RG$(WP%)
7510  PRINT "Current value = ";VQ(WP%)
7515  PRINT : INPUT "New value ? (-999 to leave unchanged): ";NV
7520  IF NV >  - 900 THEN VQ(WP%) = NV:RC$(WP%) =  STR$ (VQ(WP%))
7555  RETURN
7560  REM edit character-type entries
7570  PRINT : PRINT WO$;".  ";VN$(WP%);RG$(WP%)
7580  PRINT "Current value = ";RC$(WP%)
7590  PRINT : INPUT "New value ? (N to leave unchanged): ";NV$
7600  IF NV$ < > "N" THEN RC$(WP%) = NV$
7615  RETURN
7620  REM edit carrier gas value
7625  PRINT : PRINT WO$;".  ";VN$(WP%);RG$(WP%)
7630  PRINT "Current value = ";RC$(WP%): PRINT : INPUT "New value ? (blank to leave
      unchanged): ";NV$
7635  IF NV$ = "" THEN 7650
7640  IF NV$ = "HE" OR NV$ = "H2" OR NV$ = "N2" OR NV$ = "AR" THEN RC$(WP%) =
      NV$
7650  RETURN
8000  REM save a file
8010  HOME : PRINT "SAVE A FILE:": PRINT "---- - ----": PRINT
8020  IF MF$ = "Y" GOTO 8040
8025  FOR I = 1 TO 3
8030  IF FT$(I) = "Y" THEN SF% = I
8032  NEXT
8035  GOTO 8060
8040  PRINT "Data file, format file, or none ? (D/F/N): ";
8042  GET KS$: IF KS$ < > "D" AND KS$ < > "F" AND KS$ < > "N" GOTO 8042
8044  IF KS$ = "N" THEN  RETURN
8046  IF KS$ = "D" THEN TF% = 1
8048  IF KS$ = "F" THEN TF% = 2
8050  PRINT KS$
8058  IF FT$(TF%) < > "Y" THEN  PRINT : PRINT "No such file in memory": RETURN
8060  ON TF% GOSUB 8100,8400
8080  RETURN
8100  REM save data file
8110  HD$ = "SAVE DATA FILE":UL$ = "---- ---- ----"
8120  GOSUB 6200: REM show file contents
8130  PRINT : PRINT "CURRENT FILENAME IS ";DF$
8140  INPUT "ENTER NEW FILENAME ('N' to use current name): ";KS$
8150  IF KS$ < > "N" THEN DF$ = KS$
8160  PRINT : PRINT "PROCEED ? (Y/N): ";
8170  GET KS$: IF KS$ < > "Y" AND KS$ < > "N" GOTO 8170
8180  PRINT KS$: IF KS$ = "N" THEN  RETURN
8190  HOME : PRINT : VTAB (11): POKE 1403,25: PRINT "WRITING FILE ";DF$;" NOW ..."
8200  PRINT CD$;"OPEN ";DF$;",D2"
8210  PRINT CD$;"WRITE ";DF$
```

```
8220    PRINT PTS
8230    PRINT MAX
8240    FOR I = 1 TO PTS
8250    FOR J = 1 TO MAX
8260    PRINT YP(I,J): PRINT XP(I)
8270    NEXT
8280    NEXT
8290    PRINT CD$;"CLOSE ";DF$
8390    RETURN
8400    REM save rate vbles file
8410    HD$ = "SAVE RATE VARIABLES FILE":UL$ = "---- ---- --------- ----"
8420    GOSUB 6400: REM  show file contents
8430    PRINT : PRINT "CURRENT FILENAME IS ";FF$
8440    INPUT "ENTER NEW FILENAME ('N' to use current name): ";KS$
8450    IF KS$ <  > "N" THEN FF$ = KS$
8460    PRINT : PRINT "PROCEED ? (Y/N): ";
8470    GET KS$: IF KS$ <  > "Y" AND KS$ <  > "N" GOTO 8470
8480    PRINT KS$: IF KS$ = "N" THEN  RETURN
8490    HOME : PRINT : VTAB (11): POKE 1403,25: PRINT "WRITING FILE ";FF$;" NOW ..."
8500    PRINT CD$;"OPEN ";FF$;",D2"
8510    PRINT CD$;"WRITE ";FF$
8520    FOR I = 1 TO 11
8560    PRINT RC$(I)
8580    NEXT
8590    PRINT CD$;"CLOSE ";FF$
8690    RETURN
9000    REM get default filenames
9010    PRINT CD$;"OPEN FILENAMES,D2"
9020    PRINT CD$;"READ FILENAMES"
9030    INPUT DF$
9040    INPUT FF$
9050    PRINT CD$;"CLOSE FILENAMES"
9500    RETURN
```

Program "PRESSMONITOR"

```
10      PRINT  CHR$ (4)"PR#3"
20      LOMEM: 32768
30      DIM IN$(20)
40      DIM SEL(20,2)
50      DIM SL(100,2)
55      DIM FM(400)
60      LS = 120
70      LA = 25
80      CD$ =  CHR$ (13) +  CHR$ (4)
120     PRINT CD$"BLOADATTENT"
130     PRINT CD$"BLOADTEMP1"
140     PRINT CD$"BLOADCONVERT"
150     PRINT CD$"BLOADMADMAIN"
170     PRINT CD$"BLOADTEMP2"
280     HOME
290     Z = 0:D = 0: REM :TO ALLOW SETTING UP STEP
295     DZ = 0
300     NF% = 0:XU% = 0
340     HOME : PRINT "MONITOR NEUTRAL REACTANT FLOW:": PRINT "------- ------- -------
        ---": PRINT :IN$(1) = "3"
350     AD = 2
360     S = 3:S$ = "DELAY(20=1SEC)":RG$ = "1:256": GOSUB 760:DD = VO
370     PRINT
380     POKE 25040,AD: POKE 25042,DD
390     S = 9:S$ = "CHANNEL NO":RG$ = "0:7": GOSUB 760:CH = VO
400     TT = 0
410     PRINT
420     CH = CH + (TT * 16)
430     POKE 25060,CH
440     AGAIN = 1
450     PRINT
460     HGAIN = 1
470     PRINT
474     POKE 31232,0
475     POKE 31233,0
476     POKE 31235,0
477     POKE 31234,0
480     CALL 24576: REM  AD SAMPLE
505     XH =  PEEK (31232)
507     XL =  PEEK (31233)
510     XH = (XH * 256) + XL
520     SH =  PEEK (31234)
530     SL =  PEEK (31235)
540     SH = (SH * 256) + SL
550     BH =  PEEK (29408 + TT * 2)
560     BL =  PEEK (29408 + TT * 2 + 1)
565     V1H =  PEEK (25051)
567     V2L =  PEEK (25050)
570     BH = BH * 256 + BL
580     P1T = (XH * BH) / (HGAIN * AGAIN)
582     P2T = (SH * BH) / (HGAIN * AGAIN)
584     P1T = P1T / 8141
586     P2T = P2T / 8141
590     SLOPE = (P2T - P1T) / (DD * .05)
610     CH =  PEEK (25039)
```

```
620   CL =  PEEK (25038)
630   CT = CL + (CH * 256)
635   SLOPE = SLOPE * 10
640   TEXT : HOME : PRINT  CHR$ (4)"PR#1"
650   PRINT SLOPE
660   PRINT  CHR$ (4)"PR#3"
680   IF KX$ = "Y" GOTO 710
690   PRINT "PROCEED WITH FLOW MEASUREMENTS ? (Y/N): ";
695   GET KX$: IF KX$ <  > "Y" AND KX$ <  > "N" GOTO 695
700   PRINT KX$: IF KX$ = "N" GOTO 1220
710   XU% = ( PEEK ( - 16368)) - 64: REM read keyboard buffer
720   NF% = NF% + 1
730   FM(NF%) = SLOPE
740   IF XU% = 8 GOTO 1450
745   IF XU% = 23 THEN AUT = 0: GOTO 290
750   GOTO 340
760   PRINT S$;"(";RG$;")?<";IN$(S);">";: GOSUB 1020:OK = 0: IF A > 0 THEN IN$(S) = A$:
      GOTO 800
770   A =  LEN (IN$(S)): IF A = 0 GOTO 980
780   FOR I = 1 TO A: IF  MID$ (IN$(S),I,1) = "," THEN B = I + 1:I = A
790   NEXT
800   IF S = 4 OR 5 GOTO 990
810   L =  LEN (RG$): IF L = 0 GOTO 990
820   PRINT  A$
830   PRINT L
840   R$ = "":R = 0: FOR J = 1 TO L
850   IF  MID$ (RG$,J,1) <  > ":" THEN R$ = R$ +  MID$ (RG$,J,1): IF J < L GOTO 970
860   IF  VAL (R$) = 0 AND  ASC (R$) <  > 48 GOTO 930
870   IF R = 0 THEN VO =  VAL (IN$(S)): IF VO <  VAL (R$) GOTO 950
880   PRINT  VO
890   IF R = 1 THEN  IF VO >  VAL (R$) GOTO 950
900   IF R = 2 THEN V1 =  VAL ( MID$ (IN$(S),B)): IF V1 <  VAL (R$) GOTO 950
910   IF R = 3 THEN  IF V1 >  VAL (R$) GOTO 950
920   R = R + 1:OK = 1:R$ = "": GOTO 970
930   IF IN$(S) <  > R$ THEN R$ = "": GOTO 970
940   OK = 1: GOTO 960
950   OK = 0
960   J = L
970   PRINT R$: NEXT
980   IF OK = 0 THEN  PRINT  CHR$ (7);"INVALID ENTRY;CHECK (RANGE)":AUT = 0: GOTO
      760
990   VO =  VAL (IN$(S)): RETURN
1000  IF B THEN B$ =  LEFT$ (IN$(S),B - 2): RETURN
1010  B$ = IN$(S): RETURN
1020  A = 0:B = 0:A$ = "": IF AUT = 1 AND S < LS AND  PEEK ( - 16384) < 128 THEN  PRINT :
      RETURN
1030  AUT = 0
1050  GET C$:C =  ASC (C$): IF C > 31 GOTO 1200
1060  IF C <  > 8 GOTO 1120
1070  IF A = 0 GOTO 1020
1080  PRINT C$;" ";C$;:A = A - 1
1090  IF A > 0 THEN A$ =  LEFT$ (A$,A)
1100  IF A < 1 GOTO 1020
1110  GOTO 1050
1120  IF C = 13 THEN  PRINT : RETURN
1130  IF C = 27 AND ES THEN  GOSUB 11000:AUT = 1: POP : POP : GOTO 110
1140  IF C = 1 THEN AUT = 1:LS = 50:DTET = 1: GOTO 1020
1150  IF C = 4 THEN  PRINT : PRINT CD$;A$: POP : GOTO 760
```

```
1160    IF C = 7 THEN  GOSUB 730 GOTO 1050
1170    IF C = 20 THEN  GOSUB 840 GOTO 1050
1180    IF C = 19 THEN  GOSUB 840
1190    IF C = 24 THEN  PRINT  CHR$ (92): GOTO 1020
1200    IF C = 44 AND B = 0 THEN B = A + 2
1210    PRINT C$;:A = A + 1:A$ = A$ + C$: GOTO 1050
1220    PRINT CD$;"RUN OPTIONS,D1"
1450    HOME : INPUT "ENTER RUN NUMBER ? (1-30): ";RN$
1460    NM$ = "FLOWFILE" + RN$
1500    PRINT CD$;"OPEN ";NM$;",D2"
1510    PRINT CD$;"WRITE ";NM$
1520    PRINT  NF%
1530    FOR I = 1 TO NF%
1540    PRINT FM(I)
1550    NEXT
1560    PRINT CD$;"CLOSE ";NM$
1570    PRINT CD$;"RUN OPTIONS,D1"
```

Program "COLLIRAT"

```
10      REM ** PROGRAM COLLIRAT **
15      REM This program calculates the collision rate coefficient for an
20      REM ion-molecule reaction, based on Su & Chesnavich's method
25      REM (involving parametrization of collision rate by trajectory
30      REM calculations). Ref: J.Chem.Phys 76,5183 (1982)
40      CD$ = CHR$(13) + CHR$(4)
50      PRINT CHR$(4): "PR#3"
100     GOSUB 1000
110     REM initialise program
120     REM ----------
300     GOSUB 3000
310     REM input variables
320     REM ----------
400     GOSUB 4000
410     REM perform calculation
420     REM ----------
500     GOSUB 5000
510     REM display results
520     REM ----------
600     IF NG$ = "Y" GOTO 300
700     END
990     REM ----------
1000    REM initialise program
1010    GA = 1.6605E-24: REM grams per amu
1020    QI = 4.80298E-10: REM ionic charge in esu
1030    KB = 1.38062E-16: REM Boltzmann's const. in erg/K
1040    PI = 3.1415927
1500    RETURN
1990    REM ----------
3000    REM input variables
3010    HOME: PRINT "INPUT VARIABLES:": PRINT "----- ---------": PRINT
3020    INPUT "Reaction title ? : ";RT$
3030    PRINT: INPUT "Mass of ion ?     (in amu): ";MI
3040    INPUT "Mass of neutral ? (in amu): ";MN
3050    RAM = MI * MN / (MI + MN)
3060    PRINT "Reduced mass = "; INT(RAM * 100 +0.5)/100;" amu"
3070    PRINT: INPUT "Polarizability of neutral ? (in cm3): ";PN
3080    PRINT: PRINT "Dipole moment (in esu cm) <NB 1 Debye = 1E-18 esu cm>"
3090    INPUT "Permanent dipole moment of neutral ? (in esu cm): ";DM
3100    PRINT: INPUT "Temperature ? (in degrees C): ";TC
3110    PRINT: PRINT: PRINT "                Any changes ? (Y/N): ";
3120    GET KS$: IF KS$ <> "Y" AND KS$ <> "N" GOTO 3120
3130    PRINT KS$: IF KS$ = "Y" GOTO 3010
3500    RETURN
3990    REM ----------
4000    REM perform calculation
4010    RGM = RAM * GA: REM convert reduced mass to grams
4015    TK = TC + 273.2
4020    KL = 2 * PI * QI * ((PN / RGM) ^ 0.5)
4030    X = DM/ (((2 * KB * TK) ^ 0.5) * (PN ^ 0.5))
4040    K1CAP = 0.4767 * X + 0.6200
4050    IF X <= 2 THEN K1CAP = ((X + 0.5090) ^ 2) / 10.526 + 0.9754
4060    KC = K1CAP * KL
4500    RETURN
4990    REM ----------
```

```
5000    REM display results
5010    PT$ = "N"
5020    IF PT$ = "Y" THEN PRINT CHR$(4);"PR#1"
5025    HOME
5030    PRINT "ION-MOLECULE COLLISION RATE CALCULATION:": PRINT "--- -------- ---------
        ---- ----------": PRINT
5040    PRINT RT$
5050    PRINT: PRINT "Calculated collision rate k(c) = ";KC
5060    PRINT: PRINT "Collision efficiency K(cap) = ";K1CAP
5070    PRINT "Capture rate k(L) = ";KL
5080    PRINT: PRINT
5090    PRINT "Reduced mass = "; INT (100 * RAM + 0.5) / 100;" amu"
5100    PRINT "             = ";RGM;" grams"
5105    PRINT
5110    PRINT "Polarizability of neutral = ";PN;" cm^3"
5120    PRINT "Permanent dipole moment of neutral = ";DM;" esu cm"
5130    PRINT "                                   = "; INT(1E20 * DM + 0.5) / 100;" Debye"
5135    PRINT
5140    PRINT "Temperature = "; INT (100 * TK + 0.5) / 100;" K"
5150    IF PT$ = "Y" GOTO 5200
5160    PRINT: PRINT "Do you want a printout ? (Y/N): ";
5170    GET PT$: IF PT$ <> "Y" AND PT$ <> "N" GOTO 5170
5180    PRINT PT$: IF PT$ = "Y" GOTO 5020
5200    IF PT$ = "Y" THEN PRINT CHR$(4);"PR#3"
5210    PRINT: PRINT: PRINT "More calculations ? (Y/N): ";
5220    GET NG$: IF NG$ <> "Y" AND NG$ <> "N" GOTO 5220
5230    PRINT NG$
5500    RETURN
```

ERRATA:

The following amendments should be made to the text:

p. 10, 5 lines from bottom. "frequencies" should read "rates".

p. 20, 7 lines from bottom. "is commonly" should read "can be"; reference 60 quoted on this line should be replaced by reference 61.

p. 30, equation {1.ix}. "k = ln ..." should read "k = - ln ..."

p. 63, line 2. "poymerisation" should read "polymerisation".

p. 70, line 8. "-0.705" should read "0.705"

p. 71, line 2. "-6.448" should read "6.448"

p. 74, table 3.2, note 'c'. "rate coefficient, using" should read "rate coefficient, in units of 10^{-9} cm^3 $molec^{-1}$ s^{-1}, using". The same amendment should be made to note 'c' in **tables 4.2** (p.100), **5.2** (p. 142), **6.1** (p. 201) and **7.3** (p. 242).

p. 98, table 4.1. This table has two notes 'b'. The second of these should be changed to 'c'; likewise, the existing note 'c' should be changed to 'd', etc.

p. 107, table 4.5. "geometries", in the title of this table, should read "properties".

p. 117, table 4.7. The printed value of k_2 for reaction with C_2H_2, ">0.06", should read ">0.6".

p. 147, equation {5.iii}. "[CF+]" should read "[CF_3^+]".

p. 206, 4 lines from bottom. "HC_3N^+" should be indented appropriately.

p. 213, line 5. "C_2H_2N+" should read "$C_2H_2N^+$".

p. 218, line 14. "was" should read "is".

p. 234, 3 lines from bottom. "though" should read "thought".

p. 245, line 13. "from from" should read "from".

p. 248, reaction (7.16). "H_2" should read "*e* ".

p. 255, line 4. ":C4N+" should read "C_4N^+".

p. 324, reference 233. "(1991) In press" should read "**105** (1991) 43".

p. 329, reference 280. "(1991) In press" should read "**248**(1991) 272".